

4

AD-A202 825

AFGL-TR-87-0234

Adapting Schottky Diode Detector Technology
to a Space Platform

Joseph Kristl
Ronald Huppi

Stewart Radiance Laboratory
139 Great Road
Bedford, MA 01730

10 February 1988

Final Report
July 1986-July 1987

DTIC
SELECTED
DEC 19 1988
S E D

APPROVED FOR PUBLIC RELEASE; DISTRIBUTION UNLIMITED

AIR FORCE GEOPHYSICS LABORATORY
AIR FORCE SYSTEMS COMMAND
UNITED STATES AIR FORCE
HANSCOM AIR FORCE BASE, MASSACHUSETTS 01731

"This technical report has been reviewed and is approved for publication"



DAVID J. KNECHT
Contract Manager



CHARLES P. PIKE
Branch Chief

FOR THE COMMANDER



RITA C. SAGALYN
Division Director

This report has been reviewed by the ESD Public Affairs Office (PA) and is releasable to the National Technical Information Service (NTIS).

Qualified requestors may obtain additional copies from the Defense Technical Information Center. All others should apply to the National Technical Information Service.

If your address has changed, or if you wish to be removed from the mailing list, or if the addressee is no longer employed by your organization, please notify AFGL/DAA, Hanscom AFB, MA 01731. This will assist us in maintaining a current mailing list.

Do not return copies of this report unless contractual obligations or notices on a specific document requires that it be returned.

REPORT DOCUMENTATION PAGE

1a. REPORT SECURITY CLASSIFICATION Unclassified		1b. RESTRICTIVE MARKINGS	
2a. SECURITY CLASSIFICATION AUTHORITY		3. DISTRIBUTION / AVAILABILITY OF REPORT Approved for public release; distribution unlimited	
2b. DECLASSIFICATION / DOWNGRADING SCHEDULE		4. PERFORMING ORGANIZATION REPORT NUMBER(S)	
4. PERFORMING ORGANIZATION REPORT NUMBER(S)		5. MONITORING ORGANIZATION REPORT NUMBER(S) AFGL-TR-87-0234	
6a. NAME OF PERFORMING ORGANIZATION Stewart Radiance Laboratory	6b. OFFICE SYMBOL (if applicable)	7a. NAME OF MONITORING ORGANIZATION Air Force Geophysics Laboratory	
6c. ADDRESS (City, State, and ZIP Code) 139 Great Road Bedford, MA 01730		7b. ADDRESS (City, State, and ZIP Code) Hanscom AFB MA 01731	
8a. NAME OF FUNDING / SPONSORING ORGANIZATION Air Force Geophysics Lab	8b. OFFICE SYMBOL (if applicable) PH	9. PROCUREMENT INSTRUMENT IDENTIFICATION NUMBER F19628-86-K-0035	
8c. ADDRESS (City, State, and ZIP Code) Hanscom AFB MA 01731		10. SOURCE OF FUNDING NUMBERS	
		PROGRAM ELEMENT NO. 61101F	TASK NO. LCDP 6I
		WORK UNIT ACCESSION NO. AB	
11. TITLE (Include Security Classification) Adapting Schottky Diode Detector Technology to a Space Platform			
12. PERSONAL AUTHOR(S) Joseph Kristl, Ronald Huppi			
13a. TYPE OF REPORT Final	13b. TIME COVERED FROM Jul 86 to Jul 87	14. DATE OF REPORT (Year, Month, Day) 10 February 1988	15. PAGE COUNT 282
16. SUPPLEMENTARY NOTATION This research was partially supported by the In-house Laboratory Independent Research Fund, Rome Air Development Center			
17. COSATI CODES		18. SUBJECT TERMS (Continue on reverse if necessary and identify by block number)	
FIELD	GROUP	infrared, sensors, thermal, Schottky barrier, space surveillance, electro optical	
19. ABSTRACT (Continue on reverse if necessary and identify by block number) Schottky barrier focal plane arrays have demonstrated superior performance in imagery and sensitivity in cameras deployed on the ground and on airborne platforms. This study determines the feasibility of placing a camera using one of these arrays in space in the space shuttle cargo bay or on the Shuttle Pallet Satellite. The basic operation and performance of platinum silicide schottky barrier detectors is first discussed. Then a detailed analysis of all of the technical issues involved in constructing a space based Schottky camera are examined at length. Optical performance, cryogenic cooling, image compensation, data recording, system control, host platform restraints, and relevant MIL-SPECS are covered. A preliminary design that meets all of the design criteria is then described. It is concluded that this application is feasible and would be an extremely valuable research tool to investigate infrared properties of objects in space.			
20. DISTRIBUTION / AVAILABILITY OF ABSTRACT <input type="checkbox"/> UNCLASSIFIED/UNLIMITED <input checked="" type="checkbox"/> SAME AS RPT <input type="checkbox"/> DTIC USERS		21. ABSTRACT SECURITY CLASSIFICATION Unclassified	
22a. NAME OF RESPONSIBLE INDIVIDUAL David Knecht		22b. TELEPHONE (Include Area Code) (617) 377-3240	22c. OFFICE SYMBOL AFGL/PHK

Contents

Table of Contents

1 Overview	1
1.1 Overview	2
1.2 System design goals	2
1.3 Schottky-diode detector technology	2
1.4 Camera component design options	3
1.5 Documentation and testing	4
1.6 Proposed design	4
1.7 Conclusions and summary	5
2 Design goals for the SBS Camera project	5
2.1 System capabilities	5
2.2 Optical performance	6
2.3 Mechanical performance	6
2.4 Modularity	6
2.5 FPA and signal processing technology	6
2.6 Radiometric calibration	7
2.7 Mission performance	7
2.8 Redundancy/error recovery	7
3 Schottky diode detector technology	8
3.1 Detector operation	8
3.2 Current state-of-the-art in arrays	16
3.3 Radiometric calibration	17
3.3.1 Theoretical approach	17
3.3.2 Implementation	22
4 Camera component design issues	23
4.1 Optical design	23
4.1.1 Overview	23
4.1.2 System optical performance requirements	24
4.1.2.1 HH-G platform: mounted in cargo bay	25
4.1.2.2 SPAS platform: free flight	25
4.1.3 Optical design options	26
4.1.4 Tracking capability	28
4.1.4.1 Host platform tracking data	30
4.1.4.2 Sun trackers	31
4.1.4.3 Earth horizon trackers	32
4.1.4.4 Magnetometers	32
4.1.4.5 Star trackers	33
4.1.4.6 Gyroscopes	34
4.1.4.7 Summary of tracker options	34
4.1.4.8 Mechanical tracking implementation	34
4.1.5 Focus control	36
4.1.6 Visible wavelength tracking camera	37
4.1.7 Cryogenic cooling of optics	40
4.1.8 Radiometric calibration sources	41
4.1.9 Bandpass filters	42

Contents

4.1.10 Summary of optical system	44
4.2 Cryogenic cooling system	45
4.2.1 Cooling requirements	45
4.2.2 Liquid cryogenics	51
4.2.3 Solid cryogenics	52
4.2.4 Closed cycle mechanical coolers	55
4.2.5 Joule-Thompson cryostats	58
4.2.6 Summary	61
4.3 Signal processing	63
4.3.1 Theoretical approach	63
4.3.2 Calibration of measured signal	66
4.3.3 Physical considerations	72
4.3.4 Redundancy requirements	73
4.4 Data recording system	74
4.4.1 Overview	74
4.4.2 SBS Camera data outputs	75
4.4.2.1 Analog image data formats	77
4.4.2.2 Digital image data formats	79
4.4.3 Analog video recorders	79
4.4.4 Digital recorders	81
4.4.4.1 HDDR magnetic tape recorders	81
4.4.4.2 Digital video	82
4.4.4.3 Hybrid analog video/digital recorders	85
4.4.4.4 Mechanical disks	86
4.4.4.4.1 Writable optical disks	86
4.4.4.4.2 Magnetic disks	87
4.4.5 Redundancy requirements	88
4.4.6 Summary	89
4.5 SBS Control system	90
4.5.1 Overview	90
4.5.2 Control system tasks	90
4.5.2.1 System initialization	91
4.5.2.2 Diagnostic mode	91
4.5.2.3 Calibration mode	97
4.5.2.4 Data collection mode	98
4.5.2.5 System shutdown	99
4.5.2.6 Telemetry interface	99
4.5.3 Design requirements of control computer	99
4.5.3.1 Addressing/memory map considerations	100
4.5.3.2 Interrupt handling requirements	100
4.5.3.3 Program code and data requirements	100
4.5.3.4 Processor speed/computational capabilities	101
4.5.3.5 Processor interface to user	101
4.5.3.6 Mass storage requirements	101
4.5.3.7 Other requirements	101
4.5.3.8 Software development tools	102
4.5.4 Types of control systems	102

Contents

4.5.5 Summary	103
4.6 Host carrier restraints	103
4.6.1 Payload platform overview	103
4.6.1.2 Shuttle overview and coordinate system	104
4.6.1.3 Hitchhiker-G (HH-G)	104
4.6.1.4 Shuttle Pallet Satellite (SPAS)	105
4.6.2 Overview of payload restrictions	105
4.6.3 Mechanical interface	106
4.6.3.1 HH-G mounting	106
4.6.3.2 SPAS carrier	106
4.6.3.3 Recommended materials	107
4.6.3.4 Payload mechanical design	108
4.6.4 Thermal factors	108
4.6.4.1 Environmental heat loading	109
4.6.4.1.1 Shuttle cargo bay emission	109
4.6.4.1.2 Solar flux	110
4.6.4.1.3 Earth emission and reflection	111
4.6.4.2 Thermal modeling of payload	111
4.6.4.3 Payload temperature control methods	112
4.6.4.3.1 Surface coatings	112
4.6.4.3.2 Thermal insulation	113
4.6.4.3.3 Heat sinks	114
4.6.4.3.4 Phase change materials	114
4.6.4.3.5 Heat pipes	114
4.6.4.3.6 Louvers	114
4.6.4.3.7 Heaters	115
4.6.5 Pressure factors	115
4.6.6 Dynamic load factors	115
4.6.6.1 Acceleration load limit factors	115
4.6.6.2 Sinusoidal vibrations	116
4.6.6.3 Random vibrations	117
4.6.6.4 Acoustic noise vibrations	117
4.6.7 Electromagnetic and magnetic extremes	117
4.6.7.1 Environmental	117
4.6.7.2 Shuttle produced	118
4.6.7.3 Electrostatic concerns	119
4.6.8 Electrical power interface	119
4.6.8.1 Hitchhiker-G	119
4.6.8.2 SPAS	121
4.6.9 Platform-SBS telemetry interface	122
4.6.9.1 Hitchhiker-G	122
4.6.9.2 SPAS	124
4.6.9.3 Data storage facilities	124
4.6.9.3.1 Hitchhiker-G	125
4.6.9.3.2 SPAS	125
5 Documentation and testing	125
5.1 Payload class	125
5.2 MIL - DOD specs	127
5.2.1 Safety program: MIL-STD-1574	128

Contents

5.2.2 Reliability program: MIL-STD-1543	128
5.2.3 Electromatnetic compatiability: MIL-STD-1541	129
5.2.4 Configuration control: DOD-STD-480	129
5.3 Space qualification levels	130
6 Proposed camera design	130
6.1 Overview	131
6.2 Physical mounting of system	134
6.2.1 Layout for SPAS ESP	134
6.2.2 Layout for HH-G plate mount	134
6.3 Schottky camera dewar/electronics	134
6.3.1 Focal plane array	134
6.3.2 Dewar assembly	135
6.3.3 Detector chip timing and readout electronics	136
6.4 Optics module/visible TV camera	136
6.5 Trackable mirror and calibration system	137
6.6 Payload aspect tracking system	138
6.7 Cryogenic cooling system	138
6.8 Image compensation system	139
6.9 Data (visible and infrared) recording system	139
6.10 SBS Control system	141
6.11 Summary	142
7 Conclusions	143
References	145
Appendix A Listing of VMODEL software program	150

Accession For	
NTIS GRA&I	<input checked="" type="checkbox"/>
DTIC TAB	<input type="checkbox"/>
Unannounced	<input type="checkbox"/>
Justification	
By _____	
Distribution/ _____	
Availability Codes	
Dist	Avail and/or Special
A-1	

Contents

List of Figures

Section 3.1

- 3.1-1 Potential energy diagram of Schottky-diode detector
- 3.1-2 Schematic diagram of detector
- 3.1-3 Spectral response of Schottky-diode detectors
- 3.1-4 Schottky detector response to blackbody emission
 - (a) 200 degrees K
 - (b) 300 degrees K
 - (c) 500 degrees K
 - (d) 1000 degrees K
- 3.1-5 Usable temperature range for different spectral bandpasses
- 3.1-6 Voltage-radiance response for 160 by 244 element array
- 3.1-7 Drawing of platinum-silicide Schottky-diode detector
 - (a) physical layout
 - (b) potential wells links to physical components
- 3.1-8 Block diagram of focal plane array

Section 3.2

- 3.2-1 Characteristics of current 160 by 244 element FPAs
- 3.2-2 Performance and noise characteristics for current 160 x 244 element array

Section 4.1

- 4.1-1 Layout of single pixel on Schottky-diode FPA
- 4.1-2 Overall pixel arrangement in focal plane array
- 4.1-3 View from Space shuttle cargo bay
- 4.1-4 Cassegrain - Ritchey-Chretien reflecting telescope design
- 4.1-5 Proposed Ritchey-Chretien design for SBS Camera optics
- 4.1-6 Use of tracking mirror to control instrument FOV position
- 4.1-7 Possible mechanical implementation of tracking mirror
- 4.1-8 Focus control by moving reflective optical assembly
- 4.1-9 Spectral response of silicon CCD visible band video camera
- 4.1-10 Block diagram of visible band tracking unit
- 4.1-11 Calibration source for SBS Camera
- 4.1-12 Locations for calibration sources in SBS payload
- 4.1-13 Bandpass filter wheel in SBS optical system
- 4.1-14 Filter bands used in current SAIRS camera
- 4.1-15 Complete block diagram of proposed SBS Camera optical system

Section 4.2

- 4.2-1 Plot of emitted radiance vs temperature in SBS Camera band
- 4.2-2 Candidate solid cryogenics for SBS Camera
- 4.2-3 Sample split-Stirling cooling engine
- 4.2-4 Physical dimensions of CM-4 cooling engine
- 4.2-5 Schematic diagram of Joule-Thomson cooling system

Figures

4.2-6 Refrigeration vs temperature for argon and nitrogen used in a J-T cooling system

Section 4.3

4.3-1 Block diagram of image compensation system used in SAIRS instruments

4.3-2 Specifications of A/D module used in SAIRS (MOD-1205)

4.3-3 Drawing showing physical dimensions of double-VME bus card

4.3-4 Drawing showing dimensions of 9 slot VME-bus motherboard

Section 4.4

4.4-1 D-1 digital video tape layout

4.4-2 Drawing showing physical dimensions of Odetics DCRR-32 recorder

4.4-3 Block diagram of optical disk writing mechanism

Section 4.5

4.5-1 Modified block diagram of camera electronics with diagnostic test test points added

4.5-2 Photograph of GMX Micro-20 single board computer

4.5-3 Block diagram of GMX Micro-20 single board computer

Section 4.6

4.6-1 STS (shuttle) orbiter coordinate system

4.6-2 Diagram of HH-G plate mounting payload configuration

4.6-3 HH-G plate mounting payload envelope - side aspect

4.6-4 HH-G structural assembly of plate mounting system

4.6-5 HH-G available locations in cargo bay for payload mounting

4.6-6 Drawing of Shuttle Pallet Satellite (SPAS) platform

4.6-7 SPAS drawing showing locations of platform subsystems

4.6-8 Examples of instrumentation mounted on SPAS platform

4.6-9 SPAS platform coordinate system

4.6-10 Coordinate system of Equipment Mounting Plate (ESP)

4.6-11 Functional block diagram of SPAS platform

4.6-12 Mechanical detail of SPAS Equipment Support Plate

4.6-13 Equipment envelope for ESP mount

4.6-14 Equipment envelope for SPAS while stowed in cargo bay

4.6-15 Equipment envelope for inside face of ESP

4.6-16 Equipment envelope for inside face of ESP

4.6-17 Solar spectral irradiance curve

4.6-18 Earth emission and reflection heating of payload

4.6-19 Emittance of selected surface coatings as a function of wavelength

4.6-20 Cargo bay pressure change vs time after shuttle lift-off

4.6-21 Maximum cargo bay pressure decay rate during ascent

4.6-22 Cargo bay repressurization during reentry after vent door opens

4.6-23 Sinusoidal vibration design and test requirements (SPAS)

4.6-24 Random vibration certification levels

(a) HH-G payloads

(b) SPAS payloads

Figures

- 4.6-25 Payload acoustic level testing (cargo bay during liftoff)
 - (a) HH-G payloads
 - (b) SPAS payloads
- 4.6-26 Standard interface cabling on HH-G plate mount
- 4.6-27 Interface between shuttle power and HH-G payload
- 4.6-28 Schematic of actual payload power interface to HH-G payload
- 4.6-29 SPAS power distribution system for experiments
- 4.6-30 Pinout of J2 signal cable connecting HH-G payload to shuttle
- 4.6-31 Bi-level command interface specifications
- 4.6-32 Serial command interface electrical characteristics and timing
- 4.6-33 Additional electrical detail on serial interface characteristics
- 4.6-34 RD serial link electrical and timing specifications
- 4.6-35 SD serial link electrical and timing specifications
- 4.6-36 Electrical interface for KU-band medium data rate link
- 4.6-37 Data and clock signal timing for medium data rate link
- 4.6-38 Digital timing of high speed PCM interface
- 4.6-39 Electrical details of PCM high speed interface
- 4.6-40 Electrical characteristics of IRIG-B MET signal provided to payload
- 4.6-41 Command, timing, and interface lines provided in SPAS Data Handling Subsystem (DHS)
- 4.6-42 Electrical interface on SPAS payload for each experiment
- 4.6-43 Signal characteristics of serial interface on SPAS payload
- 4.6-44 Timing of serial interface signals on SPAS serial interface

Section 5

- 5.1-1 Comparison of program characteristics of space programs of each payload class
- 5.1-2 Items that must be included in statement of work for design and building of payloads of each class
- 5.1-3 Comparison of review items included in the statement of work for payloads of each class
- 5.1-4 Additional comparisons between space payload programs of each class
- 5.1-5 Typical design factors used in each of the payload class categories
- 5.1-6 Typical computer resource requirements for space experiments of each class
- 5.1-7 Typical construction requirements for each of the payload classes
- 5.1-8 Comparison of test requirements for payloads of each class
- 5.1-9 Typical fabrication and test requirements for components to support the first flight item of each class
- 5.1-10 Applicability of Space Division directives for each payload class
- 5.1-11 Applicability of Space Division's commander policies in management requirements for payloads of each class

Section 6.1

- 6.1-1 Component level block diagram of the SBS Camera payload
- 6.1-2 SBS Camera dewar block diagram
- 6.1-3 Cryogenic cooling system block diagram
- 6.1-4 Major optical components and axes of SBS Camera
- 6.1-5 Diagram of tracking system
- 6.1-6 Image compensator block diagram
- 6.1-7 Block diagram of SBS payload control computer components

Figures

- 6.1-8 Data recording system
- 6.1-9 Payload to host platform telemetry interface
- 6.1-10 Block diagram of payload power interface

Section 6.2

- 6.2-1 SPAS Equipment Support Plate mounting payload layout
- 6.2-2 HH-G plate mount payload layout

Section 6.3

- 6.3-1 SAIRS dewar wiring diagram
- 6.3-2 Connector pinouts used in SAIRS dewar
- 6.3-3 Internal cooled assembly of detector dewar
- 6.3-4 Mounting of cooled assembly to outer dewar unit

Section 6.4

- 6.4-1 Physical configuration of camera reflective optics module
- 6.4-2 Implementation of focus control
- 6.4-3 Visible video camera implementation

Section 6.5

- 6.5-1 Drawing of tracking mirror assembly
- 6.5-2 Extended source calibrators around tracking mirror assembly

Section 6.6

- 6.6-1 Sketch showing gyroscope and mounting to plate

Section 6.7

- 6.7-1 Gas storage mounting for cryogenic cooling system

Section 6.8

- 6.8-1 Physical dimensions of electronics mounting assembly

Section 6.9

- 6.9-1 Photograph of Ampex DCRSi recording unit
- 6.9-2 Tape cassette used in DCRSi recorder
- 6.9-3 Physical envelopes of each recorder component

Section 6.10

- 6.10-1 Functional block diagram of SBS control computer software code

1 Overview

Recent advances in platinum silicide (PtSi) focal plane arrays have made it possible to build and use very high quality infrared cameras that are sensitive in the 1.1 to 5.7 micrometer spectral region. The technology has been proven in cameras that have made ground based and airborne measurements of targets and backgrounds. This design study is intended to lead to a space-based camera utilizing the state of the art in PtSi technology. This camera would fill an important gap in the infrared community's data base and knowledge by making calibrated measurements of the shuttle, other space targets, and earth based or near earth targets. The resulting data would be extremely useful to current DoD research.

The design of a spacecraft payload usually requires several iterations before it is complete. The first pass is the initial feasibility study. This initial study determines the mission performance requirements that the payload must meet. It also examines the payload carrier restraints, which in this case are the restraints placed by the Space Transportation System (the space shuttle). In this first iteration a preliminary design is accomplished that is detailed enough to determine that all of the needs of the payload components - as well as the basic mission requirements - can be met within carrier limits such as physical size, weight, electrical loads, and thermal loads. This preliminary design is fairly detailed to ensure that all requirements are identified early on and to allow all of the scarce resources available to be allocated sensibly. At the same time, the arrangement of the subsystems is still kept very general and is subject to extensive change. After this first stage, a detailed design analysis is required. Subsystems are designed, built, and tested to see if they meet the many stringent requirements placed on space payloads. Components or designs that fail the tests are redesigned, or alternative options are used. This phase is relatively expensive and labor intensive because of the large amount of engineering effort and extensive qualification testing involved. Provisions must be made in this stage for large time delays that will be encountered as designs fail and must be reworked. The third stage in the payload design occurs after the qualification testing has been completed. At this point, construction of the actual space hardware begins. These final payloads must pass rigorous tests, of course, but these tests should be detecting flaws in manufacture instead of design. The hardware is then flown into space to accomplish the missions required.

This study provides the initial feasibility determination and preliminary design for a payload system that will contain a Schottky-diode imager. Existing platinum-silicide array camera technology will be described and a detailed analysis of the design choices involved in building a system capable of functioning on either the space shuttle or a rocket platform is presented. The primary emphasis will be on a system capable of functioning in the shuttle cargo bay (on the Hitchhiker program) as well as on the Shuttle Pallet Satellite (SPAS), a platform capable of flying free of the shuttle and then being retrieved for return to earth. The different technological problems posed by operating in a space environment will be described, and the advantages and disadvantages of several solutions to each will be shown, to illustrate the different trade-offs that can be made in the design. A preliminary design developed at SRL will be described in considerable detail. This study provides the groundwork needed for the start of the detailed design phase in this project

Section 1

described above.

This study will be divided into seven distinct parts. These seven sections are:

- 1 Overview
- 2 System design goals
- 3 Schottky-diode detector technology
- 4 Camera component design options
- 5 Documentation and testing
- 6 Proposed design
- 7 Conclusions and summary

Each of these sections is summarized below.

1.1 Overview

Section 1 provides an overview of the entire report and a summary of its contents.

1.2 System design goals

Section 2 presents proposed design goals for the new camera. First the tasks the camera will perform are briefly described, based on discussions at previous meetings with AFGL and RADC. From these requirements, optical performance criteria are derived. The mechanical design envelope that the system should be designed to is presented. Additional goals including system modularity, FPA and signal processing technology, radiometric calibration, and redundancy/error recovery are also described. Mission performance goals are derived from factors such as potential launch delays and mission time duration. These goals, in conjunction with the various limitations of technology presented in the next section, define what is possible in the design of the proposed camera and provides general guidelines towards which system goals are of primary importance. This is important information to be used in evaluating the inevitable design and construction trade-offs that will be necessary in building a real camera.

1.3 Schottky-diode detector technology

Section 3 summarizes the operation of the basic physics and technology involved in the Schottky-diode two dimensional focal plane arrays. Theoretical information collected from the published literature on the arrays is presented. The spectral response of the detector and its implications for system performance are discussed. The relationship between the detector output voltage and the radiance incident on it is derived, and the results are used to discuss the implications of the spectral distributions of signal expected from typical targets. The effects of spectral bandpass on the system performance are also presented. Noise sources are also covered. The existing and anticipated state-of-the-art available in FPAs (in terms of noise, sensitivity, etc.) is briefly described. The techniques used to make radiometric calibration of the data (i.e., the conversion of the data from pixel values to inband radiant intensities) are derived and discussed, along with a discussion of the general calibration requirements.

Section I

1.4 Camera component design options

Section 4 works through various possible solutions to the technological problems posed by a space based PtSi camera. Six major areas of concern are identified, and for each of these, several possible solutions are identified, along with a discussion of the advantages and disadvantages of each. First (section 4.1) the optical design of the system is examined. Comparisons are made between a reflective and a refractive optical design. Control over the system focus is also covered. Tracking mechanisms, to allow the camera to locate and follow targets independent of the motion of its host platform, are discussed. The questions of cooled optics (to reduce instrument background) are also raised.

Secondly (section 4.2) the cryogenic cooling system is examined. First the cryogenic cooling requirements of the camera are identified. Simple assumptions are made about the thermal mass of the components, heat generated during camera operation, and heat loss from the environment. These assumptions, when combined with the design goals presented in section 3 of this study, determine the amounts and rates of cooling required by the camera. Then the four principal methods of attaining cryogenic temperatures in this type of camera are presented: liquid cryogens, solid cryogens, mechanical cooling engines, and Joule-Thompson cryostats. The cooling capacities, mechanical and power requirements, hold times, and other advantages/disadvantages of each type of cooling option are discussed in detail.

The third part of this section (section 4.3) treats the signal processing component of the camera. The importance of real time image compensation is determined. The basic requirements of the processing electronics are set out. Then existing implementations of the image compensation circuitry (primarily in the SAIRS cameras built jointly by AFGL and RADC) will be discussed. Power and size requirements, additions needed for diagnostic interface, and important areas for redundancy are identified and discussed.

The fourth area discussed is data recording. Data handling requirements, both in total quantity as well as data rates, are presented. Data output formatting is then covered in this section. Possible analog and digital formats are presented, along with a discussion of the advantages of each approach. Both image data and system status information must be recorded during missions. The size, power, and durability limitations imposed on the recorders are briefly covered (additional detail on the environment and resources available for each of the possible camera host systems is presented in section 4.6). Then examples of commercially available recorders are shown to see what is possible using the current state of the art. Technologies discussed include analog and digital video recorders, high density digital recorders (HDDR), and digital optical disks.

Section 4.5 discusses the camera control system. First the need for an intelligent, programmable controller in the camera is established. Then performance requirements, tasks, and limitations of the system are developed. The advantages of building a custom control computer are compared to commercially available microprocessor-based systems.

Section 4.6 presents the constraints imposed by each of the possible host carriers of the camera: the Hitchhiker-G (HHG) and the Shuttle Pallett Satellite (SPAS). The

Section 1

mechanical interface required for each type of carrier is described. Environmental factors, such as temperature, pressure, dynamic flight stresses, and electromagnetic effects are described in detail using data provided by NASA. Available power amounts and types are described. Additional mechanical and thermal concerns that will be important in the payload design are covered. The telemetry and avionics interface for each of the possible carriers is also discussed.

1.5 Documentation and testing

Section 5 briefly summarizes the documentation and testing required to certify the resulting payload for space flight. First the standard types of payload classification used by DoD are described, with a summary of the testing and construction requirements imposed by each. This camera is then identified as either a Class C or Class D payload. For these classifications, the applicable MIL - DoD and NASA official specs are listed. Selected MIL specs that have an important bearing on the proposed camera are discussed in greater detail. Attention is also given to the impact of additional formal testing on the total costs and effort of the project.

1.6 Proposed design

Section 6 presents a detailed proposed design for this camera system. This design represents only one solution out of the many possible, but it represents the authors' choices of the many trade-offs, based on past experience and understanding of AFGL/RADC requirements. The proposed design is as detailed as time constraints and resources permitted.

The proposed Schottky-diode imaging system will consist of 10 distinct components:

- (1) Schottky camera dewar/electronics
- (2) Optics module/visible TV
- (3) tracking mirror/calibration system
- (4) tracking system
- (5) cryogenic cooling system
- (6) image compensation electronics
- (7) data recording system
- (8) control system
- (9) shuttle/telemetry interface
- (10) power supplies

Section 6.1 provides an overview of each component of the proposed camera system design. Section 6.2 discusses the physical mounting of the system on the plate mounts for each of the two host platforms under consideration here. Section 6.3 examines the Schottky camera dewar and associated FPA electronics. Section 6.4 presents the optical arrangement and the optional visible band video camera. Section 6.5 covers the trackable mirror and calibration system. Section 6.6 details the payload aspect tracking system. Section 6.7 discusses the cryogenic cooling design selected. Section 6.8 describes the image compensation electronics in general terms. Section 6.9 addresses the data recorder mounting and configuration. Section 6.10 discusses the control computer system characteristics.

Section 1

1.7 Conclusions and summary

The results of this study and the lessons learned are presented in a condensed form. The recommended next steps to take in the development of this camera are also presented.

2 Design goals for the SBS Camera project

Eight design goals are proposed for this project. The design goals identify the system's capabilities and also determine the limitations that the eventual system must operate within. The design proposed by SRL in section 6 of this report meets all of these goals.

2.1 System capabilities

Design and build an instrument utilizing the newest advances in Schottky-diode focal plane array technology that will make infrared measurements of the space shuttle while in orbit. The camera system will provide radiometrically calibrated spatial imagery in the 1.1 - 5.5 micrometer wavelength band. The camera will be used to investigate the infrared signature of the space shuttle, including such phenomenology as

- * shuttle fuselage signature (all viewing aspects)
- * shuttle rocket plumes
- * contamination immediately surrounding shuttle ('glow')

It will also be capable of measuring other events in space, such as satellite or rocket firings, as well as earth based targets. Some capabilities will also be added so that the camera can make measurements of point source targets, which is an important class of targets requiring investigation. Bandpass filters will be used to make spatial maps of the features of interest in different spectral regions. The camera will have a motor driven focus and be able to focus on objects ranging from a few meters distance out to tens of kilometers. Visible band imagery will be taken and recorded at the same time for documentation. The data will be processed in real time and recorded using a recording system independent of the platform. Some limited amount of data will be accessible through the real-time telemetry stream. The camera will be controlled by an onboard microprocessor-based system capable of operating the entire system, detecting failures and enabling backup systems, putting the instrument through pre-programmed operational sequences, and accepting commands from the telemetry link. Calibrated sources will be observed by the camera to verify the radiometric accuracy of the data. The system should utilize commercially available components whenever possible, to reduce the cost of the system. The system should have adequate resources to operate independently of the host platform (with the exception of power), so that the payload is non-intrusive and thus more likely to be fit into the anticipated tight schedule anticipated for space on the shuttle over the next several years.

Section 2

2.2 Optical performance

One of the primary objectives of the SBS system is to measure the shuttle infrared signature and its related phenomenology. The optical performance needed for this is driven by the physical size of the shuttle and the range from the shuttle to the camera. Thus the camera should be capable of resolving shuttle detail through the planned operating ranges. The system should also be capable of observing other space based or earth based targets.

An additional optical requirement of the system is that it must be able to track targets of interest independently of the motion of the platform on which it is flown. None of the platforms being considered for this camera has sufficient tracking stability to allow the camera to track relatively small targets at long ranges. Thus the camera must be able to control and move its field of view independently so that it can observe targets or events of interest without making any demands on the host platform. This tracking must be stable enough to prevent image smearing during the integration time of each image (1/30 second).

2.3 Mechanical performance

The SBS camera will be primarily capable of flying as either a payload in the shuttle cargo bay (Hitchhiker-G, abbreviated HH-G) or as a payload on the Shuttle Pallet Satellite (SPAS). Size, weight, power requirements, and thermal considerations will be made compatible with both sets of payload requirements (documented in section 4.6). The system will be designed and constructed to meet all applicable NASA safety requirements and testing (documented in section 5). Since the system will consist primarily of independent components mounted on a flat aluminum plate (for HHG and SPAS), the camera will also be capable of being remounted to fly as a small payload in an unmanned rocket.

2.4 Modularity

Each of the major subsystems in the camera will operate as independently as possible of each other. This includes physically separating components, separate power supplies, separate control and diagnostics. This modularity will prevent problems in one subsystem from propagating throughout the rest of the system. It will also ease repair and modification of the system if that proves necessary. Modularity will also make possible the reconfiguration of the system to meet the needs of different missions.

2.5 FPA and signal processing technology

The basic system will utilize existing technology and components whenever possible in order to hold down total costs and simplify the development and testing cycle. AFGL and RADC have already developed working PtSi cameras that utilize sophisticated signal processing technology to correct for defects and non-uniformities within the focal plane array. This basic technology should be incorporated into the proposed camera, although it is recognized that significant redesign of the actual electronics will be necessary to reduce power, add redundancy, and add control and diagnostic test points accesable by an on-board

Section 2

computer system.

2.6 Radiometric calibration

The image data output by the SBS camera system should be calibratable. This means that the maps of pixel intensity (images) output from the camera can be converted into maps of inband irradiances or radiant intensities. To do this conversion it is required that the basic relationship between the signal incident on the detector and the voltage read out of it are well understood. It is also mandatory to document all of the changes applied to the signal as it is processed by the electronics prior to recording. A complete model must be developed of the system so that the recorded signal can be correlated with the irradiance incident on the detector in a repeatable way. This will require the measurement and recording of all variable controls (such as gain corrections or background subtractions) while the data is collected. Scenes of known radiance should be observed during the mission to verify the accuracy of the calibration model. Radiometric calibratability also mandates extensive testing in the laboratory to provide initial calibration constants, and then verification during the mission to measure any drift or deviation from the pre-mission laboratory calibration. In addition to the extended source radiometric calibration, it is also desirable to characterize the MTF (modulation transfer function) of the system so that the effects of the camera on the scene (artifacts) can be removed from the data so that true scene can be analyzed. This type of calibration will make the SBS camera far more useful for research than a simple camera that only gives imagery and is required to meet the target signature characterization goals detailed previously in section 3.1.

2.7 Mission performance

The SBS Camera system is being designed to operate after being launched into space from a variety of platforms. It should be capable of handling not only the actual data mission requirements but should also not be adversely affected by the delays and additional requirements imposed by the carriers. To meet the demands of a space shuttle launch, the camera should be prepared to encounter pre-launch delays of up to 20 days in duration, and then perform missions of up to 10 days in duration. This means that the instrument must not require hands-on maintenance or preparation (such as refilling or cryogenics or optical alignment) during these time periods. For launch on an unmanned rocket platform the time requirements are far less stringent, since such a flight would be a sub-orbital one: up to 5 days pre-launch delay, and up to 3 hours of mission time. During actual missions the camera should be capable of a minimum of 2 separate data runs of a minimum of 5 hours duration. This means that the instrument should be capable of going from its 'stowed' state to an operational state twice, and the recorders or data links should be capable of handling data in sufficient quantities and rates to store 5 hours of useful data, as well as any calibrations or additional checkouts required. The system should be capable of completely stand-alone operation, requiring only power from the host. The on-board control system should be capable operating the camera without telemetry.

2.8 Redundancy/error recovery

The system will contain as much redundancy and error detection/recovery

Section 2

capability as is practical. It is important to identify all single point failures in the design of the instrument. A single point failure is a component whose failure would be serious enough to jeopardize the success of the mission. A goal of the design is to eliminate or at least minimize all single point failures in the final camera design. The instrument should be capable of identifying, diagnosing, and correcting these problems itself as much as possible. Alternate operating procedures should be developed to handle failures that do not incapacitate the system.

3 Schottky-diode Detector Technology

3.1 Detector operation

The operation, characterization, and fabrication of metal-semiconductor Schottky barrier detectors has been exhaustively described in the published literature. This section briefly summarizes some of the information available, in order to make this report complete and also to point out some of the unusual features of Schottky-barrier arrays that impact upon camera design. A reasonably complete set of published articles on the topic can be found in the references for this section, at the end of the design study.

Schottky diode detector operation is based on the potential barrier created when a metal and a semiconductor are placed in contact. This barrier can be labeled Φ_{ms} . The barrier is approximately equal to the energy difference between the work function of the metal and the electron affinity of the semiconductor. This is illustrated in the potential energy diagram shown in Figure 3.1-1. It is important to note that the value of Φ_{ms} depends on the properties of both the metal and the semiconductor. For reference, the value of Φ_{ms} for platinum on p-type silicon is 0.27 eV. Early work on this technology used palladium-silicide junctions. Substantially better long wavelength response (out to 6 micrometers) is now achieved using platinum silicides (PtSi). The SBS camera is intended to be a mid-IR camera (the MWIR region is usually assumed to lie between 2 and 6 micrometers), and so little attention will be given in this discussion to the new iridium silicide arrays, which exhibit response out to 14 micrometers (the LWIR region) but which are still in a very early experimental stage.

A schematic diagram illustrating the basic layout of the PtSi detector is shown in Figure 3.1-2. There are 5 basic layers in the detector: the AR (anti-reflection) coating, the silicon substrate, the metal silicide film, a dielectric, and an aluminum layer on the back. Before the detector is exposed to infrared radiation, the metal silicide has a reverse bias voltage applied to it, which causes the electron depletion region to expand into the silicon. There are two basic steps to the detector operation: charge integration and readout. During charge integration, infrared energy passes through the AR coating and into the detector. Radiation with photon energies less than the band gap energy of silicon pass right through the substrate. This band gap energy is approximately equal to 1.1 eV, and will be represented here by the symbol E_g . This property of the substrate determines the short wavelength cutoff of the detector system. The infrared energy that passes through the silicon substrate is then absorbed in the metal silicide. This absorption excites the atoms in the silicide and creates photocurrent components (negative charge and positive holes). The potential barrier that exists between the metal silicide and the silicon

Section 3

has already been noted. The holes with energy greater than 0.27 eV pass through the potential barrier and are injected into the silicon substrate. This photoemission of majority carriers into the silicon substrate creates a net negative charge that accumulates on the metal silicide electrode. This negative charge is read out at the end of the staring time using a network of CCD shift registers and is a measure of the infrared signal.

The detector schematic in Figure 3.1-2 shows why PtSi Schottky barrier detectors are said to be 'back-illuminated'. The infrared photons pass through the substrate before they are absorbed in the silicide film. Other typical infrared detectors do not observe scenes through their substrates.

From the simple discussion above it can be seen that the spectral energy window of a Schottky barrier detector is given by

$$\Phi_{ms} < hv < E_g \quad (3.1-1)$$

where

Φ_{ms} = metal-semiconductor Schottky barrier

hv = photon energy

E_g = substrate bandgap energy

Typical silicon bandgap energies are 1.1 eV. A considerable amount of work has gone into lowering the barrier energy of the metal-semiconductor barrier, since lower potentials extend the sensitivity of the detector into longer wavelengths. A typical value for a thin-film PtSi detector is 0.27 eV. These two energies result in an operating wavelength band of 1.2 - 5.7 micrometers. The spectral response of current platinum-silicide detector arrays, illustrating the charge generated as a function of wavelength within the band of operation, is shown in Figure 3.1-3.

The plot in Figure 3.1-3 demonstrates that the system is very efficient in the short wavelength regions around 2 micrometers, and then the quantum efficiency decreases as the wavelength increases, until it finally drops to zero at the long wavelength cutoff. Most of the radiated thermal energy from room temperature targets is at wavelengths longer than 4 micrometers, where the quantum efficiency of the diodes is lowest. This is why Schottky-diode detectors have been labeled low efficiency devices, and indeed why they were largely ignored for years, since they were relatively inefficient in collecting thermal radiation in comparison to other detector materials, like indium antimonide, which have efficiencies of 50 percent or higher in this same band. These arguments, of course, ignore several strong advantages inherent in the operation of Schottky-diode detectors. For example, because a 2 dimensional array is used, each detector integrates its signal over a relatively long period of time (in comparison to a scanning line array), offsetting some of the differences in quantum efficiency. Schottky-diode arrays are based on silicon technology, which makes them easy to work with (in comparison to other, more exotic, techniques required for other detector materials), which results in better yields, improved noise performance, and much better array response uniformity. Recent demonstrations of platinum-silicide detector based cameras have outperformed other systems based on alternative technologies, which has led to the large amount of favorable attention that has elevated this infrared detection

Section 3

approach into an accepted technology today.

At this point it is useful to derive, in a non-rigorous manner, an expression for the detector response in terms of volts per incident radiance. The selection of these units will become clear in section 3.3. This expression will allow predictions to be made about the ultimate system performance. It also allows quantitative testing of tradeoffs made in the camera design on the camera performance. This equation is also used to determine the requirements for radiometric calibration of the system. The derivation followed here is based on that presented in the 1979 paper by Capone et al¹, and additional detail can be found there, if required.

First it is assumed that the detector is mounted in a cold cavity and is observing an extended source radiating at a temperature T_s through an aperture of F-number F . The detector response is then found by multiplying the source photon flux density by the photoyield of the detector and then integrating over wavelength. Thus the final equation will have the form

$$\text{response} = E_s = \int_0^{\infty} (\text{photon flux} * Y) \quad (3.1-2)$$

where Y is the photoyield relation for PtSi detectors. Note that this approach will calculate the detector response in terms of the number of electrons per pixel generated by the incident infrared radiation. These electrons are read out and then amplified on chip before being read by the camera electronics. The final 'chip output voltage' will thus be related to the gain of the on focal plane amplifier and the gate capacitance at the chip output.

To use this approach, the source photon flux density must be quantitatively characterized. For simplicity, this derivation will assume the source is radiating as a greybody with a Plank spectral distribution of energy. Note that this assumption is sometimes false: for example, a source radiating strongly in selected molecular lines (such as a plume of heated engine exhaust) has a decidedly non-Plankian shape. Another complication that can invalidate this assumption is that a scene can consist of a number of objects radiating at different temperatures, all with spectral energy distributions of different shapes. A common example of this is a scene containing reflections of solar radiation. The source solar spectral distribution is shaped like a blackbody (except around atmospheric absorption bands), but the source is so hot that the shape is completely different from room temperature sources in the wavelength band of these detectors (1.1 - 5.5 micrometers). Because of these complications, the assumed spectral shape of the incident radiation is kept in a separate term, and this separate term is manipulated during radiometric calibration of the camera data.

Using a blackbody source, the photon flux can be written as

$$\text{photon flux} = \int_{\lambda_1}^{\lambda_2} \frac{c_3 * d\lambda}{\lambda^4 * (e^{c_1/\lambda T} - 1)} \quad \text{photons.cm}^{-2}.\text{sr}^{-1} \quad (3.1-3)$$

where

Section 3

$$\begin{aligned} \lambda_1 &= \text{short wavelength end of bandpass} \\ \lambda_2 &= \text{long wavelength end of bandpass} \\ C_2 &= \frac{hc}{k} = 14388 \\ C_3 &= 1.8837E23 \text{ } \mu\text{m}^3 \cdot \text{cm}^{-2} \cdot \text{sec}^{-1} \end{aligned}$$

The other requirement for generating this response function is quantitatively describing the photoyield of the PtSi detector. Numerous derivations of this exist in the published literature. Here the general equation for Schottky emission is simply presented:

$$\text{photoyield} = Y = \frac{C_1 * (hv - \phi_{ms})^2}{hv} \text{ electrons/photon} \quad (3.1-4)$$

where

- C1 = a constant related to the physical properties of array
- ϕ_{ms} = barrier height (discussed briefly above)
- h = Planck's constant
- ν = frequency

At the long wavelength cutoff, the photoyield = 0, and the barrier height becomes

$$\phi_{ms} = \frac{1.24}{\lambda_c} \quad (3.1-5)$$

The photoyield equation can be rewritten in terms of wavelength and for the specific case of a PtSi detector as

$$\text{photoyield} = Y(\lambda) = 1.24 * C_1 \frac{(1 - \frac{\lambda}{\lambda_c})^2}{\lambda} \quad (3.1-6)$$

in units of electrons per photon. The constant labeled C_1 is usually called the emission coefficient and provides a relative measure of the overall efficiency of the process of majority carrier emission into the silicon substrate. Increases in the value of this constant increase the responsivity of the detectors at all wavelengths. Steady progress in the fabrication of PtSi focal plane arrays has resulted in the increase of this constant from 0.05 in the early devices to as high as 0.4 in current FPAs. Two factors that have a strong influence on this constant are the thickness of the metal-silicide layer and the physical quality of the silicide-substrate junction.

Now the photoyield can be combined with the photon flux to derive an equation that will give the number of electrons per pixel generated by the incident infrared radiation. Both the geometry of the detector and the integration time introduce additional terms shown outside of the integral. This equation is

Section 3

$$E_s = \frac{A_\lambda * t_i}{4F^2} * \int_{\lambda_1}^{\lambda_2} \left[\frac{C_3 * d\lambda}{\lambda^4 * (e^{c/\lambda\tau} - 1)} * 1.24 * C_1 \frac{(1 - \frac{\lambda}{\lambda_c})^2}{\lambda} \right]$$

photon flux
photoyield
(3.1-7)

where

- A_λ = active pixel area = (pixel area) * (fill factor)
- t_i = integration time in seconds
- F = system F-number
- λ_c = Schottky cut-off wavelength (dependent on specific chip)

This equation can be reorganized into the form below

$$E_s = \frac{1.24 * C_1 * C_3 * A_\lambda * t_i}{4F^2} \int_{\lambda_1}^{\lambda_2} \frac{(1 - \frac{\lambda}{\lambda_c})^2}{\lambda^5 * (e^{c/\lambda\tau} - 1)} d\lambda \quad (3.1-8)$$

Note that the response predicted by this relation is in practice degraded by optical transmission losses and cold shield inefficiencies. This results in a reduction in the measured signal level. It also introduces a diffuse signal component with no image content. This component is removed in the image processing electronics planned for the camera system. The measurement and calibration of this degradation is analyzed in the sections of this study treating radiometric calibration (section 3.3) and signal processing (section 4.3). For now, the source radiance incident on a detector element is caused by two primary sources: the scene radiance and the instrument internal radiance (i.e., glowing optics). Each of these radiance sources generates some electrons in the detector. The total number of electrons generated is given by

$$E_{total} = (\epsilon_s N_s) \tau_{opt} + \epsilon_{opt} N_{opt} \quad (3.1-9)$$

where

τ_{opt} = transmission of the optics

ϵ_{opt} = emissivity of the optics

The final output voltage of the chip is simply the conversion of the total number of detector electrons into a voltage:

$$V = \frac{E_{total} eG}{C_g} \quad (3.1-10)$$

where

- e = electronic charge
- C_g = output gate capacitance in farads

Section 3

G = gain of the output amplifier

This final voltage is what the camera electronics actually measures from the focal plane.

These equations have been implemented in a simple BASIC computer program called VMODEL (listed in Appendix A). This program allows the spectral shape of the Schottky detector response to be combined with the Plank shape of blackbody emission to calculate the voltage (number of electrons) measured from the detector as a function of wavelength. The results of these plots for 4 scene temperatures are shown in Figure 3.1-4. The four temperatures used are 200 K (cold scene), 300 K, 500 K, and 1000 K. The chip and system parameters used to make these plots is shown in the comments at the beginning of the VMODEL listing in Appendix A. In this wavelength band, the distribution of the radiated energy from the scene undergoes large changes as the temperature is increased. This change illustrates the importance of careful selection of bandpass filters for the system. The filter bandpasses can be matched to the expected apparent temperatures of the target to be measured, and optimum bandpasses exist. It is also important to note the values of voltage plotted on the Y axes of these plots. For a cold scene (200 K), the peak system response is around 5.3 micrometers, and it measures only about volts (for a 0.1 micrometer wide band at that wavelength). A wide bandpass is needed to collect adequate signal from this scene. The 300 K scene peaks around 4.5 micrometers, but the voltage at the peak is almost .12 volts. A 1 micrometer wide filter centered around this maximum will collect about 1 volt response from the detectors, which is over a third of the way to detector saturation. This same band measuring a 500 K source would be completely saturated. Thus either narrow bandpasses or neutral density filters are required to use a Schottky-diode detector to accurately measure bright targets. A table listing the approximate maximum temperatures than can be measured using selected filter bandpasses is shown in Figure 3.1-5. Of course, as the unsaturated temperature operating range is increased with a narrow bandpass, the accuracy of the measurement (the noise equivalent temperature) increases. In addition, the quality of the imagery, while a subjective notion, is decreased in narrower bands, since the same temperature distribution results in less image contrast as the band is narrowed. Thus the wide dynamic range of Schottky-diode detectors is partially offset by the even larger changes in signal level that can be anticipated in this band as the apparent temperature of targets increases. The selection of the filter bandpasses is affected by all of these considerations. The availability of a filter wheel that allows change of system spectral bandpass during data collection eases the choices that must be made, since wideband filters can be included in the wheel for accurate measurements of low radiance targets or scenes along with narrow filters that allow measurement of brighter target features.

Now that the signal output from the detector can be modeled, it is important to examine the primary sources of noise in the signal. Four primary sources exist. First is the shot noise in the background signal itself, which is due to statistical variations in the background flux. This noise source is proportional to the square root of the number of electrons generated by the background signal. Secondly there is background transfer noise, which is noise introduced during the transfer of charge from the detector to the FPA output through the CCD registers. The primary mechanism responsible for this in the surface channel CCD readouts is fast interstate trapping noise. CCD readout noise was the dominant noise source in the

Section 3

early PtSi arrays. Recent improvements have greatly reduced this noise mechanism. The noise electrons from this source are proportional to the square root of the product of the number of CCD gates and their transfer efficiency. The third source of noise is the KTC noise picked up in the on-focal plane amplifier and output gate. This noise source is small compared to the signal shot noise and pattern noise because the focal plane is cooled to at least 77 K. It is proportional to the square root of the capacitance at the output gate. The fourth source is fixed pattern noise in the array. This pattern noise can be traced to the array manufacturing process, and is due mostly to current lithography technique limitations. This pattern noise can be greatly reduced through signal processing and is treated in section 4.3.

These Schottky-diode detector arrays exhibit a very large dynamic range, demonstrated to be on the order of 70 dB or more. This large dynamic range is due to the combination of a very low noise floor in the best detectors along with the large potential well that is created in the substrate. The potential well can hold a large number of electrons before becoming saturated. This dynamic range characteristic translates into an ability to measure very bright targets against low signal level backgrounds without detector saturation, which is a very useful feature for an infrared detector in this band, where large contrast and signal level swings are common. The detector also exhibits a built-in blooming control, that prevents saturated signals from affecting neighboring detectors that are not observing the same large signals. Small flaws in the system optics can result in effects that resemble detector blooming, however.

As with any two dimensional array of detectors, providing methods of reading data from all array elements is difficult, due both to the large numbers of detectors (39040 in a 160 x 244 PtSi array) and to the need to keep as much of the FPA sensitive to the source infrared radiation as possible. The signal readout elements are not sensitive to the infrared signal, and any space they take up on the array surface is dead space, since any signal on this part of the focal plane is lost. This lost energy may be critical if small or weak targets are being measured. Dead regions on the focal plane also introduce modulation into the image caused by small angular movements of the optics on the order of a single pixel angular size, because different pieces of the scene being viewed come in and out of view. This modulation is easily seen with a point target. When the point source is imaged onto the silicide, a bright spot is seen in the image, but when the image of the point moves onto the dead space next to the silicide, the point vanishes or is reduced greatly in intensity. This is the source of the commonly encountered 'flickering' seen in point sources on PtSi cameras. The ratio of infrared detector area to the total area of the focal plane is usually called the fill factor of the array.

The most successful solution to date to the readout problem has been the use of CCD readout registers on the focal plane. This technology has been developed jointly at RCA and RADC at Hanscom AFB, MA. The readout registers are located right next to the silicide detector elements. This approach has the advantage of using existing chip fabrication technology, since monolithic silicon chip layout is quite advanced. The primary disadvantage is the large amount of space required on the focal plane, which results in low fill factors. The current best fill factor that has been accomplished with this approach has been on the order of 40%. Other solutions to the readout problem have used hybrid focal plane structures, where two pieces are joined together to build the detector. One piece holds the silicide cells,

Section 3

while the other contains the readout mechanism. This approach has been used by Hughes on arrays of 256 x 256 and up to 256 x 400 elements. The detectors are connected to the readout bus by a wire that is bump-bonded between the detector and the bus chip. This approach reduces the fill factor problem (fills of 80% to 85% have been demonstrated), but it introduces additional concerns about the mechanical strength and durability of the bump bonds and the wires. Array fabrication is also made considerably more complicated, since many thousands of bump bonds are required for the array. A third readout mechanism has been demonstrated (in the laboratory only so far) that mounts the infrared sensitive silicides on one side of a chip and the CCD readout registers on the opposite side. This also solves the fill factor problem, but the technology is still in an early stage at the time of this writing.

Of course, fill factor is not the only item driving detector performance. The detector's basic sensitivity and the noise background are in many ways far more important, especially to an instrument designed to make calibrated radiometric measurements of targets and backgrounds. To date the RCA/RADC chips utilizing CCD readouts have demonstrated the best overall response performance of the PtSi arrays available today. Thus the discussion of detector detail below will focus on chips of that design.

One characteristic of the CCD readout devices used in the current Schottky-diode detector arrays is that they introduce a non-linear shape into the detector voltage-radiance response. For low signal levels, the CCD registers function normally, and the charge collected at the metal-silicide junctions is read out in a buried channel mode. Above a certain level of charge, however, the buried channel mode becomes saturated, and the CCD registers transition to a surface channel readout mode that has a reduced transfer efficiency. This efficiency decreases further as the signal increases, resulting in a non-linear shape imposed on the voltage that is read out of the chip as the incident flux on the focal plane increases. On current arrays, this transition occurs when the chip voltage is around 0.8 volts. A plot of the voltage measured vs incident radiance for one of the detector arrays used in the current SAIRS camera at AFGL/RADC is shown in Figure 3.1-6. Note that several sharp bends, or kinks, are present in the curve during the surface channel readout mode. Although this results in a non-linear relationship between measured signal and incident radiance, extensive work has demonstrated that the shape of this curve stays quite constant over time, and that measuring one or two single points on it allows this shape to be fit through those points, which then allows calibration of the detector output at these high signal levels.

The physical layout of a single detector is illustrated in Figure 3.1-7. The (a) part of this figure provides a block diagram showing the physical arrangement of the different elements of a single pixel. The infrared signal enters through the bottom (in the figure), passes through the silicon substrate, and encounters the metal-semiconductor boundary of silicon and platinum, where electron emission takes place. The PtSi layer is surrounded by an N-type guard ring to reduce the dark current leakage. The transfer gate and the CCD shift register can be seen on the right of the pixel. This register is not sensitive to infrared radiation and thus represents dead space on the focal plane. Part (b) of this figure is a potential diagram illustrating the readout of the signal from the detector. During the signal integration, the transfer gate labeled 'First Poly' is held high, isolating the detector

Section 3

from the CCD readout register, which is at a lower potential (voltage) than the detector. To read out the signal, the transfer gate goes low, allowing the charge to flow from the detector into the lower potential of the CCD register. The transfer gate then goes high again, allowing the detector to begin integrating charge from the scene. The signal in the CCD register is eventually clocked to the chip output.

Due to the large number of detectors and readout elements, PtSi focal plane arrays are fairly complex devices. Since silicon chip fabrication techniques can be used, however, it is comparatively easy to fabricate the arrays. A block diagram of a 64 x 128 element array is shown in Figure 3.1-8. In this example layout, there are vertical columns of detectors alternating with columns of CCD shift registers. All of the vertical columns of CCD shift registers are connected to a horizontal row of shift registers at each end. The transfer gate then controls the movement of charge from the detectors to the columns of CCDs. Consider the vertical blanking interval of a standard RS-170 video signal to be the start of the display of a frame of data. During this vertical blanking time, the charge signal accumulated in the PtSi detectors is transferred to the vertical column registers. The lines are then read out one at a time. During the horizontal blanking preceding each video line, the pixel data for that line is transferred to the serial output register. This serial output then goes to an on-chip amplifier and is then output from the chip. If the camera is to use the entire video image area for data display (512 x 240 points for non-interlaced video), individual pixels as well as entire lines have to be duplicated (section 4.3). Note that while all of this readout is taking place, the entire array of PtSi detectors are integrating signal for the next frame of data output. Thus the integration time for each pixel is equal to the frame time.

3.2 Current state-of-the-art in arrays

It is difficult to list the performance characteristics of the state-of-the-art in Schottky-diode focal plane arrays because of the rapid advances currently occurring that are improving sensitivity, reducing noise, and increasing the fill factor. It is reasonable to assume that these steady improvements will translate into a detector array for the SBS Camera that will perform better and exhibit superior sensitivity to that attained today.

The current standard in terms of pixel numbers and fill factor is the 160 x 244 element array made by RCA and RADC. The fill factors of these arrays is on the order of 39 percent of the focal plane area. A table summarizing the pertinent array characteristics is shown in Figure 3.2-1. For comparison, the chip parameters of the current 64 x 128 element arrays are also shown in this table. Arrays with larger numbers of detectors, as well as higher fill factor, have already been demonstrated, but their noise floors and sensitivity are not as good as the 160 x 244 element arrays. Active development of 512 x 512 element arrays has already begun, though these arrays are at least two years away.

A table illustrating the performance and noise characteristics obtained with a current 160 x 244 element platinum-silicide array is shown in Figure 3.2-2. These calculations were made using a computer program written at RADC (by F. Shepherd) that calculates the predicted background and scene signals, noise levels, detectivities, and quantum efficiency that can be expected given the basic array parameters. This program runs on an Apple II computer. A version of it was moved into IBM PC

Section 3

BASIC to allow it to be run on that computer as well. These numbers allow creation of a good set of baseline parameters that can be used to evaluate the capabilities of the proposed SBS Camera system.

3.3 Radiometric calibration

3.3.1 Theoretical approach

Two basic steps are involved in radiometric calibration of a camera such as the SBS. First, a quantitative relation must be established between the infrared energy incident on the detector to the signal that is read out of it. Secondly, a quantitative relationship must be determined between the detector signal output and the electrical signal recorded on the camera's mass storage device. The first step is easier to solve in the general sense, since it depends primarily on the physics of the detector and the optics. Indeed, this step has already been completed in the non-rigorous derivation of detector response presented in section 3.1. The second step is very instrument design dependent and must be solved separately for each camera. Note that the second step, while actually easier, is usually the one that is neglected and is where the biggest errors come in. It is mandatory to have a reliable 'characterization' process that effectively describes the transfer function of the entire electrical package.

For the purposes of this discussion, instrument calibrations are defined as observing scenes of known radiance with the camera. If everything about the instrument, ranging from component temperatures to electrical settings, was known to arbitrary accuracy, there would be no need to perform this type of calibration. In practice, mathematical models describing the output of real instruments tend to break down, usually either because they make simplifying assumptions that become invalid or because they do not know the state of each system component accurately enough. Thus calibrations must be done to verify the understanding of the instrument: data. When camera data is collected on a source of accurately known radiance, errors that have slipped into the instrument model can be identified and corrected for. Measuring calibration scenes with the instrument in a state as close as possible to its state when measuring data scenes of interest allows modeling of the performance of the system without necessarily understanding all of its component behavior.

When properly calibrated, the image pixel intensities from the camera will represent inband scene radiance values. The units of radiance ($\text{w.cm}^{-2}.\text{sr}^{-1}.\text{inband}$) are used to describe the energy from extended sources that completely fill the instrument field of view. In a PtSi focal plane array, each detector has its own instantaneous field-of-view (IFOV), and for the purposes of calibration, each pixel should be treated as a separate instrument. The basic detector response equation presented in section 3.1 also described the source infrared flux in terms of radiance units. Note that for the measurement of point sources, when individual pixels may be underfilled by the target of interest, this calibration treatment may have to be modified to be an irradiance calibration ($\text{w.cm}^{-2}.\text{inband}$).

The basic approach used to calibrate the SBS camera will be based on what has been called the ' R_{peak} ' approach. This approach makes a few assumptions about the behavior of both the detector and the scene radiance that greatly simplify the

Section 3

camera modeling process. These assumptions are valid over a wide range of practical measurement situations, and allow the radiometric calibration of the image data to be done easily and in a straightforward manner.

As discussed in section 3.1, each PtSi detector accumulates negative charge as infrared radiation is incident on it. This charge is directly proportional to the integrated total of the incident energy during the pixel staring time and is read out as discussed earlier through CCD shift registers. The output voltage has already been related to the incident energy in the equation that expressed the total electrons expected from the detector. This equation can be rewritten as below:

$$V_{\text{out}} = \int_0^{\infty} \left[N_{\text{sc}}(\nu) \tau_{\text{at}}(\nu) \tau_{\text{op}}(\nu) + \epsilon_{\text{op}}(\nu) \text{BB}_{\text{op}}(\nu) \right] \text{FR}(\nu) R(\nu) d\nu + V_{\text{ns}} \quad (3.3-1)$$

where

- V_{out} = detector output voltage
- $N_{\text{sc}}(\nu)$ = radiance of the scene element being observed
- $\tau_{\text{at}}(\nu)$ = path transmission from instrument window to scene
- $\tau_{\text{op}}(\nu)$ = transmission of instrument optics and window
- $\epsilon_{\text{op}}(\nu)$ = emissivity of optics
- $\text{BB}_{\text{op}}(\nu)$ = blackbody radiance at temperature of foreoptics
- $\text{FR}(\nu)$ = spectral transmission of bandpass filter
- $R(\nu)$ = detector responsivity (in units of volts/radiance)
- V_{ns} = voltage measured when scene and instrument radiance is zero

Basically this equation identifies two sources of the radiation incident on the detector: radiance from the scene (target), and radiance from internal instrument emission. This total radiance is multiplied by a response function to arrive at the voltage output from the detector. A theoretical expression for this response function has been presented and discussed already in section 3.1.

The term V_{ns} represents the noise floor of the instrument. Its magnitude can be calculated from a theoretical analysis of the noise mechanisms, or it can be measured by observing an extended source at the focal plane temperature (nominally 77 degrees K), where the net radiative energy transfer should be zero. It should be noted that this term is only partially independent of the scene radiance, since shot noise (the random variations in the background signal) is directly proportional to the magnitude of the observed signal.

Section 3

To convert the image data from voltage to radiance, the above equation must be solved for $N(\nu)$. This is not difficult to do algebraically, but in practical terms it is difficult because all of the variables are functions of wavelength. Typically the SBS camera will be operating in a fairly wide bandpass (up to several microns wide), and many of the parameters listed above are strong functions of wavelength in the 1.1 - 6 micrometer band. The heart of the 'R_{peak}' approach to calibration is to make two basic assumptions: one is about the detector^{peak} responsivity, and the other is about the scene radiance. Each of these assumptions will be described in detail.

Assumption 1: the detector response is equal to a constant times an average response plus an additive constant. Mathematically, this can be expressed as

$$R(\nu) = R_{\text{peak}} * \overline{R(\nu)} \quad (3.3-2)$$

where

R_{peak} = normalization constant

$\overline{R(\nu)}$ = average response, or shape of detector response

The average response function represents the shape of the response vs wavelength. This assumption says that the basic shape of the detector responsivity does not change, but that a normalization factor is required that can change in magnitude. It frees the calibration from having to depend on the magnitude of the detector response calculated from the theoretical equation from section 3.1. What would change in this equation? When the SBS camera is operating in a space environment, as opposed to a laboratory environment, small changes can take place that will effect the magnitude of the detector response. One example is temperature drift of the instrument, which will affect the background radiance levels seen by the detector. Temperature drifts usually introduce small changes into the behavior of the electrical circuits processing the camera signal, which then shows up in the measured signal. Even in a well designed camera this factor can change significantly at unexpected times during field operation of an instrument. Thus this first assumption allows use of the theoretically derived response curve. The normalization factor will be calculated from the calibration measurements, and will force the calibration model, in an additive fashion, to fit the real data.

Assumption 2: The scene radiance can be treated as the product of a scene radiance scale factor and a function that describes the scene radiance distribution. This is expressed as

$$N_{\text{sc}}(\nu) = N_q * \int_0^{\infty} \overline{N_{\text{sc}}(\nu)} d\nu \quad (3.3-3)$$

where

N_q = scene radiance scale factor

$\overline{N_{\text{sc}}(\nu)}$ = assumed relative scene radiance distribution

This assumption is important because over wide spectral bands in the MWIR region

Section 3

it is impossible to precisely determine the spectral distribution of the scene radiation without a supporting interferometer. Different scenes can have very different spectral energy distributions: a radiating blackbody distributes its energy over a broad wavelength band, while heated gases emit most of their energy in relatively narrow emission bands. This wavelength dependence is further complicated by the strong slope in the spectral response of PtSi detectors: a 1 volt signal from the detector in the 4 to 5 micrometer band corresponds to a much larger scene radiance than a 1 volt output in the 2 to 3 micrometer band because of the large changes in quantum efficiency (photoyield). This effect has already been illustrated in the plots shown in Figure 3.1-4. Thus an assumption must be made about the spectral distribution of the scene radiance in order to calibrate the data. Frequently scenes are dominated by emitting or reflecting greybodies, and so this assumption follows a spectral shape calculated from Plank's blackbody law. Once the shape is known, the value of the radiance scale factor above is measured from the recorded data. The importance of filter shape should also be noted in connection with this assumption. Flatter filter bandpasses with sharp edge slopes (approximating a square bandpass) are more accurate in this connection than sharply peaked bandpasses.

Applying these two assumptions to the basic equation set out in (3.3-1) yields the following equation

$$V_{out} = N_q R_{peak} \int_0^{\infty} \overline{N_{sc}(\nu)} \tau_{at}(\nu) \tau_{op}(\nu) FR(\nu) \overline{R(\nu)} d\nu + R_{peak} \int_0^{\infty} \epsilon_{op}(\nu) BB_{op}(\nu) FR(\nu) \overline{R(\nu)} d\nu + V_{ns} \quad (3.3-4)$$

Now this is solved for the scene radiance scale factor:

$$N_q = \frac{V_{out} - R_{peak} \int_0^{\infty} \epsilon_{op}(\nu) BB_{op}(\nu) FR(\nu) \overline{R(\nu)} d\nu + V_{ns}}{R_{peak} \int_0^{\infty} \overline{N_{sc}(\nu)} \tau_{at}(\nu) \tau_{op}(\nu) FR(\nu) \overline{R(\nu)} d\nu} \quad (3.3-5)$$

To make the final step to inband scene radiance, the equation set out in out in assumption 2 (3.3-3) is used.

Several of the parameters needed to use this approach can be assumed to be measured once in the laboratory and not to change greatly over time. These include the emissivity of the foreoptics, the spectral transmission of the bandpass filter(s), the transmission of the instrument optics, and the shape of the detector response. If part of the path between the scene and the detector passes through the atmosphere, its transmission can be estimated from an atmospheric model such as LOWTRAN or

Section 3

measured independently with an interferometer. In a space environment, path transmission over the spectral bands of the SBS will be very close to unity.

The actual value of the 'R_{peak}' factor is determined using sources of known radiance, or calibrators. These radiance sources are placed in front of the instrument optics. Since the scene radiance is known accurately, it is possible to solve for R_{peak}. A typical calibrator for this type of application is a heated surface with a very high emissivity. The temperature is measured, and the radiance source is considered to be a blackbody spectrum at the calibrator temperature. Note that for the shorter wavelength bands covered by PtSi arrays (1.1 - 3 micrometers), the temperature required to produce an adequate signal to noise ratio might become too high because of safety or power considerations. In this case, an alternate calibration source such as a tungsten lamp with a known spectral output can be used for these measurements. For this simple derivation of the R_{peak} solution, the calibrator will be assumed to be a radiating heated calibrator.

For a calibrator at temperature T₁, the output voltage is

$$V_{out1} = R_{peak} \int_0^{\infty} \left[N_1(\nu) \tau_{at}(\nu) \tau_{op}(\nu) + \epsilon_{op}(\nu) BB_{op}(\nu) \right] FR(\nu) \overline{R(\nu)} d\nu + V_{ns1} \quad (3.3-6)$$

For a calibrator at temperature T₂, the output voltage is

$$V_{out2} = R_{peak} \int_0^{\infty} \left[N_2(\nu) \tau_{at}(\nu) \tau_{op}(\nu) + \epsilon_{op}(\nu) BB_{op}(\nu) \right] FR(\nu) \overline{R(\nu)} d\nu + V_{ns2} \quad (3.3-7)$$

If these two equations are differenced, R_{peak} can be solved for:

$$R_{peak} = \frac{V_{out1} - V_{out2} - (V_{ns1} - V_{ns2})}{\int_0^{\infty} \left[N_1(\nu) - N_2(\nu) \right] \tau_{op}(\nu) FR(\nu) \overline{R(\nu)} d\nu} \quad (3.3-8)$$

This approach can be used for both laboratory calibrations as well as calibrations made during an actual mission.

This 'R_{peak}' approach has been used to radiometrically calibrate other infrared spatial instruments to high levels of absolute accuracy. It is attractive because it is relatively simply to use. This method is proposed as the calibration technique to be used for the SBS camera.

The second step in calibration is to understand the relationship of the recorded signal to the detector output signal. This requires an extensive understanding of the

Section 3

total camera system electronics. A detailed discussion of this problem can be found in section 4.3.

3.3.2 Implementation

To determine the practical requirements for a calibration system on the SBS Camera, it is important to consider the radiance sources required, the types of data needed, and the calibration procedures that must be followed.

It is important to allocate time and resources to carefully map out the voltage/radiance response of the detector (and the entire camera system) under controlled conditions in the laboratory before the system is deployed in space. As noted in section 3.1, PtSi arrays using CCD readouts have two distinct regions in their voltage/radiance response. From 0 to about 0.8 detector volts of output (using the current 160 x 244 detector in SAIRS as an example), the voltage is very linear with radiance incident on the focal plane. At this point the detector charge saturates the buried channel and the charge transfer switches to a surface channel readout mode. The voltage/radiance curve assumes a non-linear shape beyond this point. The shape of this curve seems to be reasonably stable for a given detector over time, and can be mapped out in considerable detail in laboratory measurements.

Due to this non-linear nature of the PtSi array voltage-radiance response, it is desirable to have several different radiance sources so that the R_{peak} factor can be calculated for different parts along the response curve. The goal of calibrating the instrument immediately before or after data collection, however, is not to completely characterize the system's response, but rather to provide a few data points that can be compared to more extensive laboratory calibrations. In addition the presence of a filter wheel means that the radiance values chosen for these calibrators must be carefully matched to the bandpasses of the filters used. It is adequate, for a field calibration, to have two radiance values in the linear region, and then only a single radiance value in the non-linear region, so that its position can be estimated. This requirement matches the practical considerations of instrument size and power consumption that limit the number of field calibrators that can be provided. As noted earlier, as the filter bandpasses go to shorter wavelengths, or as the total bandpass of a filter becomes narrower, higher temperatures are required for the radiating calibrator surface to get sufficient signal from the detector to stay above the noise levels.

The temperature stability requirements imposed on the calibration sources have a direct impact on the ultimate accuracy of the radiometric calibration. If the detector array has a noise equivalent temperature around 0.03 degrees at room temperature, then to make calibrated measurements to the full accuracy of the FPA requires radiating calibrators whose temperature can be determined to that level of accuracy. The source must also be uniform across the field of view to this level to ensure accuracy in the calibration. Note that this is an exceptionally difficult requirement, especially for calibrators that are exposed to the space environment outside the payload. Adequate thermal mass should be added to the calibrators to reduce temperature changes during the measurement as much as possible.

Finally, the derivations of focal plane radiance in this section also depend on the accurate determination of the instrument self-emission. This is especially important

Section 3

if uncooled optics are utilized, since temperature drifts will introduce changes in the background flux. The temperatures of the optical system are important not only during calibration, but also during data collection, since large drifts will invalidate earlier calibration results and require a new calibration measurement to be made.

3.4 Summary

This section has described the basic operation of Schottky-diode detector operation, and the characteristics unique to platinum silicide systems have been identified. Since one of the goals of the SBS Camera system is calibration and understanding of the measured signals, an analytical relation between the voltage output of the detector and the measured scene flux has been discussed. Performance and noise characteristics of currently available 160 x 244 element platinum-silicide arrays have been presented. Finally, preliminary requirements for calibration measurements to be made during data missions have been examined. The next section of this study examines the issues raised during camera design and implementation.

4 Camera component design issues

4.1 Optical design

4.1.1 Overview

The platinum silicide sensors consist of a 2 dimensional array of detectors arranged on a single silicon substrate. There are a number of physical characteristics of these arrays that have important implications for the optical design of the SBS system. First of all, not all of the area of each pixel on the array is sensitive to infrared radiation. This is illustrated by the diagram in Figure 4.1-1, which shows the layout of a single pixel from one of the current 160 x 244 element PtSi arrays. Over half of the total pixel area is filled by the CCD readout electronics and the detector guard rings. For this particular example, the infrared sensitive fraction of the total pixel is only 39%. Work is proceeding on advanced arrays that will increase this fill factor considerably, but the fill will never equal 100%. Thus there will always be some detector area in each pixel (referred to here as 'dead space') on which incident infrared radiation will be lost. This has important implications in choosing the spot size of each IFOV on the focal plane. Two choices exist for the final spot size: it can be made equal to the total pixel area (active area + readout electronics), or it can be made equal to the active area only. If the spot size is made equal to the active detector array, more of the incident infrared radiation is measured by the detector, but artifacts are encountered when small point source targets are measured. As the single bright (or dark) point source moves across the active sensing area, it is measured accurately, but as it moves across the dead spots in the array it disappears, leading to a flickering of the image as it moves across the array. If the spot size is made equal to the total pixel size, a point source target will not flicker as its image moves across the focal plane, but a fraction of its energy will always be lost, since it will be falling on the dead space in the array. Thus the trade-off is one of sensitivity vs an image artifact. It is important to remember that the SBS Camera is intended not only to collect imagery

Section 4.1

but also to make radiometric measurements of targets. When the image is flickering on the focal plane it is impossible in a practical sense to know what fraction of the target is on the sensitive area and what fraction is on the dead area. This makes accurate radiometric measurements of point source targets very difficult. Primarily for this reason, the final spot size of the optics should be made equal to the total pixel size. The trade-off in sensitivity is worth the gain in calibratability.

It is also important to understand the reasons why the current arrays are laid out as they are. Each pixel is a rectangle twice as long in one direction as the other. In the 160 x 244 element arrays, the pixels are twice as long in the 160 element direction as they are in the 244 element direction. This is illustrated in Figure 4.1-2. These numbers were selected because they closely match the 4:3 aspect ratio typical in video displays. An interlaced video (television) image consists of 480 visible lines (240 in each field). Each of these lines nominally contains 512 picture elements. To create a video image from the array with the correct 4:3 aspect ratio, each of the 160 horizontal lines of detectors is displayed 3 times, to arrive at a total of 480 visible lines. Each of the 244 pixels in each line is displayed twice, to arrive at 488 horizontal elements total. Thus the aspect ratio of this display is 1.31, which is very close to the standard television 1.33. The importance of maintaining the proper aspect ratio is the elimination of geometric distortion in the displayed image. When the aspect ratios are matched in this manner, a square object observed by the array will be displayed on a monitor as a square object. This improves the image quality of the current PtSi cameras such as the SAIRS, which output their data in the form of a video signal.

Since the array operates in a staring mode, there are no moving parts to worry about in the optical design (with the exception of focus control and the optical tracking system). This allows use of a relatively simple optical design and is one of the advantages inherent in a PtSi MWIR camera. This is offset somewhat by the requirement that the image quality be maintained over the fairly large area subtended by the focal plane array. The image defects for the pixels near the edge of the array away from the optical axis must be small.

Due to practical considerations (limitations of physical space) the size of the clear aperture, or entrance pupil, of the system must be limited. One consideration is the limitation of physical space available on the equipment support plate; a 40 inch aperture is not practical on a plate that measures 28 x 28 inches. Another limitation is imposed by the need to provide a trackable system: as the clear aperture is increased, the size of the system that must be tracked (either lens or mirror) increases, and its fragility also increases. These physical limitations must be balanced against the fact that, for an image of an extended object, the amount of energy collected from a small piece of the object is directly proportional to the area of the clear aperture of the system.

4.1.2 System performance requirements

The primary goal of this system is to map out the shuttle infrared signature, providing calibrated measurements of its fuselage and plume. The optical performance criteria will thus be derived from the requirements imposed by observing the shuttle from both the HH-G and the SPAS platforms. Obviously if the system is successfully flown, it will be used to measure other space based targets and

Section 4.1

possibly ground targets as well. It is likely that objects (such as satellites or rocket burns) observed at very long ranges will be another important class of targets that this system must be capable of measuring. These targets will appear as point sources to the SBS camera. To make radiometric measurements of this class of targets it is important to provide adequate frequency response in the system to see them and also to make provisions for point source calibration measurements (as opposed to observing large extended source calibrators that fill many pixels).

The requirements of having high enough spatial resolution in the camera imagery to see detail in the target must be balanced off against having such a small field of view that tracking of the camera becomes too difficult. In addition, targets must not appear so large in the camera that it takes an excessively long time to scan the entire target in several filter bands. Thus the requirements of making close in, resolved measurements make very different demands on the optical performance from those of long range targets.

Specific performance criteria must be derived for each of the two primary platforms that the SBS will be flown on: the HH-G and the SPAS.

4.1.2.1 HHG platform: mounted in cargo bay

If the SBS Camera system is flown on a Hitchhiker payload mounted in the cargo bay its ability to measure the shuttle infrared signature would be extremely limited. Figure 4.1-3 shows the view from the front of the cargo bay looking aft. The round canisters mounted in the bay in this photo are Get-Away Special payloads. An Equipment Support Plate carrying the SBS system would be mounted approximately in these types of positions. The camera would be able to look around the interior of the cargo bay, which is not a very useful set of data in relation to the shuttle's signature. If the camera was mounted in a forward position, there is some chance it could look aft and observe the vertical stabilizer and parts of the plumes of the engines when firing. In order to be able to look around the cargo bay, the SBS would need to be able to change its focus from about 1 meter to 30 meters distance (30 meters is the approximate distance from the front of the cargo bay to the vertical stabilizer). The camera would be able to observe objects in the bay, and could also see part of the vertical stabilizer of the shuttle if mounted in the maximum forward position.

In addition to mapping the shuttle signature, the SBS Camera may be tasked to measure other space based or earth based targets. This could be accomplished while deployed in the cargo bay. The SBS Camera would have to look out of the bay, and depend upon the maneuvering of the shuttle to move targets within its trackable field of view. Since the shuttle normally flies inverted, with the earth visible over the top of the shuttle, earth targets could also be easily observed in the HH-G configuration. Thus a HH-G deployment of the SBS Camera would not allow useful measurements of the shuttle itself, but could be used to measure alternative targets also in orbit, other experiments released from the shuttle cargo bay, or earth based targets.

4.1.2.2 SPAS platform: free flight

The SPAS platform is capable of free flight independent of the shuttle (once it is

Section 4.1

removed from the cargo bay by the shuttle robot arm) and and fly out to distances of 40 kilometers. From this vantage point the SBS camera could observe the external shuttle surface from all aspects, if desired. The optical performance needed for this is driven by the physical size of the shuttle and the range from the shuttle to the camera. The shuttle length is 37 meters, and its wingspan is 24 meters. In meetings with AFGL and RADC representatives, the minimum and maximum operating ranges expected with the SPAS platform are approximately 100 meters and 10000 meters. At 100 meters range a 0.5 mrad instantaneous field-of-view (IFOV) subtends a 5 cm x 5 cm area on the shuttle, which means that fairly high spatial resolution imagery can be collected. The entire shuttle is 740 pixels long at this range, or about 3 fields-of-view, which makes it reasonably easy to scan the entire ship. The wingspan is 480 pixels long, which is also about 3 fields-of-view (in the vertical direction). At the long range position (10 km), each 0.5 mrad pixel is 2.5 x 2.5 meters. The entire shuttle is about 18.5 pixels long and its wingspan is 12 pixels long. Thus a recognizable outline of the entire shuttle can still be seen at this range, and larger phenomena (such as a glow, or long plumes) can also be comfortably fit within a single instrument field-of-view.

Thus deployment on the SPAS platform is the only realistic way in which the shuttle signature can be mapped in detail. Other targets, either in orbit or on earth, can also be mapped from the SPAS platform in a manner similar to that from the cargo bay. Since there is no dimension information available on other possible targets, it is difficult to plan the optical performance required to see them. It is clear, however, that the shuttle dimensions represent an upper bound on the possible size of space based targets, since it is larger than most payloads currently put into orbit. If the target views earth from a nominal orbit altitude of 100 miles, each pixel will subtend an area of 0.05 x 0.05 miles, or 265 x 265 feet, at the earth's surface, which is fairly low resolution (near the size of a football field). Providing adequate resolution to measure shuttle-sized targets at the earth's surface, however, would require about a factor of 10 reduction in the IFOV size, which would reduce the total field of view to a point where target tracking would become difficult and platform stability would become a difficult issue.

Thus from the above discussion and the detector characteristics the following set of optical parameters can be specified for the SBS Camera system: approximately 0.5 x 0.5 mrad IFOV, and a total field of view in the area of 87 x 87 mrad (5 x 5 degrees). The actual numbers will be more rectangular due to the pixel shape on the focal plane and the uneven number horizontal rows vs. vertical columns of detectors. The system focus should be adjustable from a few meters distance to infinity. The system F number should be in the range of 2 or 3, since the cold shielding aperture stop will probably in the range of $f/2$. The system should be capable of operating over the full wavelength band of the focal plane array, which is 1.1 to 5.7 micrometers. Platform stability requirements imposed are derived separately in the discussion in section 4.1.4.

4.1.3 Optical design options

Having identified all of the criteria relevant to selecting and specifying an optical design for the SBS camera, it is now important to briefly examine the strengths and weaknesses of the different optical designs that can be selected. One basic issue involves the selection of reflective or refractive optics. A reflective

Section 4.1

design uses mirrors to do all the optical tasks, while a refractive design uses changes in the refractive index of solid materials (lenses) to fulfil optical requirements. For space applications, reflective designs are inherently superior to refractive designs for infrared systems. Coated mirrors are physically more robust than lens optical elements, particularly in the infrared, where many optical materials (such as germanium) are brittle. This is an important consideration on a satellite platform, which is subjected to a considerable amount of physical stress during liftoff, and is also exposed to stresses while on station caused by temperature extremes. Reflective designs also have advantages in simplicity of design and good off-axis signal rejection. They have no chromatic aberration, which is an important advantage in the particular wavelength band under consideration for the SBS Camera (1.1 - 6 micrometers), where finding suitable refractive materials with constant indices of refraction over this wide range is very difficult. This advantage becomes even more important if a visible wavelength camera is also observing the scene, because then the chromatic aberration must be negligible from 5.7 down to 0.4 micrometers. The curvature required in the mirror surface is much less than that required in a refracting lens, which allows the reflectors to be built with a much smaller focal ratio than an equivalent lens system. This translates into a more compact optical system, which is an important advantage for the SBS Camera, which must be contained within a very limited physical envelope. Reflective designs are constrained to a relatively small field of view, but the FOV under consideration for the SBS Camera, derived from the mission and performance requirements, is small enough to fit within these constraints. For these reasons, only reflective type optical designs will be considered in detail for the SBS Camera.

The simplest type of reflecting design is the astronomical telescope, or the Newtonian telescope. In this approach a concave primary mirror forms an image that is reflected off to the side by a flat secondary mirror. This simple approach is very limited in terms of total angular field, off-axis rejection (baffling is very difficult), and focus design. A more practical design for an SBS Camera type of imager is the Cassegrain reflecting telescope, illustrated in Figure 4.1-4. This design has a primary concave mirror and a secondary convex mirror. Its advantages include a compact size and the location of the image straight along the optical axis. Off-axis signal rejection is a problem, but baffling can be added in (as shown in Figure 4.1-4) to block stray reflections off the mounting tube. A more significant problem is that the coma present in the image increases very rapidly as the distance from the optical axis increases, which limits a Cassegrain design to a very small usable field of view. This coma problem is solved using the modification to the mirrors proposed by G Ritchey and H. Chretien. They modified the curvature of the two mirrors by introducing a slight flattening around the edges of both the primary and the secondary, which changes their shapes from paraboloids to hyperboloids. This makes the focal length of all rays equal and removes the coma restriction. Usable fields of view of several degrees can be attained using the Ritchey-Chretien reflecting design. The system is still compact and all reflective.

The following discussion is not a detailed optical design for the SBS Camera. It is instead intended to demonstrate that the optical performance requirements, derived from the missions intended for the system, can be attained in a physical package that can be fit into the physical limitations of the SBS Camera payload. It also represents only one of a number of possible solutions to the optical design problem. This general optical solution is incorporated into the proposed design described in

Section 4.1

section 6 of this study.

The diameter of the primary mirror in the Ritchey-Chretien system represents the entrance aperture of the system. The effective clear aperture is reduced by the obscuration created by the secondary mirror, which is typically on the order of 30 percent. This diameter determines the diffraction limit of the optical system. Its minimum value must be great enough so that the optical performance required (0.5 mrad IFOV) is above the diffraction limit. This places a lower limit on the mirror diameter of around 2 centimeters. To obtain adequate light collection, the actual diameter will be considerably larger than this, so this limit will not adversely affect the design. An optical unit with a focal length of around 8 inches and an F number of 2.5 can be obtained for an entrance aperture of 3.5 inches diameter. This focal length provides adequate room to locate the detector dewar behind the Ritchey-Chretien mirror assembly. The F number is fast enough to collect a fair amount of signal and thus produce reasonable images for the target signals and detector responsivity expected (discussed under system performance predictions in section 2). A 3.5 inch entrance aperture would result in a tube containing the mirrors that would be around 4 inches inner diameter and about 5 inches long. This leaves room for anti-reflection baffling both on the tube and around the two mirrors, which is essential for off-axis signal rejection. A sketch of this proposed optical unit is shown in Figure 4.1.5. The control over this type of system focus is discussed in section 4.1.5, while the target tracking systems compatible with these specifications are discussed in section 4.1.4.

This optical system can be built as a one-of-a-kind optical unit specific to the SBS Camera only, or an off-the-shelf commercial optical system could be purchased and mounted into the camera. For example, a reflective system manufactured by Nye Optical Co. of Spring Valley, CA, is reported in the Infrared Handbook (p. 9-40) with optical characteristics close to the performance requirements described above. Other manufacturers manufacture a variety of reflective (and refractive systems) that meet the specifications, and could in theory be purchased off-the-shelf. A certain amount of testing would be required to certify that the system could meet the vibration and acceleration loads imposed by the shuttle (section 4.6). Design and construction of a custom optical unit would probably involve less effort over the long run, however, since the unit could be designed to the physical vibration specifications from the start.

4.1.4 Tracking capability

An additional optical requirement of the system is that it must be able to track targets of interest independently of the motion of the platform on which it is flown. None of the three platforms being considered for this camera has sufficient tracking stability to allow the camera to track relatively small targets at long ranges. Thus the camera must be able to control and move its field of view independently so that it can observe targets or events of interest without making any demands on the host platform positioning hardware for anything more than coarse aspect corrections (on the order of several degrees along any axis). There are two components to a tracking system to correct for host platform motion. First, there must be a system that can read out the platform angular aspect position to the level of accuracy required. The angular values must be monitored, and when a deviation is observed in the data, the amount of compensating motion required to cancel out the angular motion must be

Section 4.1

computed. Then the camera tracking system must move the instrument field of view by this amount to cancel the apparent motion. Both of these components require complex solutions.

In general the SBS Camera system will have two distinct types of pointing accuracy requirements. First is an absolute pointing accuracy that will allow the camera to acquire targets and track them even during motion of the host platform. This type of independent tracking by the SBS Camera is required for the initial target acquisition process, and will be needed to maintain track in its relatively small field of view without making excessive demands on the host platform for aspect angle corrections. The second type of tracking needed is motion to counteract jitter, or small motions, in the platform to keep the image stable enough to prevent smearing. Each of these requirements is discussed in more detail below.

The requirements of absolute pointing accuracy can be determined by considering the types of motion anticipated from the host platform. If the platform moves 1 degree along any axis within 1 second, this translates into 0.58 mrad of motion during a single frame integration time. This rate of motion is expected for the SPAS platform, whose angular aspect is controlled by bursts of cold gas from gas bottles. These bursts cause a jerking motion in the aspect of the platform, and each jerk is on the order of one or two degrees minimum over a few seconds of time. The shuttle itself uses a number of small jets to control orbiter access during an orbit, so the problem is not as severe for the case of the HH-G payload. Since all shuttle orbits are low-earth orbits, however, residual torques must be expected from the attitude control systems of either host system, and neither system has been designed to provide the level of tracking stability indicated above. Thus pointing information of the camera reference plane must be acquired in real time of sufficient accuracy to allow the camera tracking system to balance out the overall platform motion, within certain limits.

The question of platform angular jitter makes considerably harder demands on the tracking system. The angular slew of the tracked target must be kept below a maximum acceptable level during data collection. This requirement is imposed by the mode of operation of the Schottky-diode detector arrays. These arrays are integrating devices, which means each pixel is collecting scene information for a period of time determined by the frame rate. In current devices, this is a period of time equal to 1/30 second (0.033 sec). If scene elements move significantly during this integration time, the image will be blurred and streaked and have other motion artifacts. Such artifacts complicate radiometric calibration of the measured data, because the target energy is spread out as a complex function of time over several pixels while all are being integrated. With an IFOV of 0.5 milliradian, the tracking platform must maintain stability to within one-half of this angular size during the integration to prevent degradation of image data. This translates into 0.25 mrad stability over 33 milliseconds, which is a fairly high degree of stability. Note that, since this is a vibration type of noise, with an average value near zero, measurement is required of the magnitude of the platform motion at this accuracy, but not of the platform aspect angles. The tracking system must then be accurate enough to provide the required compensating motion. A way is also needed to inform the system when the camera is trying to move the field of view, in which case the tracking system might try to compensate out desired motions, which would lead to poor tracking performance. Thus the jitter requirement above is a lower limit on

Section 4.1

performance; an upper threshold must also be placed on the system (when the average value of the motion is not equal to zero), beyond which it will not try to correct for motion. The absolute angle pointing accuracy should not be a difficult requirement to attain in practice. Providing adequate guaranteed stability to prevent image jitter is considerably harder. A choice might be made in the final design that this added level of protection is not worth the additional effort, and some image smearing might be accepted instead.

In the following sections, the possible sources of platform (and camera) aspect information are considered first. Then a possible implementation of this tracking system is examined in detail.

There are two potential sources of payload aspect angle information: aspect data calculated by the host platform (the shuttle or the SPAS), or data measured by an independent sensor built into the SBS Camera payload. Note that depending on the host platform calculated data would increase the dependence of the payload on the host platform beyond that specified in section 2.1. The accuracy requirements of this aspect angle position must be around 1 arc-minute to correspond to 0.25 mrad pointing accuracy.

4.1.4.1 Host platform tracking data

When the SBS Camera system is flown on the HH-G host platform, shuttle calculated orbit position and aspect data is available to the payload through the asynchronous uplink telemetry services provided. The physical details of this data interface are covered in more detail in section 4.6.9. This service allows interrogation of the orbiter state/vector attitude relative to a fixed reference point (the fixed point used is Greenwich true of date Cartesian or Aries mean of 1950). In addition, data giving the orbiter attitude rates about each of its axes is also available. The angles of the SBS system as mounted in the cargo bay can be added to this information to determine the camera pointing aspect. One significant disadvantage to depending on this information is that time lags can be introduced (by the communication overhead between the payload and host) of up to 5 seconds duration. For a slowly moving target, this is not a significant time delay, and could be tolerated, but it could introduce problems for more rapidly moving targets, or during the initial target acquisition phase. Unformatted versions of the raw shuttle positioning and aspect data are available over a second data link at a rate of approximately once per second. This data would require additional processing in the SBS control computer to convert it into a usable form, but the time delay is greatly reduced. The formats and types of this data are described in section 4.6.9. In general, this source of aspect information would be adequate for deployments of the SBS system on the HH-G platform, and no additional tracker would be required.

When the SBS Camera is deployed on the SPAS host platform, positioning and attitude information of the SPAS is not available to the platform in real time. Thus the SBS payload cannot use this service for tracking the shuttle or other targets (the only information available is mission elapsed time data). This deficiency is important, because tracking considerations will be the most critical on the SPAS platform, which potentially will have more movement inherent in it than the shuttle, and target acquisition and tracking will be correspondingly more difficult. A limited bandwidth of telemetry is available, and provisions could be made to access

Section 4.1

positioning data through some interface with the mission controllers, but this would use up the majority of telemetry bandwidth that can be expected, and this link must be kept open for normal ground control interface commands to the payload. Thus some provision must be made in the SBS Camera design for an independent aspect tracking system to be used for SPAS deployments of the SBS Camera. Four possible technologies for measuring aspect information in orbit are discussed in the following sections.

4.1.4.2 Sun trackers

Aspect tracking systems using the sun as a source are the most commonly used tracking system on satellites. The angular radius of the sun is nearly orbit independent (0.267 degrees) and is used as an approximate point source in many sun sensors. Because the sun is so bright, the sensor design is simplified. There are two primary types of sun trackers. First are the sun presence sensors, which are systems that indicate the presence of the sun in the field of view of the instrument. This type of sensor is used to protect sensitive cameras from signal saturation and overload, as well as overheating. They provide a constant signal when the sun is in the field of view which, ideally, is a step function that signals, via a logic state, the presence or absence of the sun. Current Schottky-diode focal plane arrays are fairly robust, and brief direct solar illumination should not damage them. However, depending upon the optical design, extended solar illumination focused on a small part of the focal plane will certainly cause damage. Thus a sun presence detector would be a useful safeguard on the SBS Camera that would allow protective action (such as replacement of a cover over the optics) to be taken to prevent this damage. A sun presence sensor does not provide angular position information, however.

The second type of sun tracker provides a signal that measures the angle between a reference plane and the vector to the sun. A variety of analog and digital schemes are used to do this. Analog detectors generally limit their field of view (using aperture stops) to a conical shape, and then the amount of solar energy measured, which is the photocurrent from the detector, varies as a function of the cosine of the angle from the system reference plane. Bars or masks can be used to shadow part of one or more solar cells to arrive at a similar effect. Digital sun trackers usually pass the sunlight through a slit and onto a series of detectors arranged to provide a greyscale readout of the position of the illumination through the slit. The greyscale pattern is etched onto a reticle placed over the solar detectors. The output of these sensors provides a digitally coded version of the sun angle to the reference plane. All of these types of sensors can be extended to two-axis readouts by having a separate system along each axis. Note that, because of the relatively large angular size of the sun and the assumption made that it is a point source, accuracies using these methods are usually limited to about a tenth of a degree of angular resolution. Digital sun position sensors have been developed that use multiple reticle patterns (on the same slit) to allow interpolation that improves the accuracy down to one arc-second of resolution. For example, a multiple reticle system built by the Adcole Corporation was employed on the Solar Maximum Mission payload. The angular measures output by these sensors are combined with the known position of the sun (stored as a table of coordinates vs time in a small memory bank) to allow computation of the absolute angular position of the reference plane of the detection system.

Section 4.1

Sun trackers are the simplest systems of the trackers discussed here because they can rely on a single very bright object for positioning information. Their other advantages include small mass, simple optics, and low power consumption. They work best for earth or near earth orbits, where the sun is relatively bright and at a constant range. Note that they are useless when the platform is in the earth's shadow, which for an east-west near-earth orbit from Cape Kennedy (29 degrees north latitude) is approximately half the time. Solar illumination can be made more constant for near-earth orbits (characteristic of the space shuttle) only over certain orientations of polar orbits from Vandenburg AFB in California. It is this limitation that severely restricts the usefulness of sun trackers for aspect information for the SBS Camera system.

4.1.4.3 Earth horizon trackers

Earth horizon sensors are also commonly used for aspect information on near-earth satellites. Because of the large size of the earth, which can fill up to 40 percent of the sky, the horizon is a convenient reference to use. The earth horizon is most definite in the strongly absorbing atmospheric carbon dioxide bands around 15 micrometers wavelength, and thus many horizon sensors use a narrow infrared band centered on this feature. This band has the added advantage of having a relatively constant signal over both day and night, and is less susceptible to spurious reflections of sunlight. Most horizon sensors employ some method of scanning the sky over the sensor with a relatively small field of view detector since wide FOV sensors (like the solar position sensors described in the previous section) cannot accurately determine the position of the large and dim earth. The times between acquisition of signal (when the sensor scans from space onto the earth) and loss of signal (scanning from the earth back onto space) are compared with the earth's width and a reference signal (midscan) that has the largest time delay between acquisition and loss. The midscan position represents a scan across the middle of the earth. This information is combined with the known earth position to derive angular aspect information for the satellite.

Horizon sensors typically have angular resolution only down to about a tenth of a degree. This is because the atmosphere causes a blurry, rather than a sharply distinct edge signal, at the horizon. Most earth horizon sensors find use as an inexpensive error signal input for gross attitude control systems on earth resources, communications, or weather satellites. The relatively poor angular resolution of these systems does not improve significantly over the positioning information already available on the host platforms for the SBS, and thus earth horizon sensors will not be considered further in this study.

4.1.4.4 Magnetometers

Magnetometers measure both the direction and magnitude of the earth's local magnetic field and derive platform aspect information from this data. The magnetic field can be measured using induction in a wound coil or solenoid. Several coil schemes are currently employed to attain vector direction and magnitude information. More elaborate magnetometers employ devices that measure the magnetic field using quantum effects (such as nuclear magnetic resonance), but these systems are far too large to be considered for use on a payload such as the SBS Camera. There are several general advantages to the use of magnetometers for

Section 4.1

trackers: they are physically small, lightweight, consume very little electrical power, and generally have no moving parts. They are not extremely accurate, simply because the magnetic field around the earth is not known to the accuracy required, and local fluctuations from the standard models can introduce significant errors into the aspect determination. Presently available magnetometers are limited to about several arc-minutes of pointing accuracy. Systems with this level of accuracy weigh about 1.3 kilograms and consume about 1 watt of 12 VDC. The physical size is around 700 cubic centimeters for the magnetic sensor and 1200 cubic centimeters for the electronics. Care must be taken in the placing of these sensors in the payload to avoid stray magnetic effects from the electronics in the payload.

4.1.4.5 Star trackers

Star trackers measure the positions of stars and compare their angular positions with the known coordinates of the star stored in a star catalog. Star trackers are generally the most accurate type of tracking systems available, with accuracies down to a single arc-second attained in existing designs. Three general types of star trackers are in use. First are star scanners, which use the motion of the spacecraft to provide the searching function. Note that since the host platforms anticipated for the SBS payload will not be rotating in a regular manner, this type of tracker is not suitable for use in the SBS Camera. The second type of star tracker is a gimbale system, which has a mechanical system that can search out and track selected stars. The final class of star trackers are fixed head units, which use electronic searching and tracking through a large detector or an extended array of detectors. All of these systems determine the angles of their reference plane to a known star, whose celestial coordinates are stored in a star catalog. The angles of the platform are determined from this information.

A gimbale star tracker has a detector with a very small optical field of view (typically less than one degree). It has a much larger effective field of view gained through motion of the field of view on the gimbal mount; systems have been used on payloads with half-cone angles as large as 43 degrees. The basic idea is to determine the position of a star with respect to a null point (usually in the center) of the optical FOV. The star's position is then read out from the gimbal angles. In some designs small scanning devices are combined with slits over the detector to create a circular motion of the star on the FOV. Feedback mechanisms are used to reduce the radius of the star motion, which provides better automatic tracking capabilities. Once a star is acquired, it is identified from the stored star catalog. This system requires that at least the coarse coordinates of the platform aspect be known, so prevent the star catalog from growing too large. Gimbale star systems usually have a good accuracy over a large effective field of view, but the primary disadvantage is that the gimbal assembly is usually large and heavy.

Fixed head star trackers do not use a moving mechanical assembly to scan and acquire stars. Instead they employ an extended array of detectors, such as a CCD array, or a vidicon system. The detector array is read out, and the pattern of charge corresponds to a star pattern that is then fed into a microprocessor system. The microprocessor compares the pattern to a star pattern stored in a star catalog. In some designs, the detector array FOV is scanned electronically for a bright star first by systematically reading out the elements and only accepting a signal above a pre-set threshold that corresponds to the bright star. When the bright star is acquired,

Section 4.1

the position of the surrounding star pattern is determined. Fixed head star trackers are smaller than gimballed units, and generally do not use any moving parts. They tend to cover a smaller total field of view, however, which increases their susceptibility to tracking errors and mistracks.

Star trackers generally exhibit a high level of accuracy, exceeding the requirements of the SBS Camera tracking, but are complex and sensitive to stray light and tracking errors (picking up the wrong star, for example). Sun shades are an important part of any star tracker's design, because the low luminance levels of typical stars can be masked or overwhelmed by stray light entering the system. Even the best star trackers are usually not usable within 30 degrees of the sun.

4.1.4.6 Gyroscopes

Gyroscopes have seen considerable use to determine aspect position of payloads in space. A basic gyroscope uses a rapidly spinning mass to sense changes in the inertial orientation of its spin axis. Rate-gyros and rate-integrating gyros are commonly used to determine payload orientations. Rate gyros simply measure the rate of change of the platform angular position, while rate integrating gyros carry the measurement a step further by directly measuring the angular change. Rate integrating gyros usually mount their spinning mass in a low friction liquid, where the spin axis is supported by either gas or ball bearings. Accuracies down to an arc-minute can be obtained with these devices, and typical power consumptions are in the range of 15 watts. The system weight is around 1 kg, and the size is small (around 6 cm diameter, 11 - 28 cm length). A rate-integrating gyroscope would offer the required aspect tracking accuracy for the SBS Camera in a package that could fit in the system. These types of gyroscopes are already commonly used in space applications, and so space capable systems are not hard to locate. For example, Northrop makes a line of both types of gyroscopes that are small and would suit the needs of the SBS Camera.

4.1.4.7 Summary of aspect angle tracking options

Several schemes for determining the camera aspect angles have been described above. Three systems have the basic angular accuracy required for tracking: a sun tracker, a star tracker, and a rate-integrating gyroscope. Sun trackers are limited to use only part of the time, and on that basis are excluded from consideration, although they may be completely adequate for certain mission configurations. Thus either a star-tracking system or a gyroscope based system could be used on the SBS for basic angular tracking data.

4.1.4.8 Mechanical options to implement tracking motion

Once the angular drift rates are measured and known, provision must be made in the SBS camera design to move the field of view of the camera in a direction opposed to the platform drift, so that the two motions cancel and the camera FOV is allowed to stare at a fixed point in space. All solutions involve moving some part of the camera optical system. Moving the reflective optics assembly on a gimbal is not attractive because of the complications added to the optical system. Additional optical elements would be needed to relay the image from the gimballed portion to the fixed dewar. Moving the entire system (optics, visible TV tracker, and dewar) is

Section 4.1

not attractive because of its large total mass, which will be on the order of 3 to 5 kilograms. The required mechanical stability would be difficult to attain, and the positioning control devices would be complex and thus prone to failure.

One relatively simple solution is to fix the entire optical system to the mounting plate and add a movable flat mirror in front of the entrance aperture. This mirror would nominally reflect the optical axis from parallel to the mounting plate to 90 degrees away, allowing secure mounting of the optical system. This arrangement is illustrated in Figure 4.1-6. If mechanical control over the angle of the mirror to the fixed optical axis was added, the mirror could move the instrument field of view and counteract the platform motion. A mechanical arrangement that allows the mirror to move in three dimensions about a fixed pivot point is shown in Figure 4.1-7. Stepper motor control is provided over three points out near the mirror of the edge. A fixed pivot point is provided in the center. The size of the mirror, as well as the design of the pivot points, determines the tracking limits of the system. Motion can be provided at the pivot points using precise stepper motors. Sample calculations have shown that providing a trackable field of view of 10 degrees in any direction from the 90 degree normal plane of the mounting plate should be feasible, and refining this design could potentially provide tracking of the field of view up to the obscuration limits (i.e., when the field of view runs into the SBS payload components mounted on the plate around it).

While designing this mirror system is possible, it does pose some demanding requirements on fabrication accuracy and stiffness. This can be shown through some simple calculations. Using a circular field of view that is 3.5 inches in diameter (see earlier discussion in section 4.1.3), the mirror's must be 5 x 5 inches just to reflect the entire field of view up at a 90 degree angle. The mirror does not need to be square, due to the projected shape of the field of view, but for simplicity a square mirror will be assumed in these calculations. To deflect the optical axis by 174.533 milliradians (10 degrees), while maintaining accuracy on the order of 0.25 mrad, requires having a resolution of around 1/700 of the total mirror motion. The length of a mirror required to deflect the FOV 10 degrees is 6.1 inches, so we will use a nominal mirror length of 6.5 inches total. If the mirror is fixed in its center, the edges must travel around .57 inches to move the FOV 10 degrees. To maintain 0.25 mrad accuracy, the mirror motion must be accurate to within 1 mil (one thousandth of an inch). The total jitter in the mirror must also be less than this number. Thus the stiffness and accuracy requirements imposed on the tracking mirror are rather demanding, but not impossible. The mirror would need to be fabricated from a very stiff material (such as beryllium) to prevent flexing and the introduction of image distortion into the collected imagery.

Another alternate solution to this problem is the addition of gyroscopic stabilization directly in the mirror mount design. British Aerospace, for example, manufactures a mirror mount that incorporates two gyroscopes that hold a mirror in a stable position and compensate for hand-held motion in the optical system being stabilized. Such a system could be adapted to the SBS requirements, and this type of stabilization might correct the jitter problem.

This amount of tracking capability gives the SBS Camera a considerable ability to follow a target independent of the platform motion. For a target at 100 meters distance, 10 degrees of tracking about the center of the field of view allows motion

Section 4.1

of 16.45 meters in any direction. This allows the camera to scan back and forth across a target without any motion required of the host platform. At a range of 10 kilometers, this angular motion allows tracking up to 1.64 kilometers in any direction, which again allows the camera to follow a moving target, or to acquire a target that is not located in the proper position. If the host platform (the SPAS) can position itself within a few degrees of the aspect angles required for target measurements (coarse positioning), the tracking mirror allows a comfortable tracking margin that can both correct for errors in the host platform positioning as well as follow the target through relative motion without losing track.

This tracking mechanism thus requires that angular position of the instrument reference plane be first determined, probably by direct measurement using either a star tracker or a gyroscope. The angular information is then compared to the angular position of the target, which is either programmed into the system or is received from the ground controller operating the camera. The difference in angles is computed, and then these differences are translated into the motion required of the tracking mirror. Commands are then issued to the stepping motors controlling the mirror positioning pivots to move the mirror to the required new position. Position information on the mirror is continually read out so that the relation between the required instrument field of view angles to the target and the actual aspect angles can be recomputed. Motion continues until the error (the difference between these two numbers) is small enough to ensure that the target can be seen by the focal plane array. This computing power would likely be provided by the SBS control computer (detailed in section 4.5).

Use of a tracking mirror to provide stability to the instrument field of view makes significant contributions to the capabilities of the SBS camera. A movable mirror is a relatively simple way to introducing tracking capability. It also allows the instrument to observe calibration sources easily, as will be described in section 4.1.8.

4.1.5 Focus control

An important feature required for the SBS Camera is a real-time control over the system focus. The system must be capable of making close in (distances of a few feet) as well as long range measurements of targets and backgrounds. Thus control must be placed over the optical system focus to allow good performance over this span of ranges. Focus changes may also be mandated when bandpass filters are changed. Different filters will use different substrate materials optimized for their wavelength band that have different indices of refraction, which will cause system focus to change when filters are changed. In the wavelength bands of the SBS Camera (1.1 - 5.7 micrometers) this is commonly encountered between filters with germanium and silicon substrates. A third reason to change focus during a mission is during instrument calibrations. It is anticipated that the SBS on-board calibrators will consist of extended radiance sources only. Defocusing an image of these calibrators improves the uniformity of the radiance observed at the focal plane.

The focus control can be implemented by simply moving one of the secondary reflective elements in the optical system. A stepper motor could be used to control its position through a gear arrangement. Designing such a system that would maintain optical accuracy would be difficult, however. A simpler arrangement

Section 4.1

would be to move the entire reflective optical assembly, while leaving the detector dewar in a fixed position. This would change the optical focus at the focal plane and be mechanically simpler to operate. Such a system is illustrated in Figure 4.1-8. An important issue that arises in the design of the focus control is that of speed: how fast the element should be able to move from the closest focus to infinity. If the focus change is too slow, determining the focus in real time becomes difficult if changes (for better or worse) in scene focus cannot be detected while the focus element is moving. This must be balanced off against the need for a precise focus point. If the optics system is built with a 10 inch focal length, the reflective unit would have to be able to travel about 1 inch of distance relative to the dewar in order to change the focus from about 3 meters to infinity.

The requirements imposed by the focus control on the optical design are dictated by a number of separate factors. One crucial issue is the method used to determine and set the proper focus for the instrument. Currently the best and most reliable way to focus a camera the size of the SBS system is through manual intervention by the system operator in real time; the operator observes some scene feature at the required focal distance, and then manually uses the focus control motors to move the focusing element until the image looks sharpest. This is a very subjective technique to use, and has the additional drawback that 'real-time' control of this motor may have a time lag of up to 20 seconds added to it by the shuttle-payload telemetry interfaces (discussed in section 4.6). Despite these disadvantages, no reliable methods are known for automatically determining the system focus that can be used within the limited payload restraints of the SBS.

4.1.6 Visible wavelength tracking camera

One feature identified as desirable in discussions with AFGL/RADC representatives is the addition of a visible wavelength camera that observes the same field of view as the infrared focal plane array. This feature would offer several useful advantages during use of the SBS Camera. First is assistance in the correlation of the infrared scene data. The availability of a visible band image recorded along with the infrared data allows easier identification of targets and events that are being measured. This simplifies the data reduction and analysis process. A good example that illustrates the usefulness of this is measuring something unexpected in the infrared image of the target (shuttle) such as a hot spot along the fuselage. The visible image could be used to identify exactly where the hot spot was located, and then fuselage drawing could be consulted to determine the source of the heating. In some wavelength bands the infrared image of a target is very different than the visible band image. This advantage is particularly important at longer target ranges, since if the visible camera has greater spatial resolution than the platinum-silicide array, it will provide additional detail that cannot be derived from the infrared image. The focal plane arrays anticipated for the SBS Camera have 160 by 244 elements. The discussion below shows that significantly higher spatial resolution can be obtained from standard video cameras.

Secondly, visible camera data can be used for range and aspect angle determination. It is very useful, especially for calibrated radiometric measurements, to know the exact range to the target. It is also very useful, for mapping out the target signature as a function of angle, to know the aspect angles of the target relative to the infrared camera field of view. Both of these parameters can be

Section 4.1

determined fairly accurately from the positioning information collected on both the host platform (assumed to be the SPAS for a remote shuttle measurement) and the shuttle itself. However, if other targets are measured, this information may not be available. In this case, a geometrically accurate image of the target allows determination of these numbers. For range determination, the distance in the camera image between two points on the target is first measured. The actual distance is determined from the target design drawings, and then the measured distance from the visible image is converted into a range using the camera optics numbers. For aspect angle determination, the distance between three points widely separated points on the target is first measured. Again, using the known dimensions of the target, it is possible to make a first guess at the aspect angles required to produce the distances measured in the camera image, and then iterate the process until a suitably accurate solution is arrived at. The accuracy of these methods is determined by the resolution of the camera and the properties of the optical system. Given the recommended optical system numbers above, ranges to a few meters of accuracy and angles to within a degree could be determined in this manner. Note that this process takes place after a mission and not in real time.

The two advantages described above for use of a visible camera must be balanced against its disadvantages. The primary one is that this camera would take scene energy away from the infrared focal plane array. The only practical way (within the SBS payload restraints) to view the same field of view with two cameras at all ranges (from one meter to infinity) is to put a beam splitter in the optical path and divert half of the energy to the platinum-silicide array and the other half to the tracking camera. Thus half of the infrared energy collected by the optical system is lost. This could be a problem if faint targets were being measured, and faint targets could be objects observed in a wide bandpass filter at long physical ranges, or close objects observed in a very narrow bandpass filter. This loss of energy could be avoided by using a visible optical system that is separate and parallel to the infrared system, but a complete second set of reflective optics would be required, as well as a complex coupling between the two systems. This option is not viable for the small physical envelope of the SBS Camera payload. A secondary drawback is the increase in weight and system complexity. The cameras themselves are small (as shown below) and require little power, but the visible band information has to be recorded away somewhere for later use. This requires either an extra tape recorder or additional bandwidth on an existing one. Note that the high dynamic range required to record the infrared pixel data away is not needed for this data (see section 4.4), so a more compact and lower quality analog recording device would be adequate. Good frequency response must be maintained if the data is to be used for ranging and aspect determination. The use of the visible band imagery in real time would also require an additional high bandwidth television data link between the payload and the ground camera operators.

This visible wavelength camera could consist of either a photographic camera or a television compatible video camera. Photographic fine-grained film has considerably more spatial resolution than a video camera system (films can go as high as 5000 pixels across an image in both horizontal and vertical directions), which is an advantage for longer range aspect and distance determination. A film based system, however, is considerably more complex than a video camera, and the visible imagery is not readily available of a telemetry data link in the same way that a video signal can be sent. For these reasons, the discussion here will be

Section 4.1

limited to a video-based solution to the visible camera requirement.

Two general types of video camera are available for use in this application: picture tube based cameras and CCD array solid state cameras. Tube systems scan a beam of electrons across a photosensitive coating and generate a voltage proportional to the scene intensities and colors. Cameras that use a tube design include systems such as vidicons, newvicons, and satcoms. Solid state camera use a two dimensional CCD array sensitive to visible wavelengths that states at the scene elements and is read out pixel by pixel to generate a scene image. Tube based cameras generally have greater light sensitivity (can operate under lower lighting conditions) than CCD cameras. CCD cameras are more physically rugged, have greater geometrical image accuracy (particularly around the image corners), and have more resistance to factors such as magnetic fields. Since one of the primary uses for the visible camera system would be ranging and aspect determination, maintaining high geometrical image accuracy is very important. For these reasons, a CCD solid state camera is more suitable for the SBS application.

A wide selection of very compact and lightweight solid state CCD cameras are currently available from a variety of manufacturers that includes RCA, Panasonic, Hitachi, Sony, Magnavox, NEC, etc. Typical performance specifications can be seen in those for one device: the Pulnix TM-34 CCD video camera module. This unit utilizes a silicon CCD array with 284 (horizontal) by 491 (vertical) elements. The minimum illumination is down to 3 lux (0.3 footcandles). An automatic iris that adjusts to the scene brightness is available to allow F number variations from F1.6 to 200, and weighs only 2 ounces. The unit uses 12 VDC and, with the auto iris and power supply included, consumes only 3 watts of power. The unit operates from 0 to 40 degrees C, and the storage limits are -30 to 60 C. The vibration resistance is 7 g's (from 11 Hz to 200 Hz), and the shock resistance is 60 g's. Physical dimensions are 41.6 x 27.8 x 76.3 millimeters. The spectral response of the silicon CCD, which is typical for most of these solid state CCD cameras, is illustrated in Figure 4.1-9. The system outputs RS-170 standard video, which is compatible with all US video systems. This represents a remarkably small, lightweight, and capable camera, and is commercially available off-the-shelf at a price in the range of \$1000. Higher spatial resolution video cameras are also available, and should be considered if ranging and aspect determination will be required for targets at longer ranges.

The options available to record the video signal for later data reduction and analysis are covered more completely in section 4.4 of this design study, which treats the platinum-silicide recording options available for the SBS Camera payload. Note that a small analog video cassette recorder would be sufficient for this system. Alternately, the visible data could be digitized and stored along with the infrared image digital pixel data on a single recorder if it had high enough bandwidth and speed. Such recorders do exist, and a scheme employing this approach is described in more detail in section 6.

This visible camera tracking unit must be incorporated into the optical path of the SBS Camera. The use of a beamsplitter has already been mentioned as the best way to observe the same field-of-view as the platinum silicide infrared array. If this beamsplitter is inserted into the optical path, however, it must be placed in a place where the image rays are parallel, to prevent image degradation. The only place where the rays are parallel is in front of the Ritchey-Chretien reflective

Section 4.1

mirror assembly. This is illustrated in Figure 4.1-10. The beamsplitter approximately 5 inches square is mounted at a 45 degree angle inside a mechanical housing in front of the entrance aperture of the mirror assembly. The beamsplitter would have to be manufactured from a material highly transmissive in both the visible bands as well as the platinum silicide band; a suitable candidate material is calcium fluoride. The visible camera would be mounted on top or to the side of the unit, and would have an appropriate lens to collect the image of the field of view.

In summary, the use of a visible wavelength camera offers two important advantages in the use of the SBS Camera, which are correlation of the infrared phenomenology observed and an independent means of determining range and aspect information. Much of this information can be derived from other sources, for the specific case of measuring the space shuttle signature, which has been set as one of the primary goals for the SBS camera. Thus this visible camera system is a nice feature, but its presence is not mandatory to meet the camera performance goals detailed earlier in section 3. It is recommended that capabilities for this system be included in the design, but that it be a removable component so that, if its inherent disadvantages of its use (loss of scene signal) are important for a particular mission, the system can be removed easily without adverse impact.

4.1.7 Cryogenic cooling of optics

Another issue that must be examined in the initial design of the SBS Camera optical system is the cooling of the entire optical system. A significant improvement in overall system performance can be attained by reducing the amount of background radiation seen by the detector. Reductions in background signal levels translate into increased detector sensitivity, because the shot noise present in the background is reduced. The amount of background flux anticipated from the reflective metal mirrors themselves is low because of their relatively low emissivity. Off-axis infrared emission, from the mounting structures used to hold the optics in place, is the primary source of background expected. This problem is increased with a reflective design, since the off-axis rejection of these systems is relatively poor.

The primary disadvantage encountered with cooled optics is the large amount of cooling capacity required to maintain the optics at a stable cooled temperature. Cryogenic temperatures are required to reduce the background flux, and thus this represents an additional thermal load placed on the cryogenic cooling system. The magnitude of this thermal load is estimated quantitatively in section 4.2.1, where the performance specifications of the cryogenic system are derived. Because of the large thermal mass anticipated of the optical system and associated mounting hardware, a significant amount of cooling power is required for cooldown. The relatively large physical size of the system will also result in increased heat loss once the system has been cooled down. Another very significant problem is alignment errors that will be introduced into the optical system as it is cooled down and all of the mounting hardware contracts. One of the design goals for the SBS Camera is to have the system capable of operating in a stand-alone mode, but extensive re-alignment would be required after each cool-down. This problem could be avoided if the entire optical system were cooled on the ground (pre-launch) and kept cooled until data collection, but this would require very large amounts of cryogen that could not be fit into the physical envelope of the SBS payload (discussed in section 4.2). For these reasons, it is not practical to incorporate a

Section 4.1

cooled set of optics into the optical design of the SBS Camera without significant departures from the design goals.

Cryogenically cooling the optical elements located within the instrument dewar is a practical alternative, as shown in section 4.2. This includes a cold aperture stop, the bandpass filter wheel, antireflection baffles, and the focal plane array itself.

Given the large potential temperature variations expected in a space environment (detailed in section 4.6), some system of temperature stabilization for the optics will be required to prevent potential alignment problems. Temperature stabilization can be realized within relatively broad limits with less complicated measures than a cryogenically cooled optical system. There are several means of temperature control available (both active and passive) that are discussed more completely in section 4.6.4. The most likely solution is a combination of active temperature control, in the form of heaters, that maintains the lower temperature limit, and passive thermal control that maintains the upper temperature limit.

In summary: keeping the entire optical system (mirrors, baffles, and dewar components) cooled to a cryogenic temperature during data collection is not practical given the SBS design constraints because this would require a cooling system that could not be fit into the payload envelope. The advantages of a cooled set of optics (increased system sensitivity) are more than offset by the problems caused in cooling the optics, and so a cooled optical system is not recommended for the SBS Camera design. A single cold aperture stop and a cooled filter bandpass wheel are practical within the dewar and will be analyzed in greater depth in the next section.

4.1.8 Radiometric calibration sources

One of the design goals for this camera system is that it must produce data that can be radiometrically calibrated. The process of calibration has already been described in section 2.4, and the requirement for a limited verification of the calibration accuracy immediately before or after data collection has been established. In-flight calibration requires the complete camera system to observe sources with known radiance values. These sources must be inserted into the instrument field of view during calibration, and then removed during data collection. Ideally, they should be located as far along in the optical train as possible, in order to calibrate as much of the system as possible. A need for three independent sources was also established.

Previous analysis has already indicated that the most suitable sources for these calibrations would be extended heated sources with high emissivity surfaces. This is easily provided by manufacturing a block of metal with a high heat capacity to provide thermal stability. Heating can be provided by resistive heaters mounted inside the block, and temperature readouts can be provided using precision temperature sensors. The surface of the blocks should be machined with a 'honeycomb' structure to reduce surface reflections and provide recessed cavities in order to simulate a backbody cavity. This surface should be painted with a high emissivity paint in order to approach the behavior of an ideal blackbody. A unit with these characteristics is illustrated in Figure 4.1-11.

There are two ways to get these sources into the instrument field of view: the

Section 4.1

sources can be mechanically moved into it, or the instrument field of view can be directed onto fixed sources. In order to include the characteristics of the reflective mirror in the calibration, it is desirable to locate the sources beyond the entrance aperture, as opposed to inserting them directly in front of the dewar opening, where the focal cone is smaller. This requires the sources to be larger than the 3.5 inch aperture diameter, and thus makes mechanical insertion of these large blocks of metal less practical than re-directing the instrument field of view. A convenient way to redirect the instrument FOV is to add an additional degree of freedom to the tracking mirror described in section 4.1.4. Rotating the mirror around the optical axis of the reflective mirror assembly allows the FOV to be directed to either side of the mirror, and also down into the mounting plate. These locations are ideal for the calibration sources. This is illustrated in Figure 4.1-12. Facing the mirror down into the plate also provides a convenient 'stow' position for the mirror, that protects it from damage when the camera system is not in use. Note that this additional degree of freedom complicates the design of the tracking mirror mount, making its extended arm longer and thus more susceptible to vibrations and motion, which will translate into tracking errors. This is offset by the ease with which the calibration sources can be incorporated into the optical design. The sources will be out of focus for the system, which will improve their uniformity across the total field of view.

4.1.9 Bandpass filters

The addition of spectral bandpass filters to the SBS Camera system would add significant operational advantages to the system. The primary advantage of filters is that they divide up the relatively wide spectral response region of the Schottky-diode focal plane arrays into smaller pieces. This allows a target signature to be measured as a function of wavelength, which can provide valuable insights into the phenomenology that is creating the measured signature. A common example of this is separating the thermal and solar reflected components of a target signature. For targets around 300 degrees K in temperature, the relative intensities of these two components frequently cross over around 4 micrometers: at longer wavelengths, the emitted radiation dominates, while at shorter wavelengths, the reflected radiation is the primary source of the signature. Since these two sources have very different spectral shapes, they will exhibit different properties. Measuring a target with a 4.5 - 5.5 micrometer filter can determine the emitted component, while using a 2 - 3 micrometer filter provides a measure of the reflected component. Separating this type of phenomenology out is essential to understanding and predicting a target signature. Thus bandpass filters will add significantly to the usefulness of the SBS Camera data.

One basic way to add bandpass filters in is to mount them in a metal wheel located in the optical path. Rotating the wheel allows different filters to be selected. The proposed SBS Camera design (section 6) locates this wheel inside the cooled dewar, so that the filter self-emission is reduced, reducing the background flux seen at the focal plane array and thus increasing its sensitivity. Placing the filters normal to the optical axis reduces the effect on the system optics to simply changing the focal point of the system, which can be compensated for by focus adjustments. Typical bandpass filters consist of stacked layers of coatings that interfere with each other so that their transmission cancels outside the bandpass of interest but constructively adds within the bandpass. The layers are placed on a substrate material, which for this wavelength region is usually either silicon or

Section 4.1

germanium. Intelligent selection of materials, thicknesses, and order in the layer stack lets the filter maker build the desired spectral behavior. It is relatively simple to create arbitrary spectral bandpasses, either narrow or wide, within the platinum-silicide band (1.1 - 5.7 micrometers) using existing technology, with slopes on the bandpass edges down to the 1 percent range. Note that these two substrates have different indices of refraction, so if they are mixed together in a single filter wheel, refocusing of the system will be necessary when the filters are changed.

Another possibility for controlling the spectral band observed by the SBS Camera is the use of a circularly variable filter. This is also an interference filter. It consists of a film deposited on a circular substrate. The thickness of the film varies as a function of position around the circular substrate. Thus the interference, and the spectral bandpass, varies as a function of position around the filter. This design is simpler than a filter wheel in that only a single large filter is rotated, and it gives multiple spectral band coverage. There are several disadvantages to this approach. The primary one is that the bands in circularly variable filters tend to be narrow. It is not possible to mix narrow and wide spectral bands without making the manufacture of the filter exceedingly complex. Another problem is that the spectral shape of the bandpass regions is sharply peaked (since essentially a single layer is varying to create the bandpass), and sharp peaks like this make radiometric calibration of the data difficult (see section 2.4). A final disadvantage is that the bandpasses of the circular filter will be ordered in ascending or descending order (in wavelength). For reasons of measurement phenomenology, it is advantageous to be able to mix filter bandpasses in order to simplify the measurement. For example, if data is desired in a very narrow bandpass filter, it may be simplest to locate a wideband filter in the wheel next to this narrow filter. The camera can then acquire and track the target of interest in the wideband filter, where there is plenty of signal, and then switch to the narrow filter only after acquisition and track. This option, which may prove important in practice, is not available with a circularly variable filter.

A second issue to be resolved is the number of filters that should be incorporated into the filter wheel design. The larger the number of filters available during a mission, the greater the amount of spectral information that can be collected on a target signature. This is especially true in a spectral band like that of the platinum-silicide detectors, where the physics determining the target signature usually changes completely from one end of the band to the other. The real limitation on the number of filters allowed is a practical one. First, as more filters are placed in the wheel, the calibration requirements grow, since each filter must be characterized separately. In addition, separate background averages may need to be stored for different bandpasses, and each average takes several seconds to collect (section 4.3) Thus the camera operating overhead grows. Secondly, the filter wheel grows larger as more filters are added into it, and maintaining a cold filter wheel becomes more difficult, because the heat leaks into the system are increased. The optical system proposed for the SBS has no intermediate focal plane, and thus the filters will have to be reasonably large. The focal plane array is about 0.5 x 0.5 inches square, and if the filter wheel is a few inches in front of it, each filter will have to be approximately 1 inch in diameter to prevent vignetting of the image along the filter edges. Thus adding filters adds 1 inch disks to the wheel, which increases its size rapidly. Putting two filter wheels in removes the size disadvantage, but it greatly increases the complexity of the system, as separate motors must be maintained, and

Section 4.1

the readout mechanisms (for filter position) become less reliable. For simplicity, a single bandpass filter wheel is recommended, and a number of 8 filters has been tentatively agreed upon for the SBS Camera design. An illustration of the position of the bandpass wheel in the camera optical system is shown in Figure 4.1-13.

The final issue to be resolved is the selection of filter bandpass values. The effects of different filter bandpasses combined with the Schottky-diode spectral response has already been discussed in the performance analysis in section 2.3. It was demonstrated there that the use of certain bands significantly extends the dynamic range of the system. This must be balanced off against the loss in sensitivity that results from the filters blocking out the majority of the scene energy. To improve the calibration, relatively wide (on the order of 1 micrometer) and flat spectral bands are preferred. The bandpasses already used in the current SAIRS design are listed in the table in Figure 4.1-14. Fortunately, the lead times required for filter fabrication are less than a year, and so the final selection and specification of the filters for the system can be postponed until the project is fairly advanced. Here it is recommended that, for a four filter wheel, three positions be used for wide filters that split up the bandpass, and the fourth be used for a single narrow filter that significantly extends the dynamic range of the system (for use with bright targets).

In summary: the addition of bandpass filters to the SBS Camera design would significantly enhance the usefulness of the collected imagery in understanding the measured target signatures. A bandpass filter wheel holding several changable filters is recommended over a single circular variable filter because of increased flexibility and ease of camera use. A compromise between the desire for many filters and the practical problems posed by a large wheel leads to a recommendation for a filter wheel with four positions.

4.1.10 Summary of optical system

A set of optical performance parameters that determine the optical requirements of the SBS Camera system has been derived in this section. An optical design with the following characteristics satisfies these requirements and can be fit in the SBS design envelope: 3.5 inch entrance diameter, 10 inch focal length, with an F number around $f/\# 2.5$. The need for a target tracking and acquisition system that moves the instrument field of view independent of the host platform has been demonstrated. A workable solution has been shown to be a flat mirror, mounted in front of the reflective entrance aperture, mounted so that its angle to the fixed optical axis can be precisely controlled by motors to counter the motion caused by the host platform. Focus control in the system is best implemented through motion of the reflective mirror assembly. The value of a visible television camera observing the infrared FPA field of view was demonstrated, and an implementation of this was shown that can be easily removed from the system. The disadvantages of cryogenically cooled optics were found to outweigh the advantage gained by reduced instrument background. The general design characteristics for inflight radiometric calibrators were described, and an implementation that allows the SBS Camera to easily observe them for extended source calibrations was shown. Finally, the value of incorporating a bandpass filter wheel into the optical path was described. The final block diagram of the optical system for the SBS Camera, including the results of the analysis in this section, is shown in Figure 4.1-15.

Section 4.1

Additional details showing a possible implementation of this scheme are covered in the proposed design presented in section 6 of this study.

4.2 Cryogenic cooling system

4.2.1 Cooling requirements

Schottky barrier arrays are infrared detectors, so they are very sensitive to the backgrounds emitted by both the observed scene and the instrument itself. The detectors need to be cryogenically cooled in order to function at all, since above around 90 degrees K the dark current swamps the current generated by the infrared signal. The typical temperature range used on existing arrays is in the range from 60 to 80 degrees K, with liquid nitrogen (77 K) usually used as the coolant. There are some indications that the responsivity of the arrays increases significantly as they are cooled further down to about 40 K. In earlier arrays the CCD registers had trouble operating at these lowered temperatures, but newer designs have solved some of the problems. Careful monitoring of the absolute temperature of the array is important, because the sensitivity of the detectors does increase as they are cooled, particularly in the temperature regime around 40 to 65 K. Changes in sensitivity affect the radiometric calibration of the data.

In addition to the cooling of the focal plane array, it is important to provide cooling for the detector surroundings in order to reduce the background flux on the detector. The improvements gained in system performance can be seen by examining the common parameter D^* , which is a measure of the signal to noise ratio of the detector. One way to define D^* (from Hudson, p. 322) is

$$D^* = \frac{\sqrt{(A_d * f)}}{NEP} \quad \frac{\text{cm} * (\text{Hz})^{0.5}}{\text{W}}$$

where

A_d = area of detector (cm^2)
 f^d = equivalent noise bandwidth, Hz
NEP = noise equivalent power

The NEP of the detector is directly proportional to the total irradiance incident on it:

$$NEP = H A_d \frac{V_n}{V_s} \quad \text{Watts}$$

where

H = irradiance (rms of fundamental component)
 V_n = rms noise voltage
 V_s = rms signal voltage

Cooling of the detector surroundings, or cold shielding, limits the background flux

Section 4.2

from the instrument. As the equations above show, the detectivity D^* of the system improves as more background flux is removed. Cold shielding is mandatory, since it can easily improve the D^* by an order of magnitude or more. This improvement has the price of increasing the thermal load placed on the cryogenic cooling system of the camera, and this additional load has to be considered in the design of the instrument.

A common way to cold shield infrared detectors is to place a cooled aperture stop in front of the focal plane. The aperture stop has an opening that follows the outside envelope of the ray bundle of the scene being observed outside the camera. If the area inside the aperture stop is cooled to the same temperature as the detector, that source of background energy will be effectively eliminated. In addition, glare stops, or baffles, will be required in front of the dewar to block the reflections of stray light onto the detector. Some of these baffles may have to be cooled if they are located inside of the aperture stop.

Another important requirement is cooling of the bandpass filters and their associated mount. The bundle of energy from the scene passes through the filters, so energy radiated from warm filters is not blocked by an aperture stop. The detector array is sensitive to energy from 1.1 micrometers to its long wavelength cutoff (around 5.7 micrometers with current PtSi arrays). The bandpass filter is blocking spectral energy from the scene that is outside of its bandpass, and so no useful scene information is contained there. If the filter is uncooled, however, the filter itself is either radiating at its temperature outside the bandpass or is possibly reflecting energy emitted by its surroundings. Filters that block incoming scene energy by absorbing it can also be heated if the observed scene is bright enough. This emission contributes to the background flux observed at the focal plane and reduces the sensitivity of the system. For this reason, significant gains in system sensitivity can be realized by cooling the bandpass filters. The reduction in background flux from the filters is illustrated in Figure 4.2-1. This is a plot of inband radiance emitted from a blackbody as a function of temperature. The wavelength band is 2 - 5.7 micrometers. In this band and at these temperatures the emitted radiance is a strong function of temperature. Cooling the filters from 300 K to 240 K reduces the background emission by a factor of 10. Note that the background flux at 77 K is essentially zero. This plot illustrates that large reductions in background can be attained without cooling the filters all the way to 77 K. Cooling the filters to 150 K, for example, reduces the emission by 4 orders of magnitude and already diminishes the signal to a small fraction of the expected inband signals that will be measured. The largest improvement, of course, will result for bandpass filters that pass very little scene energy: narrow or short wavelength filters. The absolute numbers shown in Figure 4.2-1 assume an emissivity of 1, which is not realistic for coated filters, but the plot is intended to illustrate the proportional improvement that can be expected as the filter temperature is dropped.

Two major complications are introduced into the dewar design when a cooled filter wheel is used. First, practical design considerations usually dictate a filter wheel design that consists of a round wheel holding the bandpass filters connected to the rest of the dewar by only a center shaft. Such a wheel design has poor thermal contact to the rest of the cooled dewar, and thus more of the cooling takes place via radiation cooling (as opposed to conductive cooling). This can significantly increase the cooldown time required before the system can operate. Secondly, the

Section 4.2

filter wheel must be driven by some sort of stepper motor controlled by the camera. Reliable motors that operate at cryogenic temperatures are difficult to find or make, because of lubrication problems and the relatively large mass of the wheel. These problems are not unsolvable, of course, but they must be seriously considered in the design considerations of the cryogenic cooling system.

An important issue that affects the camera's capabilities is the cooldown time, which is the time required to cool the dewar and cold shields from a non-operating temperature (temperature of the system when in the stowed state) to a temperature low enough so that the system can be operated. Cooldown time requirements have a major impact on the cryogenic cooling system selected. If rapid cooldown is required, a considerable amount of cooling capacity (on the order of many watts) may be required, since the total thermal mass of the detector, cold shield, baffles, and filter wheel is not insignificant. If longer cooldown times can be tolerated, lower capacity cooling systems can do the job. The cooldown time has an upper limit imposed by the fact that the SBS Camera will have a limited amount of total time available for data collection.

To determine the performance requirements of the cryogenic cooling system, some simple assumptions will be made that allow approximation of the thermal load. Three levels of operation will be examined: cooling of detector chip and single cold aperture stop only; additional cooling of baffles and filter wheel; and complete cooling of optical system. Two important factors must be evaluated. First, the cooldown time is an important consideration, as noted above. Secondly, the constant heat loss during operation must be estimated.

The thermal mass of just the detector and a single cold aperture stop is relatively simple to estimate. The thermal mass of the silicide detector itself is small compared to its cold finger mount and the aperture stop. A single aperture stop can be made very thin, as it has no mechanical demands made on it. We will assume for simplicity that aluminum is used, and its total mass of this first option is on the order of 0.05 kg. If the baffles and filter wheel are added into the cooling requirements, the thermal mass that requires cooling is increased considerably. We will assume that the total mass of the cooled assembly increases to 0.25 kg of aluminum. The filter substrates in the wheel also require cooling, but the thermal mass of 1 inch filters of either silicon or germanium is small in comparison to the mass of the mechanical assembly. If the entire optical assembly is cooled, this analysis becomes very complicated and design dependent, because the reflective mirror system will have a considerable thermal mass because of both the size of the mirrors and the need to be mechanically rigid. The mass of this entire system will be modeled here by 2.5 kg of aluminum. The specific heat of aluminum is 896 joules/kilogram per degree C, so thermal load presented to the cooling system for each degree Centigrade of temperature change is:

<u>cooling requirements</u>	<u>Joules/degree C</u>
detector, aperture stop	44.8
detector, baffles, filter wheel	224
optical system	2240

Now the temperature change required must be estimated. The temperatures expected for the SPAS and HH-G payloads are discussed in section 4.6. It is assumed

Section 4.2

that the payload will not be directly exposed to solar radiation during operation for any extended length of time, and because of the large heat input that this can cause, this assumption is likely to be an actual operating restriction. The ambient temperatures of the instrument prior to cooldown will range from -100 C (facing deep space) to about -5 C (facing earth). We will use a pessimistic value for our calculation of 0 degrees C (273 Kelvin), since the cooling system should be able to operate under the full range of possible conditions. The final operating temperature of the array must be below 80 K, but it also has a wide range below this (45 - 80 K). For simplicity 73 K will be selected, to make the total temperature change required = 200 degrees. Thus the thermal loads presented for cooldown are

<u>cooling requirements</u>	<u>total Joules</u>
detector, aperture stop	8960
detector, baffles, filter wheel	44800
optical system	448000

Now time limits must be determined for the cooldown of the system from ambient to operating temperature. The design goals of the system expressed in section 3 of this study require 2 separate data runs of 5 hours duration each. The total time budget of experimentation time available on a shuttle mission of 8 days duration is only about 5 days total. If the SBS is deployed on the SPAS platform, only about 30 hours of free-flight orbit can be expected, placing a much more severe restriction on the cooldown time. We will present numbers for two cooldown rates: a rapid cooldown, which we will set equal to 1 hour, and a slow cooldown, which we will set equal to 5 hours. With these basic time assumptions, the cooldown thermal loads can be converted into watts of cooling capacity required:

1 hour cooldown

<u>cooling requirements</u>	<u>watts</u>
detector, aperture stop	2.5
detector, baffles, filter wheel	12.4
optical system	124.4

5 hour cooldown

<u>cooling requirements</u>	<u>watts</u>
detector, aperture stop	0.5
detector, baffles, filter wheel	2.5
optical system	24.8

The cooling capacities in the tables above must be further modified to include the thermal losses incurred during cooldown. Such losses are very dependent on the quality of the dewar design and insulation. It is possible to estimate these losses, however, by realizing that the larger and more massive the assembly being cooled to cryogenic temperatures, the larger the steady state thermal losses, because there will be additional mechanical links to the rest of the platform that will present thermal conduction loss. If just the detector and aperture stop are cooled, it should be possible to attain steady state losses on the order of 0.5 watts. For the detector, baffles, and filter wheel, designs with a loss of 1 watt are possible. For the complete optical system, losses of several watts must be expected, and so we will assume 5 watts steady state loss. With these additional considerations, the cooldown requirements become:

Section 4.2

1 hour cooldown

<u>cooling requirements</u>	<u>watts</u>
detector, aperture stop	3.0
detector, baffles, filter wheel	13.4
optical system	129.4

5 hour cooldown

<u>cooling requirements</u>	<u>watts</u>
detector, aperture stop	1.0
detector, baffles, filter wheel	3.5
optical system	29.8

Note that, in the above calculations, perfect thermal conductivity throughout all components of the system was assumed. While this may be reasonably approximated in a large or massive dewar, it is very possible that some components will be in relatively poor thermal contact with the rest of the system. A good example of this is the filter wheel, whose only conductive thermal contact with the rest of the dewar might be through the center shaft. Radiative cooling then becomes the dominant cooling process for the wheel, and cooldown times might be significantly increased as a result. These calculations are only intended to provide general guidelines in the evaluation and selection of a cryogenic cooling technology to utilize in the SBS Camera system.

In addition to cooldown time considerations, the cryogenic system must be capable of maintaining the system at its selected operating temperature. This is generally less demanding than the cooldown requirements, since the heat losses of a well designed dewar are generally small. Current PtSi arrays generate heat while operating on the order of 100 milliwatts, which is a fairly low load. The arrays do require a large number of electrical connections (on the order of 60), so the potential for significant thermal leaks through the chip wiring exists and must be provided for. Fortunately, the detector operation is not affected by using wires with relatively high resistances (a few hundred ohms), so low conductivity wires such as Constantan (a 60% copper, 40% nickel alloy that has relatively low thermal conductivity while still maintaining good electrical conductivity) can be used. One important additional consideration is maintaining temperature stability during operation. Since the responsivity of PtSi arrays is dependent on temperature, changes in array temperature must be kept below a minimum level. Small temperature fluctuations in the cooler are usually minimized by putting a considerable thermal mass directly behind the detector, which buffers the microtemperature variations (but adds to the cooldown time requirements).

For this analysis, the steady state losses described above will be added to the chip heat dissipation to arrive at the steady state heat load during system operation:

<u>cooling requirements</u>	<u>watts</u>
detector, aperture stop	0.6
detector, baffles, filter wheel	1.1
optical system	5.1

Section 4.2

The final design requirement imposed on the cooling system is the ability to maintain adequate cooling capacity prior to system operation. In the design goals in section 3, potential holds on the launch pad of up to 20 days must be anticipated, and the mission duration can be up to 10 days. Thus the cooling system must be able to last through a time duration of up to 30 days in a stowed state before providing the required cooling power. This additional time requirement is important for a cooling system using stored cryogenics (liquid or solid), since heat will be absorbed and cryogen will be lost during this waiting time. For other cooling technologies that store their energy differently (cooling engines or Joule-Thompson coolers), hold times on the order of 30 days make no difference, since cold materials are not being stored. For stored cryogenics, the heat loss depends strongly on the design and quality of the dewar used to store the material. The dewar is subject to both radiative heat loss and conductive heat loss. The radiative heat loss can be estimated by assuming that the surface of the inner vessel at temperature T_1 (cryogen temperature) is completely enclosed by a much larger surface maintained at T_2 (assumed to be ambient temperature, or 300 K, since the bulk of these delays will occur prior to launch). The net radiant exchange can be calculated by

$$q = \epsilon * \sigma * A_1 * (T_1^4 - T_2^4)$$

where

- q = net radiant exchange (watts)
- ϵ = emissivity of the surface (assumed to be low, or 0.01)
- σ = Stefan-Boltzmann constant ($5.669E-8 \text{ W.m}^{-2}.\text{K}^{-4}$)
- A_1 = area of inner surface (m^2)
- T_1 = temperature of inner surface (stored cryogen)
- T_2 = temperature of environment (300 K)

A simple examination of this equation shows that, as larger amounts of cryogen are stored, the volume of the storage vessel increases, and the radiating area of the inner vessel increases. For large volumes of stored cryogen, this area term becomes large enough to become the dominant source of heat loss over the course of the mission. Thus simply increasing the amount of stored cryogen leads to diminishing increases in total cooling capacity of the system.

The conductive heat loss is very dependent on the exact design of the dewar and the storage vessel. Typically it can be made smaller than the radiative heat loss through careful design and the use of superinsulating materials. In the analysis presented here radiative losses will be assumed to be the dominant source of loss for the cryogen storage vessels (if any). Conductive heat losses for the dewar will be estimate from the actual performance of similar dewar designs already in use.

It is apparent from the above discussion that the initial cooldown of the system imposed the most demanding operational requirements on the cooling system. It is also clear that, given the power and physical size restrictions imposed by the host platforms on the SBS Camera system (discussed more fully in section 4.6), cooling of the entire optical system will present thermal loads that will swamp the capacity of any practically available cooling system. From the discussions on detector performance in section 4.2.12, it is also clear that reduction of the background levels seen by the detector lead to large increases in overall system sensitivity through

Section 4.2

reduction of the noise. Thus the first cooling option discussed above (detector and a single aperture stop) would lead to a significant trade-off in overall system performance. Thus the performance requirements used for the cooling system will be those for cooling of the detector, baffles, and a cooled filter wheel. These performance specifications are summarized in the table below:

<u>operating mode</u>	<u>watts (minimum)</u>
system cooldown	
1 hour	13.4
5 hour	3.5
system operation	1.1

The system must be capable of doing this twice, and so should have a total cooling capacity (expressed in Joules) of $68000 * 2 = 136000$ Joules. Note that this specification is a minimum one, and some safety margin would have to be added in to the design.

With the above requirements in mind, four cryogenic cooling technologies will be considered in detail in the following sections. The basic mechanisms, and the advantages and disadvantages of each in a space environment, will be detailed. One notable omission from the following list that has been used in space applications is the radiative cooler. This system has been popular on satellites with long cooling lifetimes (many months or years). Such systems, however, are very dependent on the camera orientation, as they cool by radiating energy off into the cold deep space background. Such a cooling system would impose many operating restrictions on a camera such as the SBS. In particular, operation in the shuttle bay on a Hitchhiker-type payload would be nearly impossible, as usual shuttle orbits tend to face the cargo bay towards earth. The cooling capacity of these systems is also relatively low. A radiative cooler would also be difficult to operate in the laboratory. For these reasons, this cooling technology has been rejected from consideration for the SBS camera design.

4.2.2 Liquid cryogenics

The use of liquid cryogenics for cooling takes advantage of the cooling provided when a liquid is converted into a gas. The energy absorbed by this process can be determined from the heat of vaporization of the liquid. The actual temperature attained is controlled by the coolant selected and the gaseous pressure maintained over the liquid. The liquid is kept in thermal contact with the focal plane and the rest of the dewar components that require cryogenic cooling.

Lists of candidate liquids can be found in references such as the Infrared Handbook. Two very common liquids used in the temperature range of the Schottky-diode camera are liquid nitrogen (77 K boiling point at 1 atm pressure) and liquid argon (87 K boiling point at 1 atm). If the pressure over these liquids is reduced, the temperature of the liquid can be reduced to their solidification temperatures. These liquids have found wide use in laboratory systems because of their low cost, easy availability, and ease of handling.

The main disadvantage of liquid cryogenics in a space payload is that, quite simply, solid cryogenics have more cooling power per unit mass (or volume) of coolant. Solid

Section 4.2

cryogenics inherently absorb more heat as they are converted to gases (as discussed in the next section). Solids are harder to work with in a laboratory, but in a remotely located payload such as the SBS Camera, the slight additional trouble of converting the liquid to a solid pays off in additional cooling. In addition, the use of solids simplifies the dewar design, because the cryogenic material must be kept in thermal contact with the dewar elements, and liquids tend to float away, requiring additions such as large surface area structures in the cryogen container to maintain contact via surface tension.

Thus liquid cryogenics can be ruled out for use in the SBS Camera payload simply because solid cryogenics provide more cooling and are easier to handle. The advantages and disadvantages of solid cryogenics are covered completely in the following section.

4.2.3 Solid cryogenics

The use of solid cryogenics for cooling is based on the sublimation of a solid into a gas that is then dissipated into space. The cooling capacity is determined by the heat of sublimation of the solid. The heat of sublimation is the sum of the heat of vaporization and the heat of fusion of a material, so solid cryogenics inherently provide more cooling power than liquid cryogenics. The temperature is controlled by the coolant material and the pressure maintained by the vent gas. As the cooler absorbs heat from the instrument, the solid is transformed into gas. As the gas accumulates, its pressure and temperature would normally increase. In a solid cryogen cooler, the duct of the exhaust gas to space is normally designed to maintain a constant pressure. This design pressure can be used to match the temperature at which sublimation occurs to the instrument requirements. The minimum vapor pressure is in theory 0 but in practice is usually around 0.1 millimeters of mercury. The maximum operating pressure is at the substance triple point. A plot illustrating some candidate solid cryogenics for the temperature range required by PtSi arrays is shown in Figure 4.2-2 (from the IR Handbook p. 15-22). The operating minimum and maximum temperatures are shown using the criteria mentioned above.

An important issue to resolve is whether these candidate solids could be used within the SBS payload restrictions. The primary determinant of this is the mass, and subsequent volume, of the storage vessel required to store the solid cryogen. The following table simplifies this analysis:

<u>material</u>	<u>heat subl (J/g)</u>	<u>density (g/m³)</u>
nitrogen	224.7	1022100
argon	185.6	1714000
oxygen	226.8	1302400
methane	568.7	498200
carbon monoxide	293.1	929200

The basic requirement is for 130000 Joules in addition to the storage vessel loss. The mass required to provide this cooling is shown in the following table:

Section 4.2

<u>material</u>	<u>mass req (g)</u>	<u>volume (cm³)</u>
nitrogen	551	539
argon	668	390
oxygen	547	420
methane	218	438
carbon monoxide	423	455

These values are not unreasonable for the SBS camera. However, the potential loss of cryogen during hold times prior to launch must also be added in. This storage vessel loss is a significant factor. For simplicity, this analysis will assume that all of the loss encountered during cryogen is radiative heat loss, since this cannot be avoided. The net radiant exchange relation shown back in section 4.2.1 will be used to estimate this loss. This equation shows that, as the area of the stored cryogen (inner container) increases, the radiative loss increases proportional to this area. If argon is selected from the above table (smallest volume for cooling), and if a spherical storage vessel is assumed (to minimize the surface area), the radius of the inner vessel would have to be about 5 cm, given the density of solid argon. This vessel would experience a steady state radiative loss of 0.14 watts, which, over a period of 20 days, translates into a heat load of 241920 Joules, which is twice the refrigerative capacity of the solid argon. In other words, the solid would be completely evaporated before launch during a 20 day hold. This effect can be compensated for by increasing the mass of the stored argon, but its area also increases, so a significantly larger amount of cryogen is required. Some sample calculations indicate that a mass of 8082 grams of solid argon (heat capacity of 1500000 joules total), with a volume of 4715 cm³, could be stored in a spherical vessel with radius 10.4 cm. This vessel would experience a steady radiative loss of 0.63 watts, which over a 25 day hold time would consume 1360800 joules of the total. This would still leave just enough refrigeration required to perform the mission. This sample analysis illustrates that, for any solid cryogen, the mass of cryogen must be greatly increased to meet the pre-launch hold requirement (as much as a factor of 10 in the case of argon above). Given the relatively small physical envelope of the SBS payload, the size of the cryogen storage vessel can only be increased to a certain point (whose exact value depends on the physical design of the rest of the system). This demonstrates the diminishing returns gained from increasing the amount of stored cryogen.

This greatly increased storage volume required for the cryogen can be reduced if the pre-launch hold time requirements are relaxed. For example, if access to the payload was allowed within three days of launch (in other words, the cryogen could be replenished on the ground 3 days prior to launch during a delay), then the total hold time would be 3 days pre-launch and a maximum of 8 days on station. For these conditions, the example of solid argon discussed above would be considerably reduced. A mass of 2694 grams of solid argon (500000 joules of cooling), in a volume of 1571 cm³, would have a radius of 7.2 cm, which results in an average radiative heat loss of 0.3 watts. This heat loss would consume 285120 joules over 11 days, and would still leave adequate cooling capacity (214880 joules) to perform the mission requirements. This volume of storage vessel (the inner vessel would be about the size of a basketball) could be accommodated in the SBS payload. Similar calculations can be easily performed for the other cryogens listed above. This gain

Section 4.2

requires relaxing the pre-launch access time for the SBS payload, which is currently considered a significant disadvantage in the overall design.

Of the cooling candidates listed above, several have serious problems that effectively prevent further consideration of their use for the SBS. Oxygen, methane, and carbon dioxide are all potentially hazardous gases: solid oxygen and methane are potentially explosive, and carbon monoxide can be dangerous to handle in the laboratory. In addition, methane and carbon monoxide have molecular bands that are active in the 1.1 - 6.0 micrometer wavelength band. Thus the presence of these gases around the instrument can introduce errors into calibration and data measurements by selectively absorbing part of the incident radiant energy. These problems could be worked around if any of these gases offered significant advantages in cooling power over the easier to work with argon and nitrogen, but they do not. For these reasons, argon and nitrogen emerge as two serious candidates from the above short list.

Solid cryogenics have been used to attain hold times of up to 1 year in duration on various long-term satellite projects. Dewar designs with this level of performance have been described in the literature. It is important to note that all of these very long hold times were obtained by using very large volumes of cryogen and limiting the thermal loads on the cooling system to small fractions of a watt. These limitations become unrealistic for a space based system that will be operating in close proximity to the earth (at times observing it) and to a large platform like the space shuttle, which radiates a considerable amount of thermal energy. Since the SBS Camera is assumed not to be the primary instrument on its host platform, it will not have exclusive control of the platform aspect, and thus would not be able to employ the elaborate schemes used by the long-hold time satellites to minimize incident thermal radiation. In addition, the year-long hold time payloads usually employ solid hydrogen, which has a very large cooling capacity (heat of sublimation) in relation to its density, and is thus a particularly good cooler. Solid hydrogen operates at a temperature far below the current optimum temperatures for Schottky-diode arrays, however, and so the temperature would have to be maintained higher through controlled heat leaks by the cooling system. In addition, the volatile nature of hydrogen is a significant disadvantage when compared to solids such as nitrogen or argon.

There are several general advantages to use of solid cryogenics. They have more cooling capacity than equivalent volumes of liquid cryogen. Solid cryogen systems are mechanically fairly simple, since no complex plumbing is required. The only major need during system operation is to exhaust gas at a pressure equal to that chosen to maintain the system operating temperature, which is relatively simple to do into the vacuum of space. The plumbing required to load in the cryogen and solidify it can be a separate attachment that is used only during system fill on the ground. The electrical power requirements of a solid cryogen system are quite low, since only cryogen level sensing is required. A properly designed system should be capable of operating at all attitudes of the instrument, since the solid does not move.

Solid cryogenics do present a number of significant disadvantages to the SBS design requirements. A solid cryogen system employing nitrogen or argon would have a relatively large mass and volume because of the long pre-launch hold times built into the system design goals outlined in section 3. If these design goals are relaxed,

Section 4.2

the cryogen system will become smaller (as discussed above), but the potential for a launch pad hold causing problems is correspondingly increased. Of the volume and mass of the system, the volume requirement is the one that causes the most trouble, as the mounting areas allocated for the instrument on the HH-G and SPAS platforms are not very large. Again, if the design goals are relaxed and the instrument is allowed to grow larger than a single mounting plate (see section 4.6), then additional space becomes available for the cryogen. The tradeoff is increased instrument complexity (cryogenic linkage between two independent plates) and increased experiment size, which demands more of the host platform and makes the instrument more intrusive. Another disadvantage is that filling of the cryogen requires access to the payload as close to the launch as possible, which could provide problems.

Summary: for the instrument and design goals being considered in this study, the mass and volume requirements imposed by solid cryogens precludes their use on the SBS camera. If the pre-launch holding time requirements are relaxed, then a solid cryogen system of manageable size could be accommodated within the SBS design envelope. Alternative cooling technologies exist that can meet the design requirements, and thus there is not a pressing need to relax those basic design goals.

4.2.4 Closed cycle mechanical coolers

Closed cycle coolers, or mechanical refrigerators, absorb heat at a cryogenic temperature and then reject it at a higher ambient temperature. The work that is required to accomplish this is provided by a compressor that compresses the gas and moves it through the system as required. The gas is raised to a high pressure, cooled in a heat exchanger to remove the heat of compression, and is then expanded to produce refrigeration. Typical coolers are hermetically sealed with helium gas used for the cooling repeatedly, leading to the name 'closed cycle coolers'.

There are three basic approaches to accomplishing this cooling that lead to four major types of mechanical coolers:

- (1) integral Stirling cycle cooler
- (2) split Stirling cycle cooler
- (3) integral Vuilleumier cycle cooler
- (4) Gifford-McMahon cycle cooler

The integral Stirling cycle cooler consists of a compressor and an expander section in a single mechanical package. The expander and compressor are run from a single crankshaft to maintain the proper phase relationship between the cooling stages throughout the system. This represents the most efficient design of the cryogenic cooling engines, in terms of work expended to cooling power obtained. The primary disadvantage is that the compressor and the heat exchanger are located near the detector being cooled. This usually leads to serious microphonics (vibrations) and causes problems in keeping the heat output away from the cooled detector. Integral Stirling engines usually are not built to have very high heat pumping capacities, at least in relation to the capacities determined necessary in section 4.2.1.

The operation of the split Stirling cycle cooler is very similar to that of the integral Stirling cycle cooler described above. The difference is the split system

Section 4.2

separates the compressor, motor, and heat exchanger from the gas expander unit. This gains the advantage of isolating the cooled item from vibrations and heat. The longer gas line that connects the two pieces adds a considerable amount of volume to the working gas, and this increased volume decreases the efficiency of the engine. Thus the tradeoff in this design is decreased cooler efficiency for a given energy input. On current designs the practical limit on the length of the gas line is 1 to 2 feet. Both types of Stirling engines are physically small and require relatively low levels of power. They are characterized by a relatively short operating life and relatively low levels of cooling power.

The integral Vuilleumier cycle cooler replaces the mechanical compressor present in a Stirling engine with a thermal compressor. The thermal compressor is present in a motor driven hot displacer and a gas driven cold displacer. The power input provided to the cooler moves the hot displacer back and forth. This reduces wear with corresponding increases in operating life, and also reduces power consumption. However, Vuilleumier cycle coolers are considerably less efficient than Stirling engines, so more power overall is required to provide the same level of cooling. Gifford-McMahon engines use a separate high speed compressor and low speed gas expander. These engines can be built physically large to provide large amounts of cooling (several watts), but they represent the physically largest and least thermally efficient of the cryo-engine technologies. The weight and power consumption of such an engine is typically very large compared to the design envelope for the SBS Camera, and thus are impractical under the current set of design goals.

One representative cooler with characteristics suitable for use in the SBS Camera is the CM-4 Cryogenic cooler manufactured by CTI-Cryogenics. This unit is a dc-brushless, 1 watt split-Stirling engine that cools to 77 degrees K. A picture of the unit is reproduced in Figure 4.2-3. This picture was taken from some promotional literature received from CTI-Cryogenics. Because of the split-Stirling design, the expander has to be located at the cooling points on the dewar, but the compressor section can be located several inches to a foot away in a more convenient location. The physical dimensions of the expander section are shown in Figure 4.2-4. Due to its small size, it would not be difficult to locate several of these expanders around a dewar of the size anticipated for the SBS Camera. The unit requires 45 watts of input power, which is reduced from most other split-Stirling coolers due to improvements in design. The cooldown time of the cold finger on the expander is only 3.5 minutes from room temperature to 77 K. One complete cooler unit weighs 3.5 lbs, and the compressor unit physical size is 3 inches diameter by 6 inches length. The MBTF is approximately 1000 hours of use. Note that this particular unit is not qualified to meet either military standards or for space use. It is intended to illustrate what can be attained using current technology (even though it is an older model). The acoustic noise output of the unit is an important consideration because of potential microphonic problems (discussed below).

Closed cycle mechanical coolers offer several design advantages for the SBS camera. Pre-launch hold times do not pose a problem to the cooling system, since the energy is not stored in a cold cryogen that is dissipating over time. Mechanical coolers can be cycled on and off repeatedly, allowing the system to be shut down when not required. No significant gas is vented from the instrument as in a solid cryogen system. Mechanical coolers are also quite reliable, at least in comparison to the mission times being considered for the SBS Camera. Typical Stirling machines,

Section 4.2

for example, have lifetimes on the order of 2500 to 3500 hours MTBF (the one discussed above has a MBTF of 1000 hours). While this is a serious problem for operational systems that must be on station for extended periods of time, this is not an important limitation for a design such as the SBS Camera, which will operate for less than 100 hours total on a typical mission. Military and space qualified versions have been developed under past programs and exist today.

Several very significant disadvantages exist to using a closed cycle system on this type of camera design. The two primary ones are cooling capacity and heat dissipation. The inherent inefficiency of these mechanical cooling engines leads to consumption of a relatively large amount of electrical power for a small amount of thermal cooling. Small closed cycle Stirling coolers exist with cooling capabilities on the order of 1 watt at 77 degrees K. Typically about 100 watts of electrical power is required to attain this level of cooling. Virtually all of this energy is converted into excess heat that must be dissipated in some manner. Engines with more than a watt of cooling power generally require additional heat exchangers beyond simple radiating metal sinks, and some require forced air cooling. The larger the cooling capacity, the larger the heat dissipation problem, which quickly becomes serious on a small system such as the SBS located in a space environment. To meet the performance goals determined in section 4.2.1, 3.5 watts of cooling power would be required for a cooldown of 5 hours duration, which represents a maximum acceptable cooldown time. This performance level could be approached using three split-Stirling coolers with 1 watt cooling capacity each of the type described above. Cooldown time would be increased to 6.3 hours (without any safety margin). Two of the cold fingers would be placed near the focal plane array, and one would be strategically placed at another point near maximum thermal mass on the dewar assembly. At least 135 watts of heat would have to be dissipated for 6 hours prior to system operation. Approximately one kilowatt of the total energy budget would also be expended for each system cooldown (this limitation is significant only on the SPAS, where the battery capacity puts a limit on the total energy consumption). Note that the loss of 6 hours of time might significantly impact upon the total time available for data collection on a mission. After the initial cooldown period, two engines could be shut off to conserve electrical power and serve as a backup in case of failure in the primary engine during camera operation.

The solution described above is practical within the constraints of the SBS payload design envelope. If this cooling approach was pursued, several engines would have to be procured, qualified to meet the requirements of flight on a shuttle payload, and testing would be required to see if the simple calculations done above can be realized in practice on a mock-up design of the dewar. Some additional disadvantages associated with mechanical coolers that would have to be considered in such a design are considered below.

An additional problem with mechanical coolers is the reduction in cooling capacity over time. Because of the steady mechanical wear on the seals of the pistons and other moving parts, leaks develop. As the seals leak, gas blows past the piston, which reduces the system efficiency. Pieces of the worn products from seals or pistons accumulate in the gas passages in the cooler, reducing efficiency over time. Leaks in the outer case introduce impurities into the helium gas, which also reduces cooler efficiency. Dry lubrication is done internal to the cooler with Teflon compounds and special greases, but these substances have limited lifetimes.

Section 4.2

Fortunately, these processes occur over a period of time that is large (several hundred hours) in comparison to the total on-station time requirements of the SBS Camera payload, and thus are not considered to impose a significant limitation.

The use of mechanical coolers can introduce problems related to microphonics and thermophonics. Microphonics are defined as steady mechanical vibrations induced by the cyclic operation of the cooler compressor. This type of vibration can potentially induce systematic noise into the Schottky-diode detector output. Microphonic problems have been encountered in PtSi imagers that have used cryo-engines in the past. This problem can usually be reduced or corrected by putting mechanical damping into the system to reduce the amplitude of the vibrations. Thermophonics are fluctuations in the temperature of the cold finger of the cooling engine. The cold finger of these engines typically varies in temperature by a number of millidegrees as the device works through its cooling cycle. These variations in temperature can have serious effects on the operation of the Schottky-diode detector array, since the response of the array is known to be a strong function of temperature in certain operating regions. The problem can be reduced by adding a thermal mass that acts as a temperature buffer between the cold finger and the detector, but this adds to the total load that must be cooled before the camera can begin operation.

In summary: split-Stirling engines represent a cooling technology that could be used on the SBS Camera payload. Their cooling capacity is relatively low, but current models are small enough (in terms of power consumption and physical size) to allow the use of several cooling units in the payload. Thus the advantages of long pre-launch hold time and repeated cycling can be realized. These advantages must be offset against the increased power consumption, increase in cooldown time, and large heat dissipation that must be dealt with.

4.2.5 Joule-Thompson cryostats

A Joule-Thompson cooling system is basically an open cycle cooling technology in which high pressure gas is expanded in a Joule-Thompson expansion valve. The Joule-Thompson effect uses the ratio of temperature change to pressure change in a real gas during expansion. The internal energy changes during expansion, and cooling results. A schematic diagram of a Joule-Thompson cooling system is shown in Figure 4.2-5. High pressure gas enters the top and travels through a long finned tube with a large surface area. This pre-cools the incoming gas, since this finned tube is in contact with the exhaust of spent gas that has already been expanded and is still cold. The gas then passes through the orifice, where it expands rapidly and is cooled and liquifies. The stream of liquid is directed to flow along the surface of the container to maintain good thermal contact. The liquid stays along the walls (held by surface tension), while the evaporated gas separates from the liquid and is collected in the center. The liquified gas collects at the bottom of the container in a reservoir that provides the needed cryogenic cooling. The exhaust gas travels back up through the heat exchanger and is eventually vented away.

The amount of cooling attained is directly related to the orifice diameter and the pressure of the incoming gas. Simple Joule-Thompson cryostats have fixed orifices, and the gas flow (and resulting refrigeration) varies only with the source gas pressure. Other Joule-Thompson cryostats have variable diameter orifices that allow

Section 4.2

the amount of refrigeration to be regulated as desired. This study will not go through an extensive of Joule-Thompson coolers, as this is readily available in the published literature. The relevant issues for this study are the amounts of gas storage required, as well as the total cooling system volume, weight, and power required to provide adequate cooling for the SBS Camera dewar. The refrigeration capacity is directly related to the total mass and pressure of the stored gas. The cooling produced can be related to the change in enthalpy in the cryogen caused by the Joule-Thompson effect as shown by

$$Q_R = H_a - H_b$$

where

Q_R = ideal refrigeration in watts-minute/liter of gas
 H_a = enthalpy of gas leaving cryostat
 H_b = enthalpy of gas entering the cryostat

Solutions of this equation for nitrogen and argon gas, two commonly used gases to produce temperatures in the range required for the Schottky-diode detector, are shown in Figure 4.2-6. This plot allows the selection of an input pressure for the gas storage bottle. Note that there are optimum pressures for refrigeration capacity and that they are different for the two gases. These maximum values of refrigeration are not the optimum pressures for total system cooling capacity, because even though the heat absorbed per liter of gas flow decreases at higher pressures, the total amount of gas continues to increase. This plot simplifies calculation of the gas quantity required to meet the performance specifications of the SBS Camera cooling system. The volume of gas required to produce a given amount of refrigeration for a given period of time can be expressed as

$$V = \frac{T * Q_1}{(P_t - P_{op}) * Q_r}$$

where

V = water capacity of the gas tank in liters
 T = time in minutes required to maintain cooling
 Q_1 = specified refrigeration in watts
 P_t = operating pressure of tank in psi
 P_{op} = operating pressure of cryostat in psi
 Q_r^{op} = ideal refrigeration in watts-minute/liter

Most, but not all, of the gas stored in the cylinder can be used for cooling, because eventually the pressure in the tank drops below the cryostat operating pressure. This fact is incorporated in the above equation. The above equation is based upon a more detailed discussion giving its derivation in the J. Buller article [].

Now the tank volume required can be calculated for the following two operating conditions: cooldown and camera operation. For simplicity (and brevity) it will be assumed that the tank pressure = 6000 psi, which results in a $Q_r = 0.87$ for nitrogen and 1.37 for argon. The regulator cut-off pressure will be set at 500 psi, which is a

Section 4.2

reasonable value.

(1) initial cooldown: 1 hr cooldown needs 13.4 watts
5 hr cooldown needs 3.5 watts (derived in section 4.2.1)

	water volume of tank (liters)	
	<u>nitrogen</u>	<u>argon</u>
for 2 cooldowns of 1 hour:	.34	.21
for 2 cooldowns of 5 hours:	.44	.28

Note that the slower cooldown rate requires slightly more gas.

(2) operating condition: 1.1 watt constant loss

	water volume of tank (liters)	
	<u>nitrogen</u>	<u>argon</u>
for 2 runs of 5 hours:	.14	.09

Thus the total volume nominally required for nitrogen gas is 0.92 liters (920 cubic centimeters), while for argon it is 0.58 liters (580 cubic centimeters). This translates into a fairly small bottle, and the mass is not unreasonable. For example, a bottle with an internal radius of 4 cm and a length of about 20 cm would meet the requirement shown above for nitrogen. It is easy to add safety margin into this allocation of stored gas, which is important, since these are only rough calculations, and extra margin would be needed. Note that newer gas mixtures (of a proprietary nature) exist that give substantially enhanced cooling capacity, and thus the volumes and total mass of gas could be decreased even further if required.

Many candidate coolers exist with individual cooling capacities ranging from milliwatts up to 10 watts cooling capacity. It must be realized that the primary market for Joule-Thompson coolers over the past several years has been guided missile applications: a system that contains a heat seeking infrared sensor. In this type of system, small cooler size and very rapid cooldown times (room temperature to 77 K in a matter of seconds) are part of the operational requirements. Usually only the detector is cooled in this application, so thermal capacities on the order of one-quarter to one-half of a watt are typical, although higher capacity systems have been sold. Other current markets include instrumentation that requires small amounts of cooling (in probes) to operate. Coolers with capacities up to 10 watts using standard gases are marketed by Air Products of PA.

Hybrid Joule-Thompson coolers have been described [SPIE, 1982]. These two stage coolers, used for space applications, have a pre-cooling stage where the temperature of the gas is dropped using a passive radiative cooler. This increases the efficiency of the system. These hybrid coolers can also be used to provide cooling on demand (as opposed to continuous cooling), which allows the system to match its cooling capacity (which might be several watts of refrigeration when operating), to the thermal losses experienced by the dewar, which might be 1 watt or less. This type of Joule-Thompson system provides a significant quantity of liquid cryogen, and then shuts off. With the expander non-operational, it is possible to control the

Section 4.2

pressure of the liquid, thus adjusting its temperature. Indeed, the pressure can be reduced enough to solidify the cryogen to result in additional cooling. Contact between the liquid and the walls of the dewar (the cold finger) is maintained by having a metal honeycomb structure on the walls of the chamber, which holds the liquid to it using surface tension and thus works even in zero gravity conditions.

There are several advantages to using Joule-Thompson coolers in the SBS payload. First is the availability of the large cooling capacities required for fairly rapid cooldown of the dewar (on the order of 1 hour time). A second advantage is the very low electrical power consumption by the system, as the only power it would use would be monitoring and operating of the gas valves in it. This level of power consumption would be on the order of a few watts, which reduces the heat that must be dissipated and is an important advantage in the limited power budget on the SPAS. A third advantage is the large amount of safety margin that can be provided while still staying within the SBS design envelope. An ample amount of gas (even double the minimum required) could be provided as safety against component failure, gas leaks, or thermal leaks developing during a mission. Finally, since the cryogen is stored as a gas under pressure, pre-launch delays do not result in the significant loss of cryogen, so this type of cooling system can tolerate potentially large delays without losing its cooling capacity.

These advantages are partially offset by several disadvantages to Joule-Thompson cryostats. A common problem encountered is clogging of the orifice, which causes the cooler to stop operating. This is frequently caused by impurities in the gas such as water, which can ice up the orifice opening. Very high purity gas is required for this type of system. Once an orifice ices up, it is effectively lost, because even if it is thawed it is likely to re-freeze once it is used again. Another problem encountered in the use of these coolers is microphonics, which results from vibrations set up in the orifice by the flow past of the high pressure gas. A third disadvantage is that spent gas must be released out into the environment, though if relatively inert gases (such as nitrogen or argon) are used, this should pose no safety hazard. Finally, these coolers require that a significant quantity of gas be stored at a fairly high pressure. Special provisions would be required to prevent damage and subsequent rupture of these tanks, which could cause serious damage to the payload.

In summary: Joule-Thompson cryostats represent a technology capable of meeting the cryogenic cooling requirements of the SBS Camera. The system has large cooling capacities (relative to the SBS cooling requirements), has a fairly small volume and weight, and consumes very little electrical power.

4.2.6 Summary

The cooling system performance requirements for the SBS Camera have been derived and described, in accordance with the design goals of the camera and the payload restraints. The cooling of the detector, aperture stops, and a bandpass filter wheel pose a significant but achievable thermal load for this system. Four primary cryogenic technologies have been identified that could be used to provide this cooling. Of these, two have been shown to be capable of meeting the requirements within the payload restraints: mechanical cryo-engines using a split-Stirling design, and Joule-Thompson cryostats. SRL believes that the Joule-Thompson technology is the better of the two systems for the SBS Camera for the following reasons:

Section 4.2

(1) physical considerations

In terms of overall cooler volume and weight, the mechanical cooling systems are significantly smaller than a complete Joule-Thompson system. But the size of the expansion orifices used on J-T systems are significantly smaller than the example expander shown in Figure 4.2-4. This smaller size will ease interface to the dewar. In addition, the gas storage bottles for the J-T coolers can be located anywhere on the payload, while the split Stirling engine(s) would need to be within a foot of the dewar. Thus the J-T system offers increased flexibility in payload design.

(2) lower power consumption and heat generation

This is the primary advantage that J-T coolers have over a mechanical cryo-cooler. A split-Stirling system would require at least a kilowatt of payload power for each dewar cooldown and would then consume power at a continuous rate of around 50 watts. This represents a significant fraction of the total payload power budget in a platform such as the SPAS, which must rely on batteries for power while on station. A Joule-Thompson system would only consume the power required to monitor temperature and operate the gas valves, which should be on the order of a few watts. In addition to the electrical power load reduction, Joule-Thompson coolers do not have the potentially significant heat dissipation problems that mechanical coolers would face.

(3) faster cooldown time

The sample calculations included in the discussion above indicate that a 1 hour system cooldown could be achieved with a Joule-Thompson system, while a cryo-engine based system would require at least 6 hours for each dewar cooldown.

(4) additional safety margin

The proposed configuration for the mechanical engine cooling system described above could just meet the performance requirements. In order to provide some safety margin into the system, additional cooling systems would be needed, increasing weight, power consumption, and heat dissipation problems. The Joule-Thompson system has considerable additional margin in which additional cryogen (gas) could be stored, as well as additional coolers. The J-T system thus possesses additional, but probably required, room for a safety margin.

This selection of a Joule-Thompson based cooling technology was based on the understanding of the system design requirements and performance goals as detailed here. If the mission requirements for the SBS Camera change significantly, this selection could change, and the other technologies could look more promising. In particular, if pre-launch hold time requirements were relaxed (which is not recommended), then a solid cryogen system would also become a viable option for this payload.

4.3 Signal processing

4.3.1 Theoretical Approach

This section will treat the image processing proposed for the new SBS Camera system. This image processing, performed in real time on the array data before it is recorded on mass storage, is based on previous work done with the SAIRS series of cameras built jointly between RADC and AFGL. The electronics in these cameras represents the most advanced image correction scheme currently implemented for PtSi cameras. These systems have been designed and built by Dr. William Ewing of RADC.

The basic philosophy behind these image corrections involves three steps: convert the array signal to a digital data stream as close to the dewar as possible, correct for array defects and pattern noise, and then convert the data to a form suitable for recording. All processing applied to the image data is done solely to remove array artifacts and defects in order to increase the sensitivity of the camera. No 'advanced' image processing, such as algorithmic target detection, edge enhancement, etc., is done in the SAIRS design, as the goal for that camera was to provide a source of noise free and radiometrically accurate image data. The processing applied in the SAIRS cameras is referred to as image compensation.

The presence of real-time image compensation in the SBS is important because it can significantly extend the performance of the camera system. The ultimate design goal for infrared cameras is to operate in a regime where the noise floor in the data is determined by the random statistical variations in the photon flux of the instrument background. This condition, commonly referred to as background limited (BLIP) operation, describes the best that can be theoretically attained in an infrared sensor. Shephard and Mooney have shown that reductions in the instrument noise floor alone are not sufficient to attain BLIP operation in an infrared camera under all conditions. They have demonstrated that non-uniformities in the detector array cause a fixed pattern noise, or sensor imprint, that reduces the camera's contrast signal-to-noise ratio. This additional noise source becomes dominant with even small amounts of detector non-uniformity, preventing BLIP performance of the system. In their analysis the mean square total noise (in electrons) in the array output is shown equal to

$$N_n^2 = N_f^2 + N_b + UN_b^2 \quad (4.3-1)$$

where N_f represents the camera noise floor, which is caused by all of the system noise mechanisms that operate independently of the camera signal. N_b is the statistical shot noise in the IR background. UN_b is the fixed pattern noise caused by modulation of the infrared scene by the detector array non-uniformity. This non-uniformity term is the dominant noise term that prevents BLIP operation even if the array non-uniformity in response is as low as 1%. Thus image compensation, which reduces the magnitude of the fixed pattern noise in the detector output, plays a significant role in improving the overall performance of the camera system. Its value goes beyond simple cosmetic improvements in the imagery collected. Improvements in system performance of PtSi cameras through array compensation have been demonstrated and reported in the published literature.

Section 4.3

Uncompensated array data does give credible images on the currently available CCD readout arrays used at RCA and RADC. Image defects exist, however, in even the best arrays. Gross defects, such as dead or non-functioning pixels, occasionally show up. More typical defects show up as responsivity and dark current variations in pixels across the focal plane array. Such defects are caused by diverse factors such as nonuniformities in dopants or treatment during the array manufacturing process. The transfer efficiencies of all the CCD readout registers are not equal over the chip. The active sensing area varies from pixel to pixel because of limitations in the lithographic techniques used to manufacture the chips. Shading or other optical flaws can also introduce image defects. In particular, shading proportional to the fourth power of the cosine of the angle of each pixel's field of view from the optical axis is unavoidable, and can become significant for physically large arrays. These defects form an image pattern that contains no information about the observed scene, and are thus a form of image noise. Such reductions can be achieved using fairly straightforward image processing techniques. A second class of defects involves single pixels in the array that are faulty or shorted. These 'bad' image pixel values can be mapped out in the laboratory and can be replaced in real time by the value of neighboring detectors that are operating. This type of processing, which preserves the subjective quality of the image, is separate from the image processing described below.

The solution to reducing this fixed pattern noise has been to build electronics that applies corrections to the image on a pixel by pixel basis. Currently a gain and a level correction are applied to the PtSi image data in SAIRS. The level correction reduces defects caused by dark current and optical shading variations from pixel to pixel. The gain correction reduces pattern noise caused by responsivity variations. This type of processing can be described as a '2 point' correction of the form $y = mx + b$, where 'x' is the original pixel value, 'm' is the gain correction, 'b' is the offset correction, and 'y' is the new corrected pixel value. A straightforward implementation of this would require two arithmetic steps: first an offset would be subtracted from the pixel, and then a gain term would be multiplied in. Work by B. Ewing at RADC has indicated that better performance can be obtained by using a modified '3 point' correction of the form $y = m(x + b/m) + b'$. Algebraically, this is an identical process to the two point correction described above. In practical terms, the modified three point correction splits the offset correction into two separate steps: the correction for a fixed offset and a scene variable offset. To minimize the possibilities of arithmetic overflow, it is desirable to apply the fixed offset correction first before multiplying. After multiplying, the second offset, measured by the instrument off a uniform calibration source, is then subtracted. The fixed offset is stored in non-volatile storage (PROM) and does not change from data run to data run. The other offset is collected by the instrument and stored in RAM, where it can vary from data run to data run. The primary advantage to this approach is that it allows fixed problems to the array to be corrected for, while the second offset compensates for smaller magnitude variations caused by changes in the instrument over time. Examples of such changes include filter bandpass changes, or increases in the optics temperature. This correction approach improves the image compensation when the average value of the scene moves away from room temperature, and improves it over the total dynamic range of the instrument.

The implementation of this image compensation can be seen in the block diagram showing the signal path in the existing SAIRS instruments. This is shown in Figure

Section 4.3

4.3-1. Signal compensation is applied in the following order. First is a background subtraction using values stored in a bank of PROM memory. These values are determined in laboratory calibrations and are different for each detector array. They are stored as 39040 values of 12 bits each. The second image processing step is the responsivity multiplication. The responsivity values for each pixel are again predetermined in the laboratory by measuring the array output while viewing two calibrators at different temperatures. The responsivity values are chosen so that every pixel in the array will output the same size digital step between the two sources. The current SAIRS has a single set of stored responsivity constants, one per pixel. Recent experience has shown that these numbers change slightly for different wavelength bandpasses, and so the responsivity is a function of both wavelength and band width. An optimum system would have a set of constants stored for each filter position, and would switch to the appropriate bank of PROM for each filter. This significantly increases the PROM storage requirements; with capacities of PROMs steadily increasing, however, this approach may prove practical for the SBS camera. Similarly, the responsivity values change slightly as a function of scene signal, so the quality of the correction is not maintained over the entire dynamic range of the instrument.

The third image correction applied in the SAIRS is the second background offset correction (b' in the sample equation shown above). This background correction is determined by observing a cold reference source (usually cooled to liquid nitrogen, or 77 K) with the camera. The differences in signal level between the array pixels and an arbitrary digital pedestal are stored in a bank of RAM. These differences represent the residue of offset errors present in the data after the fixed level and gain corrections have been applied. Now when the camera outputs pixel values corresponding to the temperature of the cold calibrator, pixel values equal to the digital pedestal will be output. The instrument is radiometrically calibrated in reference to this pedestal. Note that there is no special requirement that the stored background calibrator has to be at a zero or very low radiance value. Any radiance reference will do; care must be taken, if the reference is warm, that the digital pedestal is chosen so that cold features observed by the camera will not result in digital overflows during processing. This is an advantage for a remotely operated camera such as the SBS, where it may not be practical to provide a 77 degree K calibration source.

To reduce the noise in this stored background image of the cold calibrator, many frames are collected and the results are averaged together to come up with the final value of the correction. This frame averaging reduces the pattern noise in the stored correction by approximately the square root of the number of frames averaged. The Ewing SPIE paper [] contains an expression (from Shepherd) that can be used to estimate the minimum number of frames needed to minimize random fluctuations in the background. This expression is

$$k = \frac{N_{bl} + N_f^2 F^2}{N_f^2 F^2} \quad (4.3-2)$$

where

k = number of frames to be averaged

Section 4.3

N_f = number of noise electrons at the device temporal noise floor

N_{bl} = number of background electrons per pixel with f/l cold shielding

F = operating F number

This equation can be used to estimate the effect of changing the number of frames averaged in. The older 64 x 128 element cameras averaged in 16 frames, while the current SAIRS design averages 256 frames. The advantage of increasing the number of frames is the reduction in residual pattern noise. The disadvantage of increasing this number is the increase in the number of bits per storage needed to prevent overflow. In addition, the time required to collect the background image increases. For example, at 30 frames per second, the current SAIRS operating rate, the collection of a background requires about 8 seconds of time. This time requirement may adversely impact on missions that require filter changes while measuring events of relatively short time duration. This last correction is the one step that requires special actions by the camera while collecting target data. The actual operating procedure is simple. The camera is put into a 'background average' mode using its control console. A uniform cold calibrator is placed directly in front of the lens, to provide an unfocused (and thus uniform) radiance scene. The system collects 256 frames and computes their average, which is stored into RAM. The operating mode is then changed, so that this collected background will be subtracted off the image data in real time. The camera is then ready for operation.

4.3.2 Calibration of recorded signal

A procedure to relate the detector array output voltage to the energy incident on the detector focal plane has already been described in section 2.4. It is now important to follow the path of that detector voltage through the camera electronics to determine the relation between the detector voltage and the signal recorded away onto data tape. This will be examined from a radiometric calibration point of view, and all parameters needed to recreate the original voltage will be determined. It is important that all required parameters are recorded away in some form, or else the calibratability of the data will be lost.

During a data mission the detector output voltage is not directly recorded, but rather a signal that has had various gain and level corrections applied to it. It is essential to be able to trace backwards through the electronics after the fact to remove all of these signal modifications to derive the detector output voltage. The signal path block diagram is an important start in this direction. This discussion will use the SAIRS signal block diagram as an example, since the basic signal processing proposed for the SBS Camera will be modeled closely after the SAIRS design. The SAIRS block diagram has already been presented in Figure 4.3-1. This discussion will assume that the recorded signal is an RS-170 video waveform representing the scene, as is used in SAIRS. This will not be an exhaustively detailed analysis, since the actual circuitry in the SBS will be considerably different from that used in SAIRS, but instead this will work through the modeling process in a general sense to demonstrate what is required.

This derivation builds a general equation showing the relationship between the recorded signal, V_{rec} , to the detector output signal, E_{out} . In the system architecture

Section 4.3

shown in Figure 4.3-1 there are 6 major points where the signal is modified before it is digitally recorded:

- (1) sample/hold and conversion to digital value
- (2) defective pixel replacement
- (3) first background subtraction
- (4) responsivity multiplication
- (5) second background subtraction
- (6) scan conversion buffer

The analog tracking signal passes through 4 additional stages:

- (1) level control (digital addition)
- (2) gain control (digital look-up table)
- (3) D/A conversion
- (4) video signal generation

Each of these signal points will be discussed in order.

- (1) sample/hold and A/D conversion

The sampling and conversion of the detector voltage output to a digital value is a very critical point in the signal path. Errors in the conversion will be preserved throughout the digital signal path. In addition, the data is still susceptible at this point to the addition of analog noise. It is extremely important to use a high quality A/D converter and to accurately know its limitations. In basic terms, the converter must have adequate speed (faster than a 1.2 MHz pixel clock rate for a 160 x 244 detector array), resolution (12 bits, which approximately matches the 70 dB dynamic range of PtSi detectors), and must be matched to the chip output impedance. The converter must have absolute accuracy in its conversion. Other parameters that have an important impact on converter performance include conversion linearity, slew rate, and noise immunity. Poor linearity can introduce errors, slew rate errors introduce phase error into rapidly changing signals. Many high speed converters have the speed and the absolute accuracy required, but exhibit poor linearity and slew rate performance. The existing SAIRS designs use the commercially available Analog Devices MOD-1205 converter module. The specifications of this module are summarized in Figure 4.3-2. This unit is a combination sample/hold and A/D module that has 12 bits of resolution at a maximum conversion rate of 5 MHz. The voltage range is -2.048 to 2.048 volts, which sets the LSB at 1 mV. The entire unit is contained on a 5 x 5.5 inch PC board, and dissipates 13 watts of heat, so provisions for cooling must be made. Improved units have become available from Analog Devices, but a ruggedized system meeting applicable MIL-SPECS that is capable of the required performance has not been located to date.

As the signal is sampled and converted to a digital value, it is modified by the conversion electronics. Thus the digital signal can be related to the detector output signal by the relation $V_i = f_{A/D}(E_{out})$. Note that if the A/D is perfectly linear, this function would simply be a linear fit of digital values to the input voltage, as is true for the MOD-1205 used in the SAIRS.

- (2) defective pixel replacement

Section 4.3

After the analog to digital conversion, the data is read out of the unit and latched. At this point defective (dead) pixels are replaced by the values of neighboring pixels. The map of bad pixel locations is stored in a PROM (that is different for each individual array). On the best currently available arrays, there may be as few as no replacements required. The overall impact of this replacement on the signal calibration is small for extended sources. One must be careful in evaluating data collected on a point target that moves into a region where these dead pixels are located. If there are no pixel replacements, there is no modification to the detector signal, and $V_2 = V_1 = f_{A/D}(E_{out})$. If the number of pixel replacements is small relative to the total number of pixels in the array, which is a reasonable assumption given the current state of the art in arrays, the total average signal value (viewing an extended source of many pixels) will also be small. This substitution can cause artifacts (such as the disappearance of a source on a replaced pixel), which emphasizes the importance of using a defect free array.

(3) first background subtraction

The third modification applied to the detector signal is the first background subtraction used in the image compensation scheme. This subtraction is applied using a 20 bit wide ALU. The values subtracted off are stored in a PROM (determined in laboratory measurements for the specific detector array), so it is easy to determine this subtraction after the fact. As before, the subtraction is applied on a pixel by pixel basis, so the value is potentially different for each detector pixel in the array. This correction is denoted by B_1 . Note that this correction is tied to an average reference pixel value located in the center of the array, and the total background subtraction corrects for pixel deviations from the average value. The DC level information is not completely lost. The model has now grown to

$$V_3 = V_2 + B_1 = f_{A/D}(E_{out}) + B_1 \quad (4.3-3)$$

(4) responsivity multiplication

The pixels in the data stream are now multiplied by the fixed set of responsivity constants stored in another PROM. This is the second step in the image compensation scheme. Again, these numbers are fixed values, so it is easy to determine the magnitude of this correction after the fact. The multiplication takes place in a 16 bit wide multiplier. The effect of the response multiplication is denoted by the symbol M . The model now becomes

$$V_4 = V_3 * M = (f_{A/D}(E_{out}) + B_1) * M \quad (4.3-4)$$

(5) second background subtraction

Now the background values stored in RAM are subtracted off the pixels in the data stream. This is the third step in the image compensation scheme. Correction of this effect is more complicated than before because the pixel by pixel values being subtracted off are stored in RAM and are not preserved when the instrument is powered off. Every time a new background average is collected by the instrument, these values change. There are two possible solutions to preserving this information. First, provision can be made to record away these 39040 pixel values so that the

Section 4.3

subtraction can eventually be measured during data calibration. If the recording method is digital, these pixels can be read out of RAM at some convenient point and inserted into the recorder data stream. If the recorder stores an analog video signal, the RAM bank could be read out and converted into a video image for recording. A second approach is to make an assumption about how this second background subtraction works. This approach assumes that the net result of this second background subtraction is to perfectly normalize the scene values to the radiance of the calibration source used during the background average. Then, when the camera observes an object with a radiance equal to the calibration source, its output will be equal to the digital pedestal built into the instrument output. This assumption requires the image compensation process to be working perfectly. In practice this is a reasonable assumption for scenes with radiances near the value used for the background average, but its accuracy decreases as the scene radiance moves away from the background average value. The first solution to this problem is more exact, but the second approach is frequently the one used in practice, since it is easier. In the SBS Camera provision should be made to record away the contents of this RAM for later analysis. This correction will be denoted in the model as B_2 . The model now becomes

$$V_5 = V_4 + B_2 = ((f_{A/D}(E_{out}) + B_1) * M) + B_2 \quad (4.3-5)$$

(6) scan conversion buffer

The frame buffer and scan converter consists of 2 banks of RAM memory. Data is read into memory and is re-formatted to build a spatially correct image (the main correction that must be made is removal of the interlace effect in the array readout). As data from the current frame is read into one bank of RAM, the other bank, which contains the previous data frame, is read out and proceeds towards the camera output. The functions of the two banks of RAM toggle back and forth as image frames are collected. Thus a time delay of one frame time is introduced into the data stream during scan conversion. This time delay is on the order of 1/30 of a second and is usually too short to be noticed during visual inspection of the data. Note that scan conversion simply reorganizes the pixels, and does not change either individual pixel values or the total frame average value. Thus the model equation which we have been building is unchanged by this step.

Note that if a full resolution digital recorder is included in the SBS Camera system, the signal is now ready to be recorded away for later analysis. It is assumed that the digital recorder will store the pixel values exactly as they are present in the image data stream. In practice, a certain level of pixel errors are tolerated in current HDDR digital recorders (see section 4.4) that is fairly high. This error addition is a source of noise, but will be considered small enough to be ignored in this analysis. The relationship between the digitally recorded voltage, V_{rec} , and the detector output voltage is now

$$V_{rec} = (((f_{A/D}(E_{out}) + B_1) * M) + B_2) \quad (4.3-6)$$

This can be solved for E_{out} :

Section 4.3

$$f_{A/D}(E_{out}) = \left(\frac{V_{rec} - B_2}{M} \right) - B_1 \quad (4.3-7)$$

If the analog-to-digital converter is assumed to be a completely linear system, the $f_{A/D}(E_{out})$ can be replaced by a linear function, and so the equation becomes

$$f_{A/D}(E_{out}) = M_{A/D}(E_{out}) + B_{A/D} \quad (4.3-8)$$

The detector voltage is solved for directly:

$$E_{out} = \frac{1}{M} \left(\left(\frac{V_{rec} - B_2}{M} \right) - B_1 \right) - B_{A/D} \quad (4.3-9)$$

This equation illustrates the parameters that need to be measured in order to be able to analyze the recorded digital signal. The A/D converter slope and offset should be constant; thus one only requires knowledge of the two additive corrections and the multiplicative response. All of these numbers are stored in PROMs except for the second additive response B_2 , which is stored in a RAM bank. This equation allows conversion of the recorded signal to the detector output voltage, which can then be calibrated as described in section 2.4.

The SAIRS system outputs its focal plane imagery as an analog video signal. It is anticipated that a video image of the camera data in real time would be very useful for target acquisition and tracking that would be done by a ground operator of the SBS Camera system. Such a process is dependent on the types of telemetry links made available to the SBS payload (see section 4.6). The design of the real-time imagery section will likely be closely paralleled after the SAIRS video circuitry. As the signal block diagram in Figure 4.3-1 shows, this primarily involves the addition of level and gain controls, and conversion from a digital to an analog signal. It is expected that this signal will be analog recorded at the ground or shuttle tracking site to serve as a backup copy of the data in case of failure in the primary data recorder. Thus some discussion will be made of the level and gain controls and the digital-to-analog conversion process.

Once the pixel data leaves the scan conversion memory banks it has a level control applied to it. The signal level is controlled by the addition of a digital value selected by an operator control on the instrument console. As the SAIRS block diagram shows, it is basically just an ALU that adds a digital offset to every pixel in the data stream. Its use is in adjusting the signal level to improve the cosmetic appearance of the instrument output (which, for the SAIRS, is a video signal). It allows the instrument operator to select a portion of the total dynamic range of the instrument for display. This is important because of the dynamic range limitations of standard video, which does not have adequate dynamic range to hold all 12 bits of resolution. Note that this level control should be completely independent of the gain control (described in step 9). It is also important in the instrument design to synchronize controls such as the level control with the frame timing of the data. Controls should not be allowed to make changes to the data until the current frame is completed. This prevents the level value from changing in the middle of a frame,

Section 4.3

which will render the data uncalibratable.

At this point a gain control may also be applied to the digital signal, in order to control the bottom and top levels of the scene contrast observed in the final video image. By viewing only a selected portion of the total dynamic range of the sensor, it is possible to view the scene at a higher effective dynamic range, which can be useful for tasks such as acquiring and tracking faint targets. The current SAIRS system uses an analog attenuator that exhibits non-linearities in its response. It is simpler, and more effective, to use a digital attenuation system. A digital system would employ a series of pre-calculated look-up tables that would map the incoming 12 bits of data to a new set of 12 bits of output data. The higher the 'gain', the sharper the slope of the values in the look-up table. Indeed, for assistance in tracking, non-linear image compression schemes could be implemented in the calculation of the look-up table without affecting the primary data signal. This look-up table could be implemented using simply a few PROMs loaded with the appropriate numbers. Each gain setting would require 4096 locations, and so a number of gain settings could be provided in a small number of PROMs.

The next step in the SAIRS signal path is the digital to analog conversion of the data stream. The D/A converter takes the digital pixel stream and converts it into a voltage proportional to the digital value. Highly accurate D/A converters exist and are available for data rates of 1.2 MHz. The SAIRS system employs an 8 bit converter. Higher resolution converters (up to 12 bits) are available, but due to analog limitations the extra dynamic range is expected to result in little difference (each 12 bit step in a video signal corresponds to 173 microvolts, which is likely to be below the noise level of a typical transmitted video signal via a telemetry link). This level of resolution is certainly beyond the performance of typical analog recorders (40 dB of range - see section 4.4).

The data signal is now converted into a form suitable for transmission and recording. In the case of the SBS (and the SAIRS), this involves conversion to an RS-170 standard video waveform. This involves adding horizontal and vertical synchronization waveforms, vertical blanking, and matching the timing phase of the video signal. The voltage representing pixel intensity is forced to fit the RS-170 specification (discussed in section 4.4), which means it must range from 0 to 0.714 volts. The video signal is then transmitted for viewing and recording.

Note that the analysis applied to the digital pixels above could be easily extended to apply to the analog video output as well. This would simply require the addition of a few additional terms to the basic equation relating the recorded voltage V_{rec} to the detector output voltage E_{out} . It is recommended strongly that this analysis be completed before any mission, to allow calibration of the recorded analog video signal in case of a failure in the primary digital recorder.

This elaborate analysis is crucial to the calibration of the recorded data. Having this model expressed in the general form shown above allows a model of the instrument to be written into a computer program that simply takes the image data and instrument housekeeping information and converts the pixel intensities into inband scene radiances. An additional important benefit is the ability to model changes made to the instrument by simply changing individual terms in the model as required.

Section 4.3

In summary, a list can now be constructed of the parameters that must be stored during data collection for later calibration of the focal plane data. For calibration of the detector output voltage, as described in section 2.4, the following parameters need to be stored: the optics temperature, the detector temperature, the filter bandpass, and the fixed detector array parameters. To calibrate the recorded digital signal, the pixel by pixel image of the second background subtraction (from RAM) must be stored. All other values are stored in fixed PROMs, which can be accessed after the mission. Finally, for calibration of the video signal in case of digital recorder failure, the gain and level controls must be recorded, and the characteristics of the telemetry link and analog recorder used must be characterized.

4.3.3 Physical considerations

The physical size and layout of the processing electronics is an important consideration in the design of the system, since this has a significant impact on what can be done. All of the SAIRS processing circuitry has been constructed on separate boards mounted on a multi-slot bus structure. Use of this type of bus structure allows similar functions to be grouped on boards, and having separate physical boards allows easy replacement of or debugging of board problems. The construction of the SAIRS circuitry by RADC has been standardized on the basic double-VME bus board. The physical dimensions of one of these boards is shown in Figure 4.3-3. These boards have a well-designed slot connector that has demonstrated a fairly high physical reliability during aircraft and other field deployments of the SAIRS system. Other advantages of using this basic design have included wide availability of prototyping boards, final board fabrication tools, and standard bus enclosures. An illustration showing the physical dimensions of a 9 slot VME-bus backplane is shown in Figure 4.3-4. Twelve slot backplanes are also available from a variety of vendors.

The current SAIRS processing card cage has a separate mount for the analog-to-digital converter and then a card cage that is capable of holding 9 of these double-width cards. All of the actual circuitry in the current design is contained on 7 double-VME cards. The wiring is done using 'stitch-weld' type wiring. A standard VME bus backplane is used for the card slot connections, although the wiring of the backplane does not follow standard VME bus conventions. Informal discussions with Dr. Ewing of RADC have indicated that the current design can be compressed to considerably less space, since further space constraints were not a factor in the SAIRS electronics design. This device is then mounted in a 19 inch rack-mounted chassis for general use.

Power dissipation is another concern for the SBS payload design. Informal discussions have indicated that approximately 100 watts of electrical power are dissipated in the image compensation electronics in the SAIRS system. Very little attempt to conserve power was made in the design of the system, however, and it is believed that the power consumption could be reduced considerably. The reductions in power consumption through improved low power design, however, would be at least partially offset by the additions of diagnostic and backup circuitry to the basic system design (discussed in section 4.5). The initial design for the processing electronics chassis will thus assume a power dissipation of 100 watts for thermal calculations.

Section 4.3

The anticipated slot allocation in a 12 slot backplane for the SBS camera is 6 slots of image compensation electronics. The outer physical dimensions and additional detail of this enclosure is covered more completely in section 6. This would leave 6 additional slots unused. The analog-to-digital conversion system should also be moved to a single card in this backplane, with a shielded cable connecting it to the dewar output. Note that the new CAV-1205 converters from Analog Devices meet the performance specifications and are designed to mount directly in a VME bus system, so the converter could be purchased already mounted on this system. Careful provision for adequate cooling would have to be made to dissipate the large amounts of heat generated from the converter in the chassis (10 to 13 watts).

4.3.4 Redundancy requirements

Redundancy can be expensive in terms of space and power consumption in a small payload such as the SBS Camera, but the cost of backing up critical components is usually repaid through a level of improved system reliability that can mean the difference between success and failure in a mission. It is important to identify the minimum alternative configurations in which the camera can be run in order to determine strategies in case of component failure. The focal plane array itself is an obvious single point failure, but provision of an alternative one would significantly complicate the dewar and optical design of the system. The analog-to-digital converter is a critical point, since there is no provision in the proposed design for a capability to record the raw analog signal from the detector. Such an addition would require the presence of an additional recorder compatible with the analog voltages, and could also end up inserting noise into the raw detector signal. Current Schottky-diode arrays produce acceptable imagery without any image compensation at all, and thus if failures occurred in the image compensation section of the signal path, this would decrease the overall sensitivity of the camera but would not be a catastrophic failure. The scan conversion and level/gain control's importance depends upon the recorder selected for the system. If an analog recorder is selected with insufficient dynamic range to record the imagery, then the scan conversion and level/gain controls become critical points in the signal path. If a digital recorder capable of full dynamic range (12 bits) is used, the level/gain controls become important only for scaling of the image output in real time and not for the recorder. In addition, the scan conversion sections are less important if a digital recorder is used, since scan conversion can be done after the fact. Because of the inherent advantages of digital recorders, and their current availability (see section 4.4), it will be assumed that a digital recorder is employed. Note, however, that the focal plane imagery will not be available in real time without scan conversion, and thus all instrument tracking would have to depend upon the visible band TV camera or strictly on aspect and pointing information.

Thus an acceptable minimum electronic processing system would consist of the detector, A/D converter, and a digital path directly to the recorder. A redundant focal plane is impractical, since it would introduce a whole new set of reliability issues. A redundant analog-to-digital converter is certainly practical, and provisions should be made for two in the design, with the control computer (or telemetry-directed commands) capable of switching between the two. Provisions should also be added for a direct digital signal path from the analog-to-digital converter to the recorders, to allow this option as a backup strategy. A duplicate recorder is

Section 4.3

impractical, given the size constraints of the SBS Camera, but redundancy should be added by designing in systems that can make all or at least a portion of the data available over the telemetry stream for recording in a ground or shuttle based system in case of recorder failure (see section 4.4). Providing a redundant A/D system would consume an additional slot, leaving 4 slots free in the electronics backplane for mounting the control computer (discussed in section 4.5)

4.4 Data recording system

4.4.1 Overview

The recording system used to store the infrared data collected by the SBS Camera is a critical component of the system. This camera is intended to make radiometric measurements of targets and backgrounds as required. If the mission data is not reliably stored for later analysis, the mission will be a failure. One of the design goals for this system is to be capable of standalone operation (except for power). Thus a data recording system is an essential component of the proposed camera. Due to the high data rates and the relatively small physical space available for the camera, this is one of the more difficult subsystems in the camera design. This section examines the possible techniques that can be used to format the infrared image data from the SBS Camera and the recording systems available to store the data away.

There are some general points to be made about the physical limitations that will be imposed on the recording system by the space environment and platform. As detailed in section 4.6, the shuttle environment is a fairly harsh one, with extremes in vibration and temperature. Any recorder considered for this application must have a physically robust design and must be capable of reliably withstanding the environment it will be exposed to. These limitations preclude many of the existing recorders available commercially, since these devices are designed for a laboratory environment. Additional requirements include small size and low power consumption. In order to keep the entire system on a single equipment mounting plate (as proposed), the actual recorder, including all thermal insulation and shock mounting, must actually be quite small. Another important consideration is that the recorder will be operated without any user nearby to perform such functions as changing tape or media. The media must be capable of recording all data expected on a single mission without being changed. The recorder must also be remotely controllable, since it will be run by either the on-board control system or by a ground based user via telemetry links.

The approach taken in this design study will be to summarize the recording technologies available today that are suitable for an application such as the SBS Camera. Actual commercially available products representative of each category will be presented as a concrete illustration of the advantages, disadvantages, and special features of each. This study will not go excessively into the details of each system, since it is likely that the actual recorders described here will be obsolete when the actual camera system is designed and built. Note that inclusion of information on commercially available data recording systems is not intended as an endorsement of either the particular products or the companies involved. This information simply allows the system designer some specific details and performance

Section 4.4

characteristics so that general engineering decisions can be made about the eventual recording system to be made.

One of the goals of this design is to keep the recording subsystem as physically separate as possible from the rest of the system. This goal will ultimately provide the system users flexibility in selecting which recorder to use. It will also allow the recording system to be changed and updated as new technologies become available, which is an important advantage given the rapidly changing nature of recording and storage technology. If a decision is made to transmit the data over a telemetry link and record the data remotely (either on the shuttle or at a ground based station), the physical limitations on the recorder would be reduced considerably, but at a cost of overall increased SBS system complexity.

4.4.2 SBS Camera data outputs

There are two types of data that need to be recorded during an SBS camera mission. First there is the image data, the maps of pixel intensity generated by the PtSi array as it observes the target. This data accounts for the vast majority of the total data recording requirements of the system. The second type of data is housekeeping data, which consists of documentation such as Universal Time, instrument settings, etc. This data must be able to be correlated with the image data collected so that the images can be calibrated and analyzed as required.

The image processing circuitry in the SBS Camera is designed to operate on digital data. The reasons for this decision (increased dynamic range and simplification of the image processing circuitry) have been discussed in the previous section. Thus the data read out from the array is converted into a digital number proportional to its voltage as close to the dewar as possible. The digital values are manipulated in the three point correction scheme to correct for array defects and provide a radiometric reference for the data. Now the data needs to be stored away. There are two fundamental approaches that can be taken at this point. The data can be converted back into an analog signal and recorded, or it can be stored away as an array of digital numbers. The actual data rates from the detector are quite high. Current state-of-the-art PtSi arrays contain 160 x 244 elements; the entire array is read out 30 times a second in existing designs. This translates into 39040 pixel values per image. At 30 frames per second this is 1.171 million pixels per second. Since these are 12 bit pixels (and the bits per pixel may increase in future designs), the final data rate is 2.342 megabytes/sec. Given these high rates, the quantities of data collected are also very large. A system capable of recording 2 runs of 5 hours of image data total (as specified in section 3) needs to hold about 84.3 gigabytes of data.

Note that the data rates cited above are for raw camera imagery. Data compression and encoding schemes can be added to the camera that reduce the quantity of data by encoding redundancies contained in the image pixels. Typical imagery from the SBS Camera is expected to contain a considerable quantity of duplicate information. For example, consider a data image that contains the shuttle at a range of 10 kilometers. Earlier calculations (in section 4.1) have shown that the target size would be approximately 19 x 12 pixels, or about 228 pixels total. Thus the target signature data would be contained in less than 1 percent of the total image pixels. If the shuttle is being viewed against the backdrop of space, the

Section 4.4

remaining pixels will be measuring a scene colder than the detector array (deep space has a 4 degree Kelvin spectral shape), and thus the image content will be essentially zero. This is an extreme case, but it can be anticipated that a reasonable fraction of scenes will contain a large number of pixels with no useful image content. Another example of redundancy can be seen in close-up images of the shuttle, where large sections of the fuselage may have the same apparent radiance. These pixels represent redundancies that can be encoded using standard data compression algorithms. These data compression algorithms range from quite simple to very complex and computation intensive solutions. It is reasonable to expect that a simple scheme, such as run-length encoding (RLL), could reduce the total data recording requirements by a factor of 5 or 10, and for some scenes by as much as a factor of 100. Basic run-length encoding replaces a string of identical pixels with a pixel value and a number of pixels following with that value. A number of variations on this scheme exist to improve the efficiency further. This scheme is also simple to implement in hardware so that it operates in real time. Thus, if encoding is added to the instrument data processing, the data quantities can conservatively be estimated to drop by a factor of 5. Note that, while the average data rate will also drop by this amount, the instantaneous rate will not, because structured parts of a scene will not be encodable and the full pixel rate will have to be recorded. To achieve a reduction in the data rate as well, an additional hardware scheme, such as a large and intelligent data buffer, would need to be added to the compression stage, in order to smooth out these temporary variations in data rates. This type of buffer would not be a difficult design, and should be considered if encoding is selected for the SBS Camera data recording path. The primary disadvantage encountered in recording compressed scene data is that errors in the recording process become magnified. High data-rate digital recorders (discussed in section 4.4.4) achieve their high rates and capacities partially by relaxing error detection and correction information, and thus have relatively high error rates (on the order of 1 in 10^7 bits). A typical SBS Camera data frame consists of $4.7E5$ data bits, so bit errors can be expected every 22 frames on the average. In an unencoded scene, an incorrect bit would corrupt a single image pixel. In an encoded scene, an incorrect bit can potentially corrupt a string of pixels. If the compression reduces the data frame size by a factor of 5, then this corruption would be expected every 110 frames in encoded data. Thus this potential disadvantage must be balanced off against the improvements in recorded data capacity that are obtained through image compression.

An additional consideration for the recorder specifications is the minimum data integrity required for the image pixels. While it would be desirable that every pixel is recorded with complete accuracy, such a requirement imposes additional error detection and correction overhead on the recorder that reduces both recording rates and total data capacity. Maintaining a zero error rate is usually not necessary for imagery of the type expected from the SBS Camera. The fidelity of typical recorded images can usually be preserved even through error rates on the order of a few percent of the total number of pixels in the image. This process is assisted by the high frame rate of the SBS Camera. With the possible exception of engine plumes, the signature of the shuttle is not expected to vary rapidly with respect to the frame rate of 30 frames per second. This means that many frames of essentially duplicate data can be expected during measurements, which allows pixel errors to be detected and either ignored or corrected. This is an important advantage, because the high data rate digital recorders (discussed in section 4.4.4) usually have

Section 4.4

relatively high error rates.

The housekeeping information generated by the instrument is a crucial part of the data, for this allows radiometric calibration of the data and correlation to events of interest with the target. The following items need to be recorded with the proposed SBS design:

1. time information - 8 bytes using BCD encoding
2. level setting - 2 bytes (if applicable)
3. gain setting - 1 byte (if applicable)
4. reference scene temperature - 2 bytes
5. orientation data: x,y,z angles at 2 bytes each = 6 bytes total
6. instrument temperatures: 3 temps at 2 bytes each = 6 bytes
7. bandpass filter position - 1 byte
8. additional status info: 4 bytes allocated

This totals 30 bytes of housekeeping information per data frame. Note that this amount could be compressed somewhat if the need arose. Thirty bytes per frame is a data rate of 900 bytes/second, and the total data quantity is 32.4 megabytes for 10 hours of image data. Either the primary recording system needs to be capable of accomodating this additional information, or a separate recorder must be provided. The data rates are very low in comparison to the raw image data: probably on the order of only a few bytes of data per frame. Three basic approaches exist to record this data. First, a separate recorder could be provided. This is the most expensive option in terms of physical space and additional power, and precautions would have to be taken to ensure that the recorded status data could be reliably correlated with the image data later. A second possibility is to store the data on unused channels on the primary data recorder. An analog video recorder, for example, might have unused audio channels that could easily store this information in an PCM format. The third option is to actually insert the parameters into the image data stream. If the data stream is being recorded as an analog video signal, the housekeeping data could be stored on unused video lines, for example, or it could be added to the video image as inserted characters. If the data stream is digital, the bits representing the housekeeping information would simply be inserted at the start or the end of each data frame. The final choice that is made between these three options depends, of course, on the type of recorders finally selected for the system.

4.4.2.1 Analog image data formats

The most frequently used analog signal format used to display image data from cameras such as the SBS is the standard video signal that drives most televisions and video recorders. Current designs of PtSi array cameras such as the SAIRS output their data as standard video signals. The exact waveform of the standard video signal is defined by the Electronic Industries Association EIA Standard called RS-170. This standard sets out the number of vertical lines, the interlace, the waveform timing requirements, and the equipment and procedures to be used to measure the signal. The RS-170 standard defines a monochrome video signal which stores the picture brightness (or luminance) information in a voltage that varies between 0 and 0.7 volts.

Once the image data is stored as an RS-170 video signal, provisions must be made

Section 4.4

for post-mission data analysis to allow this data to be input to a computer system so that it can be manipulated for calibration and analysis. The use of analog processing or analysis techniques can be ruled out from the start, due to the higher dynamic range and lower noise thresholds that are routinely attained using digital image processing techniques. One way to do this is to use a video digitizer that converts the video signal into an array of pixel intensity values. Commercial digitizers are available for a fairly low cost that meet or exceed the dynamic range of available analog video recorders. These digitizers typically contain phase-locked loops to allow the converter to synchronize with the analog signal waveform so that the frame is converted in the proper order. The horizontal and vertical synchronization signals are used for this phase-locking process. This step in the data reduction process is an additional one imposed through the use of analog recorders.

There are several advantages to converting the camera to an analog video signal for display and recording. Video provides a low cost and standard way of displaying large amounts of information rapidly. Standard television signals display 30 frames a second of 525 interlaced lines of data. Megabytes of image data can be easily displayed on a television monitor. A wide variety of video recording devices are available to store the image data. It is also simple to verify the operation of the recorders by playing back selected portions of the data. Another advantage arises in data reduction and analysis. It is easy to rapidly scan through large amounts of video tapes to review the data and select portions of interest for analysis. Video digitizers that convert the video signal into digital form suitable for computer analysis are also inexpensive and easily available.

The primary disadvantages to this form of data storage arise from the analog nature of the video format: video images are susceptible to noise, degradation over time, and have a limited dynamic range. The limitations on dynamic range are perhaps the most serious limitation of video recorders. Even the highest quality video recorders (used in the broadcast industry) are typically limited to 40 db of dynamic range, which translates into a digital accuracy of approximately 8 bits per pixel. Given the definitions of video signals, and the limitations of most broadcast industry video equipment, this level of dynamic range is suitable for commercial applications, but represents a significant compromise for a camera such as the SBS which will be capable of operating with close to 70 db of range (12 bits per pixel). Techniques do exist for expanding the dynamic range of a video signal. One possibility is to apply a logarithmic mapping function to the pixel values before they are converted into analog video. This increases the total dynamic range of the displayed scene but decreases the measurement accuracy of displayed pixels. A second possibility is to use gain and level controls on the instrument to view only a selected portion of the total dynamic range of a scene. Pixels too bright or dark for the portion selected are simply allowed to saturate. This technique is used in the current SAIRS design to improve the capability of the instrument to display its full dynamic range within the limitations of video. For scenes with low total contrast, effective dynamic ranges equal to the full 12 bit resolution of the camera can be obtained using a gain and level control.

In summary, use of an analog recording system requires RS-170 compatibility with a capacity of 10 hours data duration. Auxiliary channels (sound channels, for example) must have sufficient bandwidth and capacity to hold the instrument housekeeping data at 900 bytes/second or 32 megabytes total. The recorded data

Section 4.4

must be of high enough quality to allow post-mission digitization of the imagery.

4.4.2.2 Digital image data formats

Since the image data is present in the instrument in a digital form, it is very possible to record the pixel values directly. There are several advantages to this approach. First the pixels are stored exactly, and there is no degradation of the image (unless part of the digital recording medium is damaged). Secondly the full dynamic range of the system is preserved. Frequency response ceases to become a limiting factor. Use of a digital approach also allows encoding schemes (such as run-length encoding) that are more reliable and preserve the full image fidelity in a more reliable manner than analog data compression techniques.

The current state-of-the-art in digital recorders is capable of handling the large data quantities and rates characterized by the SBS Camera. The main problem encountered is fitting these recorders within the small physical envelope allocated by the host platforms, as well as keeping electrical power consumption to an acceptable level. Note that compromises are possible in specifying exactly what needs to be recorded, and these compromises extend the range of recorders that can be used. For example, the high data rates are typically more of a problem than total data storage capacity. It is certainly possible to compromise in the recording scheme by deciding not to record every single frame of data read out of the instrument. A system can be designed that would record only a few frames a second at full digital resolution during the mission. For targets with stable infrared signatures that were not changing rapidly this compromise could indeed be acceptable. Another possible compromise is designing a large memory buffer capable of holding a second or two of continuous data frames. This buffer would collect a 'snapshot' of the data and then slowly spool the data out to the recording device at a slower rate. This 'snapshot' mode would maintain full time resolution, but could not provide a continuously set of data for analysis. The desirability of these compromises is strongly dependent on the nature of the mission being flown and the types of targets being investigated. Given the current rate of development in digital mass storage devices, it is likely that devices capable of handling the data rates and quantities cited above will exist in an inexpensive form in a few years. The PtSi arrays, however, are also increasing in size, with 512 x 512 arrays under development. These larger arrays will increase the data rates and quantities by over a factor of 4 when available. Thus compromises may still be necessary even with greatly improved recorders in the future.

In summary, the following performance specifications apply to any digital recorder selected for the SBS Camera system. If unencoded, raw pixel data is recorded, the recorder must be capable of handling 2.342 megabytes/second with a total capacity of 85 gigabytes. If the image data is compressed, the nominal performance requirements are for 468 kilobytes/second with a total capacity of 17 gigabytes. In addition to the image pixel data, the recorder must also be capable of handling 900 bytes/second on a secondary channel with a total capacity of 32 megabytes.

4.4.3 Analog video recorders

Analog video recorders represent a reasonably established technology. The

Section 4.4

research and development in this area has been funded by the needs of the major commercial networks for high quality video recording, playback, and editing capabilities. Portable machines have been developed as a direct result of broadcast network requirements. It is advantageous to try and take advantage of all of this existing technology, since that holds down development costs and makes repairs and upgrades simple to implement.

Two distinct types, or 'grades', of video recording devices can be currently purchased. The high quality grade consists of recorders that adhere to the 1 inch tape broadcast standard format. This standard tape format is known as the SMPTE-C format, and is a standard used throughout the broadcast industry. The second, and larger, class of machines consist of video cassette machines (VCRs) that have been driven by the demands of consumer video. There are large differences in quality, cost, and reliability between these two classes of machines. High quality broadcast machines have better image fidelity and editing capabilities, along with higher cost and larger physical size and weight. Videocassette machines have lower quality specifications, but tend to cost less and be smaller and lighter machines. One very important difference between the two emerges when the requirements of post-mission digitization of the scene video are considered. The synchronization information recorded with typical VCR-type devices is significantly poorer and contains more noise than that recorded with SMPTE-C devices. The recording of good timing information in an analog signal requires a lot of frequency response (since the timing signals consist of sharp, step-function transitions), and frequency response is usually what is compromised in VCR-type systems. The result is that VCR's have enough timing information quality to allow scene playback, but the quality is too poor for phase-lock systems to provide accurate synchronization information for digitization purposes. This introduces tearing and phase errors into digitized scenes. This is a significant problem for SBS Camera data, which needs to be read into a computer for analysis purposes. It is especially aggravated for the case of a 2 dimensional focal plane array such as the Schottky-diode arrays, where each image pixel is created by a separate detector. If real-time image compensation has not been applied, there will not be adequate phase accuracy in a recorded analog signal to allow these corrections to be applied after the fact. For this reason, a VCR-type system represents a poor choice for use as the primary recorder for the SBS Camera system. Since VCR devices are available in small, ruggedized versions, they are attractive as a backup recording system, but the difficulties encountered in digitizing image data reliably from them sharply limit their usefulness.

One area where VCR-type recorders promise significantly better performance than a SMPTE-C type machine is in ruggedness and physical reliability. VCR machines enclose their recording media in a cassette, which leads to significantly enhanced reliability in comparison to open reels of tape. Ruggedized VCR machines have been used to record data in a variety of harsh environments.

Portable recorders adhering to the SMPTE-C recording standards are available for off-the-shelf purchasing. One popular model is the Nagra VPR-5 manufactured by Ampex. The unit weighs about 7 kilograms, and can be run from either a battery power supply or line power. The unit can use either 5.5 inch reels of tape, for 20 minutes of recording time, or 9 inch reels of tape, for 60 minutes of recording. This recording capacity is small relative to the data recording requirements spelled out in the SBS design goals. In addition, MIL-SPEC qualified units of this type of recorder

Section 4.4

are not available. It is not clear whether the recorder could be ruggedized enough to function reliably in the harsh vibration environment of the SBS payload, simply because it depends upon open reels of tape and a fairly complex set of mechanisms to control tape speed.

A number of companies market ruggedized videocassette recorders. These units tend to be on the order of 5 kilograms of weight, consume fairly low levels of power (20 watts), and are not significantly larger than conventional VCR recorders. Data capacities range up to eight hours of data per tape cassette.

In summary: a variety of analog video recorders are available to store the SBS Camera imagery. The recorders with high enough fidelity to preserve the image quality, however, are more fragile and susceptible to vibration and environmental damage. The ruggedized systems that could be realistically used in a space payload are not of high enough quality to preserve the camera imagery without degradation of the data. When coupled with the additional disadvantages inherent in analog recorders discussed earlier, it is apparent that this type of recording system would not be adequate for the SBS payload system.

4.4.4 Digital recorders

4.4.4.1 HDDR magnetic tape recorders

Significant advances have been made recently in high density digital recording technology (HDDR). Data rates and overall system ruggedness have increased markedly over the past few years. The development of such systems has been driven by demands for increased performance from instrumentation groups desiring the higher dynamic range and relative noise immunity of digital recording.

It is important to note that no universal standards exist for HDDR recorders (as opposed to, for example, wideband IRIG recorders). Each manufacturer decides upon a unique tape format and then constructs the machine to record input data into it. Thus use of this type of recorder implies a commitment to a particular manufacturer for upgrades or design changes.

Since no general standards exist for this type of digital recorders, this discussion will present two products that are among the current state-of-the-art in HDDR technology. The characteristics, advantages, disadvantages will be described in order to present what is possible with current technology. Both of these systems are manufactured by the Ampex Corporation, an established manufacturer of tape recorders. This discussion, of course, in no way implies an endorsement of their products, nor does it indicate that they necessarily offer the most advanced systems available. These two systems are simply representative of the two approaches common in HDDR technology today. The first system uses a hybrid approach that puts a digital front-end set of electronics onto an analog recorder. This type of digital recorder is discussed in section 4.4.4.4. The other system is a complete HDDR system available as either a laboratory (19 inch rack mount) or an 'aircraft qualified' system that meets a number of MIL-SPECS in its physical configuration and design.

An example of a stand-alone HDDR digital recorder that is currently available is

Section 4.4

the DCRS system (Digital Cassette Recording system), manufactured by the Ampex corporation. This unit is capable of recording data at rates as high as 107 megabits/second, which is 8.9 million 12 bit pixels/second, well above the current detector array data rates. An additional advantage of this recorder is that it will be capable of keeping up with the data of new PtSi detectors arrays currently in development (512 x 512 element arrays), which will have data output rates on the order of 6.8 million 12 bit pixels/second. The digital data is recorded onto a tape cartridge. One tape can hold approximately about 5 hours of SBS Camera data. The recorder also has a large memory buffer that allows scrolling through collected data, as well as freeze-framing. The unit was designed as an instrumentation recorder, and thus has extra tracks for time code, instrument housekeeping parameters, etc. It is controllable by commands sent via an RS-232 serial data interface, which allows computer control of the recorder functions. Both ground systems (19 inch rack mount) and aircraft qualified (ruggedized) versions of the system will be available, for fairly modest cost (less than \$200 K). A version with less features is currently available now. This recorder meets the basic requirements imposed by the SBS payload, and has great potential for meeting future digital recording needs with the system as well. Additional detail on this recording system can be found in section 6 of this report.

4.4.4.2 Digital video

A recent trend in the broadcast recording industry has been a move from analog to digital recording methods. This move has been hastened by the agreement upon a universal definition of digital video recording standards by a SMPTE (Society of Motion Picture and Television Engineers) committee, which is the predominant group that sets standards for the television and video industries. The new standard is known as D-1. It defines a high speed digital image format that is recorded onto magnetic tape cassettes at video rates in real time. Note that the standard describes the tape data formats and physical configurations. The actual design of a recorder capable of recording and playing back this data is left up to the recorder designers.

There are several advantages to a digital video recorder. First is the advantages inherent in the digital storage of the image data, as has already been described in general above. Secondly is the expected availability of a number of machines competing in the same market. Digital video is being driven by the demands of the broadcast industry, which represents a large potential market, so a large R&D effort currently exists. The existence of several functionally identical machines will result in better features and lower prices. Selection of the digital video standard will not lock the SBS Camera system into a particular recorder manufacturer. In addition, video machines are ideally suited for analysis of the infrared image data from a Schottky-diode array, which is essentially a continuous map of imagery. Broadcast video machines are designed to allow rapid or slow scrolling through imagery, freeze-framing, and other editing features that greatly assist in the data selection and reduction process. The presence of alternate audio tracks allows space to record instrument housekeeping information along with the data. Finally, the system is capable of handling either a digital data stream or an analog video stream, which gives flexibility to the system designer.

The D-1 digital video standard is also referred to as the 4:2:2 recording standard. An illustration of the data format on tape that demonstrates its overall

Section 4.4

characteristics is shown in Figure 4-4.1. The data is still recorded on tape using helical scan recording techniques (helical scan uses a rotating head moving past the tape, writing tracks almost longitudinally). Blocks of video information and error correction data are written to the center of the tape. Four blocks of high quality (20 bits per sample at a sampling rate of 48 khz) digital audio data are located in the center of the tape. On the edges of the tape are located time code, control, and cueing information tracks. The format and sampling of the recorded data is important, because the SBS Camera image output has to be adapted to match the recorder input requirements. Directly digitizing the SBS analog video signal would still limit the image dynamic range to 40 dB (8 bits), and would lose many of the inherent advantages of digital recording. One solution is to format the data and utilize the extra recording bandwidth set aside for color information. Color information is meaningless for the Schottky-diode imagery, since only pixel intensities (or luminance information) is generated. Color information is encoded into the D-1 digital recording standard in a complex manner. The recorder stores luminance (or brightness) information and chrominance (or color) information. Because the human eye is more sensitive to luminance changes than color accuracy, the bandwidth of the recorded luminance channel is made twice as wide. Color is normally built from three signals: red, green, and blue. In D-1 digital recorders, the chrominance and luminance information is combined into three data streams consisting of a luminance and two color difference signals. The colors are encoded according to the following scheme:

$$\begin{aligned} \text{luminance} = Y &= 0.299R + 0.587G + 0.114B \\ \text{color diff} = Cr &= 0.713(R-Y) = 0.5R - 0.418G - 0.082B \\ \text{color diff} = Cb &= 0.564(B-Y) = 0.5B - 0.169R - 0.331G \end{aligned}$$

The data sampling rates have been selected to be compatible with both 525 line (USA) and 625 line (European) systems. Thus the basic sampling rate is set at approximately 13.5 MHz, which is 864 times the horizontal frequency in 625 line systems and 858 times the horizontal frequency in 525 line systems. The two color signals, labeled R - Y and B - Y, are sampled at half this frequency, or 6.75 MHz. For each active horizontal line there are 720 luminance samples and 360 of each color difference signal. The luminance signal is stored as an 8 bit digital value, while the two chrominance signals are stored as 6 bit digital values. Thus the effective bandwidth of the luminance channel is 5.75 MHz, while the chrominance bandwidth is approximately 2.75 MHz. The overall signal-to-noise ratio of the recorder is nominally 56 dB (Y/B-Y/R-Y).

Three standard sizes of tape cassettes have been defined in the standard: a small, medium, and a large cassette. The following table summarizes their physical dimensions:

<u>cassette</u>	<u>width</u>	<u>length</u>	<u>height</u>
small	109 mm	172 mm	33 mm
medium	150 mm	254 mm	33 mm
large	206 mm	366 mm	33 mm

In addition to the overall size, two thicknesses of recording tape have also been specified: 16 and 13 micrometers. The thinner tape obviously allows more tape to be fit within a cassette and thus results in longer recording times. The possible playing

Section 4.4

times are summarized in the following table:

<u>cassette</u>	<u>16 micron tape</u>	<u>13 micron tape</u>
small	11 minutes	13 minutes
medium	34 minutes	41 minutes
large	76 minutes	94 minutes

The size and capacity of the tape cassette determines the total recording capabilities per machine, since it is assumed that no tape changing will be possible for the SBS Camera payload.

A standard digital data interface has also been defined as part of the D-1 recording standard. These recorders can accept data in either a serial or a bit parallel format. The details of this interface are covered in SMPTE document RP-125. The parallel interface consists of just a 27 MHz clock signal (for synchronization) and eight twisted pair connections, each containing a single bit. Data is transmitted in the order luminance, first chrominance, luminance, second chrominance, etc. The data is organized into blocks of 1440 video words, which corresponds to a single horizontal line of the image (720 luminance words, 360 words of each chrominance component). Timing reference information is also provided for the start and end of active video, which is used to determine the horizontal blanking regions. The serial digital interface option reformats this basic approach to use a single coaxial line connection. Note that the interface serves as both an input and an output specification, so that data is recovered from the recorder in the same format as it is input.

Because of this unusual digital data format, it is necessary to perform extensive reformatting on digital image data from the Schottky-diode detector in order to record it onto the digital video without loss of dynamic range. One possible solution to the formatting problem is to utilize the chrominance values for additional storage. Since the chrominance data values are unused by the SBS Camera, the alternating chrominance components can be paired with the luminance values to provide a 14 bit deep recorded digital word. The eight most significant bits of the infrared pixel can be stored in the luminance data word. The remaining bits are stored in the next chrominance word. This scheme has the added advantage of allowing viewing of the recorded data on a standard monochrome television monitor, and the eight bit image will make sense when viewed (since the luminance contains the eight most significant bits of the image). The primary disadvantage that this (or any other) data packing scheme encounters in the error correction scheme designed into D-1 digital video recorders. A relatively high error rate is tolerated in the recorder design (an average of several errors per frame recorded), since significant cost savings can be realized with minimal loss of image fidelity. The main error correction system in these digital recorders is interpolation: if a pixel is read off tape, and the value is known to be bad, the neighboring pixel values are used to interpolate over it and the bad pixel is replaced with a local average. This is a simple way to maintain the quality of a typical television scene, and the bad pixel is not noticed because in a normal scene neighboring image pixels have values that are correlated to each other. In the data formatting described above, this type of correlation exists in the luminance signal but not in the chrominance pixels. The least significant bits of a typical image will likely be completely uncorrelated, so this type of interpolation and local averaging would substitute in an incorrect value.

Section 4.4

This results in subtle errors being introduced into the data. Thus for this type of application, the error correction circuitry would have to be modified (or completely removed) to prevent this type of error.

There are not many existing D-1 standard digital video recorders on the market due to the relative newness of the standard. One machine has been announced by Sony, called the DVR-1000. The system is intended for use in a studio, and is clearly not ruggedized for field deployment conditions. The recorder and processing electronics are the size of a small office desk, weigh 325 lbs, and consume around 1300 watts of power. The approximate single system cost is around \$125,000. It is clearly not practical to put this system into a small payload like the SBS Camera. Intensive development is currently in progress on many additional machines of this type, including portable ones, and as the size, weight, and power consumption of these anticipated designs decreases, machines using this standard could become serious candidates for use in the SBS system within the year.

4.4.4.4 Hybrid analog video/digital data

Recording systems have been developed for storing digital data that rely on analog systems as the basic recording mechanism. These 'hybrid' systems accept digital data through some type of interface (either parallel or serial) and encode the data into an analog signal that a standard analog recorder is capable of recording. Usually error correction information is added into the analog waveform to increase the reliability of the system. During playback, the analog signal is digitized, along with the error correction information, and the data is converted back into a stream of digital data. This type of system runs into the bandwidth limitations of analog recorders when high data rates and quantities are being stored. Advanced encoding techniques are employed to increase the recording capabilities.

One common example of this type of digital recorder uses a standard video cassette recorder to store data. VCRs are widely available and low cost systems with a reasonably high bandwidth, since they must be capable of handling video data rates. Many systems have become available that encode digital data into a video waveform that is then recorded on a standard cassette. Several such systems exist for small personal computers, such as IBM PCs, that use commercial VCRs for data backups of fixed (Winchester) disks. These units hold on the order of 100 megabytes of data. In general these devices tend to have slow data rates (in comparison to the Schottky-diode FPA image output), because to maintain error rates low enough to be acceptable for computer code and data, very complex encoding and error correction schemes are required. For an application such as the SBS Camera, where the bulk of the data is imagery, such high data integrity is not necessary. Thus it is possible to relax the error correction to a certain degree, which in turn reduces the recorder overhead and allows higher recording rates.

This approach has been applied to digital instrumentation recorders as well. One example of such a system is the DCRR-32 Digital Cassette Recorder/Reproducer sold by Odetics Inc. of Anaheim California. This system consists of a hermetically sealed unit containing two videocassette recorders that are shock mounted and thermally insulated, and a second box that contains the recorder electronics and power supplies. A drawing of the unit, from the recorder manual, is shown in Figure 4.4-x. The unit is capable of handling two independent input data streams at a rate of 352

Section 4.4

kilobits per second each. The inputs must be synchronous, since they are timed by a common clock. Data is stored on a standard VCR tape cassette. Each VCR can hold 16 hours of data at this input rate, so the total recorder capacity is 32 hours of data or 8.1×10^{10} bits. Provision is made to record an IRIG time code signal on the audio tracks. Note that this input data rate is far too slow for recording all of the camera image data in real time. Two channels at 352 kilobits/sec translates into about 60 kilopixels/second (12 bit deep), which is only about 1.5 frames per second. Thus this recorder would only be able to record a fraction of the total data stream. In addition, housekeeping data would have to be mixed into the image data stream, since there are no separate channels available. The unit does have certain advantages to it. This recorder was originally developed for the CIRRUS space shuttle payload, and so the basic design has already been qualified for use on the shuttle. If time and money were scarce, use of this recorder would save the expensive testing and qualification effort that would normally have to be expended. The unit consumes little power (35 - 45 watts while operating, survival heaters use 85 watts), and its weight is fairly small (77.3 lbs for both units). Note that the specified error rate is already fairly high (less than 1 error in 10^7 bits), so reducing the error correction capabilities would probably not add much recording speed. The size is fairly large in relation to the equipment mounting plate (12 x 11 x 8.5 inches for EU, 24 x 18 x 8 for TU) but is manageable.

Thus the Odetics recorder would not be a first choice for use in the SBS Camera, primarily due to its slow recording rate, but could become a candidate if time or financial constraints on the program become serious.

A second example of a hybrid analog/digital recorder is a system sold by the Ampex Corporation called the HBR-ES (High Bit Rate Electronics System). It consists of a front end set of digital electronics that interfaces to an existing IRIG wideband analog recorder. Incoming digital data is converted, along with error correction information, into an analog signal compatible with these recorders, and on playback the analog information is converted back into a digital data stream. This device accepts a single serial bit data stream at a maximum rate of 30 megabits/second, which is approximately equal to 2.5 million 12 bit pixels/second (corresponding to a tape recorder moving at 120 ips). The unit can also accept parallel data at a comparable rate. The bit error rates are reasonably low (on the order of 1 in 10^{11}), but they do depend on the analog recorder being used. Additional analog tracks are available to record instrument housekeeping data. Note that the current version of this recorder is very large and bulky, and would have to be completely redesigned in order to fit the restrictive physical envelope of the SBS Camera payload.

4.4.4.5 Mechanical disks

4.4.4.5.1 Writable optical disks

A recent development in digital storage technology has been the development of optical disks capable of storing large quantities of data. These disks written using lasers to burn pits into reflective media; the difference in reflectivity between the pits and the unburned areas of the disks is used to store 1's and 0's onto the disk. Currently systems are available that can be written once, but cannot be erased after write. These disks are commonly referred to as Write Once Read Mostly (WORM)

Section 4.4

disk drives. They are distinguished from the more commonly available CD-ROM disks by their ability to be written with data. A block diagram illustrating the basic writing mechanisms of an optical disk is shown in Figure 4.4-3. Currently the drives are available in two disk sizes: 12 inch and 5 inch diameters. The larger disks have greater capacities, but the drive units themselves are physically larger. The smaller drives are compatible with the 5.25 inch standard drive form factor that has become popular with personal computers. These drives can be easily interfaced into a small computer that accepts the incoming data, reformats it for the optical disk, and then writes it out.

A WORM disk drive has been purchased by SRL and used for real-time digital data collection on a separate program. The disk drive is the N/Hance 525, purchased from Symphony Systems of Dedham, MA. The drive unit is manufactured by Information Storage Inc. (ISI). The disk drive is interfaced into an IBM PC computer using an interface card supplied as part of the N/Hance system package, along with PC-DOS software drivers. The lower limit on the operational environmental temperature of the drive is relatively high: 10 degrees C. Informal discussions with representatives from Symphony Systems indicates this limit is placed by the diode laser used in the read/write head. The currently available drive unit is not particularly rugged, and frequent failures have been encountered in the functioning of the drive eject mechanism, which is made of plastic parts. A ruggedized, and possible MIL-SPEC qualified, version of this drive is under development and projected to be available shortly. The data transfer rates are not adequate to keep up with the image data from the SBS Camera, and are further slowed by the track to track access times, which are fairly long.

Pre-formatted disks purchased from Symphony Systems typically hold around 122 megabytes of data. Both single and double sided media are currently available, with double sided media holding around 240 megabytes of data. The currently available drive, however, has only a single sided read/write mechanism; to access data on the other side, the disk cartridge has to be manually removed from the drive, flipped, and re-inserted. Thus the additional storage capacity of double sided media is not useful for the proposed shuttle system. Informal discussions with the company indicate that the disk densities should double within the year, and double sided drives (with two read/write mechanisms should eventually become available. A disk with a 1 gigabyte capacity has been announced for availability in mid 1988.

4.4.4.5.2 Magnetic (Winchester) disks

Very large capacity fixed disks have recently become commercially available in the standard 5.25 inch form factor. Utilizing advances in bit recording density on the media and increased numbers of platters, these drives advertise capacities in excess of 700 megabytes per disk unit. The basic operation of these drives uses a magnetic coating on a fixed rotating platter. The read/write heads are electromagnets. When a current flows in the heads, a flux reversal occurs on the disk surface, which stores a bit of information. Recent improvements in these drives include new thin film metal alloy coatings that support more than 21000 flux reversal/inch, and new data encoding techniques that increase the effective bit densities as high as 31000 bits/inch. These devices fit in a standard small form factor of 3.25 x 5.75 x 8 inches and typically require a small computer to drive them (a minimum is a single board system that can be fastened directly onto the

Section 4.4

drive. Current fixed rotating disks have the opposite problems in the SBS Camera system from most tape units: they can handle the data rates (up to 10 megabytes/second), but their capacities are too limited for the data collection duration defined in section 3 of this study. Even the 700 megabyte units could store only 300 seconds, or 5 minutes, of continuous image data each. An additional limitation encountered with rotating magnetic disks is ruggedness. On current designs, the heads ride over the disk platters on a thin (less than 1 mm) cushion of air. As a result, the heads are so close to the surface during operation that a physical shock will cause vibrations in the extended arm holding the heads that can result in the heads hitting the platter surface (a disk crash). During non-operation, this problem can be circumvented by parking the heads over a section of the disk not used to store data. Note that the newest disk designs can take operating shocks of up to 40 g's and non-operating shocks up to 60 g's, so they are not as fragile as earlier generation disks.

Rotating magnetic disks are not a viable recording option for the camera design requirements as spelled out in section 3 of this study. If the total data recording times are reduced to the order of ten to 15 minutes, this technology can be seriously considered as a candidate for use in this payload.

4.4.5 Redundancy requirements

The data recording system represents a critical failure point in the SBS Camera system. If the recorders do not work, then the data collected by the system will be lost and the mission will be a failure. Thus a backup system or strategy must be provided for the data recorders in the design of the SBS Camera. One possible solution is to provide a complete second recording system in the payload that can be used in the event of any failure in the primary recorder. Due to the size of most of these recorders, and the very limited physical envelope allotted in the payload design, this option is not practical. The existing recorders (at least those examined in detail above) are too large to duplicate. Thus either the recorders must be redesigned and repackaged to fit, or alternative solutions must be sought. Naturally a repackaging of the recorders to allow two within the limited space in the SBS payload represents the best solution, but it is not clear that this is possible without huge cost and effort increases, due to physical restraints on the tape cartridge size and current transport mechanisms. A second alternative is to provide an additional recorder that is physically small enough to fit within the payload, but is a different type of recorder. For example, if the primary system is a full dynamic range, full data rate digital recorder (as recommended), a backup system consisting of a small analog video cassette type device could be provided. This recorder would record the analog imagery output by the camera's last signal processing electronics that is normally intended for real-time tracking use only. Such a backup would be of limited dynamic range and susceptible to noise, but at least the data would not be totally lost in the event of recorder failure. Housekeeping data could be placed into the video field (as inserted characters) or stored on an audio track (as discussed above in the analysis of analog recorders). A third alternative is to provide no backup recorder, but to make the data completely accessible to the telemetry streams from the payload back to the shuttle or ground control. Digital data (a selected infrared scene image) could be stored in a buffer and then spooled out over the telemetry link to a ground or shuttle based recorder. Note that the existing telemetry streams from the SPAS and the data connections from the HH-G do not have sufficient

Section 4.4

bandwidth (speed) to transmit all of the digital image data in this manner. Thus single frames, or bursts of several consecutive frames, could be selected and transmitted slowly in non-real time. This allows recording of full dynamic range data. It is possible to make special provisions for the addition of a telemetry link with sufficient bandwidth to handle the high digital data rates. Then a high speed digital recorder could be maintained as a backup on the ground, interfaced into the telemetry stream. Another alternative is to transmit the analog tracking video imagery over a television link and then record the imagery on the shuttle or ground. This option will probably be required anyways, to provide tracking and target positioning information to the ground or shuttle operators. Of course it is prudent to record whatever imagery is being received, regardless of the perceived health of the on-board data recorder.

4.4.6 Summary

The on-board data recording capability design goal of the SBS Camera payload is an important part of having a stand-alone payload, but it imposes significant additional requirements upon the system designer. Digital data recorders exist that are capable of keeping up with the data rates and quantities output by the SBS camera detector array. Units are commercially available that come close to fitting within the operating constraints of the proposed SBS payload limits. The strong advantages of digital recorders over analog recording methods, which include noise immunity, better dynamic range, and a simplified data analysis process, have been explored in detail. For these reasons, a digital data recorder seems to be the best solution to the on-board data recording requirements of the SBS Camera. Of the digital recording devices currently available, high density magnetic tape drives offer the best overall performance in terms of speed, data quantities, and size. A class of instrumentation recorders, sold for instruments such as the SBS Camera, can be procured off-the-shelf and modified to meet the space environment needs of the SBS Camera.

Recording redundancy is another important issue raised in this section. It has been determined that there is probably not room for two of these recorders in the SBS payload envelope. Thus provision should be made to make the image data accessible to the telemetry stream so that remotely based recorders could provide additional backup. A single telemetry-based television link could provide an analog backup of the focal plane array infrared imagery. If a high speed digital data link becomes available, additional circuitry should be provided in the SBS Camera design to allow selected frames to be transmitted in case of recorder failure.

Several alternative recording systems have also been identified if the basic data collection requirements of the SBS Camera system are modified. Slower but less costly tape systems are available if the mission does not require consecutive data frames but still demands a large data recording capability. Faster and less cost disks exist if the data rates remain high (or increase), but the total data storage requirements drop significantly.

4.5 SBS Control System

4.5.1 Overview

The capabilities of the control system built into any satellite system that must operate remotely have an important impact on the overall design and expected performance of the system. For this study a control system is defined as a programmable, computer like system capable of initializing and operating the SBS system without human intervention. A better overview of this system component can be gained by listing its primary characteristics. It will have a programmable CPU that can run prewritten programs or be overridden by software or commands downloaded through the telemetry stream. It will have its own memory and operating system. It will control a hardware diagnostic interface to all major system components, and will be capable of putting the hardware through programmed sequences of operations. The control system will monitor test points during system operation to detect and identify faults, and will be robust enough to handle hardware and software failures without catastrophe. It will not be used to analyze or process image data from the camera in real time.

There are several advantages to be gained from incorporating such a stand-alone control system in the SBS Camera design. It will provide increased diagnostic capabilities that will allow operators to isolate and work around failures in the hardware during a data mission. The system itself should provide a level of fault tolerant operation. It should reduce dependence on ground or shuttle based real time control of the system, which reduces the interface requirements and reduces cost. A programmable system should also be able to adapt to changing mission conditions, which can mean the difference between getting data or getting none.

The main disadvantage to having such a control system is that it significantly increases the system complexity and level of design effort. This translates into increased development cost and time requirements. If properly implemented, such a system should greatly enhance the overall reliability of the SBS Camera, and given the relative scarcity of space on shuttle flights expected for the next several years, such reliability will pay off in the long run.

4.5.2 Control system tasks

There are 6 major tasks that must be accomplished by the control system once the SBS camera is on station in orbit:

1. system initialization
2. operate system in diagnostic mode
3. operate system in calibration mode
4. operate system in data collection mode
5. system shutdown
6. telemetry interface to shuttle/platform

Of these tasks, only the last one, the telemetry interface, may be required of the control system at all times; the other tasks will be restricted to times allocated during the mission for data collection. In the design goals section, this has been

Section 4.5

identified as two independent data runs of at least 5 hours in duration.

The requirements and additional detail on each of these tasks is contained below.

4.5.2.1 System Initialization

System initialization consists of all the steps required to bring the camera system from a stowed to an operational state. It is expected that, from launch until the system is in orbit, the system will be in this stowed state, where all fragile surfaces and components will be covered and the camera will be mechanically arranged from maximum physical stability. Prior to collection of data, the camera will have to reconfigure itself into an operational state. Depending on the final design, this may be as simple as removing a few covers over the optics or as complex as moving entire subsystems into proper physical configuration.

In addition to physical changes to the instrument, several other tasks must be performed during system initialization. The control computer must bootstrap itself into operation and verify that it is working properly. Other tasks include enabling the cryogenic cooling system, heating or cooling calibration sources, powering up the data recorders, powering up the processing electronics, and making a complete diagnostic check of all system components while the dewar is being cooled down.

4.5.2.2 Diagnostic mode

Diagnostic mode is intended to allow the control computer to evaluate the health of the entire camera system. This mode will allow operators of the camera to determine the presence of hardware faults during or prior to a mission and to take appropriate action as required. All major subsystems of the SBS Camera should be designed with a diagnostic interface to indicate fault conditions. A simple example of this can be shown with the RAM memory buffers in the system. The buffers can be designed with an extra parity bit. When a parity error is detected during a memory access (using standard parity detection logic chips), a test line would change logic state, and the control computer would detect this failure. The computer could then take appropriate action, which could range from switching in an alternate bank of memory to simply flagging the data frame as possibly containing an error from a failure in the RAM memory. These test lines should be tied to an interrupt driven scheme so that the control computer does not waste all of its time polling test lines. In an interrupt driven system, a test line that changes logic state generates an interrupt on the computer, which then suspends the task it is currently executing to service the interrupt request.

There are two distinct levels of diagnostic attention that the control computer can have over the camera system. The first is error detection, which is simply determining that a hardware failure of some sort has taken place. The second level is error correction, where the computer not only detects the error but takes action to isolate or correct the hardware failure. The second level is far more complex than the first, and the need for it depends heavily on the actual design of the camera. Some errors in a system can be tolerated, and simply noting that they have occurred represents sufficient action. For example, if one of three temperature sensors on a calibration source fails, the calibration data collected on that source is still usable,

Section 4.5

because the other two temperature readouts provide sufficient information for later analysis. In this case the temperature sensor data can simply be flagged as unusable. Other failures, such as failure of one stage in the image processing electronics, represent more serious failures that can result in incorrect data, or no data at all, being recorded during a mission. Error correction in this case might involve switching the data stream to alternative backup processing boards, if such exist, or the decision might be made to bypass the image compensation circuitry completely, using the idea that uncompensated imagery is better than no imagery at all. For example, if the PROM bank containing the stored responsivity values used for gain correction suddenly failed, and if no backup set existed, it would be better to completely bypass the response correction than to multiply by wrong or non-existent numbers. This example illustrates the importance of evaluating in detail all of the alternative strategies to be taken during system component failure during the initial design phase of the camera. It is relatively easier to incorporate hardware alternatives and backup strategies during design than at a later point in time.

There are also two levels of error detection that are appropriate for this diagnostic mode of the control computer. First is a complete camera diagnostic evaluation that exercises all important components of the system. This complete diagnostic should inject a test signal into the start of the processing path and monitor the values of the test signal at several intermediate test points to verify proper operation of all subsystems. In this manner the control computer could exercise all stages in the signal path, including the A/D, the compensation electronics, data formatting, and the data recorders. This diagnostic would be an intrusive one, in that the camera could not collect imagery at the same time. Such a complete diagnostic would only have to be run once during a data collection run, preferably at the beginning. A suitable time for this level of diagnostics would be during system cooldown, when about 1 to 2 hours of time is available during which the detector is not capable of outputting image data anyways.

The second level of diagnostic evaluation is a passive error detection mode that takes place during all data collection operation. In this mode the computer is only monitoring the complete set of diagnostic test points (via interrupts), and only takes action if a testpoint indicates that an error of some sort is occurring. This type of diagnostic is non-intrusive, and thus can take place during camera operation. It is valuable for detecting component failures that take place during data collection.

Thus the error detection system consists primarily of a set of hardware test points interfaced into the computer. It is useful to compile a list of these test points in order to evaluate the requirements they place on the control computer, so that adequate performance capability can be designed into the control system from the start. Some of these test points simply monitor the logic state of some aspect of the computer: for example, a valve is either operating or not operating. This information can be passed to the computer with a single line that has either a high or low voltage level. Other test points require more elaborate attention: a temperature sensor needs to have a number read out of it and stored away in the computer. A distinction will be drawn between these two types of test points, since the second requires significantly more work by the computer. The complete system diagnostic capability adds the requirement for a signal injector into the data path in front of the analog to digital converter, and the addition of latched test points where the signal values can be read by the computer. A modified block diagram of

Section 4.5

the camera electronics with these diagnostic additions identified is shown in Figure 4.5-1.

The PtSi sensor should have a number of test points to ensure that it is receiving the proper biases and clocks. Test points to check the DC bias levels are easily implemented in hardware, since the DC level going into the dewar can be compared against acceptable lower and upper voltage limits. Test points should also be present on the clock signals as well, and could check both the amplitudes of the clocks as well as their frequencies. In addition, the relationship of the clocks to each other is critical for the detector to operate properly, and a test point could be designed to evaluate this relationship. Note that if no redundant detector driver circuitry is provided, there is little the control computer can do if a failure is detected. It is possible to design the circuitry so that levels, clock frequency, and clock phase can be adjusted by the computer, and this level of control would allow changes and adjustments to be made remotely if errors are detected in the detector voltage inputs.

The analog to digital converter (A/D) is a logical point in the data stream to inject a test signal that can be used for the complete system diagnostics. One can provide an analog test signal in front of the A/D that is digitized and then compared against a map of what the results should be. This map can be stored in a PROM memory. This test would indicate any drift or other variation in A/D parameters that is taking place during a data mission. Test signals would include a number of fixed DC reference voltages, to calibrate the absolute accuracy of the A/D, as well as AC waveforms to evaluate frequency and slew rate accuracy. The PROM memory would contain the digital equivalent of the analog signals. If the A/D conversion results are read into a small bank of RAM that the control computer can access, and if the stored PROM values are also within the control computer's memory map, statistical comparisons can be made and the results stored away with the data, or reported to the system operators via the telemetry stream. About 64 kilobytes of RAM and PROM (each) would be required to implement this level of testing. These requirements translate into addressing space requirements in the memory map of the control computer. A checksum for the PROM should be available so that the control computer can verify that the stored PROM values are functioning properly. The test signal values stored in the PROM (or RAM values) can then be used as a test signal that can be passed through the entire set of image compensation electronics, as described above.

An additional relevant capability required of the control computer is the ability to swap in an alternate analog-to-digital conversion system if the diagnostics determine that the primary unit has failed.

The electronics for the first point corrector should have test points on DC power. In addition, a PROM checksum should be available so that the control computer can verify the proper operation of the frame background pixel values that will be subtracted off in this first step. During the complete system diagnostics, the injected test signal will pass through the corrector, and since the control computer can directly read both input values and the output value of the first point corrector, it should perform this comparison to verify that the electronics (primarily the ALU) are functioning correctly. The system can do this a line at a time, or for an entire frame. This type of evaluation is a good check of the proper operation of this

Section 4.5

subsystem. Total requirements are a power testpoint and latch inputs/outputs at each end of the first point corrector.

Diagnostic evaluation of the second point image corrector (the multiplicative gain correction) is almost identical to that described for the first point corrector above. The computer should evaluate the input data to the system and compare the multiplier output data with its own independent calculation of the result. A single power testpoint and latch requirements at each end are required here. The same is also true for the third point correction. For the third point correction, the data to be subtracted off is stored in RAM, and so the control computer will have to supply pixel values into this RAM prior to performing the subtraction with this subsystem. In addition, the third point corrector has two possible modes of operation: one is the normal image compensation during operation, and the second is the collection of a background scene from a uniform calibrator, which requires the coadding of a number (64) of calibrator scenes properly into the RAM bank. The control computer diagnostic should enable this second mode, evaluate the results, and use the results as a technique of filling the RAM bank with the values needed for continued diagnostic operation.

The scan conversion buffers should have power, parity, and memory integrity checks performed by the control computer. Again, test signal data can be examined by the control computer if this memory is located within its addressing space, and the results can be compared against the known proper answers. In this manner a relatively simple software program could verify proper operation of the scan conversion memory. This would occur at the diagnostic point E5.

The final step in the signal path that should be evaluated is the data recorder. It is very useful if the recorder contains built in test equipment (BITE) that has been provided in its design. This additional option allows the control computer to access diagnostics built into the system by the manufacturer and test that all parts of the recorder are functioning properly. Most instrumentation recorders available today incorporate some sort of BITE, and this should be a criteria used to select a recorder, as described in section 4.4. BITE functions should be exercised by the control computer during the complete system checkout prior to camera operation. If BITE functions are not available in the data recorder, a series of diagnostic tests should be written into the control computer software so that some confidence in the proper operation of the recorder can be established. For example, test patterns could be fed to the computer, recorded, played back, and then compared with the original data. Test points should be available on the power voltage levels being supplied to the recorder. Additional test points, indicating such factors as the amount of tape remaining, should be accessible and checked by the control computer. Another example is the recorder temperature, which must be monitored. Most require heaters to maintain the temperature at a minimum level, and these heaters will need to be activated if the temperature drops far enough. During recorder operation, heat may also build up and exceed the temperature maximums, in which case the control computer should activate cooling (if available), or pursue some sort of cooldown strategy (which can range from shutting the recorder off to activating cooling louvers over the recorder enclosure. Since it is likely that the recorder will be hermetically sealed with gas under pressure to allow operation in the space environment, the pressure of the gas should be monitored with a test point to ensure that no leaks occur undetected. Diagnostic requirements are for 2 analog readouts

Section 4.5

and at least 4 logic state test points (exact number depends on the complexity of the BITE supplied in the recorder).

The diagnostic interface for other physical subsystems of the SBS Camera system is described briefly in the following paragraphs, with areas requiring attention highlighted.

Host platform/SBS power interface: Power is supplied from both the SPAS and the HH-G mounts on the shuttle as 28 VDC. The voltage level and current consumption of this voltage should be monitored and represent test points available to the control computer. Note that the minimum levels of fusing called out for the payload power supplies (section 4.6) use fuses that do not have a remotely readable status. The response time allocated for these test points should be reasonably fast because if main power fails, the computer may want to enable important actions to take place with the remaining power. Such actions are final design dependent but can include actions such as stowing components, shutting down certain systems like the gas flow in the cryogenic cooling system, replacing covers, etc. The loss of basic power to the SBS Camera represents a catastrophic failure condition, and actions to be taken during power loss should be evaluated carefully in the final design. Options such as providing a small amount of power via a rechargeable battery (10 to 20 seconds worth) to allow orderly system shutdown should be considered. Diagnostic requirements are 2 analog readouts and 4 test points with rapid response.

Telemetry interface: The telemetry interface exchanges information between the payload and the host platform's standard information buses. The SBS Camera telemetry interface will depend upon the control computer for basic operation, but should also have additional circuitry that will allow it to override the control computer system in event of its failure. This addition is required if the control computer fails or its operation becomes erratic, resulting in wrong commands being sent to the camera hardware, or no commands at all. Test points should be available in this system to allow the ground operators to interrogate its status directly, as well as to allow the control computer to monitor its proper operation. Diagnostic requirements are approximately 4 logic state lines.

Cryogenic cooling system: Several control computer test points are required to monitor operation of the cryogenic cooling system. The exact points required depend upon the final cryogenic cooling system selected for the system. The amount of cryogen remaining should be constantly measured, which might be a level control for a liquid or solid cryogen, or a pressure control for a stored gas system. If valves are required in the final system, these valves should have an output signal indicating their state (closed or open) so that the control computer can take appropriate action if one is in the wrong state. If cryogen or gas must flow from one point to another, the amount of flow should be monitored and if possible compared against minimum and maximum allowable limits. If the system generates heat during operation (a mechanical cooling engine), the temperature of the heat exchanger should be monitored with a sensor accessible to the computer. An additional test point should exist that changes logic state when the temperature exceeds the maximum allowed, interrupting the computer and allowing immediate action to be taken to avoid cooler damage. The items being cooled to cryogenic temperatures (the detector, the filter wheel, and the dewar walls) should have temperature sensors that can be read during operation to verify that the cooling

Section 4.5

system has attained the proper temperature. As above, test point logic could be provided for a line to change logic state for temperatures that are too warm or too cold. The approximate diagnostic requirements for the cooling system are approximately 7 test points and 7 analog readouts (temperature and flow rate).

Optical system: Again the diagnostic interface required here depends on the complexity of the final optical design. Every moving element should have a position indicator, so that the computer can read the position of the element as it is moved. In the reflective design envisions for the SBS system, there should only be a single moving component that sets the focus of the camera (not including the FOV tracking system). There should be a temperature readout of the different optical elements, as well as test points that check for temperatures at each end of the allowable temperature range. Temperatures too high or too low could introduce, through expansion or contraction of the optical elements, unacceptable errors into the optical system. It is expected that at least a single movable cover will be included to cover the camera field of view when it is not operating, so test points should be included on it. The filter wheel present in the dewar also needs position sensors on it, so that the current filter being used can be read out by the computer. The remote interface requires approximately 4 analog readouts and 5 logic test points.

Tracking system: The trackable mirror will require sensors that indicate when the system is at its limits along all three axes. In addition, three high accurate readouts of the mirror x, y, and z position will be required so that the computer can determine where the field-of-view is and where it needs to be moved to. These position readouts will probably consist of high resolution (12 bits or more) optical encoders. The control computer will need some way of reading these values in, and will then require some computation time to evaluate them and determine where they need change. If a separate SBS Camera aspect tracker (a star tracker) is included in the basic system (as recommended), it will have additional test points as well as angular positioning information that needs to be read out by the control computer. If the tracker is not included, pointing information provided by the host platform will be used to determine camera aspect. Note that, in addition to this basic diagnostic interface, the control computer will probably be used to make the required calculations of SBS Camera aspect from the tracking information (either from star tracker or data read from shuttle). This will require additional computing resources. The remote interface for the tracking system is 6 analog readouts and 8 logic test points.

Calibration system: There are two primary elements in the calibration system. First there are the heating or cooling elements used to get the calibration surfaces to the proper temperature, and then there are temperature readouts to monitor the temperature value. There can be up to three calibration surfaces, as discussed earlier. A temperature readout system should be provided for each calibrator. Additional test points should be provided so that, if the temperature goes out of acceptable range, an interrupt will be generated in the control computer so that appropriate action can be taken. The remote interface requirements are 3 analog readouts and 6 logic test points.

Housekeeping readout systems: Much of the general housekeeping information that needs to be collected from the different components of the SBS system has

Section 4.5

already been covered in the detailed discussion of each payload subsystem above. Some additional items that need attention are the time base generation and the formatting of housekeeping data for recording. The time base will be set from the host platform's mission elapsed time (MET) information. An IRIG-B formatted version of this signal is available in the HH-G platform (section 4.6), and this will also be used for timing information. Maintaining the correct time with the data as it is collected is critical to later data reduction and analysis, and thus some redundancy must be provided in the system. To ensure that the system time base is not lost, the control computer should contain its own internal clock and maintain a count of time on its own. This can be periodically compared to the time information available from the host to ensure that there is no discrepancy. Thus if time data from the host platform is lost for a period of time, the SBS will be able to maintain time information independently without compromise of the data. The formatting circuitry for recording the housekeeping information will depend on how the data is to be recorded. Several test points should be allocated for this section.

The final load of remote interface points required by the computer for the processing electronics systems is on the order of ten interfaces. The requirements for the rest of the system are approximately 24 analog, or continuous, readouts and 42 logic test points. Note that these numbers depend upon the redundancy built into the system. If redundant systems are provided, the number of test points and readouts will increase as well.

4.5.2.3 Calibration mode

Calibration is one of the operational modes of the SBS camera. As such, it primarily consists of a sequence of commands or steps that the camera must follow. The control system must have a way of issuing the command, verifying that it has been executed, and waiting for its completion. It must also have the flexibility to bypass certain steps in the sequence if some of the components involved are declared inoperable due to failure.

Two types of calibration are planned for the SBS Camera (as discussed earlier): extended and abbreviated. A brief walk-through that illustrates the steps required of the control computer during a sample calibration run is shown below. First the computer determines if an extended or abbreviated calibration is being requested. The calibrator heaters are enabled. The computer then verifies the operation and temperatures of all three calibration sources, and waits until the temperatures are stable. The system then verifies the operation of the tracking mirror. The first bandpass filter to be calibrated is selected. The mirror is commanded to observe calibration source 1. When the mirror is stable, a background image is collected for the third point corrector. The instrument parameters are read out and stored. The camera then collects and records a sample of data on that calibrator. This process is repeated for the other two calibration sources. Then the filter position is advanced, and the complete process is repeated. When the calibration has been completed, the mirror is commanded to rotate so that scene image data can be collected again.

Note that a certain amount of fault tolerance should be built into the calibration software. For example, if one calibrator refuses to heat up, or is failing, the software should be flexible enough to modify its sequence so that the calibrator is

Section 4.5

avoided, to prevent waiting forever for the start of calibration. Because of the energy that will be dissipated in heating the calibration sources, their resistive heaters should also be turned off when the system is not calibrating, to conserve electrical energy.

4.5.2.4 Data collection mode

Data collection mode is the other operational mode of the SBS camera. As the calibration mode, it also consists of a sequence of steps that the camera must go through. The actual sequence, however, is very dependent on the actual mission being flown. Anticipated examples include acquiring a target and maintaining track, scanning through filters, and possible measuring events against a pre-programmed time line. Note that the first, and most important part, of all sequences is acquiring the target of interest. This may be a physical target, or it may require simply orienting the camera to a certain set of angles and aspects required for the mission. This is the first point that the camera is required to interact with outside world. It must be assumed that it will be in a more or less random orientation when it begins. Six steps are involved in the target acquisition process. First, the current orientation of the payload reference plane is determined. A guess is then made, based on the expected target position (if available), as to what orientation is required to observe the target. The system optical axis is then moved to the first guess position. The camera should then enter a systematic search mode that scans the available field-of-view for the target. At the same time, the computer must monitor the motion of the platform and correct for changes in orientation introduced by this movement. Finally, there must be some way to determine when the target of interest is finally acquired. It is likely that this will simply be a visual display of the image to a ground operator, who will then indicate satisfactory track via the telemetry stream.

Once the target, or desired orientation, has been acquired by the camera, it must have some way of maintaining track. The simplest way to accomplish this is to have the ground operator view a version of the camera imagery, and as the target moves about in the instrument field-of-view, the operator issues the appropriate commands to the payload so that it will alter its aspect and track the target. Note that this may prove unreliable, primarily because of the potentially large communication delays between ground or shuttle station and the actual payload. These delays can be on the order of 2 - 20 seconds (discussed in section 4.6). Thus operator commands will have a built in time lag that will complicate tracking demands. It is expected that the tracking system will need to make frequent aspect corrections, since the platform will have a motion of its own and, in the case of the SPAS, will be making relatively sharp, sudden aspect corrections using jets of cold gas. Thus some consideration should be given to automatic means of maintaining target track. Unfortunately, most computation-based algorithms are not very reliable and can require large amounts of computing resources (processing and memory). For example, point source or edge detection algorithms frequently require several calculations per pixel, and the imager is collecting 39040 new pixels 30 times a second which translates into computing requirements of several million operations a second, which is beyond the capabilities of the control computer systems that can fit in the SBS payload restrictions. In addition, the true bottleneck would not be in the processing, but would be in pixel access: getting the pixel values from memory to the processor and back. Custom hardware could be added to offload part of these tasks,

Section 4.5

but the system then becomes considerably more complex. It is important to evaluate the final capabilities of the control computer in relation to the total computational overhead of simply operating the instrument to see if additional resources are available for this task. Another possible alternative is to send positioning information on the target to the SBS payload. The computer can then calculate the angular position of the camera FOV, and the angular position of the target of interest, and then make tracking adjustments as required. This greatly reduces the computational load, but the time delays discussed earlier come into play. This alternative also requires some independent method the sensing the position of the target. If the target is the shuttle, there must be some way of accessing the shuttle's own positioning information via a telemetry link in a timely manner. If the target is some other satellite, this may not be an option.

After the target of interest has been acquired, and track is being maintained on it, there are the rest of the relatively mundane data collection tasks that must be taken care of by the control computer. These tasks include monitoring of all analog sensors (temperature or pressure) and commanding changes to the hardware as required. The data recorder must be controlled and operated to store the data. If gain and level controls are included on the low resolution output of the instrument, the control computer will have to operate these. Instrument service requests received from either the ground operator or pre-programmed sequences of steps need to be put into action. Such requests include changing the bandpass filter, changing the tracking position, and changing the instrument focus. Housekeeping data must be collected from the various sensors and directed to the recorder. A continuous interface to the telemetry stream is required, both in requesting information (such as shuttle aspect and position) and responding to ground operator requests. Finally, any test points that signal an error via an interrupt must be serviced, and possible alternate instrument operation strategies must be followed.

4.5.2.5 System shutdown

This mode will put the payload back into a 'stowed' state, in which it will not be able to collect data. This stowed state will result in all power except survival heating being disabled from the system. It includes tasks such as turning off (and possibly rewinding) data recorders, disabling the cooling system, disconnecting from the telemetry system, and powering down the processing electronics. The control computer must also shut itself down in an orderly fashion.

4.5.2.6 Telemetry interface

The control computer is expected to assist in the processing of commands received over the telemetry link, and well as in sending information back to the ground or shuttle-based operators. A detailed description of the telemetry services available on the two host platforms can be found in section 4.6. Which of these services will actually be used by the SBS is very dependent upon the mission the camera is tasked to perform. The telemetry interface must be monitored, and when commands are received, they must be decoded, and the appropriate action must be taken. A command set, giving the ground operators manual control over all essential features of the SBS Camera, should be developed and incorporated into the system software.

4.5.3 Design requirements of control computer

Section 4.5

A set of performance specifications for the control computer is developed in this section. The reasoning behind each requirement is discussed as well.

4.5.3.1 Addressing/memory map considerations

It is desirable to have all PROMs and RAM present in the image compensation electronics accessible to the control computer. This allows the computer to verify the integrity of both, using checksums and parity checks, and for the RAM banks, it enhances the flexibility of the system by giving the control computer the ability to override default values stored in the banks. This also simplifies system checkout and development in the laboratory, as the development and testing of PROM values is simplified if they reside in the control computer's memory map. This translates into address requirements for seven large banks of RAM/PROM:

- (1) test signal injection PROM
- (2) defective pixel replacement PROM
- (3) background subtraction PROM (1st point correction)
- (4) response correction PROM (2nd point correction)
- (5) background subtraction RAM (3rd point)
- (6) scan conversion buffer A RAM
- (7) scan conversion buffer B RAM

On the current 160 x 244 element detector arrays, these banks must store 39040 12 bit pixel values. For the future 512 x 512 element arrays, the memory banks will need to store 262144 pixels. To maintain compatibility with future designs, each bank will be assigned 256K locations of 16 bit words. This requires 512 kilobytes of memory space. If seven banks and 1 spare are provided, a total of 4 megabytes of addressing space is needed. Note that the design does not need to allow simultaneous access to these memory banks by the camera electronics and the control computer. Only one at a time will be accessing them, which simplifies decoding circuitry and memory design.

4.5.3.2 Interrupt handling requirements

As demonstrated in the analysis of diagnostic requirements, the SBS control computer will require a robust scheme of handling interrupts generated at all the test points throughout the system. To simplify the design, several levels of priority should be available, to provide some order to the many interrupts that might be generated. Certain critical interrupts will require servicing within a maximum amount of time. One example of this is a hardware error that is detected during the processing of a data frame. The interrupt signaling the failure must be serviced before the frame ends so that the appropriate error flags can be set in the status information recorded with that frame. Thus the response time to interrupts must be significantly better than 1/30 of a second.

4.5.3.3 Program code and data requirements

It is estimated that the software required to perform all of the functions of the control computer will be at least 256 kilobytes in length. Thus provision should be made to address 256 kilobytes of PROM, which contains this code, as well as 256

Section 4.5

kilobytes of RAM, which will be needed to execute the code, and also to provide a soft copy of it so that ground operators can override the basic code if errors are found during a mission. To provide adequate backup, thus, a block of 1 megabyte of addressing space should be reserved for the basic software code. If the processor uses memory locations to carry out I/O functions, a minimum of 1 kilobyte of them should be set aside to handle all of the test and interface points anticipated. Thus the total address space requirements of the control computer are on the order of 5.1 megabytes of space.

4.5.3.4 Processor speed/computational capabilities

Since most of the functions of the SBS Camera will be performed using dedicated hardware designs, there is not a need for a great deal of processing power on the part of the control computer. The one possible exception to this may arise with the platform tracking system, which may add significantly to the computational load when the camera is scanning and searching for a target. When a tracking system is finally selected, careful attention must be paid to this computational aspect. The system will also require a moderate level of speed, simply to process any interrupts received, but it is not anticipated that any of the hardware interrupts will require a great deal of computation. Since the primary function of the control computer is to drive relatively slow hardware, computational bottlenecks should not pose major problems in the design.

4.5.3.5 Processor interface to user

The SBS control computer must be able to receive commands via the telemetry link or from a directly attached processor (for laboratory code development and system testing). It is anticipated that both of these will be serviced over an RS-232 type of interface. The computer must also be able to accept patched code, or completely new software, via this same type of RS-232 serial interface. This can likely be attained by having a minimal type of system monitor program, residing in ROM, that can be accessed at any time to override the main program, which may be going astray.

4.5.3.6 Mass storage requirements

No requirement for a mass storage device for program code or data is anticipated for this computer. The density of commercially available PROMs and EPROMs have grown high enough to make practical the storage of all program code directly in these type of devices.

4.5.3.7 Other requirements

The control computer will likely need at least 1 timer available, which will allow it to time processes, timeouts, and to maintain its own system time, which can be synchronized to the host platform's universal time via the telemetry interface. It is likely that more than one timer will be needed to fully meet the real-time operational demands of the system as described above. Another consideration is that the temperature and physical strength specifications must match or exceed the demands placed on the system by the shuttle and SPAS environment. These physical stresses are described in detail in section 4.6.

Section 4.5

4.5.3.8 Software development tools

Due to the size and complexity anticipated for the SBS control computer's operating software, a number of sophisticated development tools will have to be available for code writing and evaluation. One strong advantage to the use of an off-the-shelf computer system is the ready availability of software development tools that have been developed and debugged already. The minimum software development environment required will be a machine assembler and an operating system kernel. The availability of at least one higher level language would greatly simplify and speed code development as well. The operating system kernel should be suited to the real-time requirements of the control software, and also be able to function in an all PROM and RAM environment.

4.5.4 Types of control system

Many off-the-shelf, single board computer systems exist today, with a considerable amount of computing power in a small package and at low cost. There are several strong advantages to be gained from basing the SBS control computer on a commercially available single board computer. Among these are low cost (in comparison to the development effort to build a custom system), availability of replacement parts, and the availability of developed software tools (languages and operating systems). The primary disadvantage is that a system that exactly matches the requirements spelled out in the previous sections will not be found. Some compromises will be necessary, and usually custom hardware will be needed to interface the diagnostic and control functions with the commercially available unit. In practice, this disadvantage is not very serious, as the processing speed and capabilities of existing unit vastly exceed most of the requirements of the SBS Camera. As noted earlier, the SBS Camera should not make heavy computational demands on the control computer, because no direct image processing is undertaken by the system. The only critical requirements are in I/O capabilities and in interrupt handling. The purchase and modification of a commercially available system is far easier and more cost-effective than the design and fabrication of custom hardware capable of handling all of the functions described above.

Many commercial systems based around the 68000 microprocessor (by Motorola) exist, and exhibit the large addressing space, I/O capabilities, and speed required above. One example of such a system that would serve as a satisfactory base for the control computer is the GMX Micro-20 single board computer. A photograph of the system is shown in Figure 4.5-x. The entire board is only 8.8" x 5.75" x 0.68", and the power requirements are +5 VDC at 4.5 amps maximum, and +12 VDC at 0.15 amps maximum. A block diagram of the Micro-20 is shown in Figure 4.5-x. It is a straightforward system architecture. The CPU is a MC68020, which is a 32 bit processor, with 32 bit data and addressing paths. The unit contains 16 general purpose registers for programming. The 68020 has an addressing range of 4 gigabytes, and thus easily meets the addressing requirements of the control computer. It is available in 12 or 16 MHz speeds, which results in processing rates on the order of 2 million instructions per second. It supports memory mapped I/O, and has a rich family of support chips available from Motorola. The system supports seven levels of prioritized interrupts. Higher priority interrupts are serviced first, and lower priority ones are put on hold until all higher priority interrupts have been taken

Section 4.5

care of. By changing devices together at the same priority level, an unlimited number of devices can cause interrupts. A single non-maskable interrupt level is available for truly critical interrupts. It is possible for interrupting devices to provide their interrupt vector number to the CPU on interrupt, so that each device can be serviced by different program code. This architecture meets the demands imposed by the SBS hardware interface/diagnostic requirements projected.

The Micro-20 shown above has 512 K x 32 bits of RAM (with 1 wait state access) for program storage, and has an EPROM space of 64K x 32 bits, using standard EPROMs. For I/O ports, the unit has 4 asynchronous serial ports, and a single buffered 8 bit parallel port intended for a printer attachment. An I/O expansion connector is provided to extend the I/O and memory addressing space. It also has a floppy and hard disk controller built in, which is useful for laboratory code development and testing. The basic board contains a ROM based debugger, capable of examining and changing memory, running programs, assembling code, and accepting new code in the Motorola S format. A wide variety of language and operating system support is also available from the board's manufacturer. More detail on the unit can be found in section 6 of this design study.

4.5.5 Summary

The overall requirements of the SBS control computer have been identified and discussed in this section. The six major operating modes anticipated for the payload have also been discussed in detail. Considerable detail has been dedicated to the diagnostic functions of the computer, since this is expected to be the primary function of the control computer performed in addition to operating the payload system. A detailed list of control computer specifications were developed, based on this discussion. Use of a commercially available unit is strongly recommended because of the savings in development time and cost.

4.6 Carrier restraints

4.6.1 Payload platform overview

The SBS Camera is an infrared sensor system intended to make radiometric measurements of targets and backgrounds in a space environment. The current design effort is towards packaging a 160 x 244 element PtSi focal plane array - and all associated camera electronics and mechanical subsystems - into a system capable of being transported into space on the Space Transportation System (space shuttle). The system will be flexible and rugged enough to fly on several of the 'standard' payload orbit systems developed by NASA for space experimenters. The system will collect data on targets or backgrounds of interest while in orbit and store the data for later analysis by infrared phenomenologists.

Two possible platforms are being considered to fly the SBS:

- (1) plate mounted Hitchhiker-G payload
- (2) Shuttle Pallet Satellite (SPAS)

One of the design goals of this project is to make a system capable of flying on

Section 4.6

either of these platforms. Thus the specifications spelled out by NASA for both platforms apply to the SBS Camera; when one set of specifications is more restrictive than the other, the tighter restrictions will be designed to.

Both of the shuttle platforms have the instrument mounted on one or both sides of a large, flat aluminum plate. Because of this simple mounting system, it should be possible to adapt the system for launch on an unmanned rocket or balloon by remounting the system components on both sides of a plate that is half as wide. Thus by designing to the requirements imposed by HHG and SPAS the additional flexibility of using non-shuttle launch systems will not be lost. Unmanned launching systems do not have payload requirements as standardized as the space shuttle and so we will only mention some restrictions that have applied to previous instrumentation developed at SR¹ that has been launched on small rockets. A rocket launch of this type provides a very limited data collection time and does not match the goals defined earlier for this system. Thus no further attention will be given in this study to this payload carrying system.

4.6.1.2 Shuttle overview and coordinate system

In order to provide a common frame of reference NASA agencies have defined a coordinate system based upon the space shuttle frame. This coordinate system is defined and explained in Figure 4.6-1. In order to maintain compatibility with information provided by NASA, this coordinate system will be used throughout this design study.

4.6.1.3 Hitchhiker-G

There are four types of mechanical support systems offered under the Hitchhiker-G program:

- (1) Get-Away-Special (GAS) Canister
- (2) Plate Mounting
- (3) Additional Core Plate Mountings
- (4) Direct Mounting of Experimental Package

The SBS is being designed towards the 'Plate Mounting' system, as this seems to offer adequate resources for the camera and is reasonably compatible with the SPAS requirements. The direct mounting of the experimental package option is not needed, as the plate mounting system fully meets the needs of the SBS Camera system. A diagram illustrating the first three options listed above is shown in Figure 4.6-2. Another diagram illustrating the plate mounting system from a side aspect view is shown in Figure 4.6-3. In both of these diagrams the payloads are shown mounted against the side of the shuttle cargo bay. An exploded view of the plate mounting structural assembly is shown in Figure 4.6-4. Additional mechanical detail, such as sizes, etc., is provided in section 4.6.3 of this report: Mechanical Interface.

The Hitchhiker-G payloads can only be mounted in certain positions in the shuttle cargo bay, due to the design of the gas beam adapter that fastens the mounting plate to the orbiter. A list of these locations, along with their location in the shuttle, is shown in Figure 4.6-5. The x and z axis positions relative to the origin are provided

Section 4.6

for reference.

4.6.1.4 Shuttle Pallet Satellite (SPAS)

The SPAS is an experimental payload platform that will be launched into orbit in the shuttle cargo bay. Once in orbit the platform can be extended from the cargo bay and operated either attached to the shuttle or released completely as a separate satellite. After flying separately from the shuttle (at distances up to 50 km) the SPAS is retrieved and returned to the cargo bay and thus brought back to earth. The SPAS is reusable and provides the following services to the payloads attached to it: power distribution, data handling, telemetry links, and pointing. Two SPAS flights have been flown to date.

Two different views of the basic SPAS platforms are shown in Figures 4.6-6 and 4.6-7. Many of the SPAS subsystems are labeled in these two diagrams.

The payload interface to the SPAS platform is a metal plate called an Equipment Support Panel (ESP). A detailed mechanical drawing of this metal plate is shown later on during the discussion of mechanical interface. The instrumentation package is mounted on this plate; the ESP can then be attached to the SPAS platform on one of the many open locations on its surface. Examples of instrumentation attached to the SPAS are shown in the three parts of Figure 4.6-8. This example is from the IMPS-1 payload that is scheduled to be flown on the SPAS. The SBS Camera head, electronics, and recording systems are all being designed to fit on a single Equipment Support Panel. The similarity of the ESP to the Plate Mounting option in Hitchhiker-G makes the SBS design reasonably portable between the two platforms.

Since the SPAS platform is capable of flying free of the space shuttle, it requires its own coordinate system for reference. The NASA defined coordinate system for the SPAS is shown in Figure 4.6-9. The coordinate system for one of the Equipment Support Panels is shown in Figure 4.6-10.

A functional block diagram illustrating all of the SPAS subsystems is shown in Figure 4.6-11. The adaption kit (designed by JPL) provides power and a power distribution system to all of the experiments on the platform. It also provides a tape recorder that is capable of recording digital data produced by the experiments. All of the systems designed into the SPAS are also shown in this figure. Attitude control and maneuvering of the platform is accomplished by cold gas fired from pressure bottles. A thermal control system is provided. Radio links to the shuttle exist for SPAS control, experiment commands, and a limited amount of data telemetry. The basic SPAS services are powered by two batteries and a power distribution system that is separate from the experimenter power.

4.6.2 Overview of shuttle payload restrictions

The restrictions imposed by the SPAS requirements are far more restrictive than the Hitchhiker-G limitations. However, the usefulness of this new camera in terms of its proposed mission is extremely limited when flown on a Hitchhiker-G, since very little of the external shuttle surface can be observed from inside the cargo bay. Thus the SBS camera should be designed to meet the more stringent requirements of

Section 4.6

the SPAS system. An additional advantage of designing the system in this manner is greater flexibility in getting on a shuttle manifest, as the system will be able to fly on either type of system.

The following restrictions have been primarily extracted from two documents. The Hitchhiker-G requirements have been taken from the document "Hitchhiker-G Customer Accommodations and Requirements Specification", HHG-730-1503-02, dated November 1985. The SPAS requirements have been taken from the document "SPAS/IMPS-1 Interface Control Document (ICD)", JPL D-2838, Version 1.2, 15 May 1986. Other sources are noted in the references section of this study.

4.6.3 Mechanical interface

4.6.3.1 Hitchhiker-G Plate Mounting

A single Hitchhiker-G plate mount is capable of supporting up to 250 lbs (113 kg) of experimenter equipment. The physical dimensions of the plate are 50" x 30". Note that this is the actual plate available to mount the experiments; the actual plate is larger, but part of this additional area is taken up by an avionics box that contains the power and data interfaces to the rest of the shuttle. The relation between the avionics box and the rest of the plate is illustrated in Figure 4.6-3.

The grid of mounting holes for bolts used to fasten instrumentation to the plate is 70 mm x 70 mm spacing. The thickness of the customer hardware at the plate interface has to be between 0.125" and 0.500" (page 2-24). The payload is allowed to extend beyond the ends of the plate, but is restricted to an area defined by an 88" radius envelope (about the center of the plate). This radius is illustrated in Figure 4.6-3.

Provision has also been made to accommodate additional experiment plate mountings as part of an experiment, if additional room is required. The plates are referred to in the Hitchhiker-G documentation as "Additional Core Plate Mountings". Each additional plate provides mounting for up to 500 lbs of equipment per plate. Each plate provides a usable area of 50" x 60".

4.6.3.2 SPAS Carrier

The SPAS provides an equipment support panel (ESP) that the SBS camera can be mounted on. The ESP is illustrated in Figure 4.6-12. This panel is made of lightweight aluminum and measures 820 x 690 mm (32.3 x 27.1 in). The pattern holes used for mounting bolts are on a grid with a spacing of 70 mm x 70 mm.

The first significant difference between the SPAS mounting plate and the HHG plate is size; the SPAS mounting plate is physically smaller. The actual space available to the experiment on the SPAS ESP is even smaller, however, because the experiments are not allowed to go out to the edge of the plate. The envelope of available space on the outside face of the ESP is shown in Figure 4.6-13. A detailed drawing of the bottom edge of the experiment space is shown on the bottom of Figure 4.6-13. For the first centimeter of space above the ESP, the experiment space can be no closer than 21 mm to the edge of the plate. Then a 15 degree angle imposed on the experiment envelope reduces the available space by 14 mm. Thus for

Section 4.6

practical planning purposes, the dimension labeled 'B' in Figure 4.6-13 must be used to estimate the total area on the plate available. The values for 'B' are reported in the table in Figure 4.6-13 to be 620 x 760 mm.

The height of the experiment from the ESP (labeled as 'C' in Figure 4.6-13) does not have a fixed limit, since it depends upon the panel location on the SPAS. Different panels have different allowed clearances. One of the driving forces determining the allowed height is the stowage of the SPAS in the cargo bay during launch and re-entry. Figure 4.6-14 illustrates this for the IMPS-1 payload. Certain panel positions have a large vertical clearance that in theory could go out to the static envelope defined as 4512 mm. In actuality, center of mass and structural strength considerations would likely prohibit such a long and narrow payload. Other panel positions along the bottom of the SPAS are limited to 760 mm, and the two on the ends are limited even more by the radius of the static envelope. The maximum heights for the panels mounted on the side of the SPAS are determined by what is in the rest of the cargo bay. Certain positions are also limited by access required to the grapple fixture (the SPAS is launched and retrieved by the shuttle arm) and by the lights on the SPAS. For the purposes of this study, the height limit imposed on the lower panels (760 mm) will be used as a design guideline. Obviously it is desirable to restrict this height in the final design as much as possible for maximum flexibility. In practice, given the relative simplicity and small size of the SBS Camera, this should not be a serious limitation.

Another important difference from the HHG plate mounting is the fact that experimenter equipment can be mounted on the back of the equipment support plate as well. Since the SPAS is essentially an empty frame, a considerable amount of space is available beneath this plate. A drawing showing the equipment envelope available on the inside face of the ESP is shown in Figure 4.6-15. This space is split into two right triangles by the crossbar that is a structural support for the SPAS frame. A 20 degree angle around the edge of the experimenter area is shown in the detailed drawing in Figure 4.6-16. Each of these triangles provides approximately 2540 square centimeters of plate space for the experimenter. Note that the inner dimensions of the available space (i.e., the area within the 20 degree angle) was used to make this calculation. This is a significant addition to the experimenter space resources, and allows separate components (such as power supplies or small tape recorders) to be removed from the outside face of the ESP, which helps to compensate for the reduced space available from the HHG plate mounting.

4.6.3.3 Recommended materials

Some restrictions apply to the materials that can be used in the fabrication of the SBS Camera payload. The emphasis in determining these restrictions is on freedom from stress corrosion cracking, toxicity, flammability, and excessive outgassing, since these effects are of primary concern to the shuttle operation. For HH-G payloads, materials lists must be completed relatively early in the design process and submitted to the HH-G office for review. To simplify this process, the HH-G office has compiled lists of materials deemed acceptable for use on HH-G payloads. Materials used in the design of the payload structure, support brackets, and mounting hardware must comply with the stress corrosion cracking criteria called out in the specification MSFC-SPEC-522A. A listing of acceptable materials can be found in this document. All other materials used must be approved by the HH-G

Section 4.6

office under a Materials Usage Agreement (MUA), which is a form submitted by the payload designer. The acceptable criteria used for outgassing restrictions is a maximum of 1 percent total mass loss and a maximum of 0.1 percent collected volatile condensible materials. The specification that governs this is MTR 313-005. Materials that exceed these basic restrictions (i.e., they have less than 0.01 percent collected volatile condensible materials) are listed in MTR 313-005. This restricted list is intended for use in systems sensitive to outgassing, such as those containing optics. Materials rated to be suitably non-flammable are also indicated in this table.

Traceability is also specified for materials used in either SPAS or HH-G payloads. Three levels of traceability are specified for component materials, depending upon the classification of the components as 'safety-critical' or 'non-safety-critical'. The non-safety-critical classification applies to components whose failure will not result in the release of more than 13 grams of mass from the payload in the shuttle cargo bay. Safety-critical is a classification that applies to all other components, which are assumed to be a potential hazard to the shuttle or crew. Note that all payload components are assumed to be safety-critical, and analysis and testing is required to demonstrate that any given component can be classified as non-safety-critical. The three levels of traceability specified are:

(1) critical traceability - this level of traceability applies to all safety critical components. Each material used at this level must be directly traceable to a source tested and verified against applicable specifications.

(2) lot traceability - this applies to non-safety-critical items that are one-of-a-kind items

(3) basic traceability - implemented for high volume production items made of controlled materials. These items must be non-safety-critical.

4.6.3.4 Payload mechanical design

The process that will be followed for the design of the SBS Camera payload mechanical structure involves several distinct steps. First, a preliminary design is put together, based upon the engineering trade-offs performed to arrive at a system that can meet the basic payload mission requirements within the constraints placed on the payload. This step has been completed in this design study. Secondly, a preliminary structural design must be performed, using the physical stress loads anticipated (detailed in this section). Usually the design is then analyzed using a computer model for static, dynamic, and stress loading. The design then undergoes several iterations until it meets all of the basic safety requirements and has sufficient margins built into it to reliably operate. The payload is then fabricated and subjected to actual physical testing, where it must pass simulations of the static and dynamic loading specified by the host platform requirements. Again, several iterations may be required at this point, as problems are discovered and modifications to the design become necessary. Finally, the final structure is assembled for use on actual missions.

4.6.4 Thermal factors

Thermal factors will play an important role in the design of the SBS instrument. The temperature of the instrument will be driven primarily by the power dissipated by the system, and the temperatures encountered in either the shuttle cargo bay or

Section 4.6

on the SPAS platform. Both of these elements need to be modeled in an analysis of the instrument so that the temperature of the system components during operation can be predicted.

4.6.4.1 Environmental heat loading

Thermal considerations play an important role in the design of any space payload, and the SBS camera is no exception. This section will discuss the environmental thermal loads that the payload will experience, describe the thermal analysis that the payload must be passed through, and detail some of the methods used to add both passive and active thermal control into the system design so that it will attain equilibrium at the desired component temperatures.

Note that this environmental heat loading must be combined with the view of each component of the payload under analysis. All of the apparent temperatures given below represent ways of modeling the radiation flux observed by the spacecraft from these different environmental sources. To arrive at the total energy balanced for a specific component, the fractions of each of these sources observed by the component must be calculated and the source radiation must be multiplied by these view factors. In general, this process is complex and very dependent upon the payload final configuration.

4.6.4.1.1 Shuttle cargo bay emission

There are a number of different conditions that the payload will be subjected to prior and during the mission:

1. pre-launch and pre-deployment conditions, when payload is contained within cargo bay (also post-deployment)
2. conditions in cargo bay with doors open
3. payload deployed in space (SPAS only)

Each of these conditions imposes different thermal loads on the SBS payload. Note that the system will only be operating for second condition (HH-G) or third condition (SPAS). When system is non-operating, thermal control is not as much of a problem, since the shuttle itself will maintain reasonable temperatures (only exception is possibility of requiring heating). During camera operation, however, significant amounts of energy will need to be dissipated, and a complete thermal load analysis will be required.

When the payload is enclosed in the shuttle cargo bay, the only source of heat is radiation and conduction from the cargo bay environment. When the system is exposed to the space environment, there are several sources of thermal energy input: solar illumination, solar reflections off the earth, earth thermal radiation, and shuttle thermal radiation. Radiative cooling processes are also effected by the presence of the earth, shuttle, or deep space. Each of these factors will be briefly described to allow general thermal loading calculations to be carried out.

The first conditions of heat loading to be covered are those applying to the payload when it is in the cargo bay prior to deployment. When the system is in ground handling, the controlled temperature range ranges from 0 to 45 degrees C

Section 4.6

operating (pre-flight checks) and -20 to 45 degrees C non-operating. When the system is in an uncontrolled mode, the non-operating temperature range is -40 to 70 degrees C. The maximum rates of temperature change that could be encountered are 5 degrees C per hour in a temperature controlled environment, and 15 degrees C per hour in an uncontrolled environment. Pre-launch conditions in the shuttle cargo bay range between 7 and 27 degrees C, since air at these temperatures is circulated through the cargo bay at a rate of 450 lbs/minute. During launch and while attaining orbit, the overall temperature range in the cargo bay is 4 to 66 degrees C.

The next condition that must be planned for is for the payload in the cargo bay with the door opened. This condition applies to both the HH-G and the SPAS platform analysis. The temperatures in the cargo bay are strongly determined by the orientation of the shuttle relative to the earth and sun. A complete thermal analysis would use the following conditions for the apparent temperature in the cargo bay. There are five general conditions. First is the shuttle tail oriented towards the sun, with the cargo bay facing deep space. This is an example of the coldest environment to be encountered. The external environment has an apparent temperature of approximately -100 degrees C. The second condition is the shuttle nose oriented to the sun, solar inertial. For this case, the cargo bay receives no solar heat but some earth radiation. This is an example of a moderately cold environment, and the apparent temperature is about -50 degrees C. The third condition encountered is when the cargo bay faces earth. This is an example of a benign environment with an apparent temperature of -5 degrees C. The fourth condition is when the shuttle is rotating about its x axis, which is a commonly used method of thermal control for the entire orbiter. This is also an example of a benign environment, with an apparent temperature of 10 degrees C. The fifth condition is encountered when the cargo bay faces the sun. This is an example of a hot environment, and the apparent temperature of the cargo bay is around 40 degrees C. All of these conditions translate into a cargo bay temperature between -100 and 40 degrees C, with the qualification that the actual steady-state temperatures observed depend strongly upon the maneuvering and aspect of the shuttle.

The third operating mode that the SBS payload will encounter is when it is separated from the shuttle and in free flight facing space. This mode will of course only be encountered on the SPAS host platform. This is the harshest environment that the payload will be exposed to. When the SPAS is free of the shuttle, the thermal loading encountered by the experiment will depend on the orientation of the payload relative to the earth and the sun, since both of these are sources of blackbody radiation that will heat up the experiment. Unlike the shuttle cargo bay, the SPAS offers very little thermal mass to the experiment, and so the combination of heat generated in the instrument and that absorbed from the earth and sun will determine the temperature extremes encountered. Shading caused by neighboring experiments (or experiments mounted on the opposite side of the SPAS) will also have an impact. For this reason, the energy inputs that will be encountered from the space environment are described in detail below.

4.6.4.1.2 Solar flux

The total solar flux encountered outside the earth's atmosphere (over all wavelength bands) has an average value of 1353 watts per square meter. Because

Section 4.6

the earth's orbit around the sun is an ellipse, small variations (on the order of 3 percent) occur in this value during the course of the year. The heating caused by the solar flux on a surface of the experiment can be estimated by an equation provided in the SPAS/IMPS documentation:

$$Q_s/A = 0.14 \sin(\theta)$$

where

Q_s/A = incident solar heating in watts/cm²

θ = the angle between the sun vector and the surface

This formula assumes that the average solar flux is approximately 1400 watts per square meter. This is the maximum solar heating for a surface with a solar absorptance of 1. The heating of surfaces with lower solar absorptances can be estimated by multiplying the result of the above equation by the surface absorptance. The spectral distribution of the solar irradiance is shown in a plot in Figure 4.6-17. Because of the temperature of the sun's surface layers, the bulk of its radiated energy (95%) is at wavelengths between 0.22 and 2.7 micrometers. The emissivity of the surface through this peak of solar irradiance is usually referred to as the solar absorptance, while the emissivity beyond 2.7 micrometers is called emissivity. This spectral distribution of solar energy is exploited by certain paints that reject the bulk of the solar energy while still maintaining a high emissivity at longer wavelengths.

4.6.4.1.3 Earth emission and reflection

The earth and its atmosphere also radiate like a blackbody at the earth mean temperature. It is usually reasonable to assume that the earth emits diffusely in accordance with Lambert's law. The earth mean value of thermal emission (over all bands) is approximately 237 plus or minus 7 watts per square meter. Earth emission can be estimated using the plot in Figure 4.6-18. The angle (in this case, γ) used to read the graph is the angle between the experiment surface and a vector normal to the earth's surface. For non-blackbody surfaces, the heat input from the earth can be multiplied by the emissivity of the surface.

The earth also reflects a certain fraction of the solar irradiance onto a payload in orbit about it. This flux, commonly called the albedo flux, can be estimated by multiplying the solar flux by a scale factor that represents the average reflectivity of the earth's surface and clouds. The typical mean value used for this reflectivity is 0.3, though it can range in value from 0.1 to 0.8.

4.6.4.2 Thermal modeling of payload

The total heat input to the experiment can be estimated by performing the above calculations for all of the experiment surfaces. The heat generated by the experiment itself must also be included. This heat input is then offset by the energy radiated from the experiment surfaces. These calculations must be carefully done for any proposed experiment design, as in general the sun could be at any orientation with respect to the experiment, and it is strong enough to significantly alter the heat balance of the system. In general there is a very complex interaction between the system design, power dissipation, equipment location, and the component temperature limits. Usually a computer model is required to accurately

Section 4.6

model the thermal balance of the system. The breaks the payload down into a series of thermal nodes, and then calculates the average temperature of each component to determine where the excess or deficiencies of heat will end up. The model solves heat balance equations of the form

$$\text{heat stored} = \text{heat in} - \text{heat out} + \text{heat dissipated}$$

Heat is input to nodes by electrical power dissipation, radiation from the environment, or conduction from other nodes. Heat is lost through conduction and radiative cooling or other heat controlling mechanisms. The heat at equilibrium is calculated and then converted to an average temperature. The results from such calculations are used to determine the optimum thermal configuration for the system. Using this model the payload designer has control over variables such as the coatings, insulation, and metal structure thicknesses used, as well as additional means of active heat control. The model is then verified against actual tests of models of the payload, with heat inputs simulated using infrared sources or electric heaters.

Some heat control is provided via the host platform services. For HH-G payloads, heaters and thermostats are provided on the plate mounting that normally will maintain the plate temperature at 0 degrees C. During the extreme cold modes of operation, however, the plate temperature can go an unspecified amount of degrees colder than this. The plate mounting is heat sunk into the gas beam of the shuttle, however, and this should provide a very large thermal mass (at least when compared to the proposed camera system). The SPAS carrier framework does not provide this large thermal mass, since it is constructed from carbon fiber and titanium materials optimized for strength instead of thermal properties. Thus the SBS payload cannot count on the thermal assistance provided normally to HH-G payloads.

Note that no detailed thermal loading calculations have been made as part of this design study, as this was beyond the scope of the contract. In the proposed design presented in section 6, the total energy dissipation of the payload (and heat generated) is estimated to be fairly small, and so it is assumed that heat dissipation will not be a major concern for the SBS Camera in either the HH-G or SPAS configuration. Thermal control must be designed into the payload from the start, however, and so brief discussion of thermal control methods is presented in the following paragraphs.

4.6.4.3 Payload temperature control methods

The following section describes some general methods that are available during the SBS payload design of providing thermal control. All of these methods have been employed successfully on past payloads.

4.6.4.3.1 Surface coatings

The coating of outer surfaces of the payload components determines the nature of the coupling of the payload to the very large heat sink of space. The goal is to design a system that attains an energy balance at equilibrium in the desired operating temperature range of all payload components. Note that the actual coatings desired must be selected on the basis of a detailed thermal analysis of the

Section 4.6

payload. Modifying the surface coating provides a simple way of dissipating excess energy from selected portions of the payload, and also controlling the potentially large energy inputs from the environment that can be encountered while on station. One example of a large and highly variable environmental input is solar heating. Illumination of the payload can cause large heat inputs that could result in overheating and damage to critical components during data collection. Solar heating can be greatly reduced by coating the illuminated surface with a paint that has low emittance (high reflectance) in the peak bands of solar radiation. Usually, for purposes of radiative cooling, it is desirable to maintain a high emittance at longer wavelengths in the infrared, where the peak radiation of objects from 0 to 100 degrees C is located. An ideal coating in terms of thermal control combines these two properties. Coatings with these properties exist, such as the white paint S13-G-LO. The emittance of a few representative surface coatings as a function of wavelength is shown in Figure 4.6-19. White paints, such as S13-G-LO, are considered 'cool' coatings, because they reject the majority of ambient solar radiation while still maintaining good radiative cooling properties. Surfaces with high solar absorptance and low emissivity at longer wavelengths (such as gold) are considered 'warm' coatings, because they will trap heat from the surface and absorb the solar inputs more efficiently. Black surfaces, with a high solar absorptance and a high emissivity at longer wavelengths, maintain the surface temperature at a median point between these two extremes. Coatings can be mixed (in a checkerboard pattern, for example), so that the divergent thermal properties described above can be combined and fine tuned to achieve exactly the desired balance.

Coatings degrade after a period of time in a space environment, primarily because of the high vacuum, the impact of charged particles or micrometeorites, and solar radiation. This degradation is usually measured across time scales of years, however, and for the short times on station anticipated for the SBS payload, the changes in coating properties associated with this degradation will not be a factor.

4.6.4.3.2 Thermal insulation

Thermal insulation reduces the rate of heat flow between different nodes of the payload. Insulation can consist of a single substance, such as a low thermal conductivity foam, or a multilayer insulation, where each layer is a highly reflective radiation shield kept apart by low thermal conductance spacing material. Multilayer insulation (MLI) is commonly used in space applications because the insulating capabilities are easily tailored to the payload thermal requirements. Each layer is highly reflective so that they reflect the thermal radiation from the inner layers back. Frequently the MLI layers are separated with an evacuated space to reduce thermal conduction and held together by a small amount of low conduction material. A typical MLI used in space payloads consists of an outer layer of 25 micrometer thick aluminized Kapton. The remaining layers are aluminized mylar separated by a dacron mesh. Making the outer layer from Kapton improves high temperature protection to the payload since Kapton has a maximum temperature of 343 degrees C, while mylar is good only to 121 degrees C. The vacuum between the insulating layers can be provided using the vacuum of space. Careful attention must be paid to the design to allow for gradual venting of the gas from the insulation during ascent, as too rapid of outgassing can rip and damage the MLI layers.

Section 4.6

4.6.4.3.3 Heat sinks

Heat sinks are objects with large thermal capacities that are placed in thermal contact with critical payload components. They provide temperature buffering to the component by absorbing excess heat for a period of time without significant temperature rise (or can also provide heat if the component is cooled too much). Metal heat sinks provide an inexpensive way of smoothing out temperature variations of components that operate cyclically, and generate a large amount of heat for only part of the time. Heat sinks are also known as thermal doublers.

4.6.4.3.4 Phase change materials

Thermal buffering can also be provided using phase change materials. These systems are constructed by filling a container with a material that undergoes a phase change upon heating or cooling (usually a transition from a solid to a liquid). When this container is placed in thermal contact with a system component, it presents a large thermal load when the temperature of the component tries to exceed the temperature of the phase change, since all of the energy is absorbed by the phase changing process. This scheme has been used for components that are run periodically and present heat loads of short time duration. The result is different from that of a heat sink because, instead of a gradual temperature rise, the temperature remains stable at the phase change temperature until all of the material is converted. Of course, once the conversion is complete, the phase change system ceases to provide further thermal buffering.

4.6.4.3.5 Heat pipes

Heat pipes provide a path of very high thermal conductivity between two points. They consist of a closed tube with inner surfaces lined by a capillary wick. A liquid with suitable properties is sealed into the tube. The end of the tube where heat is input is usually called the evaporation section. Here heat vaporizes the liquid, and the pressure differences move the vapor towards the other end of the pipe. This other end, where heat flows out of the pipe, is called the condenser section. Here the vapor is condensed and loses its latent heat of vaporization. Capillary pressure transports the liquid back to the evaporator section of the heat pipe.

These pipes are ideal for payload applications where a large amount of heat is generated that must be dissipated to prevent component overheating. The heat can then be moved to another place on the payload, where it can be safely dissipated away. A variety of designs and working fluids can be selected to tailor the heat transport properties to the requirements determined from the thermal analysis of the payload.

4.6.4.3.6 Louvers

Louvers on the outer surface of a payload allow active control to be maintained over the emissive properties of that surface. These devices are useful for dealing with large changes in internal heat dissipation or in wide variations in the external environmental heat load. Louver designs operate very much like blinds on a window. When the blades are closed, the surface properties of the blades determine

Section 4.6

the radiative energy losses and inputs. When the blades are opened, the surface below the blades becomes the driver of radiation loss and energy input. This allows a surface to rapidly change the heat flow through it. Louver blades are typically driven by springs fashioned from bimetals. The activation of the system can be directly tied into temperature sensors on the surface below, or can be remotely controlled via a computer.

4.6.4.3.7 Heaters

Heaters simply use electrical energy converted into heat through resistive elements. The amount of heating provided can be controlled by modifying the amount of current flow through the resistive element. This is a straightforward way of keeping the temperature above specified component minimums. Due to the potentially very low temperatures that can be encountered in a space environment, heaters are usually provided with critical components that can be activated when the temperature drops below a certain minimum, even when the payload is not operating. This arrangement is usually referred to as survival heating, and prevents damage to components from excessively cold temperatures.

4.6.5 Pressure factors

The largest changes in pressure occur during launch of the space shuttle. Normal atmospheric pressure is maintained for approximately 10 seconds after lift-off. Then vents present in the cargo bay are opened and the gas pressure begins to change fairly rapidly. A plot of the pressure change vs. time after liftoff is shown in Figure 4.6-20. A plot of the rate of cargo bay depressurization encountered during ascent is shown in Figure 4.6-21. In orbit the atmospheric pressure is approximately $10E-13$ torr, or essentially 0.

The repressurization of the cargo bay during shuttle re-entry is shown in Figure 4.6-22. Plots are shown for two cargo bay volumes: 519 cubic meters, which represents a fairly empty cargo bay, and 212 cubic meters, which is a more realistic configuration. The times are shown relative to the opening of the vent doors. The shuttle cargo bay vent door opening occurs at altitudes between 70,000 and 94,000 feet. The Hitchhiker-G documentation indicates that the repressurization rate of the cargo bay will not exceed 0.3 psi/sec during descent.

4.6.6 Dynamic load factors

Dynamical conditions are acceleration stresses, mechanical vibrations, and acoustical vibrations. The shuttle documentation indicates that the greatest vibration conditions occur during transient excitations during liftoff.

4.6.6.1 Acceleration load limit factors

The Hitchhiker-G documentation indicates that all equipment should be designed to withstand the following limit acceleration load factors. The linear acceleration factors are given in g's, while the angular acceleration factors are in rad/sec/sec:

Section 4.6

Case	X	Y	Z	Rx	Ry	Rz
Liftoff	8.8	7.0	6.0	75	20	55
Liftoff	7.0	10.6	6.0	75	20	55
Liftoff	7.0	7.0	8.1	75	20	55
Landing	6.0	7.0	8.0	85	30	50

All of the load cases have to be considered as positive and negative, simultaneous and in all directions. The liftoff cases include the effects of combined low frequency transient loading and random vibrations. The landing case includes only low frequency transient loading and has to be combined with the effects of any thermally induced loading which may be present in the structure at landing.

In addition to these factors, all loading caused by on-orbit maneuvering also has to be considered. Since each mission is different, no hard and fast rules exist for this calculation. Generally such stresses are less than that present during the lift-off and landing case, unless the change in temperature makes thermal effects important.

4.6.6.2 Sinusoidal vibrations

Launch events such as gust loading, engine ignition and cut-off, and booster separation induce low frequency transient responses in the SPAS carrier. In the IMPS-1 documentation, these transients are modeled by applying a swept sinusoidal vibration environment to the experiment - SPAS interface. The design and test requirements that were arrived at for the IMPS-1 are listed in the table in Figure 4.6-23. Typically the measured sine wave amplitude wideband value has to be within plus or minus 10 percent of the specified value.

4.6.6.3 Random vibrations

Random vibrations are primarily generated by an acoustic field in the cargo bay during lift-off from two sources: (1) the firing of the shuttle engines, and (2) noise from the boundary layer of high atmospheric pressure around the shuttle as it passes through the atmosphere at high speed. Shocks are also encountered during liftoff, caused by the firing of pyrotechnic bolts for stage separation. These types of shock is typically of very short time duration.

A shock spectrum is usually defined as the maximum response of a single degree-of-freedom oscillator for which the natural oscillation frequency is variable. The calculation of this spectrum is fairly straightforward. The maximum response is first computed for a spring-mass system whose base is excited to the shock acceleration. The natural frequency of the system is then varied and the final shock spectrum is a plot of the amplitude of the maximum response against natural frequency. Since the spectrum depends upon the damping used, it should be specified along with the spectrum. Typical damping values range from 5 to 10 percent. Plots of maximum response obtained during the excitation are referred to as primary spectra, while plots of the response observed after the impule has ended are called residual spectra. Note that the shock spectrum decreases as a function of distance from its source.

Section 4.6

Electrodynamic vibration shakers are used for both shock and random vibration testing of the payload. A waveform meeting the specification requirements is built up and then fed to a power amplifier, which then shakes the vibration table as required. The random vibration certification requirements for the SPAS are considerably more stringent than those required for HH-G payloads. The HH-G testing levels are shown in Figure 4.6-24 (a). The payload should be capable of withstanding the specified levels for 60 seconds along the x, y, and z axes. The SPAS testing levels are shown in Figure 4.6-24 (b). Three different levels of testing are called out for the plane perpendicular to the Equipment Support Panel, for different weights of the total system. The lighter systems have more stringent testing required. The SBS system will likely fall into the 20 - 40 kg range. The testing along the two axes parallel to the ESP panel plane is called out separately, and is considerably easier than the perpendicular testing. The random vibrations are measured in frequency bands no more than 25 Hz wide. The power spectral density of the shaker input frequency has to be within plus or minus 3 dB of the specified value. The rms value of the input vibrations has to be within plus or minus 1 dB of the specified value.

4.6.6.4 Acoustic noise vibrations

The acoustic levels in the shuttle are at their maximum during lift-off, and so all testing requirements are defined relative to these levels. These levels are based on actual measurements made in an empty cargo bay early on in the shuttle program. The test requirements for the SPAS and the HH-G are similar and are presented in Figure 4.6-25. The HH-G expected flight levels and test levels are in 4.6-25 (a). The SPAS requirements, Figure 4.6-25 (b), are again split into a flight acceptance and a design/qualification/prototype level. The rms levels of the testing must be within plus or minus 1 dB of the specified level.

4.6.7 Electromagnetic/magnetic extremes

Since the SBS Camera will be either a Class C or Class D payload, very little actual testing will be required to demonstrate that the payload will not be affected by the levels of radiation described below. These levels should be taken into consideration in the camera design, however, to insure that the camera will be unaffected by them.

4.6.7.1 Environmental

Lightning near the shuttle during liftoff can induce significant magnetic fields in the cargo bay with peak amplitudes of up to 75 amperes/meter, rise times of 2 microseconds, and decay times of 100 microseconds. Note that the instrument only needs to be able to survive this condition, as it will be stowed and non-operational during launch.

When the camera is in space it will be exposed to ionizing radiation consisting of solar and galactic cosmic particles. In the cargo bay a significant fraction of these particles are shielded off by the shuttle. The following values and densities are given for operation on the SPAS, when it is operating in sortie mode clear of the shuttle. The galactic cosmic radiation is composed of approximately 85% protons, 13% alpha particles, and 2% heavier nuclei. The energy levels are between $10E8$ and

Section 4.6

10E19 electron volts. The average flux outside the earth's magnetic field is between 0.2 and 0.6 particles/cm²/steradian/sec. NASA requires that the radiation levels for a particular mission should be calculated using specific orbits and launch dates and current particle density information. Particle flux levels will be higher for polar orbits and in the Van Allen belts. A description of Van Allen radiation can be found in the report NASA TMX 73358.

Solar flares generate protons and heavy ions and can increase the incident particle stream for days. A model that can be used to estimate these changes that is accepted by NASA can be found in the following reference: Chenette, D.L., and Dietrich, W.F., "The Solar Flare Heavy Ion Environment for Single-Event Upsets: A Summary of Observations Over the Last Solar Cycle, 1973-1983", IEEE Trns Nucl Sci NS-31, December 1984.

Micrometeoroids will also hit the camera while it is operating in sortie mode on the SPAS. Typical micrometeoroids range in mass from 1 to 1E-12 grams. The average particle density is 0.5 g/cm³, and the average particle velocity is 20 km/sec. The meteoroid flux can be estimated using:

$$\text{for a mass of } 1\text{E-6 to } 1 \text{ gram, } \log_{10} N = -14.37 - 1.213 \log_{10} m$$

mass of 1E-12 to 1E-6 grams,

$$\log_{10} N = -14.339 - 1584 \log_{10} m - 0.063 (\log_{10} m)^2$$

where N is the flux of particles of mass m (in grams) or greater, in units of square meters/sec. Probabilities of camera damage, estimated from these approximations, should be estimated and the camera should be designed so that they will be acceptably low for the expected mission duration.

4.6.7.2 Shuttle produced

Electrical fields are generated in the cargo bay by the general shuttle avionics and the S-band and Ku-band transmitters. The shuttle S-band transmitters, when operating, can produce a field strength of 15 volts/meter in the 2000 - 2300 MHz band. The Ku-band transmitter can produce a field strength of 70 volts/meter. These values are worst case with the cargo bay doors open. Values may be higher for the instrument mounted on the SPAS platform when it is in free flight but near the shuttle. Adequate shielding must be put on the detector analog signal outputs (and chip bias inputs) to block noise induced by these fields during camera operation. Detailed plots are available in the HH-G documentation.

Magnetic fields are produced by the shuttle power distribution buses. The power buses are located at locations $Y_0 = +/-79$, $Z_0 = 349$ (using the shuttle coordinate system). The worst case AC magnetic fields at these points are 140 dB above 1 picotesla in the 30 Hz to 2 kHz band, which is approximately 1E-5 tesla. This value falls approximately 40 dB per decade to 50 kHz. The DC generated magnetic field is less than 170 dB above 1 picotesla, or approximately 3E-4 tesla. As the instrument is moved away from these power bus points, the magnetic flux density is reduced. The reduction can be approximated using the following formula:

Section 4.6

$$\text{dB (reduction)} = 20 \log_{10}(57R^2)$$

where R is the radial separation in meters in the Y-Z plane from the nearest power bus. For locations within 2.5 meters of the Xo = 576 or 1307 positions, the value of R should be the separation from the Xo = 576 or Xo = 1307 locations in meters.

The PtSi detector array exhibits no unusual magnetic field susceptibility, so magnetic fields should not be a major concern in the SBS camera design.

4.6.7.3 Electrostatic concerns

When the SBS Camera payload is on station in orbit, it will be exposed to solar charged particle flux and also may pass through charged particle fields from the upper atmosphere. Attention must be paid during the system design to prevent buildup of charge on exposed surfaces of the payload that could result in damaging currents or arcing during operation. The worst case of environmental charged particle interaction is on a polar orbit, passing through energized auroral fields, where the induced currents are specified to be up to 5 nanoamperes per square centimeter with an energy of 10 keV. The effects of such fields can be minimized by avoiding external dielectric surfaces where possible by providing outer conductive surfaces that are grounded to the host platform structure. In addition, MLI thermal blanketing should be grounded to the host structure (mounting plate). Unused test connectors should be covered and grounded. Connecting cables should have grounded shields and connectors should be enclosed in backshells that provide Faraday cage shielding. The SPAS specifications for a payload intended for polar orbit specify that they payload should be able to pass the following electrostatic discharge susceptibility test: survive a 3 millijoule arc discharge, from 15 kilovolts and 27 picofarad capacitance, discharged directly from each face of the unit with the return current path through the chassis ground return. MIL-STD-1541 is referenced in connection with this test.

4.6.8 Electrical power interface

4.6.8.1 Hitchhiker-G

A total of 10 kilowatt-hours of energy is allocated for a single customer on a Hitchhiker-G payload. The maximum power use at any moment is 500 watts. Note that the totals for all HH-G payloads cannot exceed 1300 watts, and the total energy available is 60 kilowatts. These numbers are single customer allocations based upon a nominal one-sixth of the total HH-G allotments, since up to 6 HH-G payloads are allowed. The standard interface cabling on the HH-G plate mount is illustrated in Figure 4.6-26. There are two basic interface cables, and one is allocated to power (the other is used for data interface between the HH-G payload and the shuttle host platform). The power is supplied as 28 VDC through the power connector J1. Two 12 gauge wires are provided in the power connector, each limited to 10 amperes by a 20 ampere fuse that is vacuum derated to 10 amperes.

The interface between the shuttle power and the HH-G payload is illustrated schematically in Figure 4.6-27. Two 28 VDC power connections rated at 10 amps provide the payload power. These circuits can be enabled through independent contacts in the DPST relay that is controlled via ground command. Each of the

Section 4.6

supplied power interfaces has an independent current measurement capability (shown in the schematic as the 'Current MON' point), and the current flow data can be accessed by the payload either in real time during flight or after completion of the mission. The survival heater power (also 28 VDC) is supplied via a separate circuit. The schematic of the actual payload power interface is shown in Figure 4.6-28. Payload signal ground must be isolated from the chassis ground for DC power at a minimum resistance of 10000 ohms. No limitation is specified on the capacitive connection between the power ground and the chassis ground. The 28 VDC return must be isolated from both of these by a minimum DC resistance of 10000 ohms. A maximum of 2 milliamps of current originating from the 28 VDC power or from the 28 VDC bi-level command lines (see section 4.6.x) can be returned via the circuit ground.

A set of transient power characteristics, narrowband emissions, and source power impedances that the payload should anticipate from the DC power system supplied to HH-G payloads from the shuttle power system is discussed below. Obviously the SBS payload should be designed to be able to tolerate these conditions. Note that none of them are particularly onerous, and that any reasonably well designed power system should be able to tolerate these conditions. Power bus ripple, transients, payload generated noise, and payload emissions are described in the following paragraphs.

In-flight DC power bus ripple is specified to be less than 0.9 volts peak-peak from 30 Hz to 7 kHz, falling 10 dB per decade to 0.28 volts peak-peak at 70 kHz, and then remaining constant to 400 MHz. If two cases of ripple occur at the same time and add, the maximum voltages at any frequency will be less than 1.6 volts peak-peak from 30 Hz to 7 kHz, falling 10 dB per decade to 0.5 volts peak-peak, and then remaining below this level out to 400 MHz. Specifications are also provided for a passive payload, which is simply a resistive simulation of the payload. In this case, the ripple on the supplied power will be less than 0.8 volts peak-peak from DC to 50 MHz. No single discrete frequency will exceed 0.4 volts peak-peak. Note that this condition applies at the mid-body power interface only.

Inflight DC power transients at DC power buses at the cargo element interface when measured common-mode will be less than 50 volts. Note that the transients may not be completely damped at time equals one second (-1 volt to 5 volts allowed). The maximum voltages allowed for these transients are plus or minus 50 volts. The inflight DC power transients at all cargo element DC power return interfaces are effectively gone within a millisecond, and the maximum voltages range over plus or minus 30 volts, so they are significantly smaller than those at the power bus inputs. In addition, the SBS payload power system must be able to withstand sawtooth transient oscillations with a maximum amplitude of 4 volts peak-peak with a base frequency between 500 - 700 Hz. This transient can occur at several of the cargo power bus interfaces, and occurs during the first 300 milliseconds of the operation of the shuttle's hydraulic circulation pumps. It can occur at any time during on-orbit operations and cannot be scheduled before flight.

Limits are also specified for variations in voltage along the power buses in the cargo bay. The common-mode voltage measured between the two furthest power bus points along the longest cargo bay dimension (which is station Xo 585 to Xo 1307 bulkhead) will not exceed 56 volts per microsecond. The peak voltage between these

Section 4.6

two points will not exceed plus or minus 2 volts. These voltage differentials are caused by the potential currents that can flow between the impedances that can exist between those two points.

Limits are placed on the HH-G payload generated noise as well. Power line conducted payload emission limits are plotted in the HH-G documentation. If the payload power system generates spikes on the shuttle DC power buses, they cannot exceed the 60 volts for 10 microseconds during normal system operation. Rise and fall times must be greater than one microsecond. The source impedances to be expected from the shuttle power bus are plotted as a function of frequency for ground power and for in-flight power in the HH-G documentation, but in general is less than 100 ohms.

Magnetic and electric field generated by HH-G payloads are limited as follows: generated AC magnetic fields at a distance of 1 meter from the payload cannot exceed 130 dB above 1 picotesla for 30 Hz to 2 kHz, falling 40 dB per octave to 50 kHz. Broadband radiated emissions must be within the envelope defined in the HH-G documentation. An additional requirement is imposed to prevent interference with shuttle radio equipment. Broadband emissions from HH-G payloads are limited to 70 dB above 1 microvolt/meter/MHz in the cargo bay in the frequency range 1700 MHz to 2300 MHz. Narrowband emissions are limited to 25 dB above 1 microvolt/meter in this same frequency band.

Limits are also specified for payload transmitters, but these are not applicable to the SBS payload, which will not have an independent transmitter and will instead depend upon the HH-G provided services for data and command interface.

4.6.8.2 SPAS

The critical mode of operation for the SPAS is the sortie mode, when the platform is not connected to the shuttle and operating under its own control. This is obviously the time when the SBS Camera will have to operate in order to collect signature data on the shuttle. Power is provided in this mode by a single Ag-Zn battery dedicated to the experiments on-board. The battery contains 500 amp-hours of charge at 28 VDC. Power is not available from the SPAS during launch, platform recovery, or power switch-over. A general schematic diagram showing how host battery power is distributed to the experiments on the SPAS is shown in Figure 4.6-29. Fuse derating factors for the SPAS are somewhat higher than those used for HH-G payloads.

The power characteristics and limits that apply to the SPAS host platform power are slightly different than those specified for the HH-G power, and will be discussed briefly here. Normal DC power line voltages can vary from 25 to 32 volts. Payloads must be able to withstand the incorrect application of voltage from 0 to 38 volts on the DC power lines for an indefinite period of time. The DC power ripple specifications are identical to those described above for HH-G. Inflight DC power transient limits and the additional noise caused by the orbiter hydraulic pumps are identical to the HH-G description. Additional limitations are placed on AC currents injected into the SPAS investigation power supply by payloads. The total current injected by all systems cannot exceed 3.16 amperes from 30 Hz to 2 kHz, decreasing 50 dB per decade to 0.01 amperes at 20 kHz, and further decreasing at 25 dB per

Section 4.6

decade to 31.6 microamperes at 2 MHz, and remaining below this level to 400 MHz. The limit for each individual payload is arrived at by multiplying these limits by the payload's fraction of the total peak power available.

Additional grounding requirements are specified for SPAS payloads. With the exception of deliberate grounding paths, the chassis ground of the payload must be isolated from all primary power leads and signal grounds by at least 1 megohm resistance. The capacitance between the chassis ground and dc isolated signal grounds must be less than 1 nanofarad. Primary power leads must be dc isolated from all signal grounds by at least 1 megohm resistance. Similar restrictions exist between the chassis ground and any ground support equipment. Specific grounding requirements may apply to individual payloads.

4.6.9 Platform - SBS telemetry interface

4.6.9.1 Hitchhiker-G

The HH-G payload system provides a standardized interface between payloads and the space shuttle. The intent is to provide an interface that is identical between the test equipment at the payload fabrication/test facility, the payload integration facility, and during actual missions on the shuttle. Six standard services are offered to HH-G payloads: (1) the bi-level command system, which offers 4 commands per payload; (2) the serial command interface, which operates at the nominal rate of 960 bits/second; (3) asynchronous uplink and downlink services that operate at 1200 baud; (4) medium rate Ku-band downlink, which operates at rates up to 1.4 Mbits/second; (5) a PCM analog data link; and (6) time data in an analog IRIG-B data format. Note that this interface is contained in the second of the two basic cables provided to interface the payload to the STS. The pinout of this signal cable is shown in Figure 4.6-30. Each of these interface services will be discussed in greater detail in the following paragraphs.

The bi-level command system consists of an interface to the shuttle that is called bi-level because the lines can either be logic false (0 volts) or true (nominally 28 VDC, acceptable between 19.5 to 32 VDC). The characteristics and general specifications of this interface are illustrated in Figure 4.6-31. The reference source for more detailed interface specifications is JSC 07700 Vol., Attachment 1 (ICD 2-19001) SHUTTLE ORBITER/CARGO STANDARD INTERFACES, Rev H, dated 16 May, 1983. The format of the command required from the Customer Ground Support Equipment to control these lines true or false is shown in the HH-G documentation. The lines can also be pulsed momentarily by the Customer Ground Support Equipment. The bi-level command meaning and use is up to the payload designers. From the timing diagrams it is apparent that communication with the payload through this service will be limited by the speed that the shuttle interface between the Customer Ground Support Equipment and the HH-G payload can process the commands.

The electrical characteristics of the interface signals and clocks for the low data rate asynchronous serial interface provided are shown in Figure 4.6-52. A description of this interface with additional electrical information is shown in the table in Figure 4.6-53. This interface operates at a nominal speed of 960 bits/second. It consists of a synchronization byte (11100101), a byte containing

Section 4.6

command byte count, a byte with customer ID number (CID) and message type info, the actual data bytes (a maximum of four bytes), and a checksum byte. Data is transmitted bit one first most significant byte first to the unique payload identified by the customer ID number. A command sent is a type 1 message. The interface is bi-directional between the shuttle and the payload, and the complete packet is passed through. Again the use of this interface is up to the payload designer.

The asynchronous uplink provides another of the low data rate interfaces between the shuttle and the HH-G payload. This link is usually referred to as the RD, or Receive Data, link. It is used to transmit customer command messages and mission elapsed time (MET) data to the HH-G payload. The uplink operates at a 1200 baud asynchronous rate, with 1 start bit, 8 data bits no parity, and 1 stop bit. The RD link electrical and timing detailed specifications are shown in Figure 4.6-39. Note that there is an additional delay time between the message leaving the Customer Ground Support Equipment and arriving at the payload is a nominal 2 to 20 seconds. This delay is caused by the overhead involved in having several different payloads issuing commands, JSC Mission control, and uplink delays. This delay can increase if uplink failure occurs and commands have to be retried. A type 2 message transmits the entire message to the payload. A type 4 message transmits MET data to the payload. Arrangements can also be made to use this service to allow the payload to access shuttle computed data such as attitude and orbit detail, in addition to mission elapsed time. The orbiter state vector and attitude data is sent relative to the Greenwich true of data Cartesian or Aries mean of 1950, Cartesian coordinate system, and orbiter attitude rates about the shuttle body axes. The MET information supplied is plus/minus 5 milliseconds of time from calculation of shuttle position/attitude information. A typical time lag encountered in sending MET information is on the order of 5 seconds duration. Again, errors in the shuttle computers or sensors can increase this time lag and significantly degrade the interface performance.

A corresponding service provided is the asynchronous downlink, referred to as the SD, or send data, interface. Data flows along this interface from payload to shuttle. The electrical characteristics and timing detail of this interface can be found in Figure 4.6-35. This is also a 1200 baud serial data link. In stead of having pre-defined message formats, the formats used on this link are negotiated with the HH-G office for each payload. Time delays comparable to those encountered on the RD link can be anticipated.

A medium data rate interface is provided through a Ku-band system in the Tracking and Data Relay Satellite System (TDRSS). This interface is intended for real-time payload support only. It is essentially a serial PCM interface. The data rate ranges from 16 kilobits/second to 1.4 megabits/second. Data is received in the same format that it is transmitted. One major advantage of this service is that it is a real-time link, without the network delays that characterize the other serial command links. The electrical interface of the KU-band link is shown in Figure 4.6-36. The data and clock signal timing is shown in Figure 4.6-37. A continuous clock at the bit rate assigned to the payload is always required. The data stream should contain a synchronization pattern to allow later recovery and analysis. Data can either be recovered on the ground using identical interfaces to those on the payload or it can be stored on magnetic tape for later use.

Section 4.6

A high speed PCM data interface is also provided. It consists of a special 5 wire interface for custom PCM telemetry interfaces. It is available only by special negotiation with the HH-G office. One wire is a continuous clock, 2 lines are data lines, and the other two are clock lines. The digital timing of this interface is shown in Figure 4.6-38. The electrical details of the PCM interface are described in Figure 4.6-39.

Finally, an IRIG-B mission elapsed time (MET) signal is provided to HH-G payloads. The payload must provide the circuitry to decode the analog signal. The electrical interface to the provided IRIG-B MET signal is shown in Figure 4.6-40.

4.6.9.2 SPAS

Data is relayed from the SPAS platform to either the ground or the shuttle through the Data Handling Subsystem (DHS). This interface is accomplished through a standard set of command, timing, and interface lines, as shown in Figure 4.6-41. Each payload hosted on the SPAS receives a serial command channel. The interface transfers a 16 bit word on this dedicated line to the experiment. The data arrives MSB first, after a header that has been pre-defined. The electrical interface is illustrated in Figure 4.6-42. The signal characteristics are defined in the table in Figure 4.6-43. The timing of the serial commands is illustrated in Figure 4.6-44.

The data telemetry stream is split into two streams: real time and stored data. The real time data includes important housekeeping and status information from the payload, and is used to monitor progress of the experiment by the ground operators. The stored data is directed to the on-board SPAS data recorder. A serial MET data interface is also provided on the SPAS.

The experiments on the SPAS are activated during two of its operating modes: the sortie mode, and the subsatellite mode. In the sortie mode, signals are transmitted between the SPAS and the shuttle through a long umbilical cable. This is attached to the port side of the SPAS to an interface connector on the data handling panel. In the subsatellite mode, communication is provided between the shuttle avionics and the SPAS by an S-band radio link. This link consists of two low-gain antennas and a NASA near-earth transponder.

Both of these links transmit data in real time at a rate of 8 kilobits/sec. Of this, 5.6 kilobits/sec is allocated to the experimenters. This is 700 bytes/sec transmission rate available for downloading of real-time image data from the SBS Camera. Using a 160 x 244 detector array, which contains 468480 bits of data (excluding housekeeping), it would take approximately 84 seconds to transmit one complete frame of imagery.

Provisions can be made to establish higher bandwidth data transmission channels between the SPAS and the shuttle. For example, it is possible to set up at least 1 television channel link from the SPAS, and this would be able to transmit imagery from the SBS Camera to the shuttle in real time. This would also allow storage of the data (with a lower dynamic range, due to the limitations of analog television bandwidth) in a recorder on the shuttle.

4.6.9.3 Data storage

Section 4.6

4.6.9.3.1 Hitchhiker-G

No standard method of data storage is provided as a HH-G payload service. Custom arrangements can be made to accommodate recorders located on the shuttle.

4.6.9.3.2 SPAS

A tape recorder is available on the SPAS platform that can be used to record data from the experiments. Its data rate can range from 32 kilobits/sec to 512 kilobits/sec. At the highest data rate available, it could record a complete frame in 0.92 seconds. The recorder has a total capacity of 5×10^9 bits, which is 6.25 gigabytes. If the entire recorder was dedicated to the SBS Camera, it could record 106728 images at 12 bit resolution, or about 1 hour of data (assuming 30 frame/sec operation). Its data rate is far too slow to keep up with the image data from the SBS Camera, however.

Since neither of the two host platforms offer a data recording capability that can adequately serve the SBS Camera system, it is mandatory that the payload contain its own recording capability. Provision for this has been made in the proposed design in section 6.

5 Documentation and testing

This section of the report presents an overview of the testing and specification levels that will have to be met by the SBS Camera payload. Both the level of pre-flight testing, and the number of MIL and NASA official specifications that will have to be met by the payload will have a large impact on the total level of effort and cost required to build and fly the SBS Camera. Since the host platform is assumed to be part of the Space Transportation System (space shuttle), NASA requirements will be involved. In addition, the camera is also assumed to have a measurement mission of a military nature, and thus military specifications (MIL specs) will also be involved.

5.1 Payload class

The general handbook that provides guidance in the area of testing and specification levels for payloads such as the SBS Camera is DOD-HDBK-343, which is titled Design, Construction, and Testing Requirements for One of a Kind Space Equipment. This handbook was specifically written to apply to space payloads that do not involve high priority missions (i.e., ones that directly impact on national goals or national prestige) or do not have long times on station. The regulation recognizes that, for this type of payload, excessive testing requirements end up wasting time and money because the cost-benefit tradeoff involved is not worth it. This is balanced off against the recognition that certain minimum levels of specification and testing are still needed because high reliability is needed for equipment used in space experiments.

The handbook defines four general classes of space payloads:

Section 5

- Class A - high priority, minimum risk
- Class B - risk with cost compromises
- Class C - economically refllyable or repeatable
- Class D - minimum acquisition cost

The formal definitions for each of these classes, taken from DOD-HDBK-345, is presented below:

Class A: "High Priority, Minimum Risk. Class A is defined as a high-priority, minimum risk effort. The characteristics for Class A usually also involve some combination of the following features: high national prestige, long life, high complexity, high use of redundancy, soft failure modes, independent qualification items, complete flight spares, highest cost, and a critical launch time. Vehicle and experiment retrievability or in-orbit maintenance is usually not possible."

Class B: "Risk with Cost Compromises. Class B is defined as a high-priority, medium risk effort, with cost saving compromises made primarily in areas other than design and construction. The characteristics for Class B usually involve some combination of the following features: high national prestige, medium life, high complexity, soft failure modes, protoflight qualification, limited flight spares, limited use of redundancy, high cost, short schedule, and a critical launch time. Vehicle and experiment retrievability or in-orbit maintenance is usually not possible."

Class C: "Economically Refllyable or Repeatable. Class C is defined as a medium or higher risk effort that is economically refllyable or repeatable. The characteristics for Class C usually involve some combination of the following features: medium to high national prestige, short life, low to medium complexity, small size, single string designs, hard failure modes, very limited flight spares, medium cost, short schedule, and a noncritical launch time. Vehicle and experiment retrievability or in-orbit maintenance is usually possible, such as typlified by Spacelab or Orbiter attached payloads."

Class D: "Mimimum Acquisition Cost. Class D is defined as a higher risk, minimum cost effort. The characteristics for Class D usually involve some combination of the following features: medium to low national prestige, short life, low complexity, small size, single string designs, simple interfaces, hard failure modes, no flight spares, lowest cost, short schedule, and a noncritical launch schedule. Vehicle and experiment retrievability or in-orbit maintenance may or may not be possible."

The general trend associated with this classification system is that the testing, construction, certification requirements, and overall costs (in money and time) are the greatest for Class A payloads and the least for Class D. This is offset by the fact that the guaranteed reliability of Class A payloads is considerably higher than that of Class D payloads. The actual classification process involves a series of management decisions where the government determines the proper balance between minimum cost and minimum acceptable risk. Additional detail on the factors to be considered in the classification decision are discussed in section 11.2 of this handbook.

It is the recommendation of this study that the SBS Camera system be classified as either a Class C or a Class D payload. This decision would allow the system builder (assumed here to be a contractor) to adhere to MIL specs as much as possible to

Section 5

insure quality and acceptability, but also allows the contractor to bypass excessive documentation and testing requirements. This would result in significantly lower costs of shorter development times for the system. Both Class C and Class D categories mesh well with the anticipated re-flyability of the SBS payload, and if system failures occur, the payload can be repaired and flown again. Since the payload is designed to be small and relatively non-intrusive, and to make relatively limited demands on the host platform resources, it should be comparatively easy to add the SBS Camera missions to typical shuttle manifests. The decision to use this payload classification does place greater responsibility on the competence and experience of the contractor(s) selected. The final decision in this area, of course, depends upon the government funding agency representatives and the specific missions assigned to the camera.

A general summary of the testing levels, showing specific testing requirements and MIL specs, is shown in Figures 5.1-1 through 5.1-11. This is a copy of the requirement matrix on pages 12 - 22 of the handbook, and allows easy comparison of the difference between all four payload classes. Note that this design study is only providing a summary of the testing and construction requirements imposed by this DOD handbook. For additional detail in this direction, a copy of the handbook (as well as many of the referenced MIL specs) is available at SRL. Figure 5.1-1 provides a general comparison of program characteristics of space programs in each of the 4 payload classes. Figure 5.1-2 lists items that must be included in the contract statement of work for design and building of payloads of each class. Figure 5.1-3 compares review items included in the statement of work for contracts of each payload class. These reviews range from program and technical reviews to component level and vehicle reviews. Figure 5.1-4 highlights comparisons between typical space experiments of each class. This table is intended to be used in combination with the information in Figure 5.1-1 to characterize each of the payload classes. Figure 5.1-5 lists the typical design factors used in each of the class categories. Figure 5.1-6 compares typical computer resource requirements for space experiments of each class. Figure 5.1-7 shows the typical construction requirements, including such items as materials traceability and assembly lot requirements, for each of the payload classes. Figure 5.1-8 compares the test requirements for each class. Figure 5.1-9 is a comparison of typical fabrication and test requirements for components to support the first flight item of each class. Figure 5.1-10 lists the applicability of various USAF Space Division policies and directives for each class. As noted at the bottom of this table, waivers from specific directives can be obtained from the commander of Space Division; this matrix is intended to provide guidance for initial programs, such as this one, in determining applicability of the different policies. Finally, Figure 5.1-11 shows the applicability of Space Division commander's policies in management requirements for space experiments of different classes.

In the detailed discussion below, the comparison between Class C and Class D payloads is emphasized, since the SBS Camera is likely to be one of these two. Summary discussions of the specifications called out, highlighting some of their requirements, are included in the following sections. These highlights can be used to estimate, in a general sense, the added costs involved in specifying each of these levels of testing and program management.

5.2 MIL - DOD specs

Section 5

Note that the following are items recommended to include in contract statement of work. This indicates that time, money, and resources must be allocated by the contractor, and funded by the sponsoring agency, to provide the level of effort called out in the regulations.

5.2.1 Safety program: MIL-STD-1574

MIL-STD-1574A is titled System Safety Program for Space and Missile Systems. The most recent version is 15 August 1979. This specification defines the requirements and characteristics of a safety program that must be established by the contractor and maintained throughout the design and testing phase of the space experiment. Its primary concern is with accident prevention throughout the program life. The full scope of the regulation can be seen in directly quoting its purpose (p. 1): "A system safety program, as specified herein, establishes administrative and technical means by which accident prevention requirements and policies are planned, managed, and implemented into the total program effort. The activities of the system safety program include: planning, management, design, analysis, research, operational functions, auditing and training. The purpose of the program is to identify significant accident risk and define methods to cope effectively with that risk within program cost, schedule, performance, and technical acceptability parameters. This standard defines the requirements for implementation of system safety programs covering the life cycle of the system. It includes the safety requirements for the following activities/periods: design, development, test, checkout, modification, production, servicing, refurbishing, maintenance, transportation, handling, training, disposal, deployment, and normal and contingency operations. This standard also defines the management and technical tasks and controls required to minimize accident risks caused by human error, environment, deficiency/inadequacy of design, and component malfunction or interactions. Risks of concern are those which could result in major injury or fatality to personnel including flight or ground crews, or damage to the system including support equipment and facilities."

Under this specification, the contractor must develop a detailed safety program, with a person in charge that is responsible for adhering to its requirements throughout the program. The safety program is referred to as the "System Safety Program Plan". Detailed logs of procedures and results must be kept during testing, and must be available to the government for review to ensure adherence. Reviews are specified of testing procedures. In general, meeting these rules requires an extensive amount of paperwork and bureaucracy. The DOD handbook specifies formal adherence to this specification for a Class C payload, but only lists it as guidance for Class D. Thus it is up to the discretion of the government (in its Request for Proposal) as to how much of the specification will be required for a Class D payload.

5.2.2 Reliability program: MIL-STD-1543

MIL-STD-1543 is titled Reliability Program Requirements for Space and Missile Systems. The most current version is dated 25 June 1982. It addresses the reliability aspects of the resulting space experiment hardware by defining reliability practices to be followed throughout the program. The scope of the regulation can be quoted

Section 5

directly: (p.1) "This standard establishes uniform reliability program practices and procedures for use during design, development, fabrication, test and operation of space and missile systems." It applies to all prime contractors and subcontractors involved in payload fabrication, and defines the characteristics of a reliability program that must be established and maintained by the contractor. The program is integrated with the design and development of the experiment. Critical item lists are made and maintained as part of this program, and the impact of design trade-offs made during construction and test of the system are also quantified as part of this program. Reliability modeling is specified, which involves creating a mathematical model of each component in the system, expressing its reliability in terms of operating conditions, and updating it as changes are incorporated in the system. All failures are documented and reviewed by a failure review board. Failure impact planning is included, and notices are given of suspect parts, materials, and processes. The review also quantifies the effects of testing, storage, shelf-life, packaging, transportation, handling, and maintenance of system components.

Provisions are made in Appendix A of this specification to tailor the reliability program for each specific payload. This tailoring is done by the contract officers of the sponsoring government agency. Note that the DOD handbook specifies reliability analysis to be conducted to the component level for Class C payloads, while it is only done to the subsystem level for Class D payloads, which is a significant difference. In addition, the single point failure justification applies to Class C critical items only.

5.2.3 Electromagnetic compatiability: MIL-STD-1541

MIL-STD-1541 is titled Electromagnetic Compatiability Requirements for Space Systems. The most recent version is dated 15 October 1973. This spec is concerned with possible interactions between the space payload and other systems in the payload or the host platform. The interactions in this case are radiated emissions, or signals added onto the power buses. The scope of this regulation is stated: (p. 1) "This standard establishes the electromagnetic compatiability (EMC) requirements for space systems, including launch vehicles, space vehicles, ground systems, and associated aerospace ground equipment (AGE). It does not apply to facilities which house such items." It gives general design guidelines for items such as determination of the electromagnetic interference safety margin, case shielding, electrical bonding, and surface finishes. It also gives design criteria to be used for wiring, grounding, isolation, and bus impedances. Very detailed emissions limits are cited. It also spells out test requirements, methods, and types of equipment to be used to determine compliance.

Configuration control: DOD-STD-480 and MIL-STD-483

DOD-STD-480A is titled Configuration Control - Engineering Changes, Deviations, and Waivers. The most recent version is dated 12 April 1978. This standard provides a systematic way of making engineering changes, deviations, obtaining waivers, and submitting revisions. It also provides for analysis of the impact of proposed changes, and defines a way to maintain information on the current configuration of a system as it is changed. The standard basically imposes a set of formal rules on the engineering change process that foces detailed documentation of

Section 5

all changes introduced during the course of a project. MIL-STD-483 makes a similar set of demands on the project. Adherence to DOD-STD-480 and MIL-STD-483 is required for Class C payloads, but is not required for Class D systems.

5.3 Space qualification levels

In recent years an additional level of component qualification has been created specifically for components to be used on space vehicles. This qualification, usually referred to as 'space' qualified, or 'S' qualified components, has been developed in an attempt to limit failures that take place in space experiments, where failures in a system on station are rarely cost effective. The basis of this qualification level is contained in MIL-STD-1547, which is titled Parts, Materials, and Processes for Space and Launch Vehicles, Technical Requirements For. The most current version is dated 31 October 1980. This standard establishes the criteria and minimum technical requirements for electronic parts in the design, development, and fabrication of space and launch vehicles. Application information provided includes derating procedures, end of life design limits, installation requirements, and aging sensitivity. Requirements and recommendations on design and construction are made. Quality assurance provisions are also discussed, including in-process controls, screening requirements, lot conformance testing, and general qualification requirements. The actual standard is quite long and detailed, and is available at SRL for reference if required. Details for the corresponding standardization and control programs required for space systems that use these components can be found in MIL-STD-1546, titled Parts, Materials, and Processes Standardization, Control and Management Program for Spacecraft and Launch Vehicles, dated 12 February 1981. This standard is also on file at SRL for reference purposes.

6 Proposed design

The philosophy of the proposed design here is to present a general payload design that will satisfy the design goals that have already been described in section 2 of this design study. A certain amount of flexibility has been put into these design goals, which have been determined from general discussions with AFGL and RADC representatives. Some of the design goals are relatively inflexible, such as the platforms that the instrument is being designed to. Other design goals are not as firm, and can be traded off in the final design. These decisions must ultimately be made by the funding agency, which will presumably have specific mission goals in mind, as opposed to this design, which is intended to meet broad specifications. As demonstrated in the discussion of the technical options in section 4, there are several possible solutions to many of the design tasks. The design presented here represents one possible solution of many. This SRL design is based on our understanding of the camera's intended mission. It is valuable to include in the design study because it demonstrates that the design of this camera within the specified restraints is indeed possible. It also sheds additional light on the design requirements and performance characteristics of such a camera system.

It is obvious that the amount of detail contained in this preliminary design is not adequate to begin construction of the payload, because such a design requires considerably more time and effort than was budgeted for on this contract. Issues such as the stress analysis, thermal loading, and safety considerations will certainly introduce major changes into the physical configuration of the eventual camera. In

Section 6

this proposed design, these issues are only covered in a general manner, and a considerable amount of engineering is left incomplete. Similarly, no feasibility testing of different concepts was accomplished, and this would be required during the detailed design and construction of the camera. In general the level of detail is restricted to the subsystem level. Since one of the goals is to keep cost low and use commercial components whenever practical, several commercial systems are selected for use in this design. Examples of this include the data recorder, the tracking camera, and the control computer. These systems would have to be tested under launch and orbit conditions to determine their desirability for use in the final design, and it is assumed that physical and electrical modifications would be necessary to these systems. The intent behind selecting and describing these commercial systems is to show what type of performance is available off-the-shelf and to identify the approximate physical and electrical requirements.

6.1 Overview

The SBS Camera system will consist of 10 distinct components:

- (1) Schottky camera dewar/electronics
- (2) optics module/visible TV
- (3) trackable mirror/calibration system
- (4) tracking system
- (5) cryogenic cooling system
- (6) image compensator
- (7) data recording system
- (8) control system
- (9) shuttle/telemetry interface
- (10) power supplies

A general block diagram of the entire payload, showing all major components of the system, is shown in Figure 6.1-1.

The Schottky camera dewar will hold the detector chip, cold baffles, cold stop, and a cooled filter wheel in a thermally insulated container. The current bandpass filter wheel design has room for 4 one inch diameter bandpass filters, though this number could be increased. The motor that drives the filter wheel is mounted on the hub of the filter wheel and must operate at cryogenic temperatures. The cooled assembly, along with the cryogenic cooler, is mounted inside an evacuated metal bottle with highly reflective insulation around it. Detector chip signals, biases, and clocks are brought in through 3 separate hermetic connectors. A warm [silicon] window on the outside of this dewar bottle allows the IR energy in the optical path to travel to the detector. Approximately 2 boards of electronics, 4 x 8 inches each, will be mounted on the side of the dewar bottle. These electronics will generate the clocks and biases required to operate the focal plane array. A block diagram illustrating the components of the dewar subsystem is shown in Figure 6.1-2.

The cooling system chosen for this design consists of three Joule-Thompson cryostats mounted directly behind the cold finger that holds the detector chip. One of these cryostats will have 10 watts of cooling capacity, while the other two will each be rated at 1 watt of cooling. Compressed nitrogen gas will be used to attain an operating temperature of 77 degrees Kelvin. The high capacity cryostat will be

Section 6

used for initial system cooldown (calculated at 1.5 to 2 hours time from 300 K) and also as an emergency backup to provide a large amount of cooling power if serious thermal shorts develop during a mission. One of the 1 watt cryostats will be used for continuous cooling to maintain the detector and filter wheel assembly at 77 K, since the current heat loss is estimated to be about 1 watt. The second 1 watt cooler is present as a backup, in case the primary cryostat fails (the most common failure mode of J-T cryostats is freezing up). A block diagram showing the major components of the camera cryogenic cooling system is shown in Figure 6.1-3. The values of cooling power assigned to each of these J-T coolers will be adjusted as the dewar design changes. High pressure nitrogen gas will be stored in two bottles approximately 5 inches in diameter and 12 inches long. Current calculations show that each bottle should give 2 cooldowns and 2 operating times of 14.6 hours duration. One bottle is primary, and the other is present as a backup.

The optical design selected for this design is based on reflective optics. A diagram identifying the major optical system components is shown in Figure 6.1-4. It is based on a simple Ritchey-Chretien reflecting telescope design with extensive baffling to block off-axis stray radiation. The optical parameters selected for the system have already been extensively discussed in section 4.1. The mirrors will be housed in a single tube approximately 6 inches long. The entrance aperture will be 3.5 inches. Focus will be controlled by motion of the reflective optics assembly relative to the fixed detector dewar. The total field of view will be approximately 4 degrees, with each pixel having an instantaneous field of view (IFOV) around 0.4 mrad. The F number of the system will be around $f/2.5$. At the exit of the reflecting tube provision will be made for an optional beamsplitter to be added in before the image enters the detector dewar. This beamsplitter, made of calcium fluoride, would allow the scene to be observed by a visible CCD TV camera, which would be used for tracking information and documentation of what was observed by the camera. The beamsplitter/camera assembly will be removable and thus an option. A fixed optical axis will be set parallel to the payload mounting plate, and the tracking mirror, visible TV beamsplitter, reflective optics module, and dewar will be fixed along this axis. A variable optical axis will exist beyond the tracking mirror assembly that will nominally be centered around a vector normal to the mounting plate surface.

A target tracking system will be present at the entrance aperture of the optics module. The major components of this system are identified in the block diagram in Figure 6.1-5. The two primary pieces of this system are a platform aspect angle determination system and a trackable flat mirror. The tracking system will consist of a commercially available rate integrating gyroscope system that will determine, in combination with the host platform aspect data, the angles of the camera optics in relation to the targets of interest being tracked. This angle information will be used (optionally either manually via ground control or automatically through the on-board computer) to calculate the mirror angles needed to acquire and track the target being measured. The flat mirror will control the orientation of the variable optical axis described above and reflect the image into the optics module. The mirror will be trackable and stabilized to provide less than 0.25 mrad jitter in the image in a single frame time (0.033 seconds). Its angle relative to the optical axis of the optics module will be controlled by three stepper motors so that the mirror can direct the field of view as required to track targets or backgrounds. This mirror will be trackable up to 10 degrees in all directions off a vector normal to the

Section 6

mounting plate of the system. The mirror will also rotate about the axis of the optics module to direct the field of view of the instrument onto extended temperature controlled sources mounted around the mirror. These close and unfocused radiance sources will be used for extended source calibration of the system data. Three calibration sources, each at a different temperature, are planned. The mirror will also rotate 180 degrees about the axis of the optics module to face the mirror towards the plate mount. This will be a 'stow' configuration that will shield the mirror surface when the camera is not being used.

A block diagram illustrating the image compensation system proposed for the SBS Camera is shown in Figure 6.1-6. The image compensator and control computer will be located in a box enclosing a card cage capable of holding 12 double-width VME bus type electronic cards. The cards will hold the electronics that will convert the detector voltage into a digital value, apply image corrections to remove array artifacts from the data and ensure radiometric calibration, scan convert the array data, and reformat the signal into a form suitable for recording. Both analog and digital outputs of the detector signal will be provided. All housekeeping functions for the instrument will also be performed by these electronics. This chassis will also hold the system control computer which will be capable of the tasks outlined in section 4.5. The control computer will consist of a commercially available CPU on a card with custom designed additional circuitry to simplify the diagnostic interface. The control computer will have its own software on-board in PROM, but will also be capable of accepting commands or input (even operating code changes) via the telemetry stream. A diagram highlighting the components of the control computer system is shown in Figure 6.1-7.

The data recording system will consist of a single high speed digital recorder and power supply. This recorder is capable of recording full resolution digital data from the focal plane array continuously up to 7.6 hours duration. The system will also be capable of interleaving visible tracking camera images with the infrared image data if a visible tracking camera is used as well, and collecting in this mode up to 3.4 hours of data. The tape will be sealed in the recorder unit prior to launch. The system is entirely self contained and controlled by the SBS control computer. The recording system is shown in Figure 6.1-8. Provision will also be made for a compact analog video recorder that can be used for either the visible tracking camera (primary function) or as an emergency backup for the infrared image data from the focal plane array.

The telemetry interface between the SBS Camera payload and the host platform (SPAS or the space shuttle) will be handled through a combination of custom built circuitry and the payload control computer. The system will use both the asynchronous serial links and the bi-level interface provided. It will also contain provisions to use the higher bandwidth telemetry links, if they are made available. A block diagram of this system is shown in Figure 6.1-9.

The instrument power supplies will take power from the shuttle (for HHG), the SPAS battery, or the rocket battery supply, and convert/filter it to generate the voltages and currents required by the SBS Camera system. This system is illustrated in Figure 6.1-10.

Section 6

6.2 Physical mounting of system

These ten system components will be physically separate subsystems that are mounted onto the aluminum plate of either the HHG or the SPAS. The primary advantage gained by keeping these components separate is flexibility in the mounting arrangement on the aluminum plate. The plate mount for the Hitchhiker-G has plenty of space to accommodate the entire system on its single surface. The reduced area of the SPAS Equipment Support Plate, however, may mandate the mounting of some of the system components on the back side of the plate. Arranging the camera system for an unmanned rocket launch would result in mounting an equal number of system components on both sides of a long rectangular plate, so that the system could be fit within a relatively small cylindrical space. Thus the system will be arranged differently, depending on which carrier it will be transported into orbit. Each SBS Camera subsystem will be designed with this mounting flexibility in mind.

Preliminary designs for all of these components will be described in considerable detail in the following sections. Right now the question of how to physically arrange the components for each of the different mounting systems will be addressed. Laying out the system in this manner is the first fundamental step that must be done, since this defines the maximum physical size envelopes allowed for each of the subsystems.

6.2.1 Layout for SPAS equipment support panel

The layout of system components for the SPAS is presented first, since it represents the smaller and thus more restrictive plate mounting option available. A possible layout of the payload on the Equipment Support Panel is shown in Figure 6.2-1. Because of inadequate room on the front of the plate, the tape recorder and its power supply have been moved to the back of the plate. Placing components on the back of the plate limits the locations on the SPAS that can be used to mount the SBS Camera payload.

6.2.2 Layout for Hitchhiker-G plate mount

The plate mounting option for the HH-G payload provides significantly more space for the payload to be spread out over. This additional space allows the tape recorder and its power supplies to be mounted on the same side of the plate as the rest of the system (which is mandatory for the HH-G plate mount, which does not have its back side available at all). The layout of system components is shown in Figure 6.2-2. Note that all components, with the exception of the recorder, are located in the same configuration as the SPAS. This increases compatibility for the payload mounting scheme between the two host platform options, and should ease transitions between them.

6.3 Schottky camera dewar/electronics

6.3.1 Focal plane array

One of the goals for this proposed camera is to maintain maximum compatibility with the existing SAIRS cameras and to use technology developed for them

Section 6

whenever possible. One place where this is very desirable is on the connector interface used on the dewar. This allows use of existing electronics units to evaluate and test the SBS dewar design, and simply enhances portability between systems. Current SAIRS dewar designs have 3 hermetic connectors that enter into the dewar. This can be seen in the SAIRS dewar wiring diagram shown in Figure 6.3-1. All of the DC biases are routed separately from the AC signals, to improve signal isolation and reduce crosstalk. The wiring from the focal plane array for each cable is sent to a Malco connector inside the dewar; this allows easy changing of focal plane arrays without having to rewire the dewar. The cables then pass into Bendex hermetic connectors, required because of the insulating vacuum surrounding the dewar. The connector containing the filter wheel control signals are also routed through a similar arrangement. The connector pinouts used in the SAIRS dewar design for each of these connectors are shown in Figure 6.3-2.

6.3.2 Dewar assembly

The detector dewar will house the focal plane array, detector pre-amp and mux electronics (on chip), cold shielding, and the bandpass filter wheel. Current plans call for all of these components to be cold (70 - 80 K). A sketch showing the arrangement of the components inside the cooled dewar is shown in Figure 6.3-3. Three J-T coolers are located directly behind the detector cold finger. Two antireflection baffles are placed between the focal plane array and the cooled filter wheel. The bandpass filter wheel will be a simple motor driven wheel that will hold between 4 and 8 bandpass filters to allow the SBS Camera to make measurements of targets and background in different spectral bands. The filter wheel shown in the drawing in Figure 6.3-3 is capable of holding 4 bandpass filters 1 inch in diameter. The wheel is included in the cooled region of the dewar to reduce the background flux seen by the detectors. A complete thermal analysis of the dewar design would be required to determine whether the filter wheels would be cooled to 77 K within the mission time planned (10 hours maximum). Note that it is not necessary for the wheel to be cooled to the focal plane temperature for the background levels to be sufficiently reduced. The filter wheel motor will have to operate at cryogenic temperatures, which means it will have to be modified for cryogenic operation. Such motors have been constructed for cooled instruments in the past at SRL. Position sensors are required to determine which filter is located in the field of view. This can be implemented using a greyscale with holes drilled along the edge of the wheel and LED's looking through them. For a four position wheel, two holes are needed; for an 8 position wheel, three holes are required. In addition, a centering readout must also be provided, so that the motor knows when to stop moving the wheel.

The internal dewar assembly will then be mounted in a larger container, with the space between them under a vacuum and containing numerous layers of MLI to provide good thermal insulation. A technique used to mount this type of custom dewar at SRL is to mount the internal assembly on a fiberglass tube, which is then secured to the outer container. This provides a strong mechanical mount for the inner assembly, but keeps the heat leaks to a minimum level. The outer shell of the dewar would then be mounted to the host platform mounting plate. A sketch illustrating this arrangement is shown in Figure 6.3-4. The dewar mounting will also accommodate the mounting of the electronics boards required for bias and clock signals, as discussed in the next section.

Section 6

6.3.3 Detector chip timing and readout electronics

The chip timing and readout electronics will be based heavily on the SAIRS designs. It is anticipated that the SAIRS circuitry can be considerably reduced in size and weight, and considerable redundancy and flexibility was designed into that system. As discussed under diagnostic considerations in section 4.5 of this study, this circuitry would have to be modified to provide test and diagnostic points. All of the circuitry currently fits on two electronics cards 4 by 8 inches in size. This circuitry would be mounted in the dewar assembly component, to isolate it from the electronic noise that will be present in the image compensation and control computer electronics enclosure.

6.4 Optics module/visible TV camera

The reflective optical design proposed for the SBS Camera system has already been discussed in detail in section 4.1. This design will be implemented as a three piece metal module: one piece contains the primary reflective mirror, the second piece contains the secondary mirror and its mounting, and the third piece is a shell that holds both together and is also the external mount onto the host platform mounting plate. This arrangement is illustrated in Figure 6.4-1. Note that it is important that the same material be used throughout the module, to avoid misalignment problems caused by thermal expansion differences between different components as the system is exposed to changing temperatures.

Note that, to simplify the optical design, a single refractive corrector element may be added to the optical system. The use of this depends upon possible complications encountered in the detailed design of these optical components. Addition of a corrector element greatly simplifies and compacts the optical system. If only short wavelength measurements are required on a mission, strong materials such as sapphire can be used for the corrector, which would reduce concerns about fracturing in the harsh vibration environment encountered during liftoff. This corrector element would likely be mounted on the front of the dewar assembly, in front of the cold aperture stop.

Focus control will be implemented by moving the entire dewar assembly along the optical axis of the system. Because the dewar assembly will have a mass on the order of 3 to 5 kilograms, making a slow and controlled movement of the assembly should not be difficult. The scheme selected here to make this movement is illustrated in Figure 6.4-2. In this arrangement, the dewar is mounted to a plate, which is then secured to the host platform mounting plate by two threaded rods. These rods are rotated by a stepper motor to move the assembly back and forth. The total amount of travel required to change the focus from close in (2 meters) to infinity is on the order of 1 inch. The material used in the rods, and the manner in which they are fastened to the host platform mounting plate, will need to be tested carefully to make sure it has adequate strength to survive expected stresses during launch as well as rigidity while on station.

The visible TV tracking assembly is considered to be an optional module that is not necessary to the functioning of the system, and could be removed without impacting on the system performance. The basic approach taken in this module uses

Section 6

a beamsplitter to select off part of the energy from the field of view for a visible band video camera. The concept has already been discussed in detail in section 4.1. A sketch illustrating the configuration of this system is shown in Figure 6.4-3. The solid-state video camera is mounted to the side of the assembly, to prevent it from interfering with the field of view of the tracking mirror. The sizes corresponding to this camera are those for the Pulnix TM-34 CCD video camera (which is a rugged camera, but is not a MIL-SPEC or space qualified model). Again, careful consideration must be given to the material used in the beamsplitter, as fracture during lift-off is a significant concern. The unit would be bolted directly to the host platform mounting plate. If the tracking camera was not required for a mission, it could be removed by simply unbolting it.

6.5 Trackable mirror and calibration system

The basic camera system will be fixed to the equipment plate and will not be movable. In order to meet requirements that the camera be able to track about and observe targets the instrument will stare at a movable mirror. The angle of this mirror to the optical axis of the fixed instrument optics will be controlled by small motors. In this manner the mirror will allow the SBS Camera to track independently of the motion of its platform to a limited extent. The operation and configuration of this mirror has already been described in detail in section 4.1. A drawing of a possible design for the mirror assembly is shown in Figure 6.5-1. The center of the mirror is fixed on a pivoting point provided by a ball joint. Three rods are attached to the back of the mirror, in a triangular shape. These rods are moved back and forth through the first fixed reference plane via gears on a stepper motor. These three stepper motors would be controlled in unison by the SBS control computer to provide controlled motion of the mirror angle to the fixed optical axis about the pivot on the back of the mirror. As shown in section 4.1, the jitter in these rods would have to be on the order of 0.001 inch to provide adequate tracking stability. The first fixed reference plane on the mirror is then mounted on a rotating axle which is controlled by a motor on the second fixed reference plane of the mirror assembly. This motor provides the rotational motion needed to turn the mirror to observe the calibrators. This arrangement provides approximate trackability on the order of 10 degrees in all directions from a vector normal to the host platform mounting plate. The actual mirror would probably consist of a beryllium baseplate (to provide low mass and high rigidity) coated with a reflective gold layer.

A complete electrical interface of these motors to the control computer is required. Test points indicating the limit positions, as well as possible malfunctions, are also required. No provision for readout of the current mirror position is provided in the design shown here. It is assumed that, on power-up, the motors would move the mirror to one limit, and then step back to the position required, and the computer would keep track of the number of steps and convert that into a mirror position. Optical encoded readout could be provided on the back of the mirror if this arrangement is unsatisfactory.

The calibration system provides for three extended source calibrators that can be observed by the instrument as the mirror is rotated about the optical axis. This arrangement is shown in Figure 6.5-2. The calibrators would consist of metal plates with a honeycomb structure on the surface observed (to increase the surface area) painted flat black with a high emissivity paint. Platinum resistance temperature

Section 6

readout would be provided by drilling into the metal block and mounting the readouts inside. Heaters would also be mounted inside each block in a similar manner. The calibrators would be bolted directly on to the host platform mounting plate. This arrangement has the additional bonus of providing mechanical protection for the relatively delicate tracking mirror assembly. The stowed position for the mirror would be rotated so that the optical axis of the instrument is directed to the calibrator below the mirror.

6.6 Payload aspect tracking system

The payload position information system provides data on the current orientation of the SBS payload reference plane, which is the plane of the host platform mounting plate. This information is used in combination with the known angles to the target (uploaded from the ground operators) to determine what motion is required in the tracking mirror to acquire the target of interest. It also provides information on the payload motion once target track is acquired, and allows the mirror to compensate for the platform motion, to allow stable target tracking. The system proposed for the SBS Camera uses a combination of host platform angular data as well as an independent readout of angular position. The host platform aspect data available to the SBS payload is described in section 4.6. The SBS Camera will complement this with a rate-integrating gyroscope that provides absolute pointing information of the platform reference plane. A number of rate integrating gyroscopes qualified for space use are available (for example, from the Northrup Corporation) that have the required angular accuracy for SBS Camera tracking. These units are described in section 4.1. A single unit would be mounted directly on the host platform reference plane. Its position outputs would be read by the SBS control computer and interpreted to provide the required aspect information so that the computer can send commands to the tracking mirror assembly. Figure 6.6-1 is a sketch showing this system. It would be mounted next to the mirror assembly, to minimize possible flexing of the host platform mounting plate between the position readout and the mirror control.

6.7 Cryogenic cooling system

The cryogenic cooling system proposed for the SBS Camera is based upon three Joule-Thompson expansion coolers. A block diagram of the system has already been shown in Figure 6.1-3. The mounting of the coolers directly behind the focal plane array in the dewar has also been shown in Figure 6.3-4. The spent gas will be vented from an opening on the dewar assembly. The gas reserve will be contained in two high pressure bottles mounted side by side on the host platform mounting plate. This is illustrated in Figure 6.7-1. It is assumed that commercial gas bottle of sufficient strength and quality could be obtained for the system. The basic gas regulators will be located near the two bottles, and will contain an interface to the control computer that allows the computer to determine the gas flow and the gas remaining in the bottles, as well as the capability to switch from one bottle to the other. The gas lines will be run down to the dewar, where a second regulator will control the flow of gas to the Joule-Thompson cryostats. This second regulator will also be controlled by the SBS control computer, which will determine the amount of cooling required (i.e., either system cooldown or operation) and control the distribution of gas accordingly.

Section 6

6.8 image compensator system

The signal path present in the image compensation electronics has already been described in detail in section 4.3 of this study. As mentioned there, the circuits used for the starting point of the system design will be the schematics of the current SAIRS family of cameras. These circuits will be modified to incorporate space-qualified components where possible, reduce power consumption, and the addition of diagnostic test points. The SBS Camera will output two types of data: digital pixel data and analog RS-170 format video imagery. The RS-170 video will be available both for quicklook purposes and also as a low dynamic range backup copy of the instrument infrared data. The digital data will contain the full dynamic range scene data and will be recorded as required on a high density digital recorder as described in the next section. No gain or level control will be applied to the digital pixel data. Gain and level will be available for the analog RS-170 video output, in order to accommodate the reduced dynamic range available in the video signal.

The image compensation and control computer electronics will be housed in a single physical enclosure that will be bolted directly onto the host platform mounting plate. The enclosure's approximate physical dimensions are shown in Figure 6.8-1. The enclosure will house a backplane of 12 slots using VME-bus type connectors. Six slots on this backplane will be allocated for double VME-bus electronic cards that will contain the image compensation circuitry. Two slots are allocated for analog-to-digital conversion modules: one is primary, while the second is a complete backup. The remaining four slots are allocated for the control computer and its backup, as described in the next section. The box will be hermetically sealed and gas will be maintained under pressure inside to facilitate component cooling. Total power consumption by the analog-to-digital conversion units will be around 25 watts; the compensation circuitry will consume approximately 35 watts.

6.9 Data (visible and infrared) recording system

As shown in section 4.4 of this report, a large variety of recorders and recording technologies are available for the SBS Camera. After studying the detailed specifications of several of the recorders available, we would recommend the specific recorder model DCRSi manufactured by Ampex Corporation. A complete manual for the system is located at SRL and is available if requested. This recorder was selected for the following reasons:

- (1) it is capable of recording full digital resolution image data from SBS camera in real time, no loss of data, for a length of time comparable to design goals (section 3);
- (2) the recorder was designed with an instrumentation interface, which means that it has provisions for computer remote control and status determination, time code and housekeeping data recording, built in test equipment so that system performance can be evaluated in real time;
- (3) both laboratory (rack mount) and ruggedized aircraft versions exist, and the aircraft version has already been certified to meet certain MIL-SPEC levels;
- (4) the power consumption, weight, and size can be made to fit within design envelope; and
- (5) the system has numerous features that aid in data reduction after mission,

Section 6

such as event marking, data shuttling, and still framing capabilities.

Note that the recording system is not space qualified, so additional work would be required in that direction. It is assumed that such a system, having already been designed for a severe environment, could be extended further as required without complete redesign. It has many attractive features, and should be available in the first part of 1988 for a reasonable cost.

A photograph of the recorder unit and power supply, taken from the Ampex literature on the system, is shown in Figure 6.9-1. This tape drive is record only, and does not have a playback option. The unit uses tape enclosed in a cassette unit that is shown in Figure 6.9-2. Data is recorded transversely on the tape by a specially designed 6 head rotating drum. One cassette holds 1750 feet of 1 inch wide tape, and its physical dimensions are 10.5" wide x 6.5" high x 1.62" deep with a weight on 2.5 lbs. The aircraft-qualified version of the tape transport unit is contained in a sealed enclosure that maintains atmospheric pressure around the tape unit for increased reliability of operation. It is assumed that this enclosure would have to be improved for operation in the space environment. The electronics module contains the recording electronics and error correction circuitry. The power supply used 28 VDC. Note that it is currently designed with a heat sink base that needs to be coupled to a cold plate for operation. Careful thermal design would be required to compensate for this in the SBS payload.

This data recorder could be designed to handle either all of the infrared imagery from the PtSi focal plane, or would have the option of interleaving together visible tracking camera imagery (digitized) in between frames if infrared data. The DCRSi can handle digital data at any rate up to 107 Mbits/sec. A single data cartridge holds 1 hour of data at this maximum rate, or a total of 385.2 gigabits of data. The raw data rate from the PtSi focal plane has already been shown to equal 14.05 megabits/second. Thus recording just the array infrared data allows storage of 7.6 hours of data, which is a good match with the mission requirements. If the visible camera imagery is digitized to a resolution of 8 bits using a flash video converter, this data could also be directed to the recorder and alternated with frames of infrared imagery. The visible camera data rate is around 15.7 megabits/second, and so the total data recording time would be reduced to 3.6 hours of data, which is still within reach of the design goals.

The physical mounting of this system onto the equipment plate involves fastening three separate modules: the tape transport, the record only electronics, and the power supply. The physical envelopes of each of these components in their present configuration are illustrated in Figure 6.9-3. The sizes are:

- (1) transport: 7.4" high x 14.1" x 11.2"
- (2) electronics: 7.9" high x 19.5" x 14.6"
- (3) power supply: 5.5" high x 9.5" x 11.0"

The weight and power associate with each component is:

- (1) transport: 33 lbs (with tape), 60 watts
- (2) electronics: 43 lbs, 250 watts
- (3) power supply: 25 lbs, 150 watts

Section 6

Note that, in an actual design, it would make sense to pay for custom reengineering of the system on the part of the manufacturer to refine the packaging to better match the available space envelope.

The image data is easily interfaced over the high speed synchronous serial data input link to the recorder. The recorder also has ample bandwidth for the housekeeping data needs. It can be directly controlled over an RS-422 interface by the SBS control computer. It also contains heaters that can provide survival heating as needed. Additional details on these details can be located in the recorder documentation maintained at SRL.

6.10 SBS control system

The control computer will not be physically separate from the image compensation electronics, but instead will occupy 2 VME-bus slots in the 12 slot backplane of the electronics module. Four slots are allocated, which should allow a complete second system to be maintained as a backup. The basic structure of the computer will be based around a commercially available single-board computer, with custom circuitry providing the I/O interface and the telemetry stream interface. This allows the component development to take advantage of established software tools, and a host of available add-ons, which should reduce development time and costs.

The single-board computer selected to be the base of this design is the GMX Micro-20, which has already been briefly discussed in section 4.5. This basic system meets or exceeds all of the requirements spelled out for the control computer in section 4.5. It seems to have a complete complement of I/O and interrupt support available, and the available microprocessor speeds (12 and 16 MHz) should provide ample computation capabilities for the anticipated load on the SBS Camera. Documentation on this system and the available options is maintained at SRL.

Currently a version of this board that uses space qualified components is not commercially available. Extensive testing would thus be required on the boards to certify that they would not fail under operational conditions. Note that many of the Motorola support chips in the system are socketed, and thus could be replaced with more rugged components. The possibility of having a custom version made from qualified components has not been investigated. It is because of concerns such as these that provision has been made to include a complete second system in the electronics enclosure as a backup.

Three major custom electronics modules would be required to complement this basic computer system. First is access to the banks of PROMs and RAM, as specified in section 4.5. The Micro-20 has provision for 16 bit access to the system data and address busses through a built-in connector. Custom hardware would be needed to allow memory-mapped access to the image compensation PROM/RAM banks. Secondly, the diagnostic hardware interfaces would need to be organized and interfaced into the computer's interrupt structure. Basic hardware interfaces would also be needed for tasks such as direct reading of sensor values (such as temperatures or pressures) by the computer. Finally, an interface is required to the telemetry of the host platform. The majority of communication would be carried out via the serial links provided. It is possible that higher communication

Section 6

bandwidth would be needed for commands, however, and a custom interface to the higher speed interfaces would likely be required. A detailed analysis of the communication requirements of the SBS has not yet been done. These needs are separate of the image data transmission requirements, which are needed for target acquisition and tracking status information by the ground operators.

The Micro-20 computer supports the operating system OS-9, which is a multiuser, multitasking operating system for the 68000 series of processors that has been around for several years. It includes such functions as a command line interpreter shell, tree-structured file system, and I/O redirection, and thus is mature enough to provide an adequate software development environment to build and debug the complex software required to operate the SBS camera. Smaller EPROM versions of the operating system exist, so that it can be run in a remote environment and used for instrument control, which is ideal for the SBS Camera.

The Micro-20 basic unit takes up an entire double VME-bus card slot in the compensation electronics chassis. All of the extra circuitry used in the custom I/O and telemetry interfaces would be located on a second card in the backplane.

A functional block diagram of the SBS Camera operating software is shown in Figure 6.10-1. The software will have eight distinct components:

1. control computer bootstrap code
 - self diagnostics
 - enable telemetry interface
 - enable operating system
 - await command from remote operator: execute when received,
jumping to one of the following blocks of code
2. SBS Camera system initialization code
3. Camera diagnostic code
4. Camera calibration code
5. Data collection code
6. Camera system shutdown code
7. enable remote operator direct control over camera
8. stand-alone ROM monitor

6.11 Summary

This section has provided a general design that meets the design goals defined in this study. On the basis of this material, a detailed preliminary design could be made and built. This general design illustrates that a camera utilizing the latest in Schottky-diode focal plane arrays could be built and flown into space. The basic design is fairly simple, small, and makes minimal demands on the host platform resources. If used on the shuttle, the payload would be reusable, and servicing between flights would be very economical. Commercially available components could be used for many parts of the system, which cuts development time and hold down costs. The payoff to be gained from this camera is a source of high resolution, high sensitivity infrared measurements of space targets and shuttle contamination sources.

7 Conclusions

This study has examined the technical issues surrounding the construction of an infrared camera that could be flown repeatedly into space on the space shuttle, mounted either in the cargo bay or on the shuttle pallet satellite. A series of design goals have been developed to guide the development effort. An overview of the operation of Schottky-diode focal plane arrays was then presented. A detailed examination of all of the major components in the payload was then conducted, with an analysis of both the problems faced as well as possible solutions. The main conclusion of this study is that an advanced camera incorporating the latest advances in this focal plane technology could be placed on a shuttle payload and flown into space. The final package required would be remarkably simple, small, and make a minimum demand upon the resources of the host platform. This simplicity arises from the fundamental simplicity of spatial cameras built using Schottky-diode technology. The resulting camera would be a very capable, general purpose infrared radiometer capable of measuring targets and backgrounds from space. The resulting calibrated imagery could be used to study and understand problems associated with the space shuttle environment, such as local contamination of the shuttle by outgassing from its surface layers. The mechanics of rocket plumes could be investigated using the high spatial and time resolution imagery that the SBS Camera would be capable of generating. This camera would also be capable of mapping out the infrared signatures of other targets in space, a task that has new relevance with the importance given the detection and placement of weapons into a space environment. This combination of low cost, short development time, and high measurement capabilities makes the SBS Camera a valuable research project for the defense community that should be undertaken.

References

Text References

Section 3

- ¹ B. Capone, L. Skolnik, R. Taylor, F. Shepherd, S. Roosild, W. Ewing, W. Kosonocky, and E. Koln, Evaluation of a Schottky infrared charge-coupled device (IRCCD) staring mosaic focal plane, Optical Engineering, Vol 18 No. 5, September-October 1979.

Section 4.2

- ¹ R.D. Hudson, Infrared System Engineering, John Wiley and Sons, 1969, p. 322.
- ² W. Wolfe and G. Zissis, editors, The Infrared Handbook, ERIM, 1978, p. 15-22.
- ³ L.G. Naes, T.C. Nast, A.E. Roche, P.B. Forney, "Two Year solid hydrogen cooler for the cryogenic limb array etalon spectrometer (CLAES) instrument", Technologies of Cryogenically Cooled Sensors and Fourier Transform Spectrometers II, Ronald J. Huppi, Editor, Proc SPIE 364, pp. 60-67 (1983).
- ⁴ J.S. Buller, "Miniature Self-Regulating, Rapid Cooling Joule Thomson Cryostat", SBRC, 1971.
- ⁵ R.V. Annable, "Hybrid Houle-Thomson cryogenic cooler", Technologies of Cryogenically Cooled Sensors and Fourier Transform Spectrometers II, Ronald J. Huppi, Editor, Proc SPIE 364, pp. 68-73 (1983).

Section 4.3

- ¹ F. Shepherd and J.M. Mooney, "Non-Uniformity Limited Performance of IR Staring Cameras", SPIE Proceedings Vol 636, Thermal Imaging, 1986.
- ² W. Ewing, "Silicide Mosaic Array Compensation", SPIE Proceedings Vol 409, Technical Issues in Infrared Detectors and Arrays, April 5-6, 1983.
- ³ W. Ewing, "Silicide Mosaic Array Compensation", SPIE Proceedings Vol 409, Technical Issues in Infrared Detectors and Arrays, April 5-6, 1983.

References

References

- B. Capone, L. Skolnik, R. Taylor, F. Shepherd, S. Roosild, W. Ewing, W. Kosonocky, and E. Koln, "Evaluation of a Schottky infrared charge-coupled device (IRCCD) staring mosaic focal plane", *Optical Engineering*, Vol 18 No. 5, September-October 1979.
- F. Shepherd and A.C.Wang, "Silicon Schottky Retina for Infrared Imaging", 1973 International Electron Devices Meeting Technical Digest, pp. 310 - 313.
- F. Shepherd, A.C. Wang, S.A. Roosild, J.H. Bloom, B.R. Capone, C.E. Ludington, and R.W. Taylor, "Silicon Schottky Barrier Monolithic IRTV Focal Planes", Advances in Electronics and Electronic Physics, VOL 40B, pp. 981 - 992, 1975.
- W. Kosonocky and H. Elabd, "Schottky-Barrier Infrared Charge-Coupled Device Focal Plane Arrays", *SPIE Proceedings Vol 443 Infrared Detectors*, August 25-26, 1983, San Diego.
- P. Pellegrini and F. Shepherd, "The Evolution of metal silicide Schottky barrier infrared focal plane detectors", *SPIE Proceedings Vol 408, Technical Issues in Infrared Detectors and Arrays*, April 5-6, 1983.
- F. Shepherd, "Schottky Diode based Infrared Detectors", *SPIE Proceedings Vol 443, Infrared Detectors*, 1984.
- M.J. Cantella, "Space Surveillance Application Potential of Schottky Barrier IR Sensors", ESD-TR-86-142, Lincoln Laboratory, 9 April 1987, ADA180848.
- F.D. Shepherd, W.S. Ewing, B.R. Capone, R.W. Taylor, and B.L. Cochrun, "Platinum Silicide Staring Sensor Evaluation", *SPIE Proceedings Vol 636, Thermal Imaging*, 1986.
- W.F. Kosonocky, F.V. Shallcross, T.S. Villani, and J.V. Groppe, "160 x 244 Element PtSi Schottky Barrier IRCCD Image Sensor", 1985.
- W. Ewing, "Silicide Mosaic Array Compensation", *SPIE Proceedings Vol 409, Technical Issues in Infrared Detectors and Arrays*, April 5-6, 1983.
- F. Shepherd and J.M. Mooney, "Non-Uniformity Limited Performance of IR Staring Cameras", *SPIE Proceedings Vol 636, Thermal Imaging*, 1986.
- F.D. Shepherd and J.M. Mooney, "Design Considerations for IR Staring Mode Cameras", *SPIE Proceedings Vol 636, Thermal Imaging*, 1986.
- B.N. Agrawal, Design of Geosynchronous Spacecraft, Prentice-Hall, NJ, 1986.
- J.R. Wertz, Spacecraft Attitude Determination and Control, D. Reidel Publishing Company, 1978.

References

- J.S. Buller, "Miniature Self-Regulating, Rapid Cooling Joule Thomson Cryostat", SBRC, 1971.
- R.D. Hudson, Infrared System Engineering, John Wiley and Sons, 1969.
- W. Wolfe and G. Zissis, editors, The Infrared Handbook, ERIM, 1978.
- L.G. Naes, T.C. Nast, A.E. Roche, P.B. Forney, "Two Year solid hydrogen cooler for the cryogenic limb array etalon spectrometer (CLAES) instrument", Technologies of Cryogenically Cooled Sensors and Fourier Transform Spectrometers II, Ronald J. Huppi, Editor, Proc SPIE 364, pp. 60-68 (1983).
- R.V. Annable, "Hybrid Joule-Thomson cryogenic cooler", Technologies of Cryogenically Cooled Sensors and Fourier Transform Spectrometers II, Ronald J. Huppi, Editor, Proc SPIE 364, pp. 68-73 (1983).

Appendix A

Listing of PtSi voltage model program

```
10 ' vmodel.bas
20 'extensive voltage model of 2D PtSi detector array
30 'based on the theoretical equations presented in 1979 paper from
40 ' Capone, Shepard, et al
50 '
60 ' last updated 9/17/86 by J. Kristl
70 '
80 ' variable definitions
90 '
100 YP=0:' photoyield in electrons/photon
110 YE=0:' photoyield in electrons/energy (radiant energy, or radiance)
120 NT=0:' number of electrons/pixel from scene observed (target)
130 NB=0:' number of electrons/pixel from instrument background
140 VS=0:' output signal voltage from scene in selected band
150 TEMPT=0:' temperature of target (scene) being observed in K
160 TEMPB=0:' temperature of instrument (background) in K
170 NOISE1=0:' photoelectron shot noise (number of electrons)
180 NOISE2=0:' incomplete background transfer noise (number of electrons)
190 NOISE3=0:' KTC noise at output gate (number of electrons)
200 NOISE4=0:' fixed pattern noise (number of electrons)
210 VSTART=0:' starting wavelength (microns) of band of interest
220 VSTOP=0:' ending wavelength (microns)
230 VSTEP=0:' wavelength increment for in-band calculations
240 '
250 ' parameter definitions (these are array dependent and user changable)
260 ' defaults are based on the existing 160x244 array flown by AFGL (preSAIRS)
270 '
280 H=4.136E-15:' Plank's constant in eV.sec
290 C=3E+14:' speed of light in microns/sec
300 E=-1.602E-19:' charge of electron in Coulombs
310 C1=.223:' quantum efficiency coefficient (%/eV)
320 C2=14380!:' hc/k in microns.K
330 C3=1.8837E+23:' (2.pi.c)*(um^3)/cm constant
340 PSI=.206:' work function of the PtSi-silicon potential barrier
350 AD=.000032:' individual detector area in cm^2
360 TS=.033:' stare time, or integration time, in seconds
370 F=2.3:' optical F number
380 LAMCUT=6!:' Schottky cutoff wavelength
390 CG=2E-13:' output gate capacitance in farads
400 G=.7:' gain of the Schottky output amplifier
410 NG=0:' number of CCD gates in the array
420 TRANEF=0:' transfer efficiency through CCD gates
430 ARRAYG=0:' rms non-uniformity of the array
440 TOPT=.4:' transmission of the system optics
450 '
460 DEFLT=1:' this variable controls use of default IRCCD parameters
470 '      1 = TRUE (use default), 0 = FALSE (user has changed values)
480 A$="":' scratch string variable used for console input/output
```

Appendix A

```

490 Q=0: scratch variable used for console input/output
500 '
510 ' print main menu
520 '
530 PRINT:PRINT "VMODEL Ver 9/17/86"
540 IF DEFLT THEN A$="DEFAULT" ELSE A$="USER MODIFIED"
550 PRINT:PRINT "Program is using ";A$;" array parameters"
560 PRINT:PRINT
570 PRINT " Select one of the following options:"
580 PRINT " (1) Calculate Schottky photoyield"
590 PRINT " (2) Response of Schottky IRCCD to a user input scene in"
600 PRINT " a user selected wavelength band (elec/pix)"
610 PRINT " (3) Schottky spectral radiance vs voltage"
620 PRINT " (4) View or change array parameters"
630 PRINT " (5) Exit program"
640 PRINT
650 PRINT " Select: ";
660 INPUT Q
670 ON Q GOSUB 700,1060,1740,2020,2050
680 GOTO 530
690 '
700 ' calculate Schottky IRCCD photoyield
710 '
720 PRINT:PRINT " Calculate Schottky IRCCD photoyield"
730 PRINT "Detector parameters used:"
740 PRINT " C1 ... quantum efficiency coefficient (%/eV)"
750 PRINT " PSI ... work function of the PtSi-silicon potential barrier"
760 PRINT
770 INPUT "Answer in electrons/photon (1) or electrons/energy(2) or quit(0): ";Q
780 IF Q=0 THEN RETURN
790 INPUT "Output on screen(1), screen/printer(2), or disk(3):";Q2
800 IF Q2=2 THEN FLE$="prn"
810 IF Q2=3 THEN INPUT "Filename: ";FLE$
820 IF Q2>1 THEN OPEN FLE$ FOR OUTPUT AS #1
830 PRINT:INPUT "Starting,ending,increment wavelength: ";VSTART,VSTOP,VSTEP
840 LAMBDA=VSTART: no use for loop because of fraction step sizes
850 IF Q=2 THEN 950
860 ' photoyield in electrons/photon
870 PRINT:PRINT "Wavelength (um) Photoyield (electrons/photon)"
880 IF Q2>1 THEN PRINT #1,"Wavelength (um) Photoyield (electrons/photon)"
890 YP=(C1*(H*C/LAMBDA-PSI)^2)/(H*C)/LAMBDA
900 PRINT " ";PRINT USING "###.###";LAMBDA;
910 PRINT " ";PRINT USING "#####^";YP
920 IF Q2>1 THEN PRINT #1," ";PRINT #1,USING "###.###";LAMBDA;
930 IF Q2>1 THEN PRINT #1," ";PRINT #1,USING "#####^";YP
940 LAMBDA=LAMBDA+VSTEP:IF LAMBDA<=VSTOP THEN 890 ELSE CLOSE #1
:GOTO 720
950 ' photoyield in electrons/energy
960 PRINT:PRINT "Wavelength (um) Photoyield (electrons/energy)"
970 IF Q2>1 THEN PRINT #1,"Wavelength (um) Photoyield (electrons/energy)"
980 YE=(C1*(H*C/LAMBDA-PSI)^2)/(((H*C)/LAMBDA)^2)

```

Appendix A

```

990 PRINT "  ";;PRINT USING "###.##";LAMBDA;
1000 PRINT "      ";;PRINT USING "#.###^ ^ ^ ^";YE
1010 IF Q2>1 THEN PRINT #1,"  ";;PRINT #1,USING "###.##";LAMBDA;
1020 IF Q2>1 THEN PRINT #1,"      ";;PRINT #1,USING "#.###^ ^ ^ ^";YE
1030 LAMBDA=LAMBDA+VSTEP:IF LAMBDA<=VSTOP THEN 980 ELSE CLOSE #1
      :GOTO 720

1040 PRINT:PRINT "Exiting photoyield section.":RETURN
1050 '
1060 ' response of Schottky IRCCD to a scene at user supplied temperature
1070 ' in user supplied wavelength band (elect/pix)
1080 '
1090 PRINT:PRINT "  Response of Schottky IRCCD to thermal target"
1100 PRINT:PRINT "Detector parameters used here:"
1110 PRINT "      AD ... individual detector area in cm2"
1120 PRINT "      TS ... stare time in seconds"
1130 PRINT "      C1 ... quantum efficiency coefficient (%/eV)"
1140 PRINT "      F ... system optical F number"
1150 PRINT "      TOPT ... system optics transmission"
1160 PRINT "      CG ... output gate capacitance in farads"
1170 PRINT "      G ... gain of Schottky output amplifier"
1180 PRINT
1190 INPUT "Output on screen(1), screen/printer(2), or disk(3):";Q2
1200 IF Q2=2 THEN FLE$="prn"
1210 IF Q2=3 THEN INPUT "Filename: ";FLE$
1220 IF Q2>1 THEN OPEN FLE$ FOR OUTPUT AS #1
1230 IF Q2>1 THEN PRINT #1,"Response of Schottky IRCCD to thermal target"
1240 PRINT:INPUT "Starting,ending,increment wavelength: ";VSTART,VSTOP,VSTEP
1250 INPUT "Temp of target scene (K): ";TEMPT
1260 IF Q2>1 THEN PRINT #1," "
1270 IF Q2>1 THEN PRINT #1,"Starting,ending,increment wavelength: ";
      VSTART;VSTOP;VSTEP

1280 IF Q2>1 THEN PRINT #1,"Temp of target scene: ";TEMPT;" K"
1290 INPUT "Temp of instrument (K): ";TEMPB
1300 IF Q2>1 THEN PRINT #1,"Temp of instrument: ";TEMPB;" K"
1310 '
1320 ' first calculate number of electrons from target
1330 '
1340 LAMBDA=VSTART:' no use for loop because of fraction step sizes
1350 ' do the integration
1360 SUM=0
1370 PIECE1=1/(EXP(C2/(LAMBDA*TEMPT))-1)
1380 PIECE2=(1/(LAMBDA^3))*(1/LAMBDA - 1/LAMCUT)^2
1390 SUM=SUM+PIECE1*PIECE2*VSTEP:' integral piece * channel width
1400 LAMBDA=LAMBDA+VSTEP:IF LAMBDA<VSTOP-.00001 THEN 1370
1410 ' then calculate NT
1420 NT=((AD*TS*C1)/(4*F*F))*1.24*C3*SUM
1430 PRINT "Electrons/pixel from target: ";NT
1440 IF Q2>1 THEN PRINT #1,"Electrons/pixel from target: ";NT
1450 '
1460 ' then calculate number of electrons from instrument self-emission
1470 '

```

Appendix A

```

1480 LAMBDA=VSTART:' no use for loop because of fraction step sizes
1490 ' do the integration
1500 SUM=0
1510 COUNT=1
1520 PIECE1=1/(EXP(C2/(LAMBDA*TEMPB))-1)
1530 PIECE2=(1/(LAMBDA^3))*(1/LAMBDA - 1/LAMCUT)^2
1540 SUM=SUM+PIECE1*PIECE2*VSTEP
1550 PRINT SUM,COUNT,LAMBDA:COUNT=COUNT+1
1560 LAMBDA=LAMBDA+VSTEP:IF LAMBDA<VSTOP-.00001 THEN 1520
1570 ' then calculate NB
1580 NB=((AD*TS*C1)/(4*F*F))*1.24*C3*SUM
1590 PRINT "Electrons/pixel from instrument: ";NB
1600 IF Q2>1 THEN PRINT #1,"Electrons/pixel from instrument: ";NB
1610 '
1620 ' compute total signal electrons
1630 '
1640 NS=NT*TOPT+NB*(1-TOPT)
1650 PRINT "Total signal electrons/pixel: ";NS
1660 IF Q2>1 THEN PRINT #1,"Total signal electrons/pixel: ";NS
1670 ' then do voltage out/pixel
1680 VS=NS*E*G/CG
1690 PRINT "Detector pixel voltage out: ";VS
1700 IF Q2>1 THEN PRINT #1,"Detector pixel voltage out: ";VS
1710 PRINT:INPUT "Another calculation(1), or quit(0): ";Q
1720 IF Q<>0 THEN 1240 ELSE CLOSE:RETURN
1730 '
1740 ' Schottky spectral voltage vs radiance response
1750 '
1760 PRINT:PRINT " Schottky IRCCD spectral voltage vs radiance response"
1770 PRINT
1780 INPUT "Output on screen(1), screen/printer(2), or screen/disk(3):";Q2
1790 IF Q2=2 THEN FLES="prn"
1800 IF Q2=3 THEN INPUT "Filename: ";FLES
1810 IF Q2>1 THEN OPEN FLES FOR OUTPUT AS #1
1820 PRINT:INPUT "Starting,ending,increment wavelength: ";VSTART,VSTOP,VSTEP
1830 IF Q2=2 THEN PRINT #1, "Starting,ending,increment wavelength: ";
      VSTART;VSTOP;VSTEP
1840 INPUT "Temp of target scene (K): ";TEMPT
1850 IF Q2=2 THEN PRINT #1,"Temp of target scene (K): ";TEMPT
1860 LAMBDA=VSTART:' no use for loop because of fraction step sizes
1870 ' do the integration
1880 SUM=0
1890 PIECE1=1/(EXP(C2/(LAMBDA*TEMPT))-1)
1900 PIECE2=(1/(LAMBDA^3))*(1/LAMBDA - 1/LAMCUT)^2
1910 SUM=PIECE1*PIECE2*VSTEP:' integral piece * channel width
1920 NT=((AD*TS*C1)/(4*F*F))*1.24*C3*SUM
1930 VS=NT*E*G/CG
1940 IF Q2>1 THEN PRINT #1,USING "#.###";LAMBDA;;PRINT #1," ";-VS
1950 PRINT USING "#.###";LAMBDA;;PRINT " ";VS
1960 LAMBDA=LAMBDA+VSTEP:IF LAMBDA<VSTOP-.00001 THEN 1890
1970 CLOSE #1

```

Appendix A

```
1980 PRINT:INPUT "Another calculation(1), or quit(0): ";Q
1990 IF Q<>0 THEN 1780 ELSE CLOSE:RETURN
2000 RETURN
2010 '
2020 ' view or change user parameters  '
2030 '
2040 RETURN
2050 ' exit program
2060 PRINT "Exiting VMODEL."
2070 CLOSE:END
```

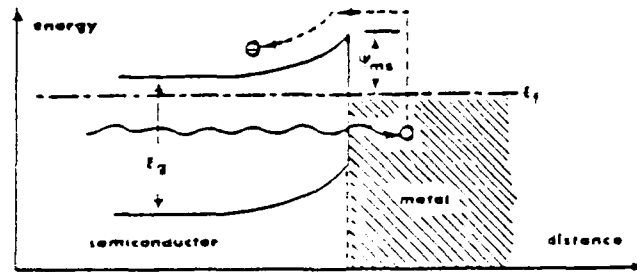


Figure 3.1-1 Potential energy diagram of Schottky-diode detector

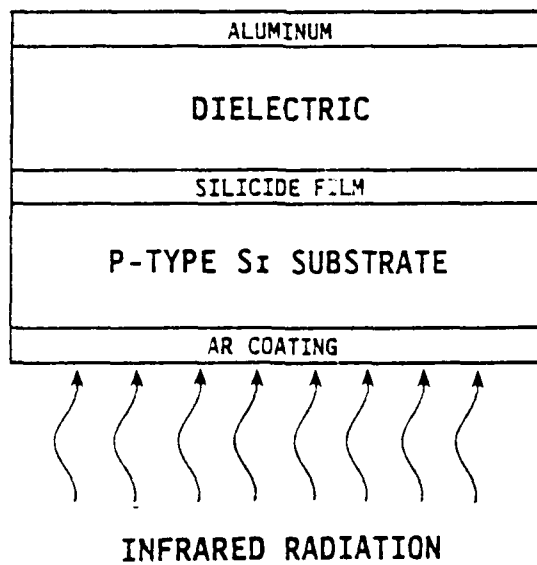


Figure 3.1-2 Schematic diagram of detector

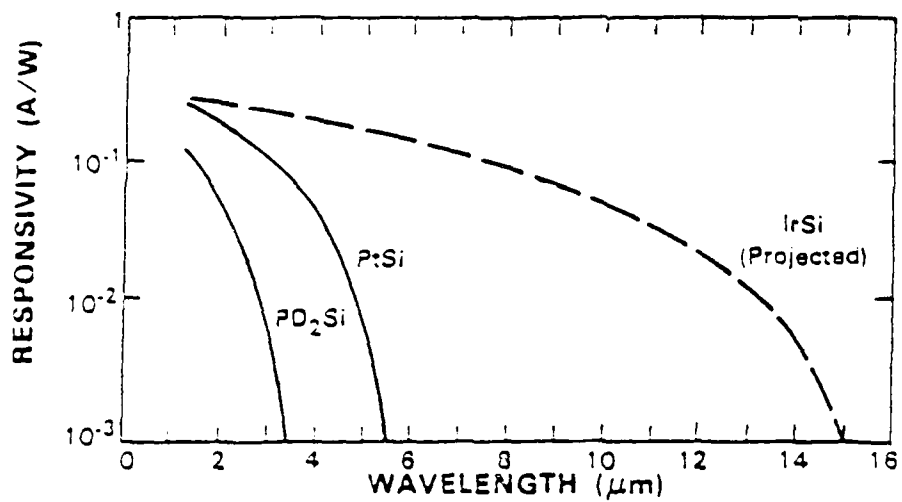
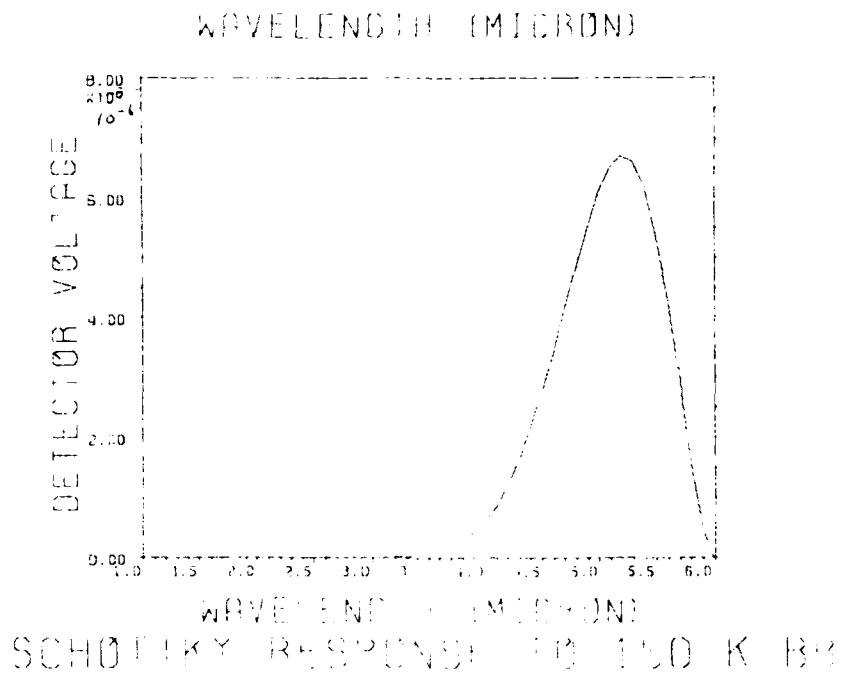
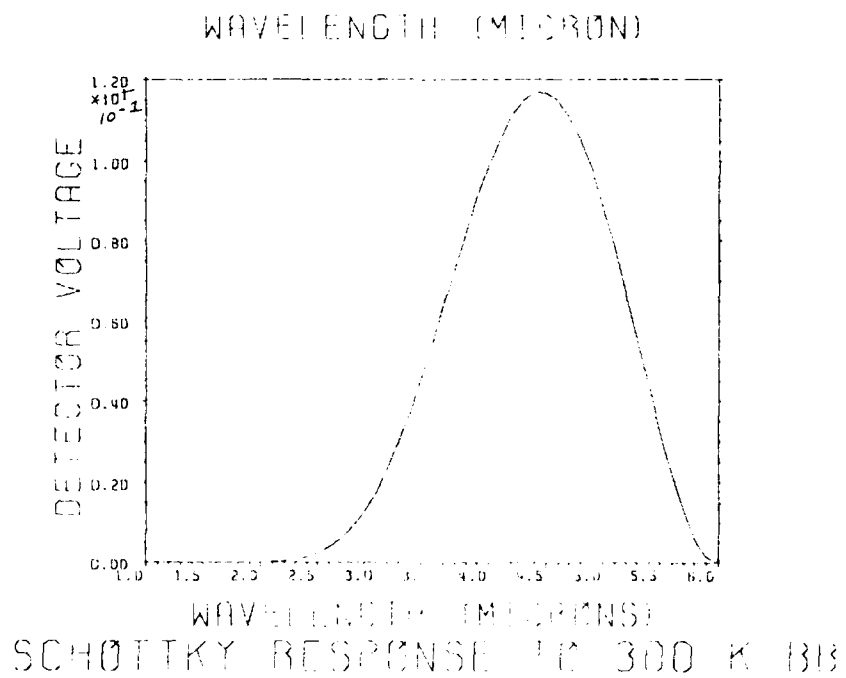


Figure 3.1-3 Spectral response of Schottky-diode detectors



**Figure 3.1-4 Schottky detector response to blackbody emission
(a) 200 degrees K**



**Figure 3.1-4 Schottky detector response to blackbody emission
(b) 300 degrees K**

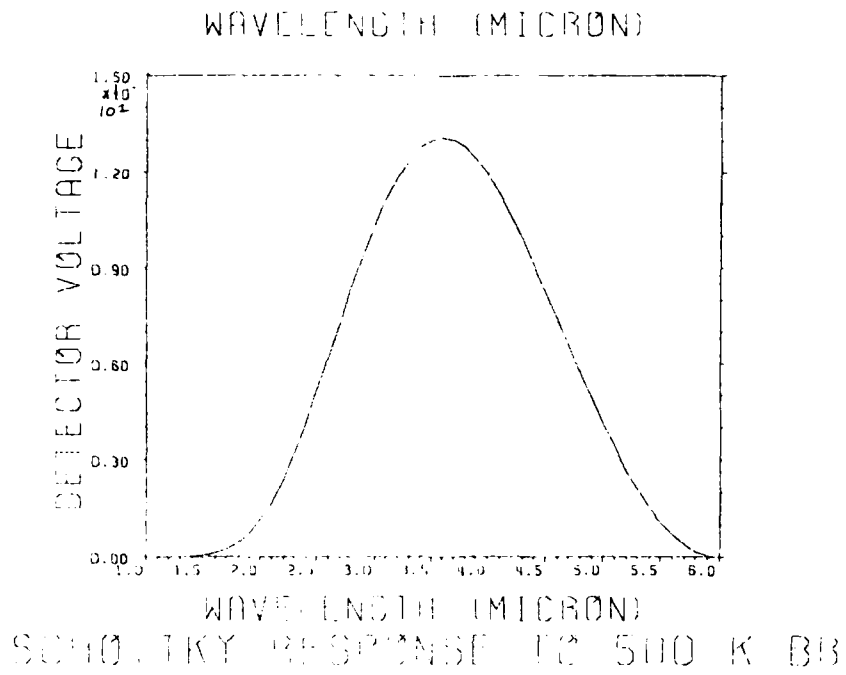


**Figure 3.1-4 Schottky detector response to blackbody emission
(c) 500 degrees K**

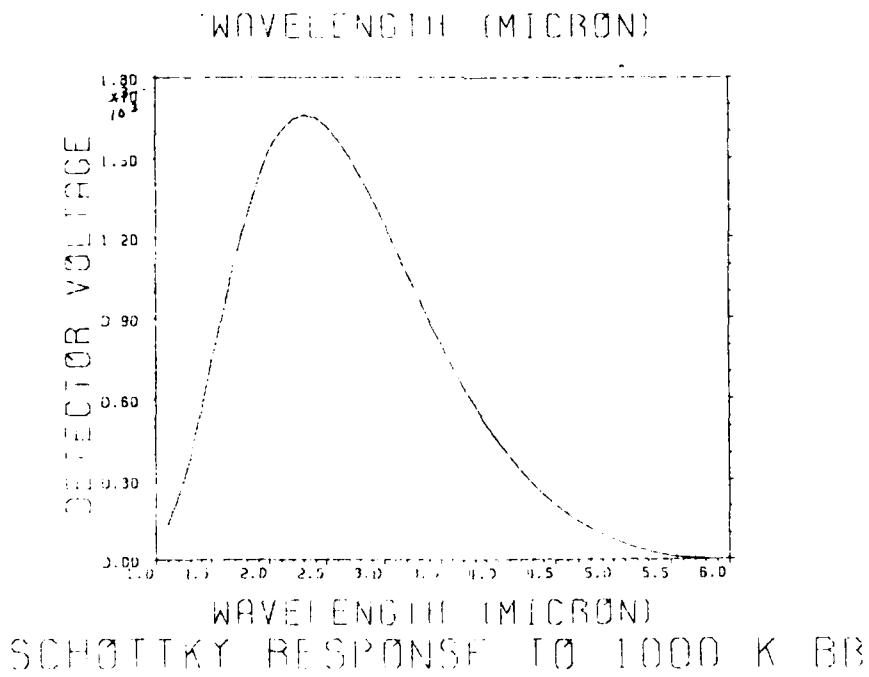


**Figure 3.1-4 Schottky detector response to blackbody emission
(d) 1000 degrees K**

Maximum temperatures that can be measured using different filter bandpasses before chip saturation at 3 V. (in degrees Kelvin).

<u>band</u> <u>(micrometers)</u>	<u>CCD readout</u> <u>transition temp</u>	<u>saturation temp</u>
3.0 - 5.5	303	340
1.2 - 5.5	303	338
4.5 - 5.5	329	384
4.0 - 5.0	318	368
3.0 - 4.0	335	375
2.0 - 3.0	385	428
1.2 - 2.0	506	554
4.6 - 4.8	380	458
5.5 - 6.0	500	660

Figure 3.1-5 Usable temperature range for different spectral bandpasses

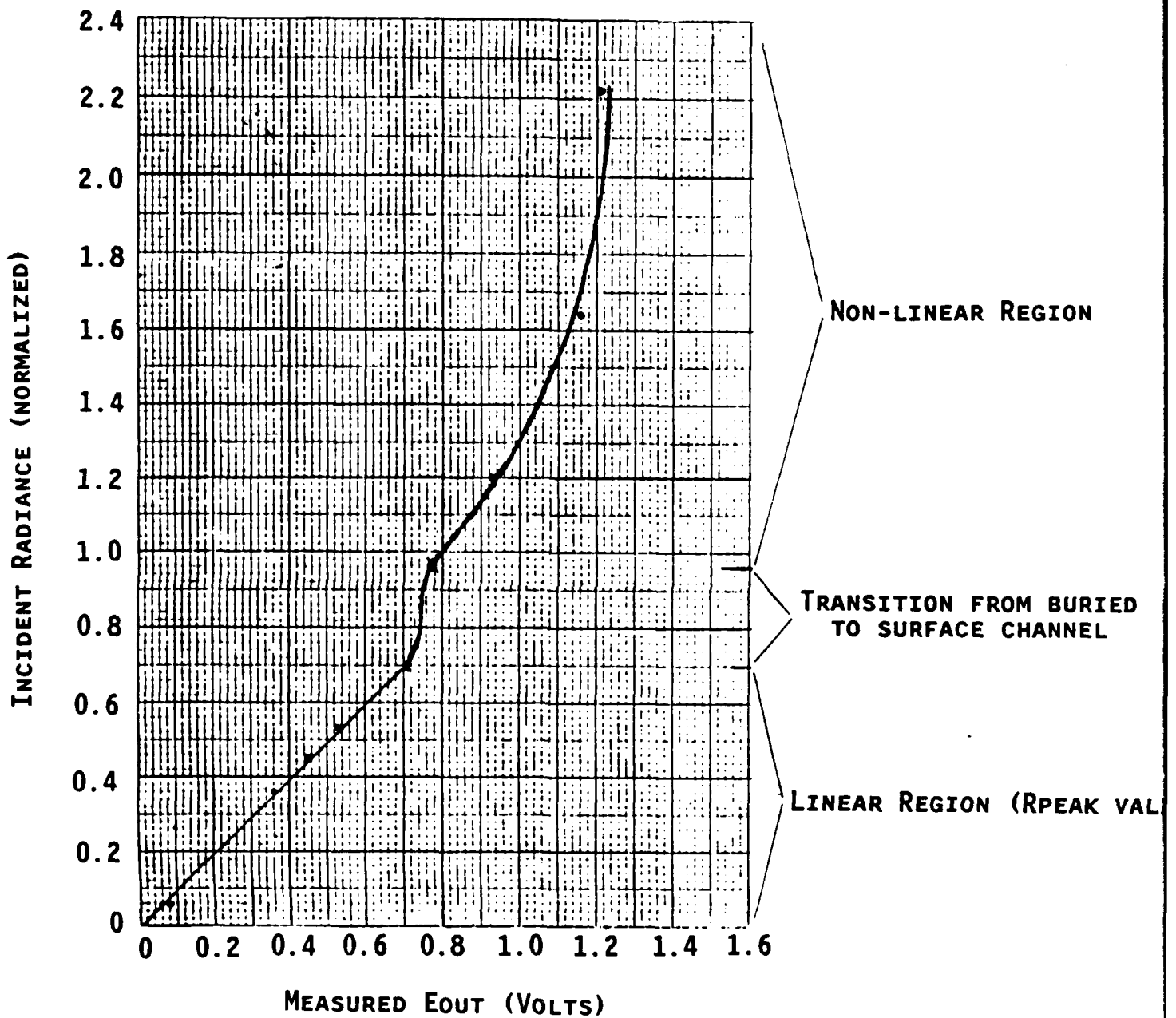
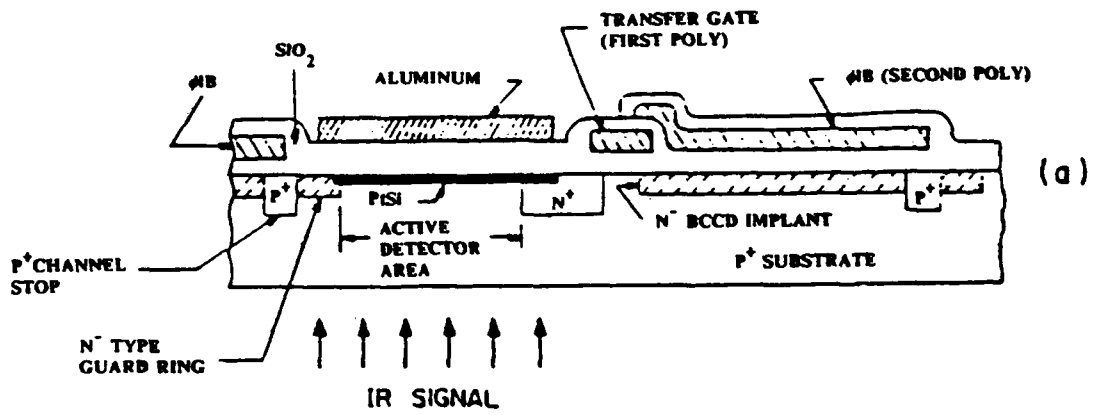
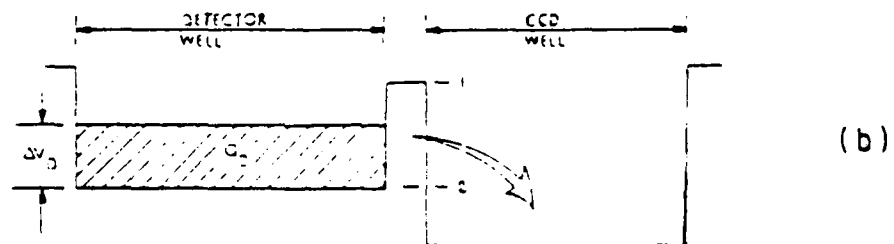


Figure 3.1-6 Voltage-radiance response for 160 by 244 element array



(a) physical layout



(b) potential wells links to physical components

Figure 3.1-7 Drawing of platinum-silicide Schottky-diode detector

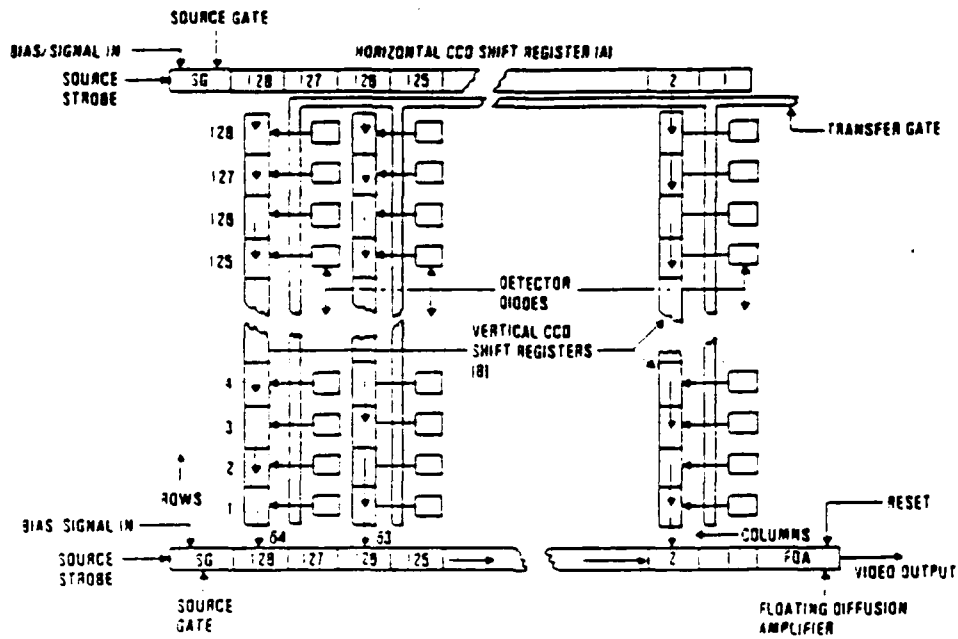


Figure 3.1-8 Block diagram of focal plane array

Array performance data from EDAMSD

(2) RCA 244 x 160 array

parameters used in calculation:

OPTICS:	
F/Number = 2	Warm emiss. = 0
Cold trans. = .9	Warm trans. = .9
Ext. trans. = 1	Cold sh.eff. = .85
PHOTODIODES:	
Q1 (1/eV) = .3	Cut-off (um) = 5.7
PSI.OP (ev) = .217	PSI.EL (eV) = .193
ARRAY:	
Pixel area = .000032	Fill factor = .39
Dark Unif. % = 0	Resp. Unif.% = 0
MULTIPLEXER:	
Noise floor = 200 e	Frame rate = 30 per sec
Gate cap (pf) = .064	Trans. gain = .5
Array/mux temperature = 30 K	

INTEGRAL PARAMETERS

Short wavelength limit:	3.4 um
Long wavelength limit:	5.2 um
Response cut-off:	5.7 um
Background temp (K):	300 K
Rel. source temp (K):	3 K

Figure 3.2-1 Characteristics of current 160 by 244 element FPAs

Array performance data from EDAM00

A. Uncompensated response - RCA 244 x 160 array

** Schottky camera response - screen 1 **

	Electrons	Voltage (mV)
Background	1210749	1515
Dark charge	339936	425
Total (w/CSE)	1764346	2208
Contrast (/K)	45705	57.1
Shot noise	1100	1.37
Total noise	1048	1.6

NEBT .029 K Limit NEBT .024 K

** Schottky camera response - screen 2 **

Background signals

Power (W)	1.115048E-09
Photons (No.)	3.457867E+08
Electrons (No.)	1210749

Noise equivalent

power (watts)	1.123684E-12
irradiance(w/cm ²)	3.309607E-08
photons (No.)	94888
temperature(K)	.127
Detectivity (D*) (A ⁻¹ W ^{-1/2})	1.78E+10

** Schottky camera response - screen 3 **

Efficiencies

quantum	.125	%
emission	.028	%

Responsivities

electron	2.9E-15	e/watt
current	.004	amperes/watt
active area	.01	amperes/watt

Figure 3.2-2 Performance and noise characteristics for current 160 by 244 element array

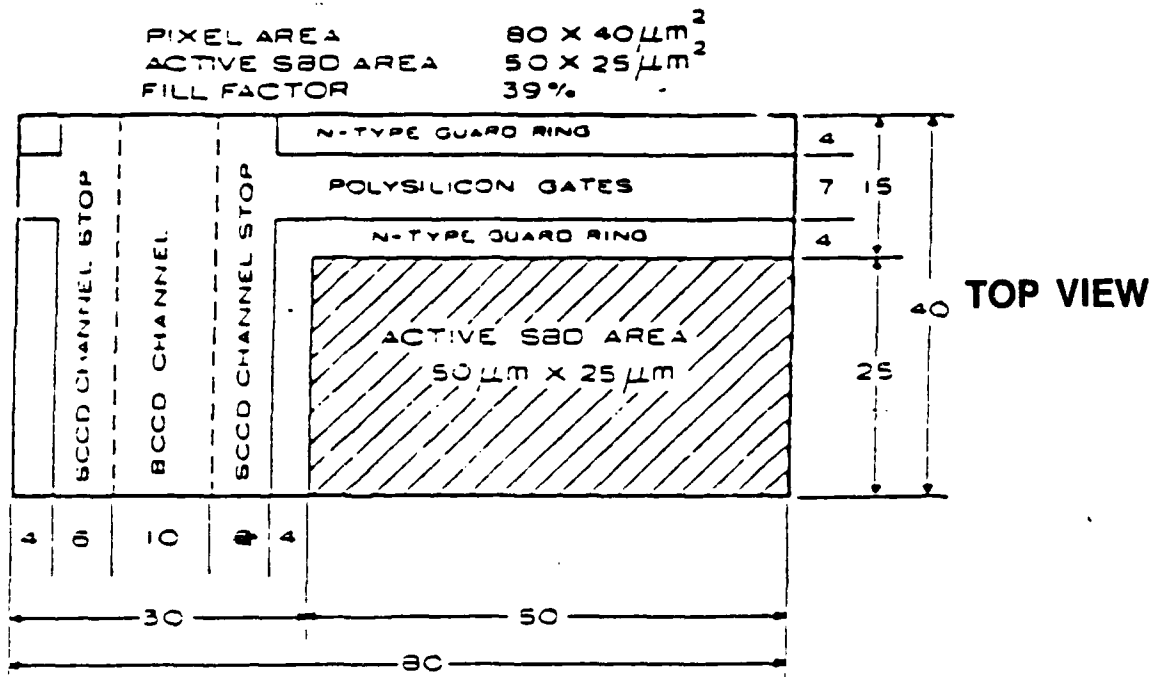


Figure 4.1-1 Layout of single pixel on Schottky-diode FPA

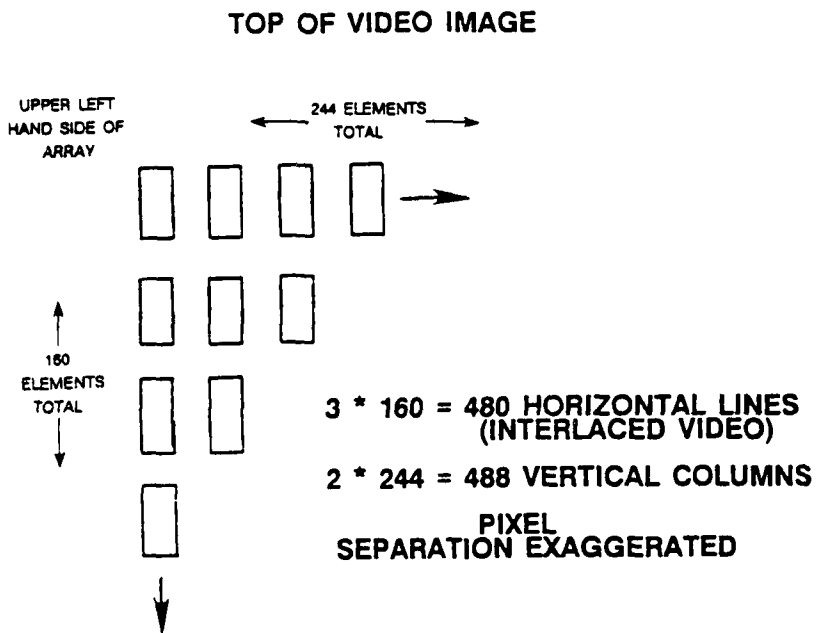


Figure 4.1-2 Overall pixel arrangement in focal plane array

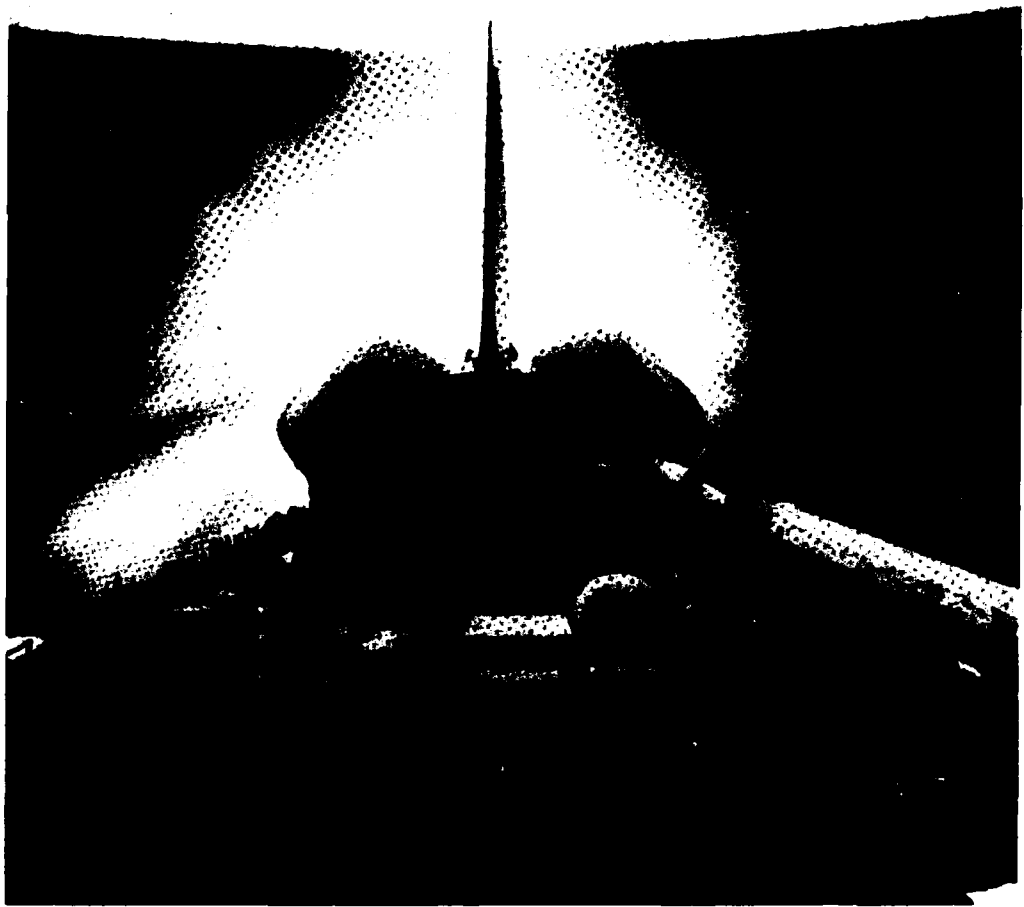


Figure 4.1-3 View from Space shuttle cargo bay

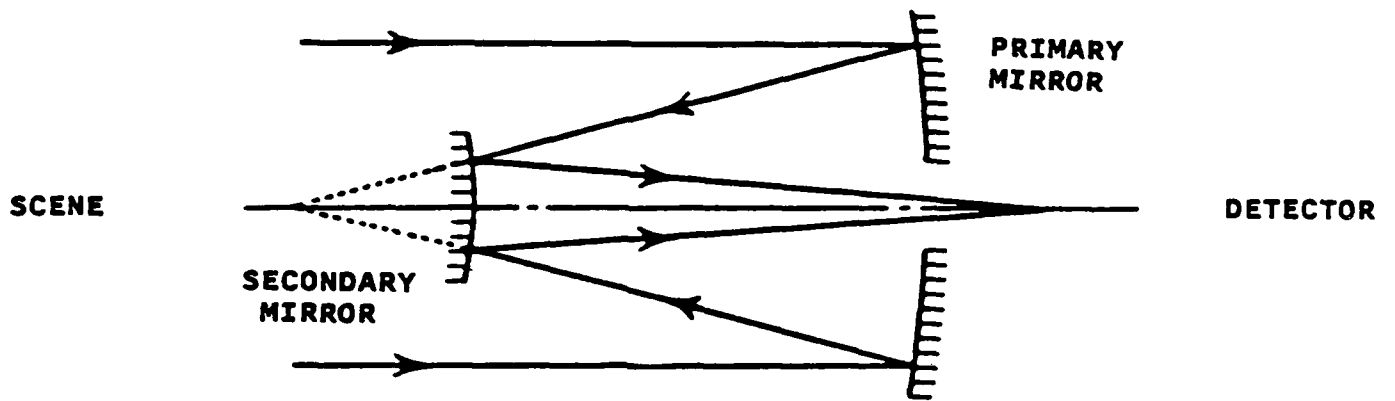


Figure 4.1-4 Cassegrain - Ritchey-Chretien reflecting telescope design

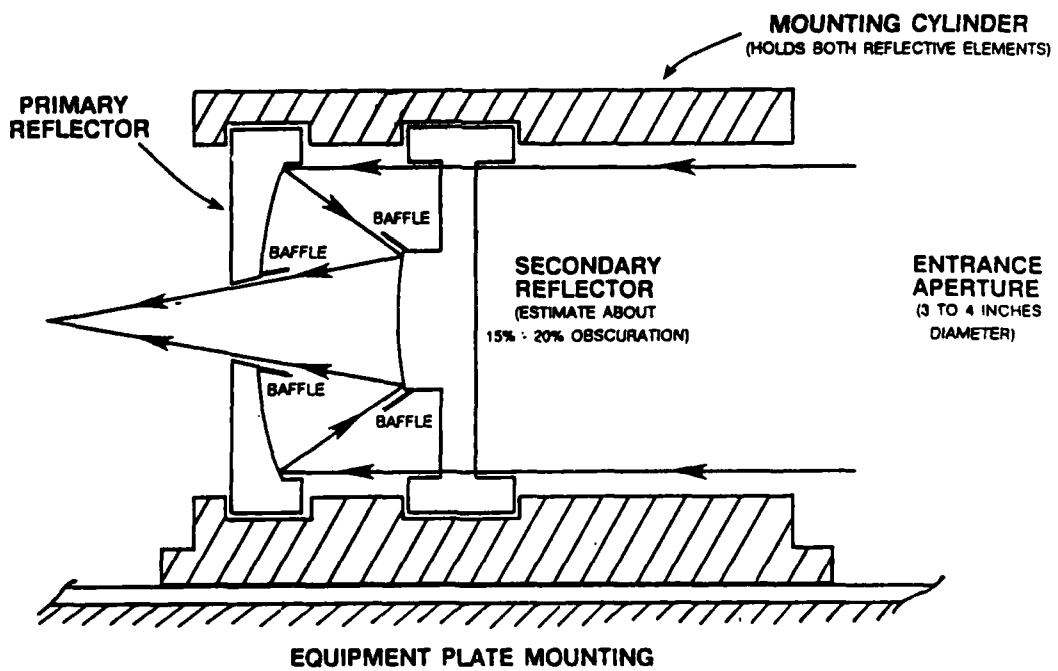


Figure 4.1-5 Proposed Ritchey-Chretien design for SBS Camera optics

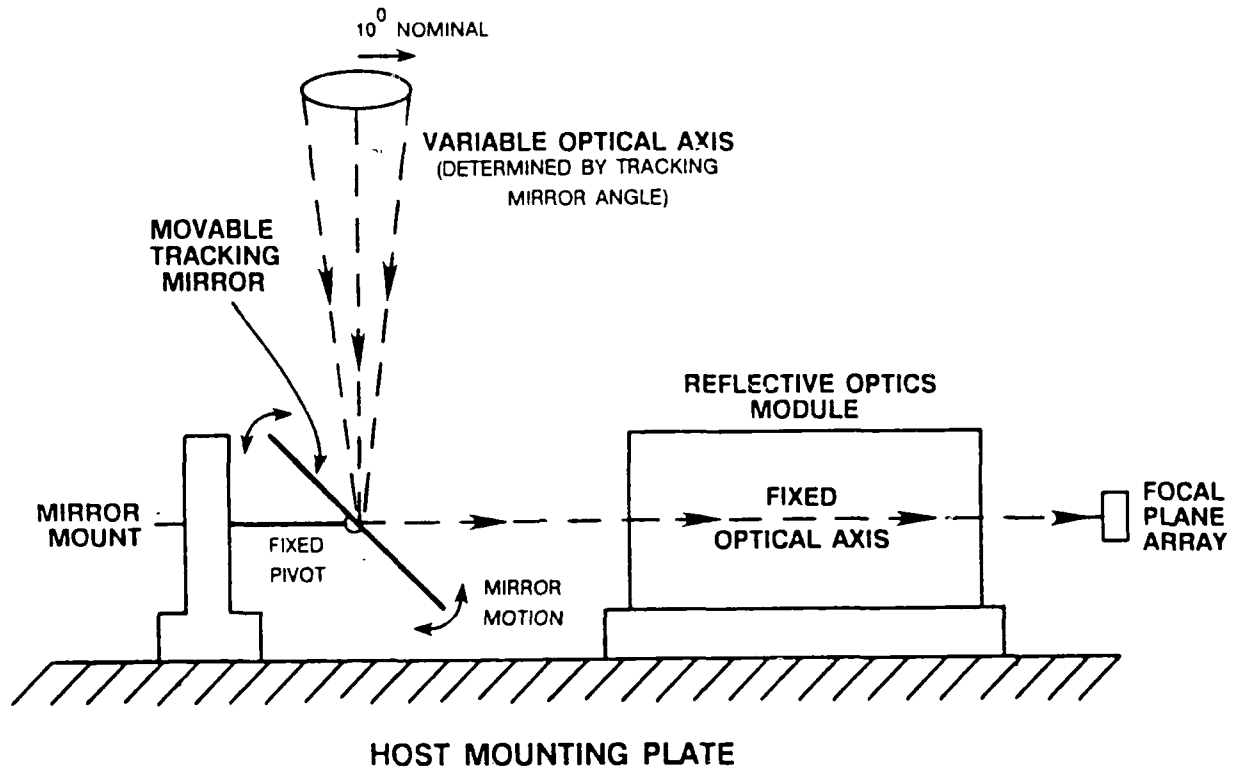


Figure 4.1-6 Use of tracking mirror to control instrument FOV position

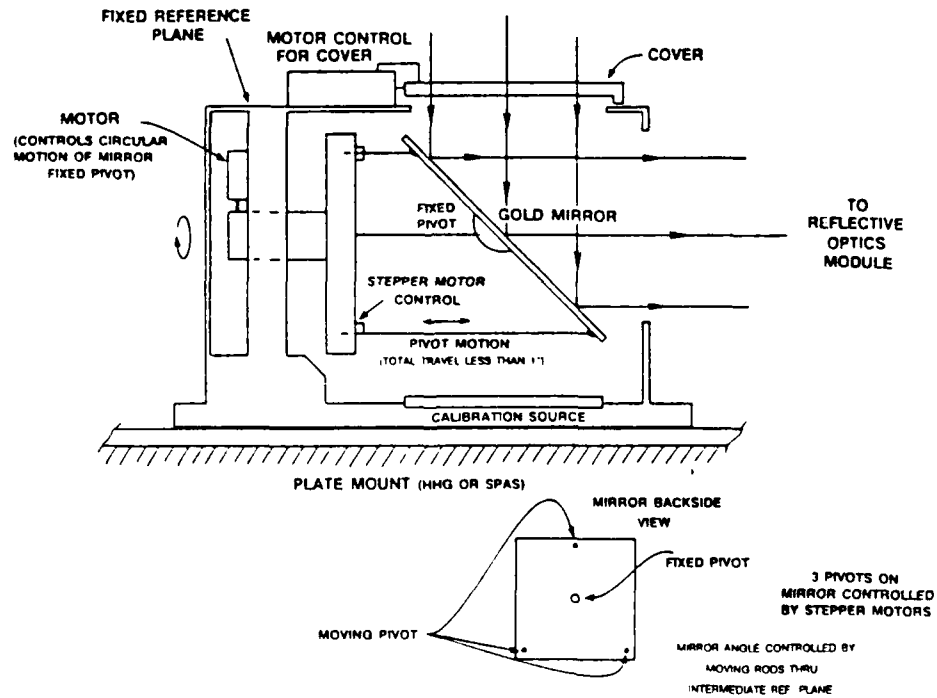


Figure 4.1-7 Possible mechanical implementation of tracking mirror

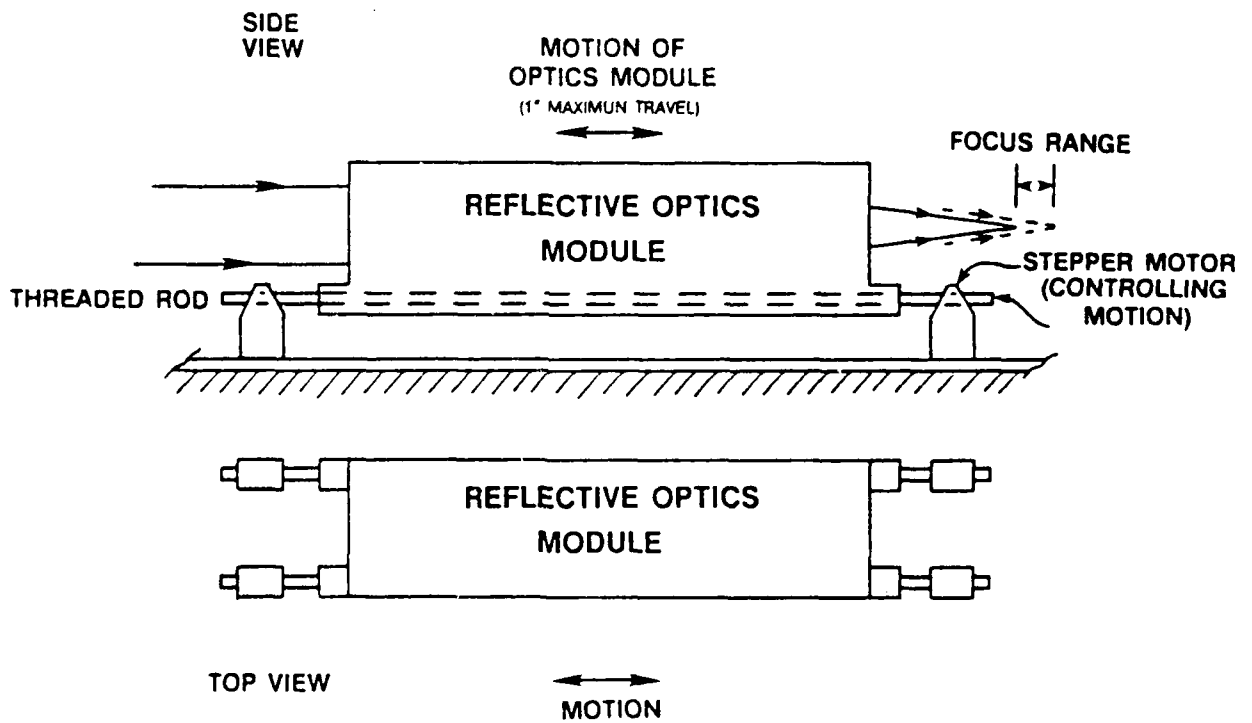


Figure 4.1-8 Focus control by moving reflective optical assembly

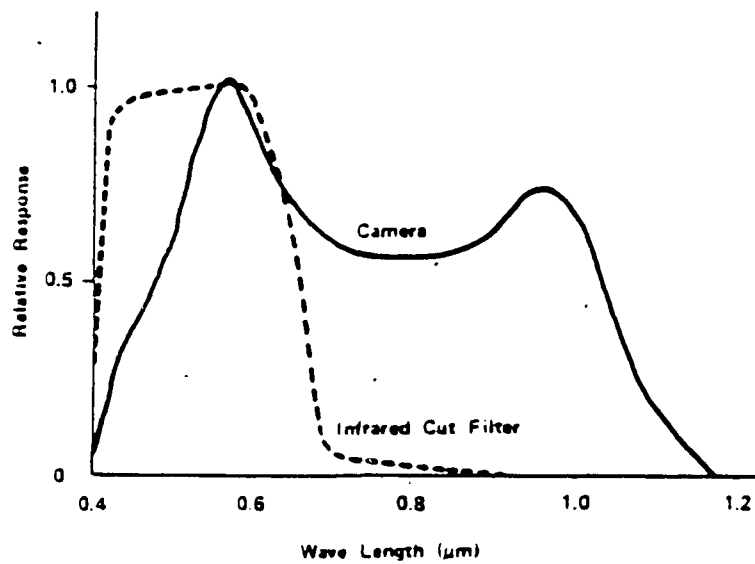


Figure 4.1-9 Spectral response of silicon CCD visible band video camera

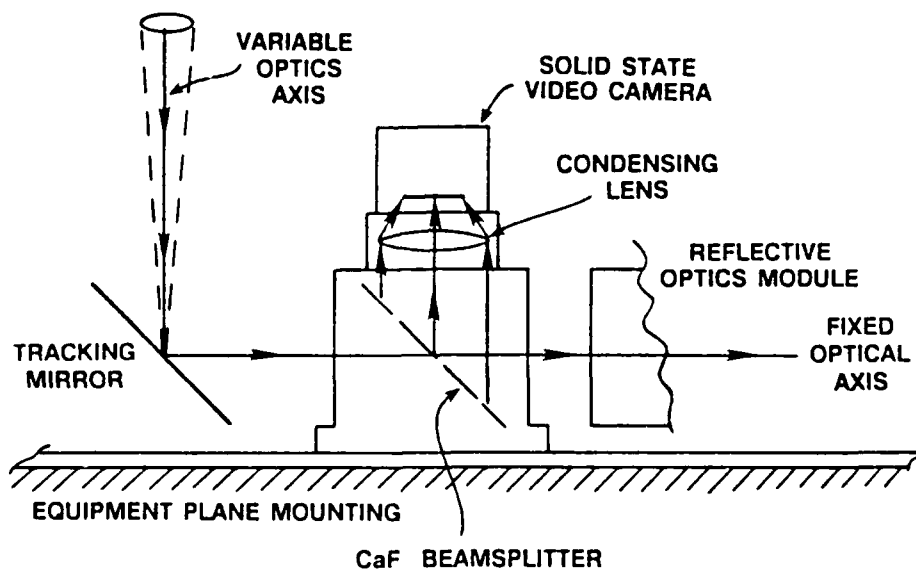


Figure 4.1-10 Block diagram of visible band tracking unit

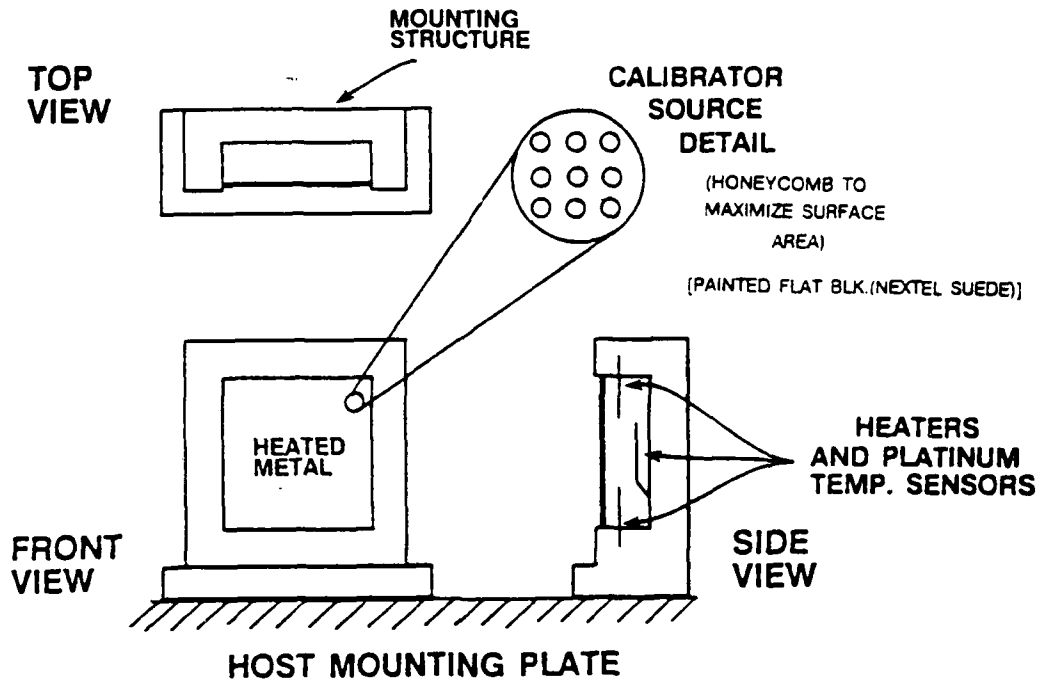


Figure 4.1-11 Calibration source for SBS Camera

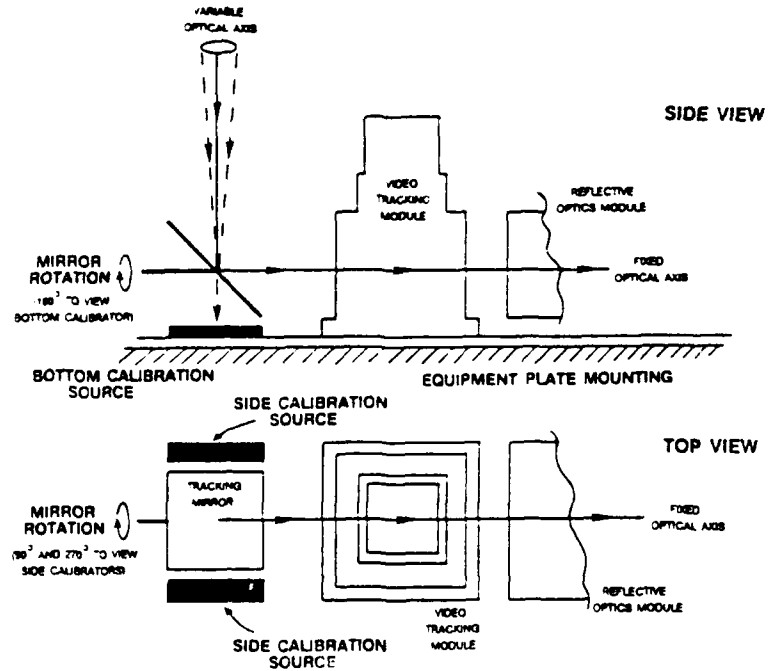


Figure 4.1-12 Locations for calibration sources in SBS payload

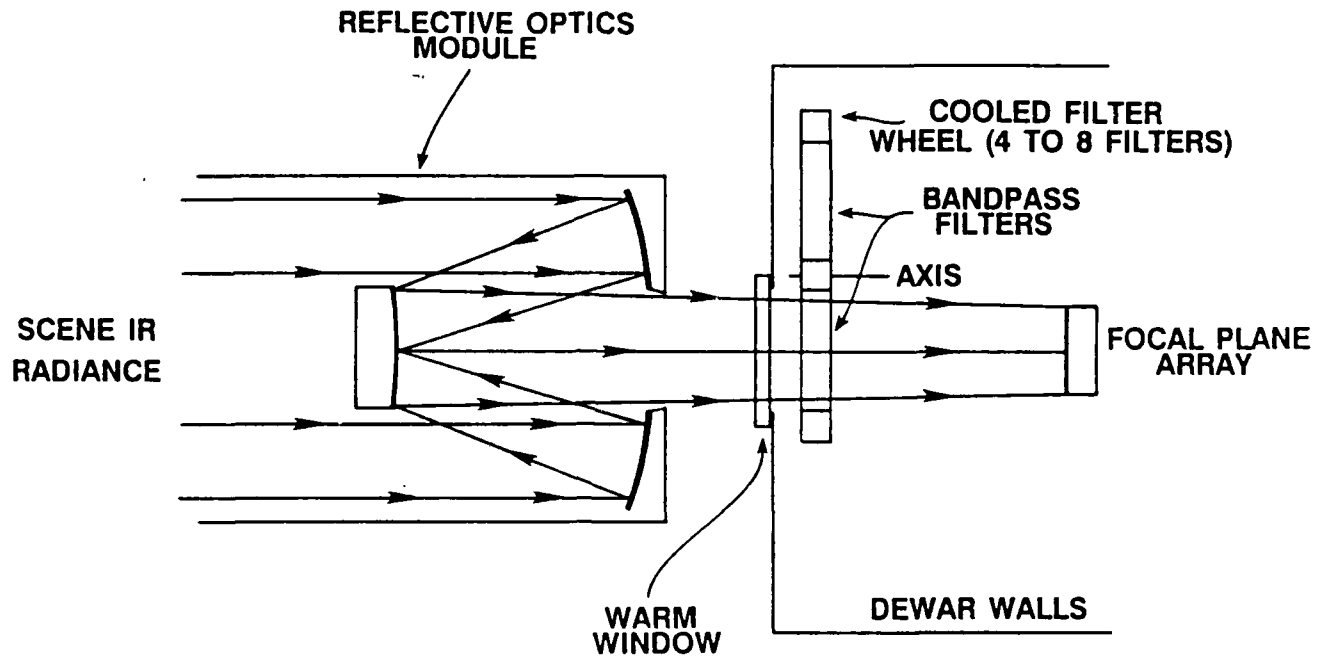


Figure 4.1-13 Bandpass filter wheel in SBS optical system

<u>wheel position</u>	<u>AFGL filter S/N</u>	<u>wavelength band (50% points)</u>
1	400	2.05 - 3.00 micrometers
2	402	3.38 - 3.83
3	406	3.90 - 4.88
4	274 + 228	3.89 - 4.92 + ND2 filter (1%)
5	410	3.60 - 5.04
6	409	4.74 - 5.41
7	387	4.21 - 4.80
8	403	3.72 - 4.22

Figure 4.1-14 Filter bands used in current SAIRS camera

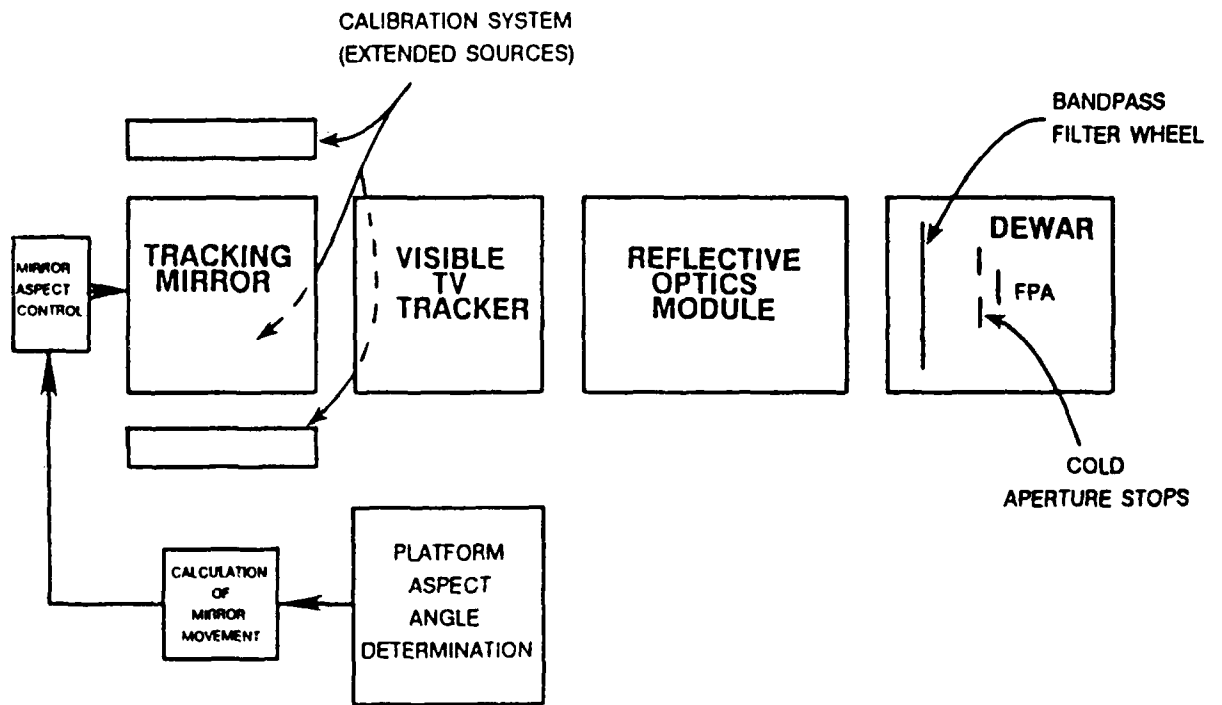


Figure 4.1-15 Complete block diagram of proposed SBS Camera optical system

3 - 5 MICROMETER BAND
(2000 - 3333 cm^{-1})

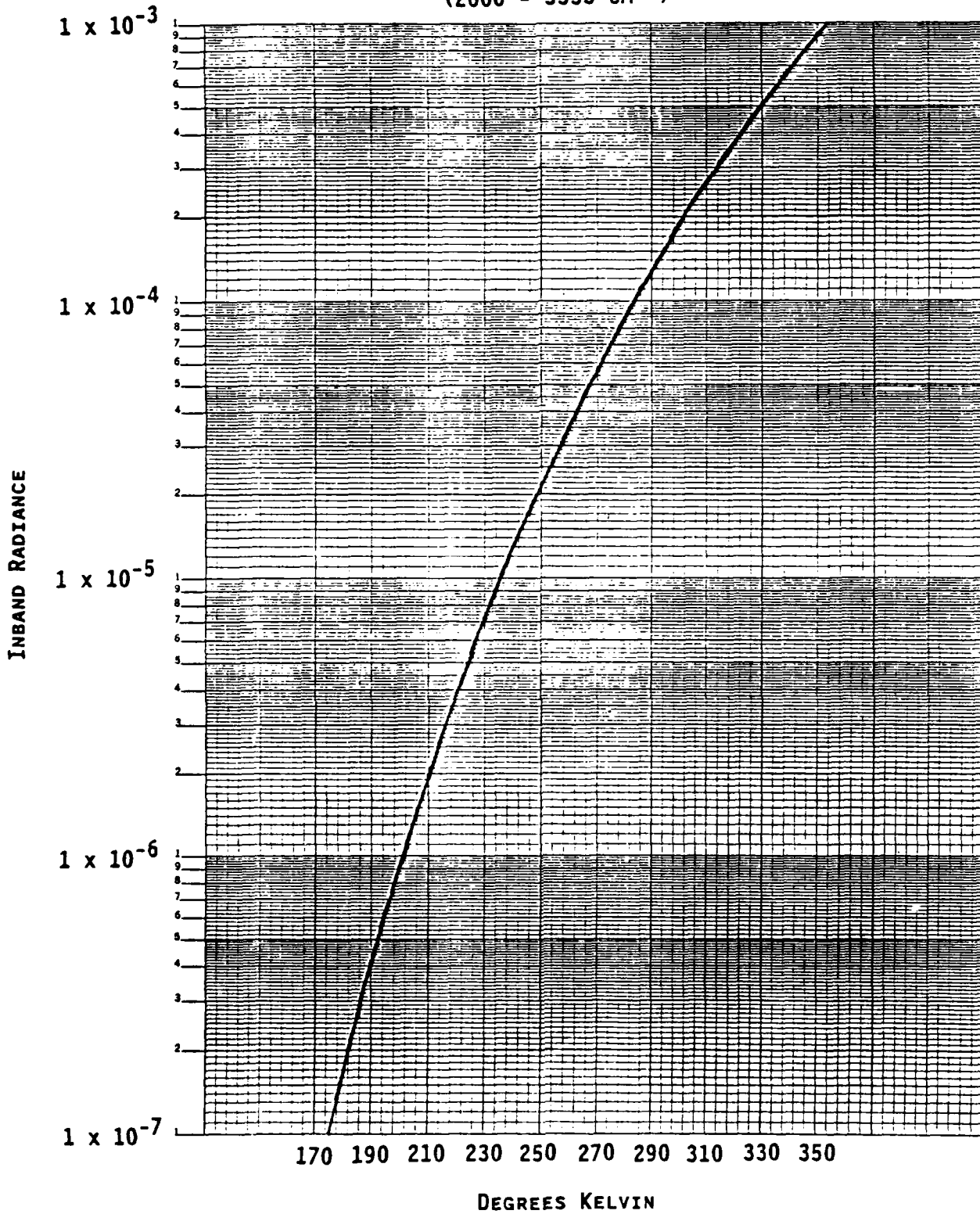


Figure 4.2-1 Plot of emitted radiance vs temperature in SBS Camera band

<u>MATERIAL</u>	<u>HEAT OF SUBLIMATION</u>	<u>DENSITY</u>
NITROGEN	224.7	1022100
ARGON	185.6	1714000
OXYGEN	226.8	1302400
METHANE	568.7	498200
CARBON MONOXIDE	293.1	929200

HEAT OF SUBLIMATION IS IN JOULES/GRAM

DENSITY IN UNITS OF GRAMS/METER³

Figure 4.2-2 Candidate solid cryogens for SBS Camera

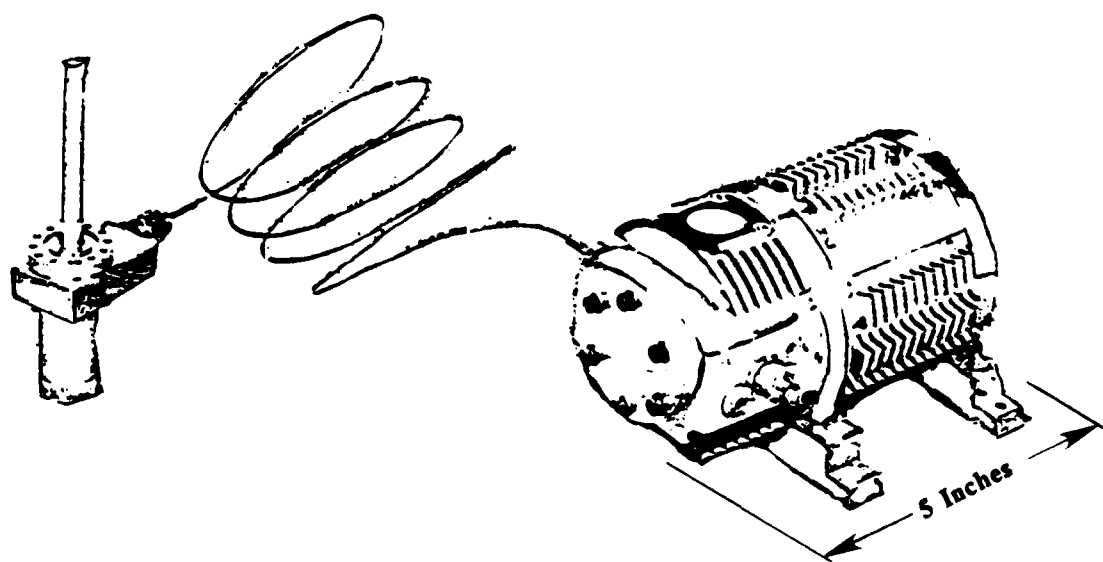


Figure 4.2-3 Sample split-Stirling cooling engine

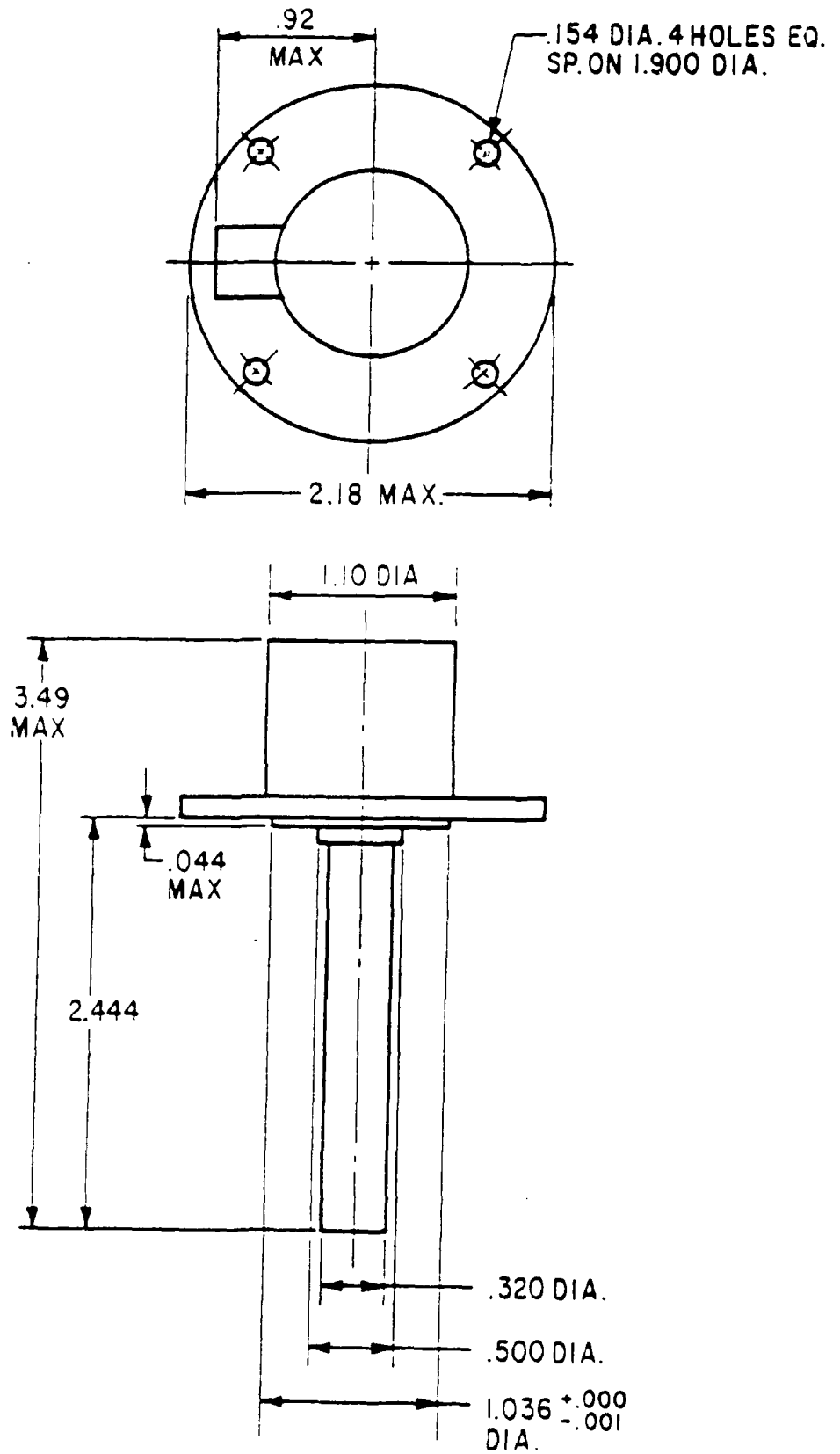


Figure 4.2-4 Physical dimensions of CM-4 cooling engine

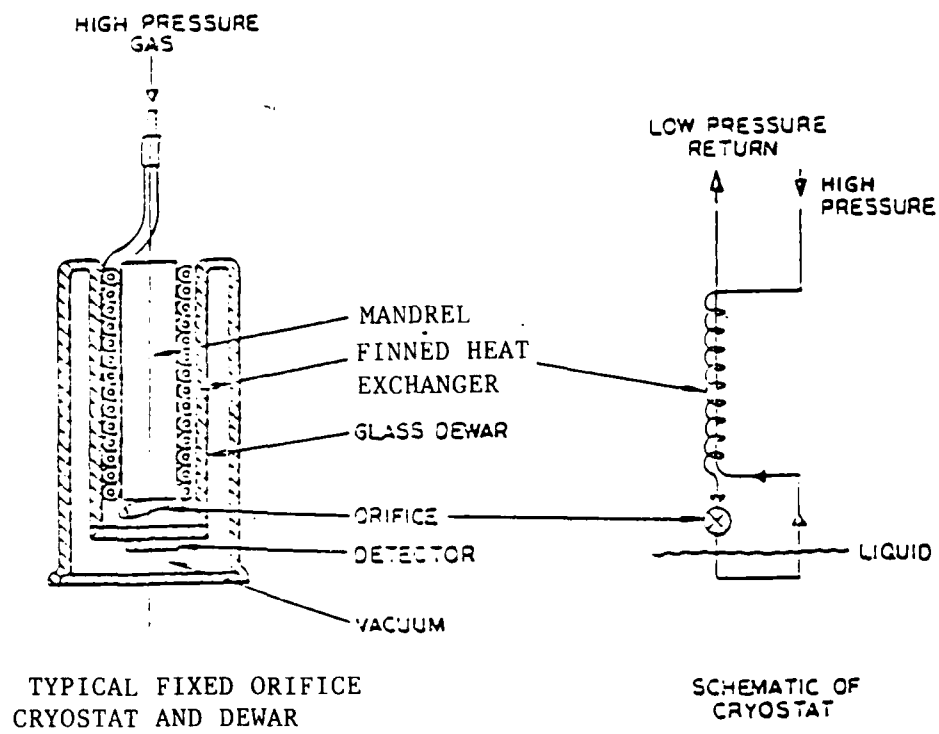


Figure 4.2-5 Schematic diagram of Joule-Thomson cooling system

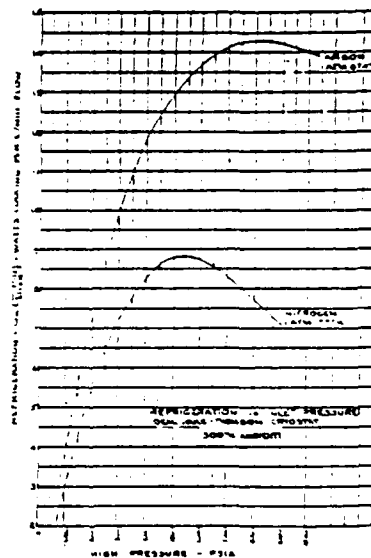


Figure 4.2-6 Refrigeration vs temperature for argon and nitrogen used in a J-T cooling system

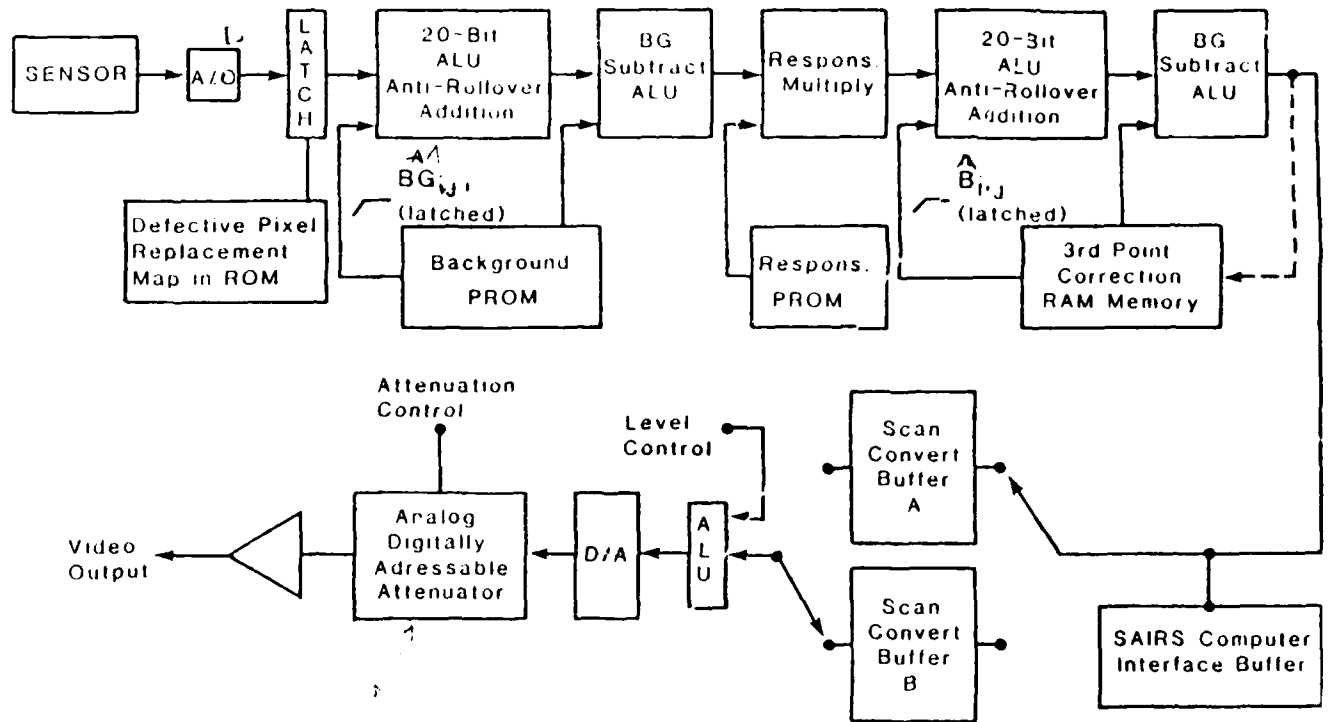


Figure 4.3-1 Block diagram of image compensation system used in SAIRS instruments

SPECIFICATIONS (typical @ +25°C with nominal power supplies unless otherwise noted)

MODEL	MOD-1205
RESOLUTION (FS = FULL SCALE)	12 Bits (0.024% FS)
LSB WEIGHT	1mV
ACCURACY (INCLUDING LINEARITY) @ DC	±0.0125% Full Scale ±1/2LSB
Monotonicity	Guaranteed (0 to +70°C)
Nonlinearity vs. Temperature	0.005% of FS/°C, max
Gain vs. Temperature	0.01% of FS/°C, type; 0.03% of FS/°C, max
DYNAMIC CHARACTERISTICS	
AC Linearity ¹ : dc to 1MHz	Spurious Signals >70dB below FS, max
.1MHz to 2.5MHz	Spurious Signals >65dB below FS, max; >68dB, typ
Conversion Time	See Text and Timing Diagram
Conversion Rate (Word Rate)	5MHz
Aperture Uncertainty (Jitter)	±25ps max
Aperture Time	30ns (±10ns from unit to unit)
Signal to Noise Ratio ²	96dB min, 98dB, typ
Noise Power Ratio ³	56dB min, 58dB, typ
Transient Response ⁴	12-Bit (0.0125%) Accuracy within 200ns
Overvoltage Recovery Time ⁵	200ns
Input Bandwidth (small signal, 3dB)	15MHz min
Input Bandwidth (large signal, 3dB)	10MHz min; flat within ±0.1dB, dc through 5MHz
ANALOG INPUT	
Voltage Range	±1.048V FS
	±4V Absolute max
Impedance	400Ω with pin 30 open, 50Ω with pin 30 grounded
Offset Voltage	Adjust to 0 with On Board Potentiometer
Offset vs. Temperature	0.02% FS/°C, type; 0.05% of FS/°C, max
Bias Current	1nA max
ENCODE COMMAND INPUT	
Logic Levels, TTL Compatible	"0" = 0 to -0.4V
	"1" = +2.4V to +5V
Logic Loading	2 Standard TTL Gates
Rise and Fall Times	10ns max
Duration min/max	25ns/50% of Duty Cycle
Frequency (Random or Periodic)	5MHz
DIGITAL DATA OUTPUT	
Format	12 Parallel Bits, NRZ
Logic Levels, TTL Compatible	"0" = 0 to -0.4V
	"1" = +2.4V to +5V
Drive (Not Short Circuit Protected)	Up to 1 Schottky TTL or
	2 Standard TTL Loads
Time Skew	10ns max
Coding	Offset Binary (OBN) or 2's complement (2SC)
Conversion Time	See Text on the Next Page
POWER REQUIREMENTS⁶	
-15V ±5%	200mA
-15V ±5%	150mA
+5V ±4%	700mA
+5V ±5%	800mA
Power Consumption	13 Watts
TEMPERATURE RANGE	
Operating	0 to +70°C
Storage	-55°C to +85°C
Cooling Requirements	500 Linear Feet Per Min (LFPM) @ +70°C
PHYSICAL CHARACTERISTICS	
Construction	Single Printed Circuit Card

NOTES

¹ AC linearity expressed in terms of spurious in-band signals generated at specified encode rates at analog input frequencies ().

² rms signal to rms noise at 100kHz analog input.

³ dc to 2.4MHz white noise bandwidth with 100Hz frequency of 512Hz.

⁴ For full-scale step input, attains 12-bit accuracy in time specified.

⁵ Recovers to 12-bit accuracy after 2 X FS input overvoltage in time specified.

⁶ ±15V supplies must be equal and opposite within 200mV and track over

temperature.

Specifications subject to change without notice.

VOL II, 11-70 ANALOG-TO-DIGITAL CONVERTERS

Figure 4.3-2 Specifications of A/D module used in SAIRS (MOD-1205)

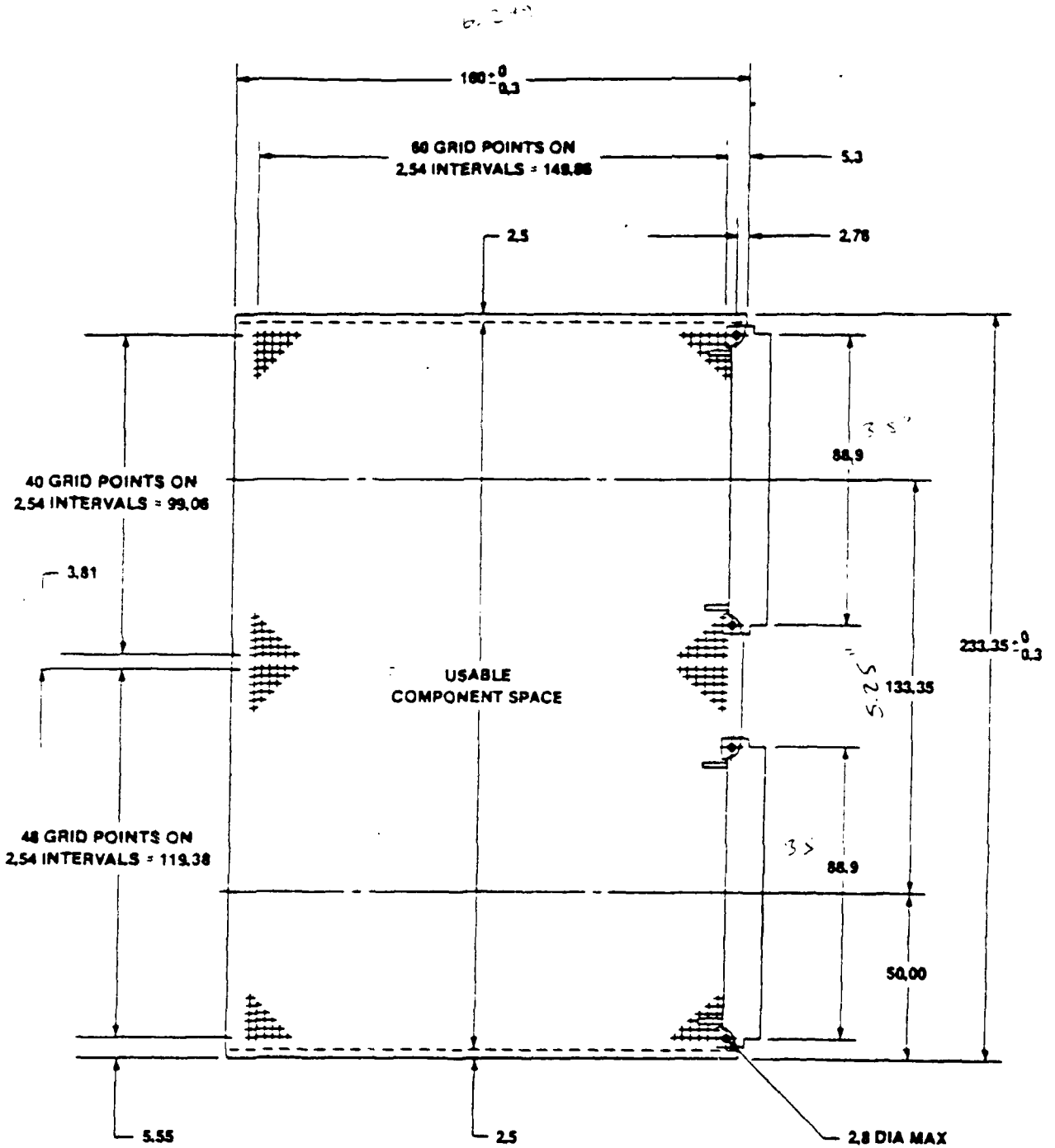


Figure 4.3-3 Drawing showing physical dimensions of double-VME bus card

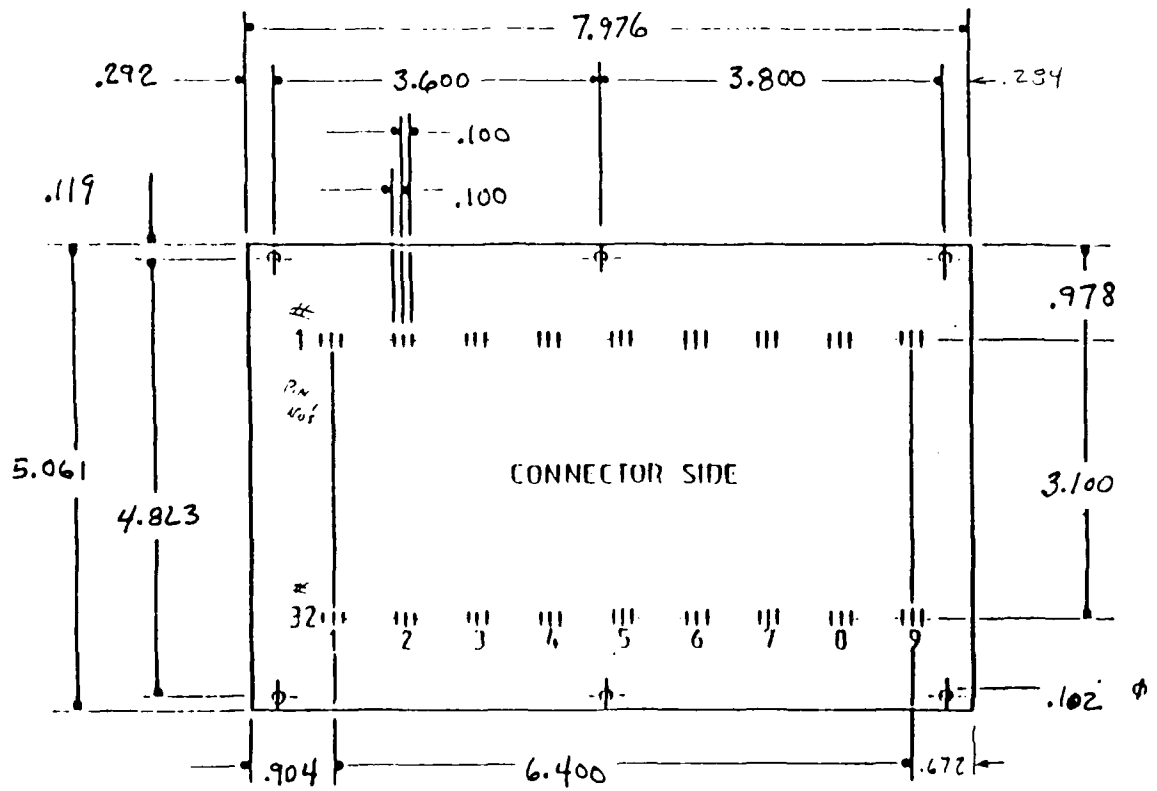
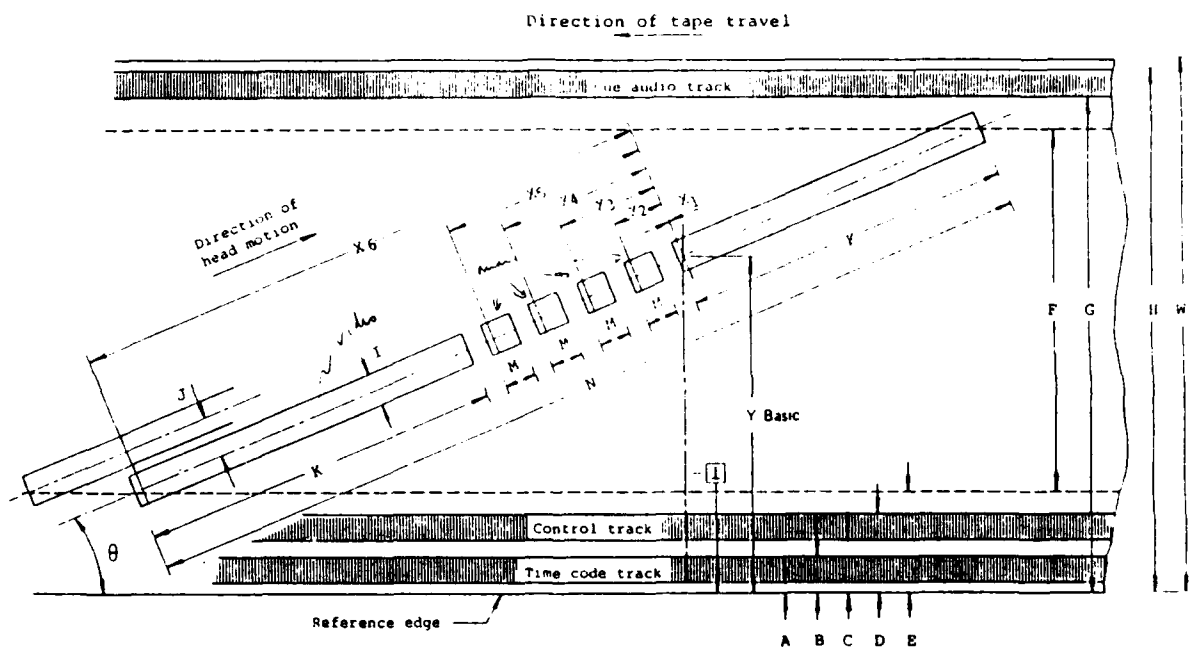
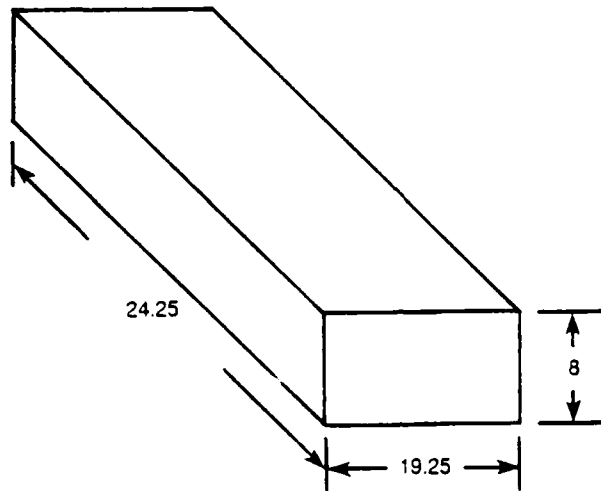


Figure 4.3-4 Drawing showing dimensions of 9 slot VME-bus motherboard

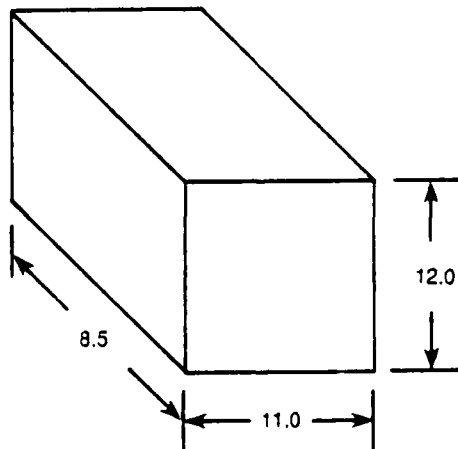


(tape viewed from oxide side, not to scale)

Figure 4.4-1 D-1 digital video tape layout



**TAPE UNIT
(T.U.)**



**ELECTRONICS
UNIT
(E.U.)**

Figure 4.4-2 Drawing showing physical dimensions of Odetics DCRR-32 recorder

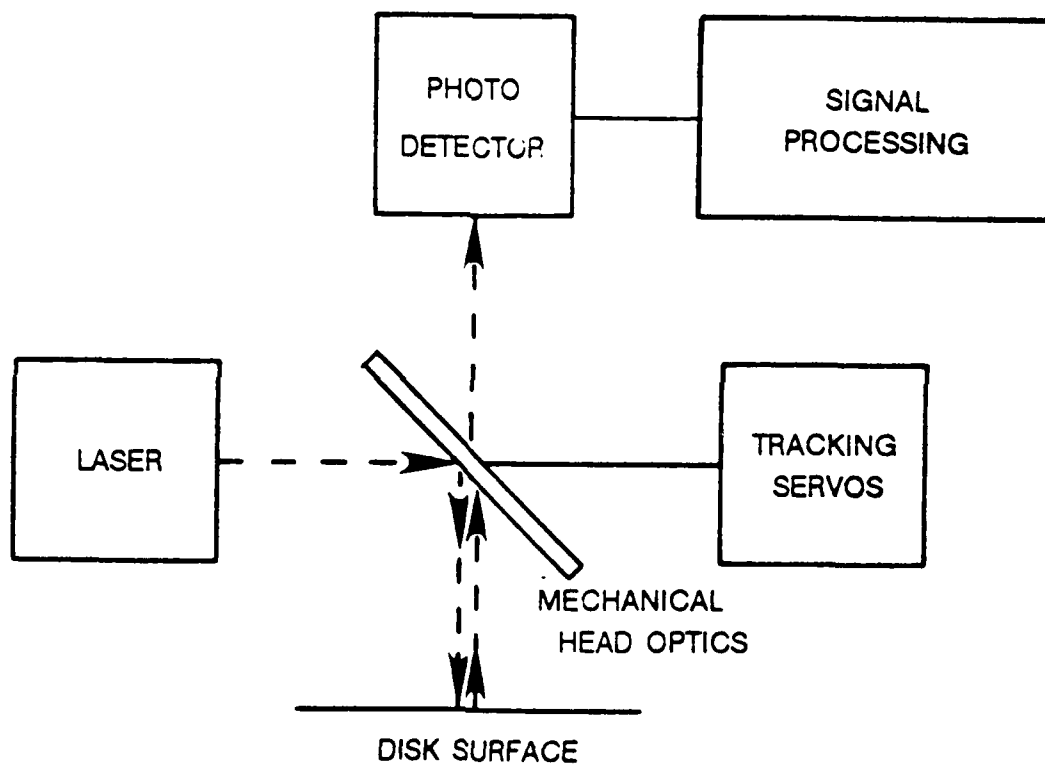


Figure 4.4-3 Block diagram of optical disk writing mechanism

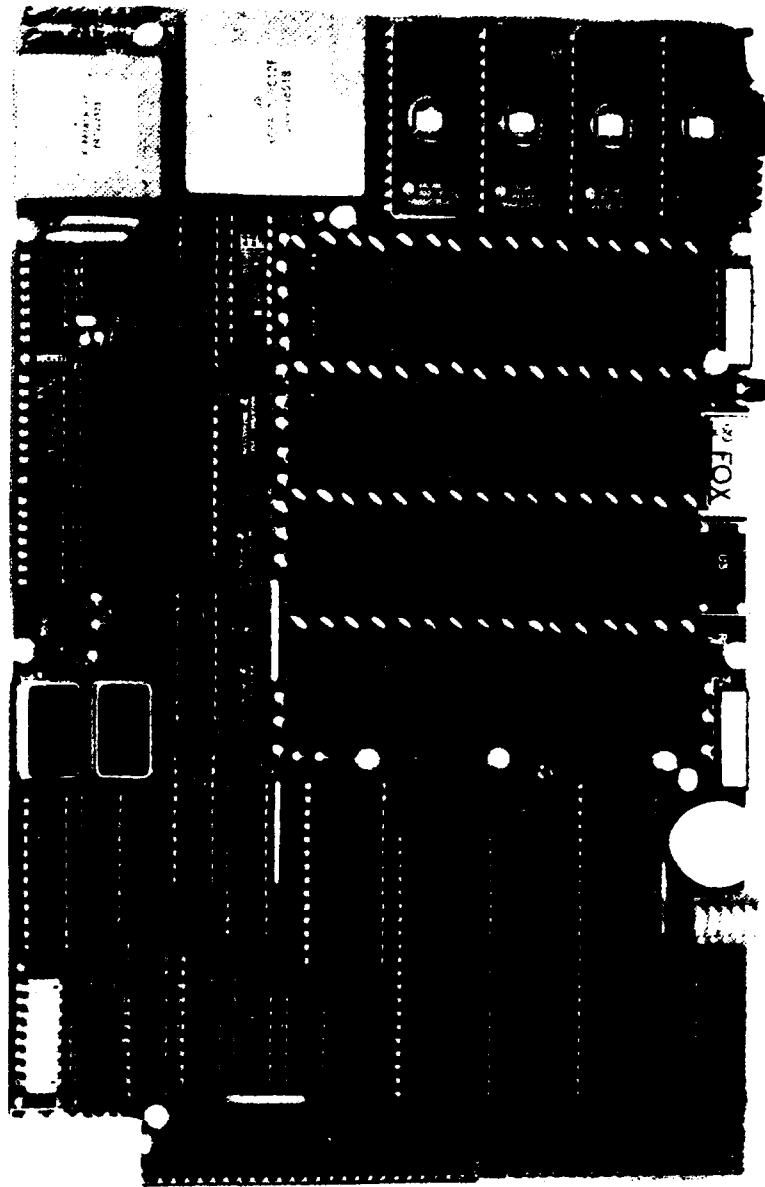


Figure 4.5-2 Photograph of GMX Micro-20 single board computer

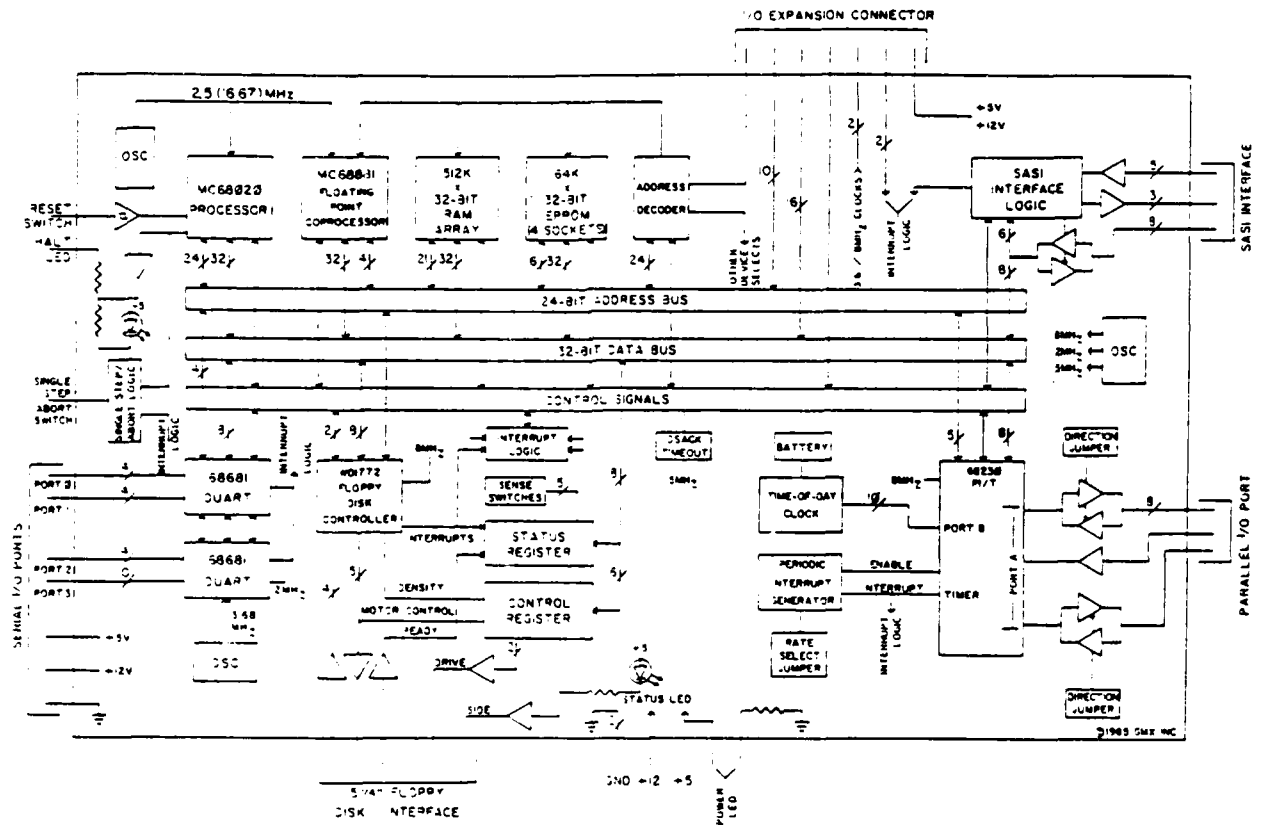
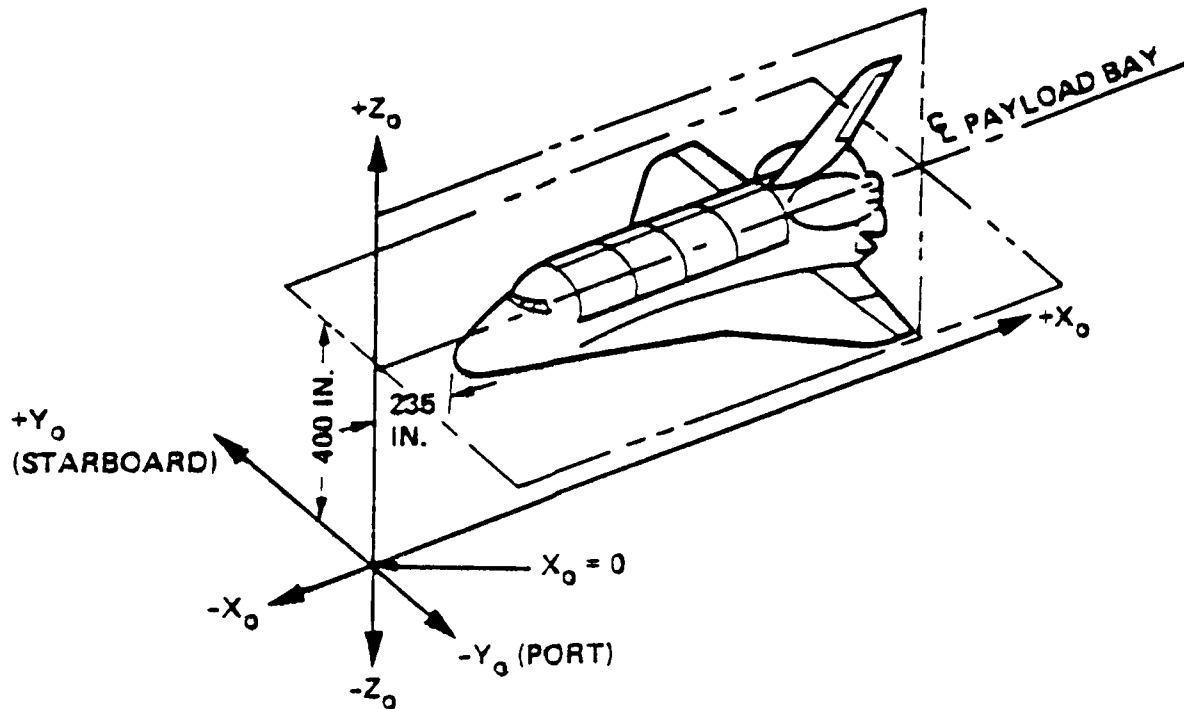


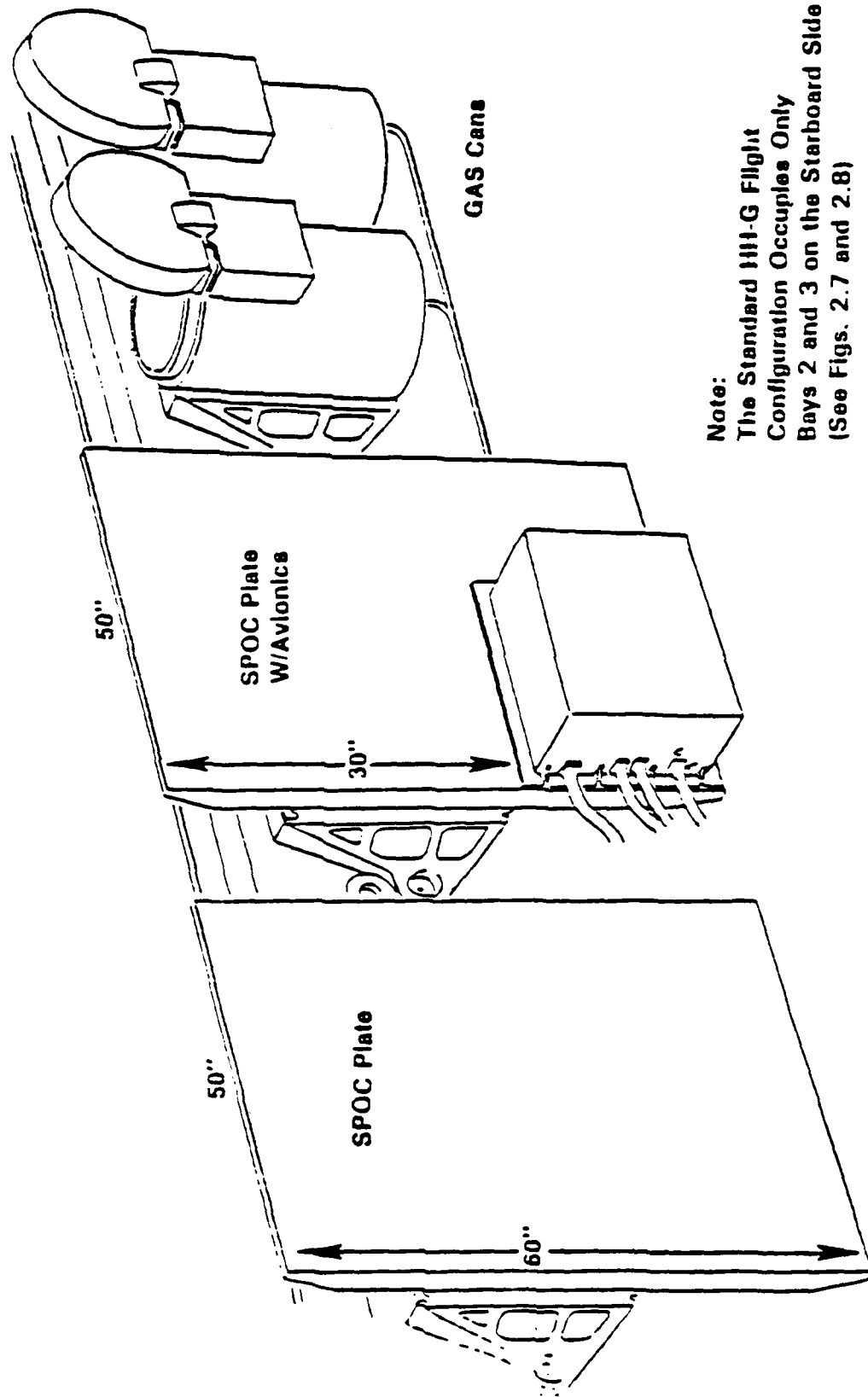
Figure 4.5-3 Block diagram of GMX Micro-20 single board computer



- ORIGIN:** IN THE ORBITER PLANE OF SYMMETRY, 400 INCHES BELOW THE CENTER LINE OF THE PAYLOAD BAY AND AT ORBITER X STATION = 0.
- ORIENTATION:** THE X_0 AXIS IS IN THE VEHICLE PLANE OF SYMMETRY PARALLEL TO AND 400 INCHES BELOW THE PAYLOAD BAY CENTER LINE. POSITIVE SENSE IS FROM THE NOSE OF THE VEHICLE TOWARD THE TAIL. THE Z_0 AXIS IS IN THE VEHICLE PLANE OF SYMMETRY, PERPENDICULAR TO THE X_0 AXIS POSITIVE UPWARD IN LANDING ATTITUDE. THE Y_0 AXIS COMPLETES A RIGHT-HANDED SYSTEM.
- CHARACTERISTICS:** ROTATING RIGHT-HANDED CARTESIAN. THE STANDARD SUBSCRIPT IS 0 (e.g., X_0).

Figure 4.6-1 STS (shuttle) orbiter coordinate system

HH-G Customer Mounting Accomodations (SPOC Plate, Avionics Plate and GAS Cans)



Note:
The Standard HH-G Flight
Configuration Occupies Only
Bays 2 and 3 on the Starboard Side
(See Figs. 2.7 and 2.8)

Figure 4.6-2 Diagram of HH-G plate mounting payload configuration

HH-G Payload Mounting Concept

Sideview

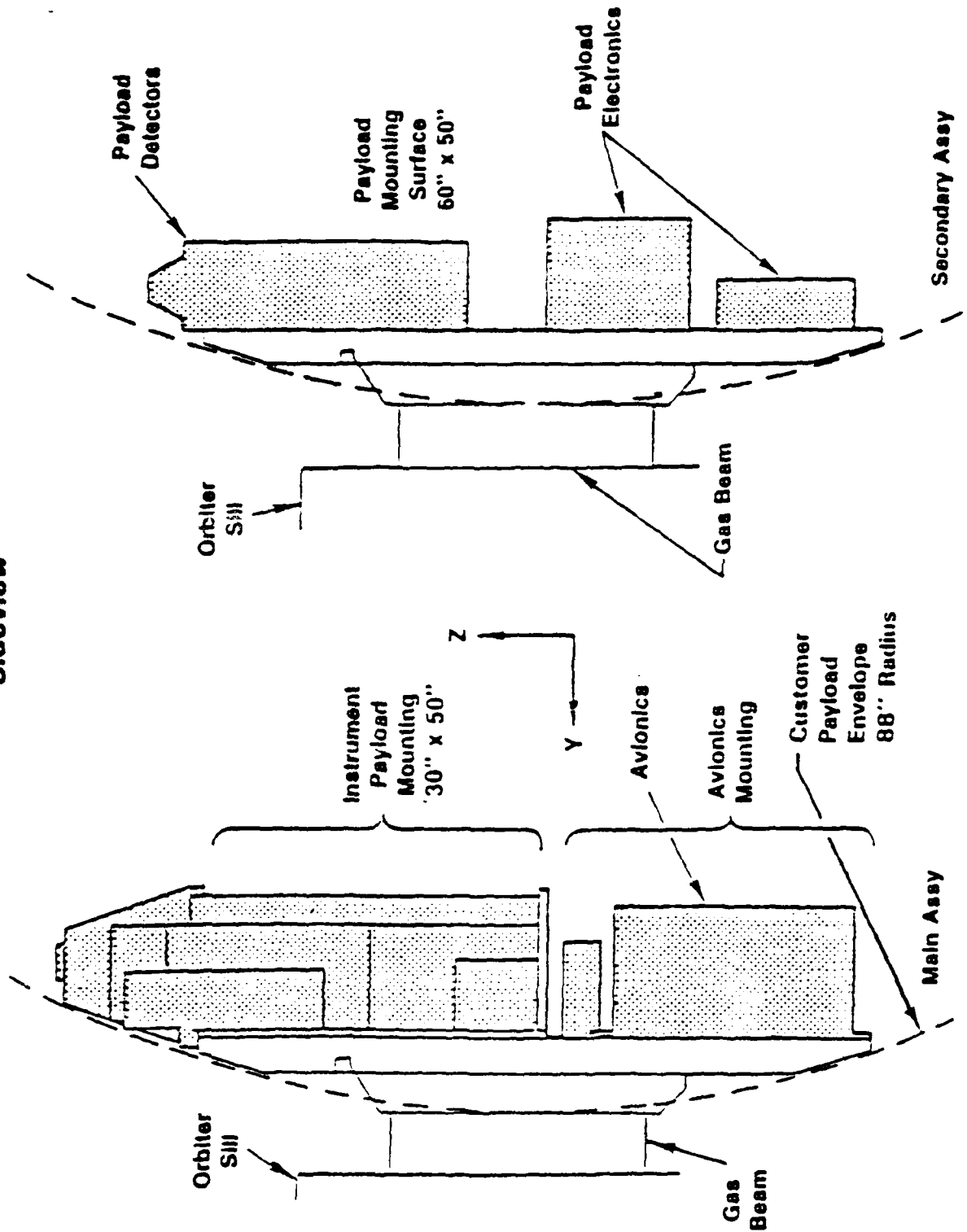


Figure 4.6-3 HH-G plate mounting payload envelope - side aspect

Hitchhiker - G SPOC Plate Structural Assembly

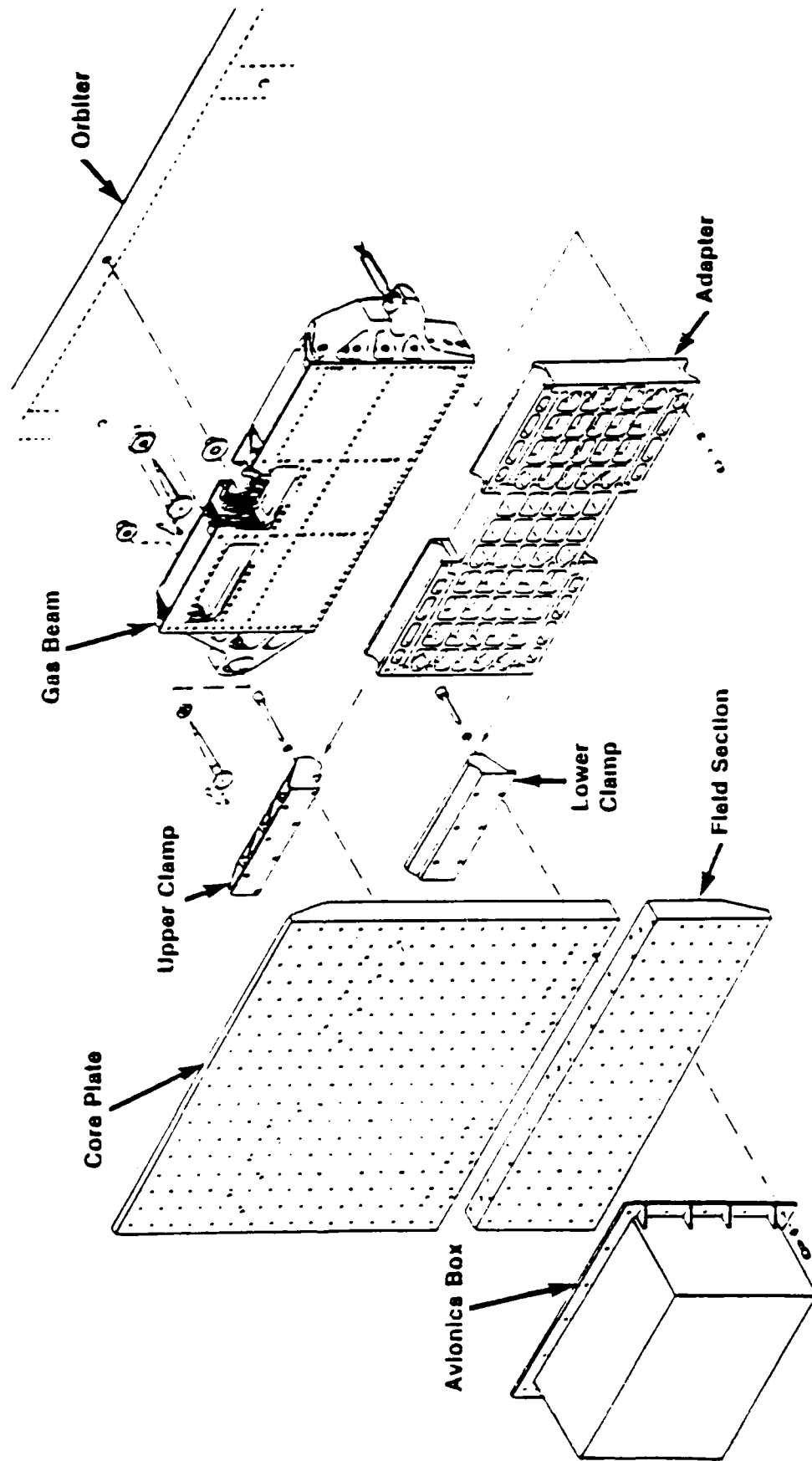


Figure 4.6-4 HHI-G structural assembly of plate mounting system

HH-G Available Mounting Locations

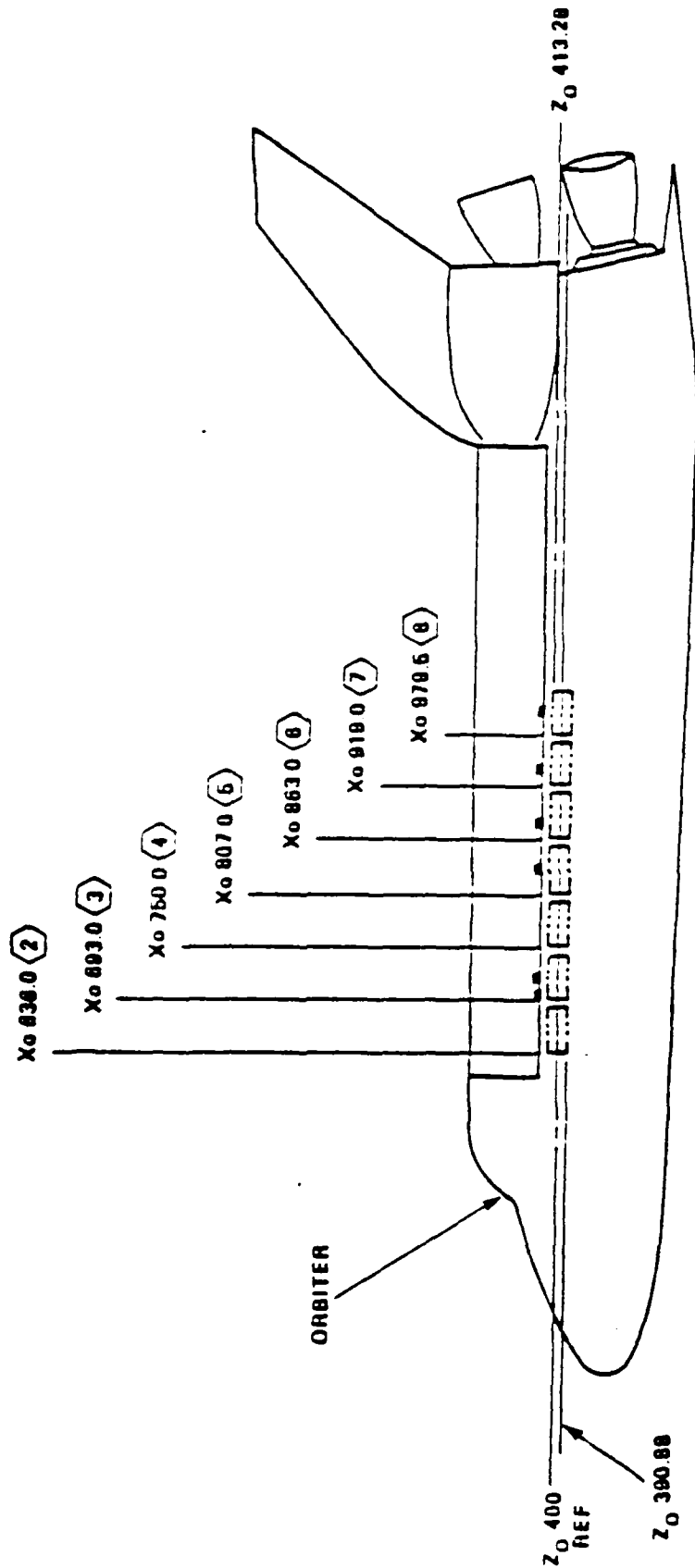


Figure 4.6-5 HH-G available locations in cargo bay for payload mounting

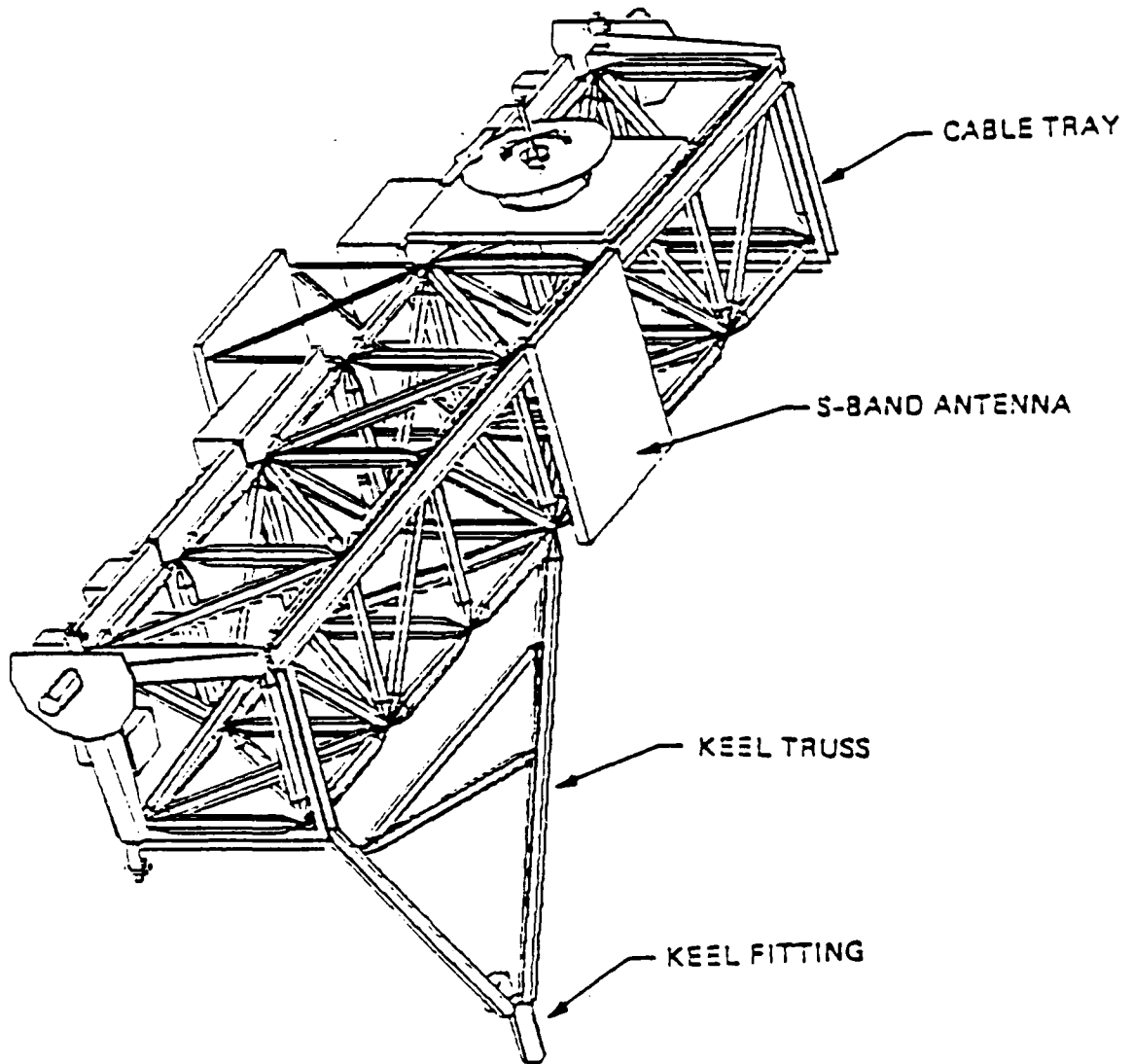


Figure 4.6-6 Drawing of Shuttle Pallet Satellite (SPAS) platform

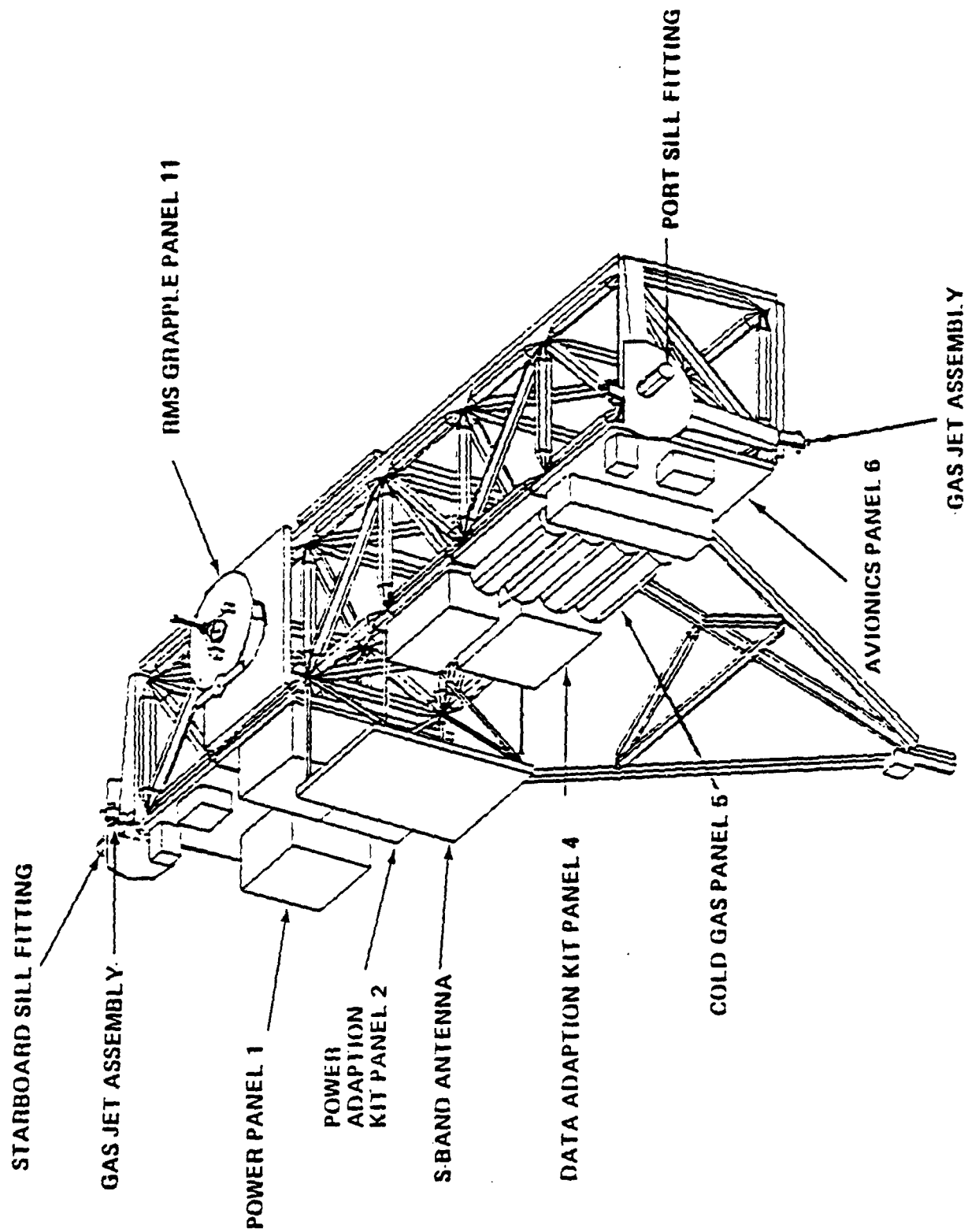


Figure 4.6-7 SPAS drawing showing locations of platform subsystems

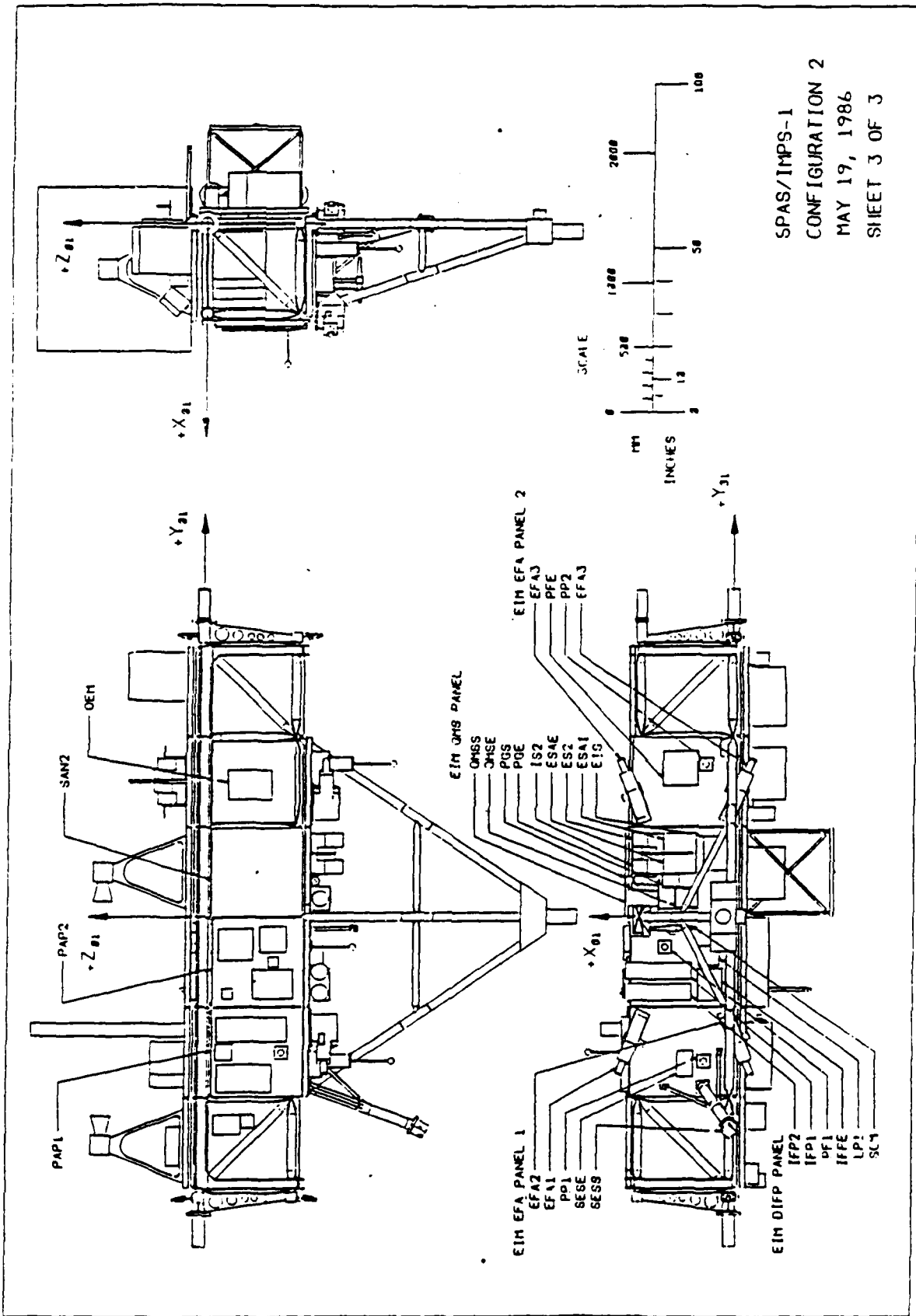


Figure 4.6-8 Examples of instrumentation mounted on SPAS platform

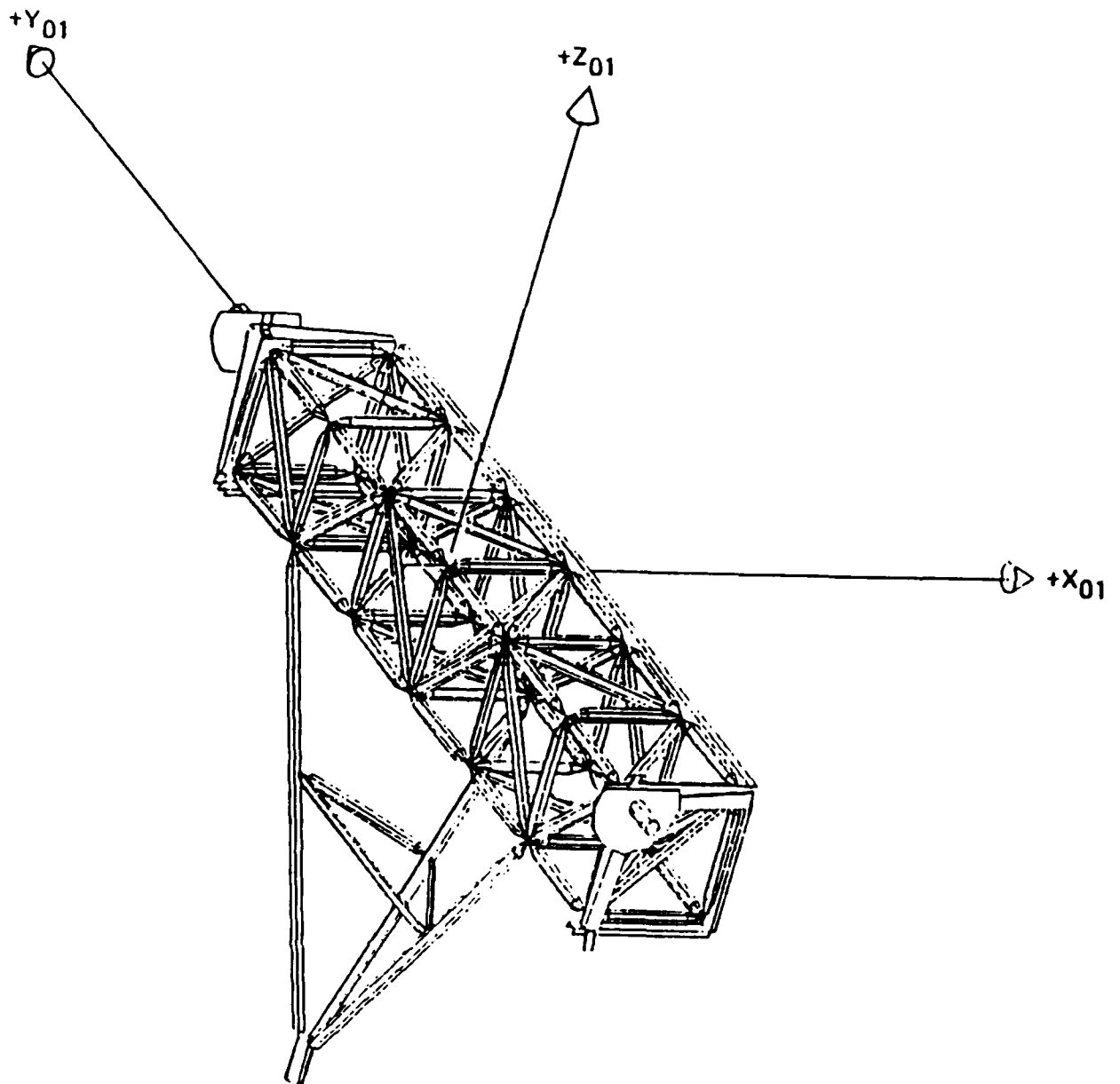


Figure 4.6-9 SPAS platform coordinate system

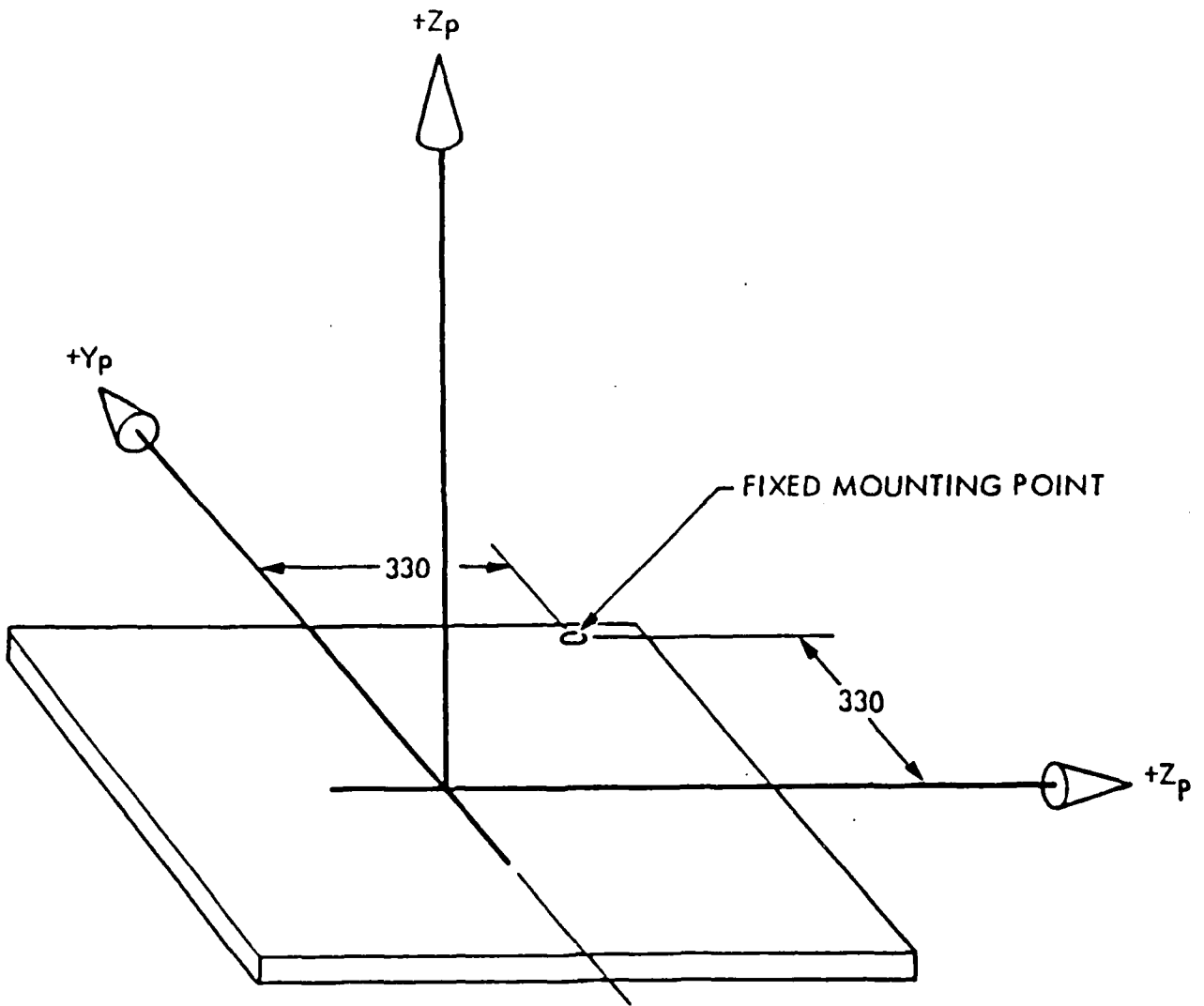


Figure 4.6-10 Coordinate system of Equipment Mounting Plate (ESP)

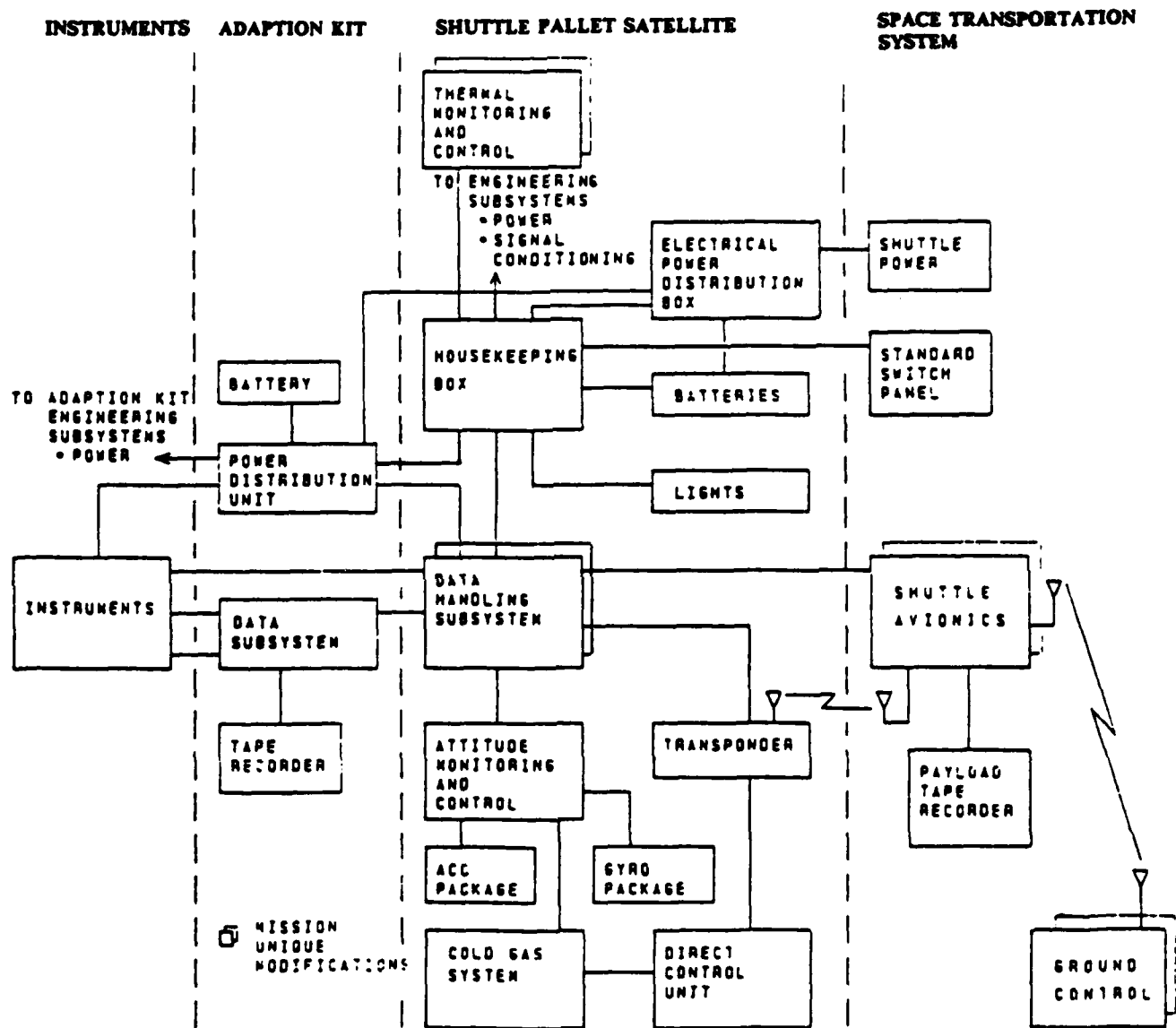


Figure 4.6-11 Functional block diagram of SPAS platform

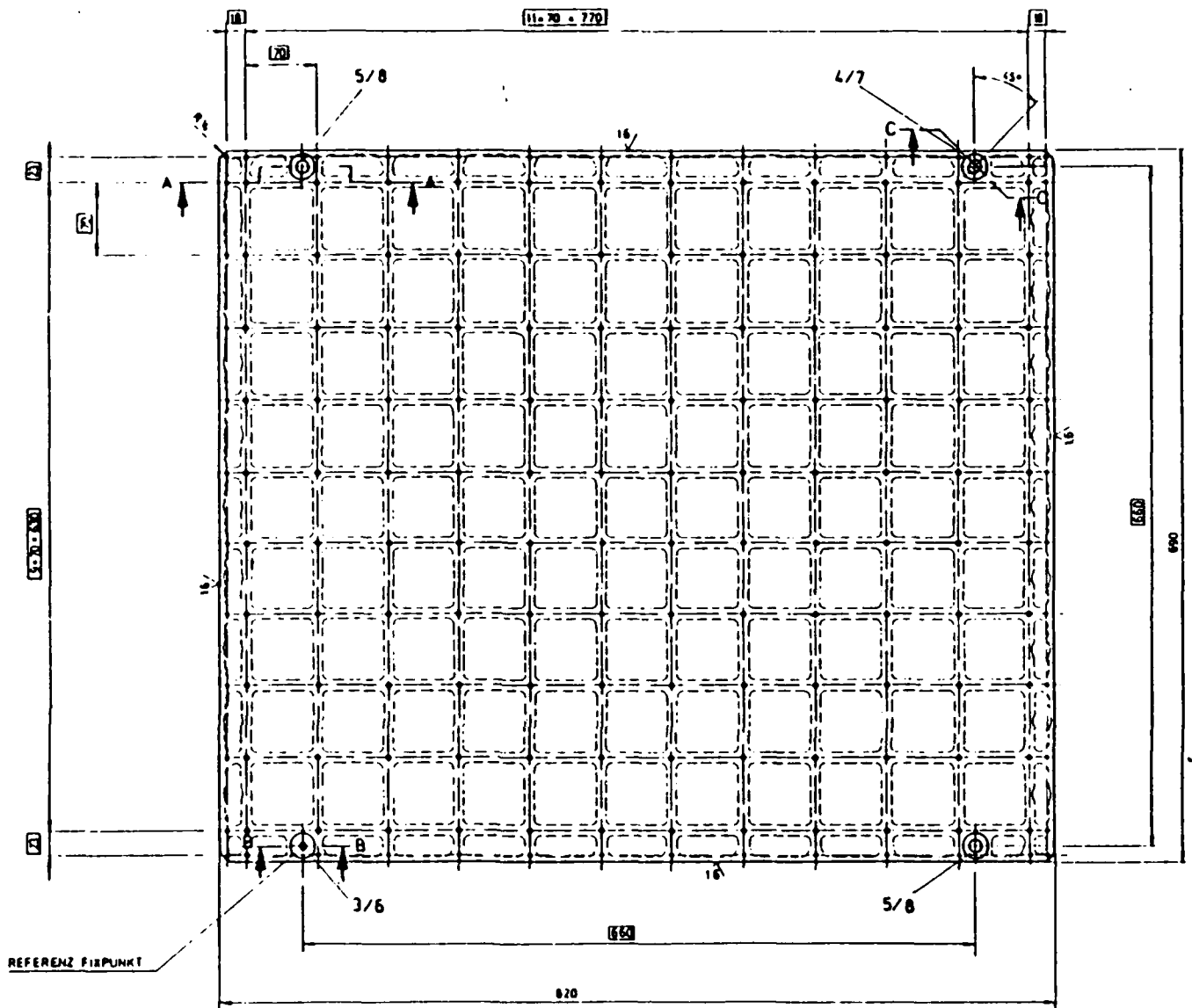
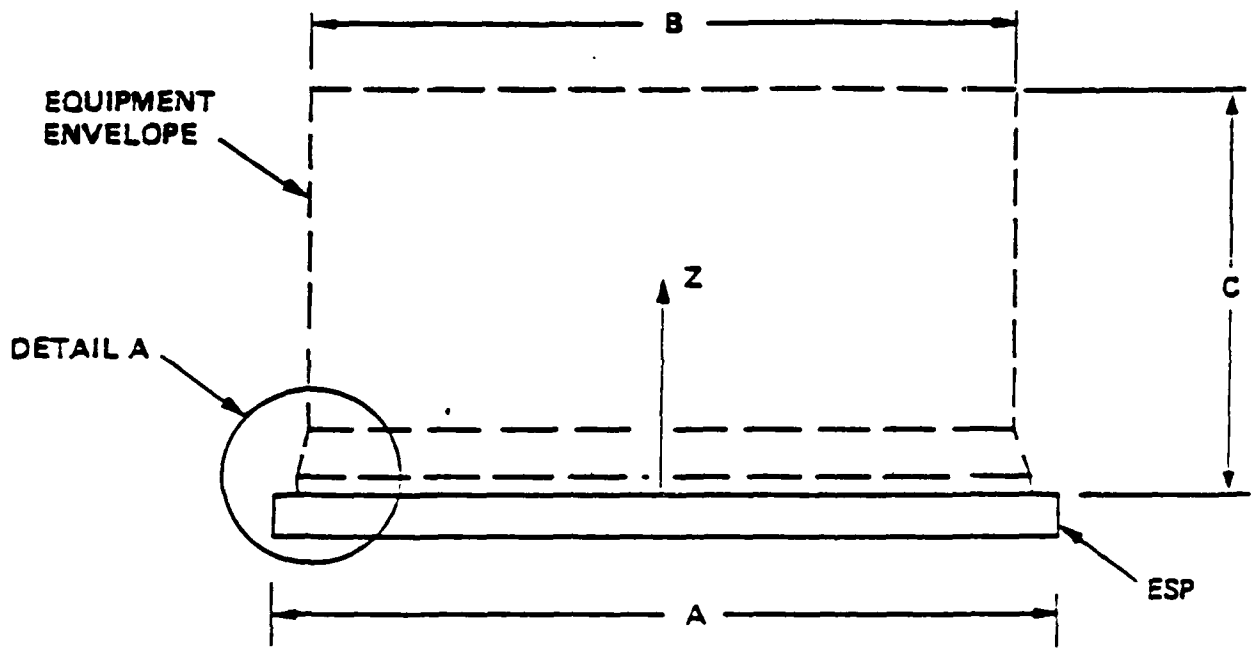


Figure 4.6-12 Mechanical detail of SPAS Equipment Support Plate



A	B	C
690 mm	620 mm	ENVELOPE HEIGHT DEPENDENT ON ORBITER DYNAMIC ENVELOPE, FIELD-OF-VIEW AND CARRIER LIGHT RESTRICTIONS
820 mm	760 mm	

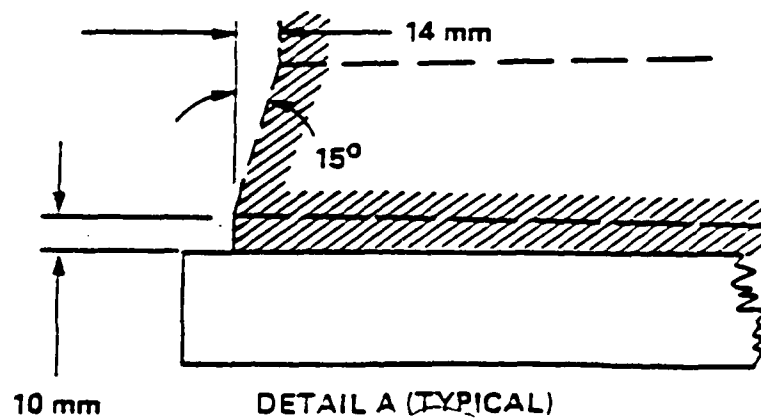


Figure 4.6-13 Equipment envelope for ESP mount

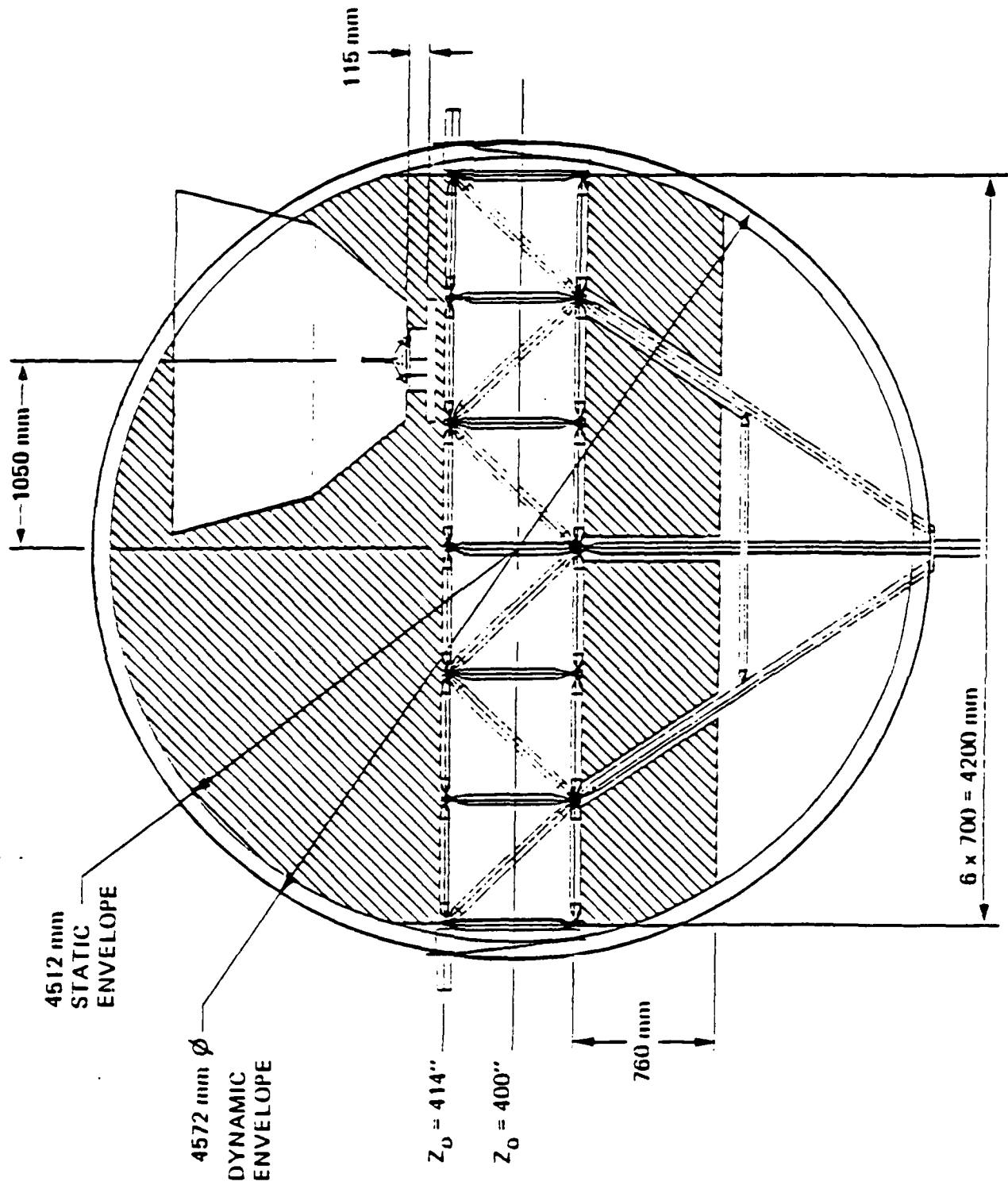
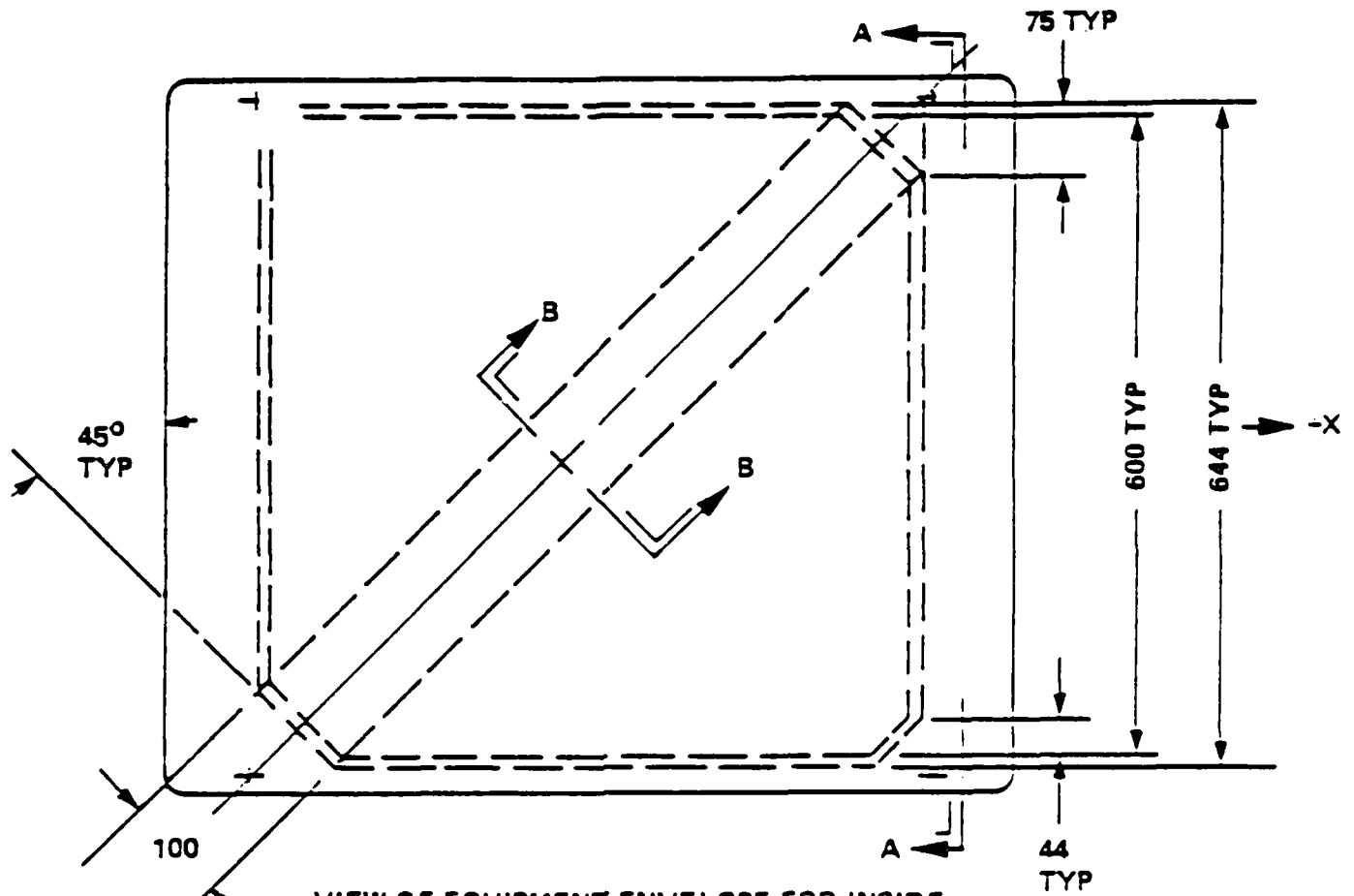
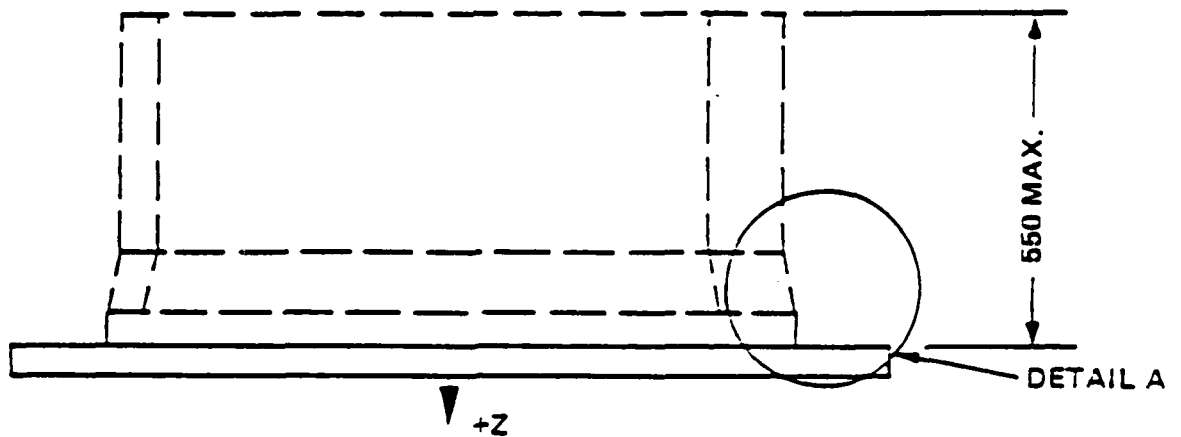


Figure 4.6-14 Equipment envelope for SPAS while stowed in cargo bay



a. VIEW OF EQUIPMENT ENVELOPE FOR INSIDE FACE OF ESP FOR PLANES 7, 9, 11, 20, 22, 24
OPPOSITE HAND FOR PLANES 8, 10, 12, 19, 21, 23



b. VIEW ON A-A

ALL DIMENSIONS IN mm

Figure 4.6-15 Equipment envelope for inside face of ESP

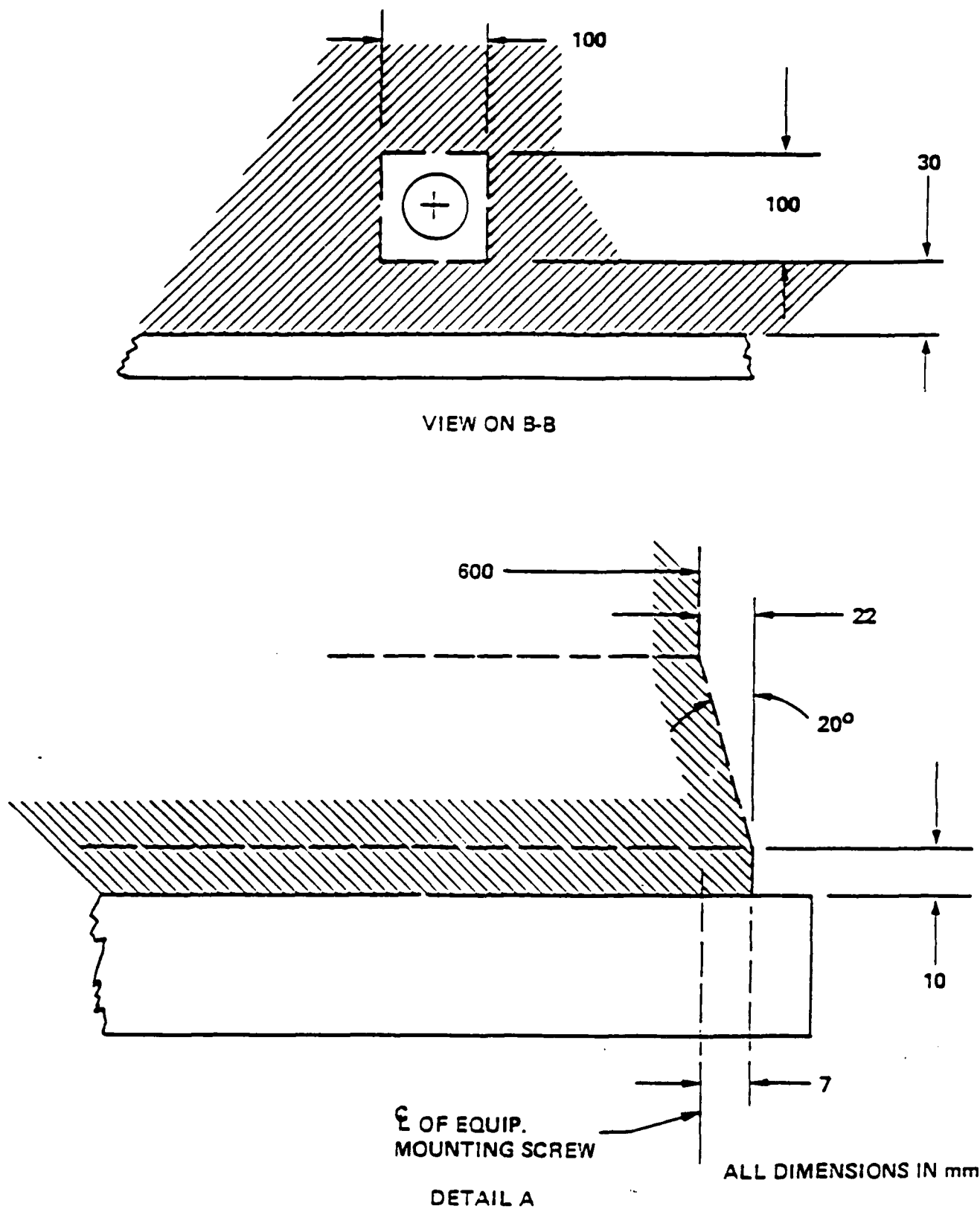


Figure 4.6-16 Equipment envelope for inside face of ESP

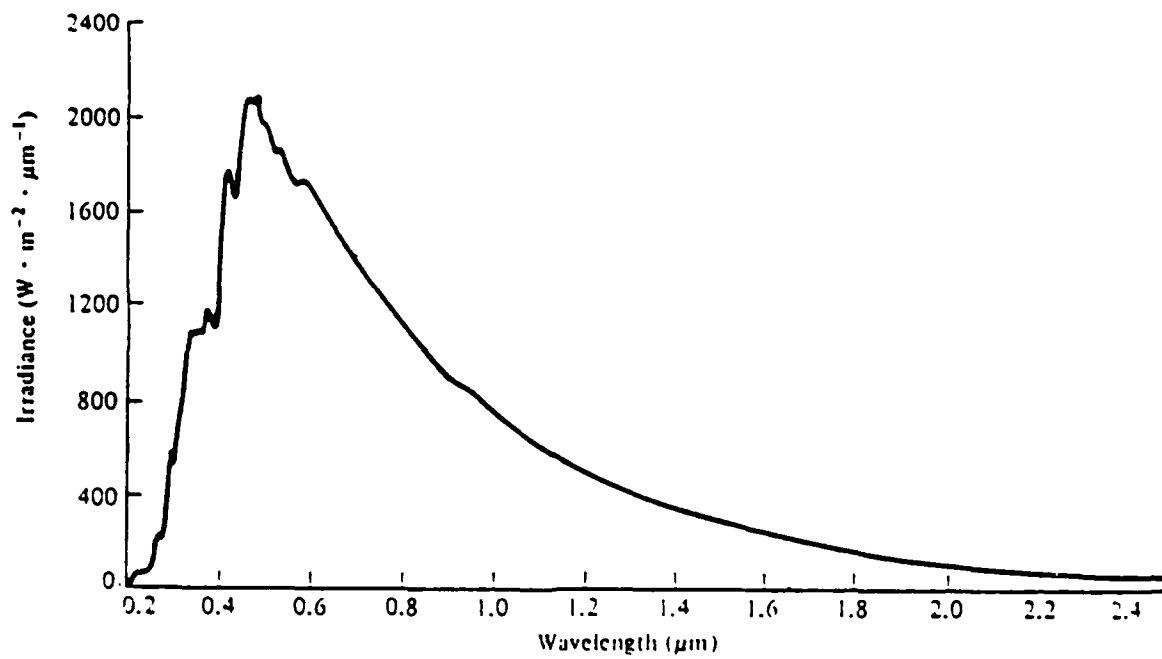


Figure 4.6-17 Solar spectral irradiance curve

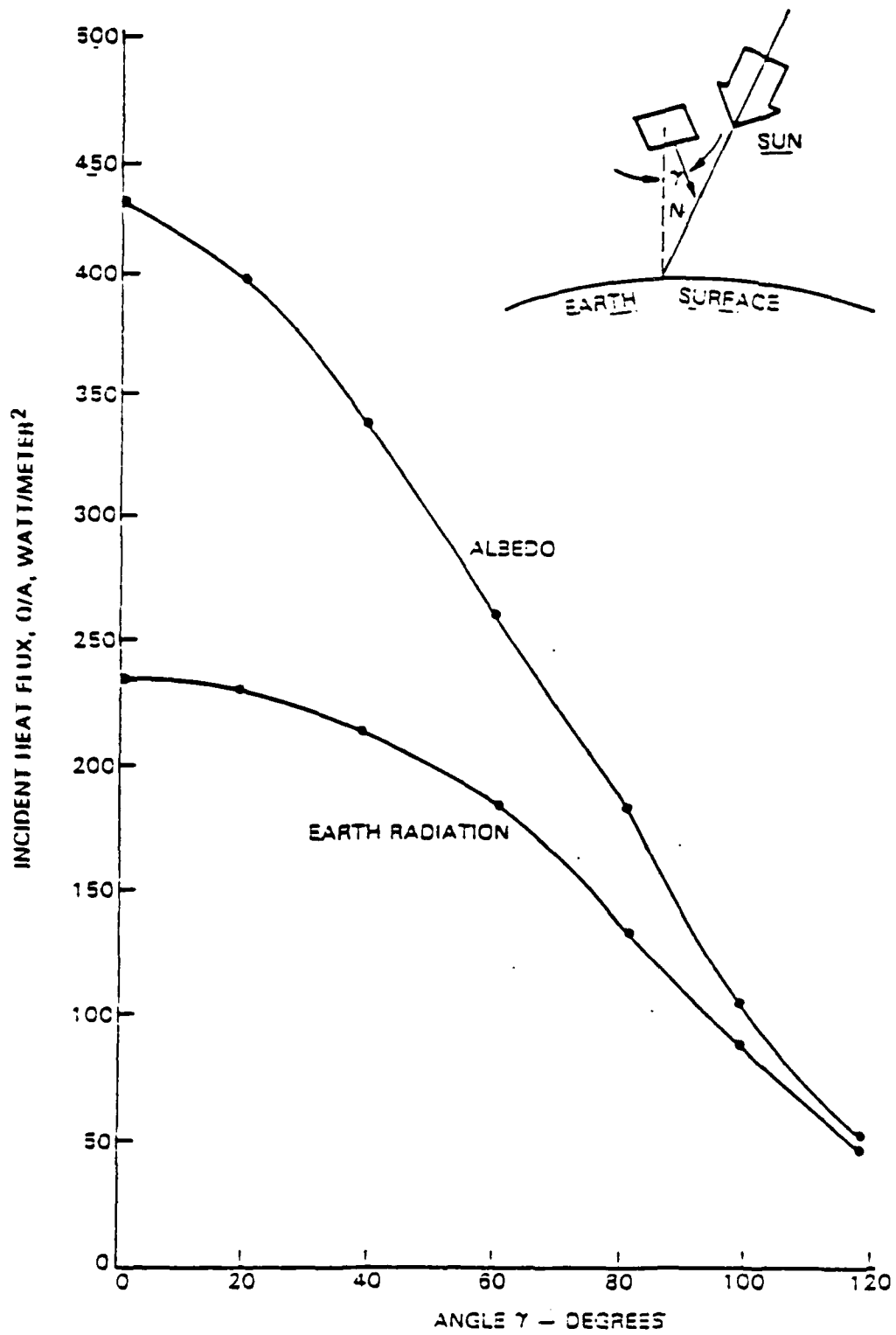


Figure 4.6-18 Earth emission and reflection heating of payload

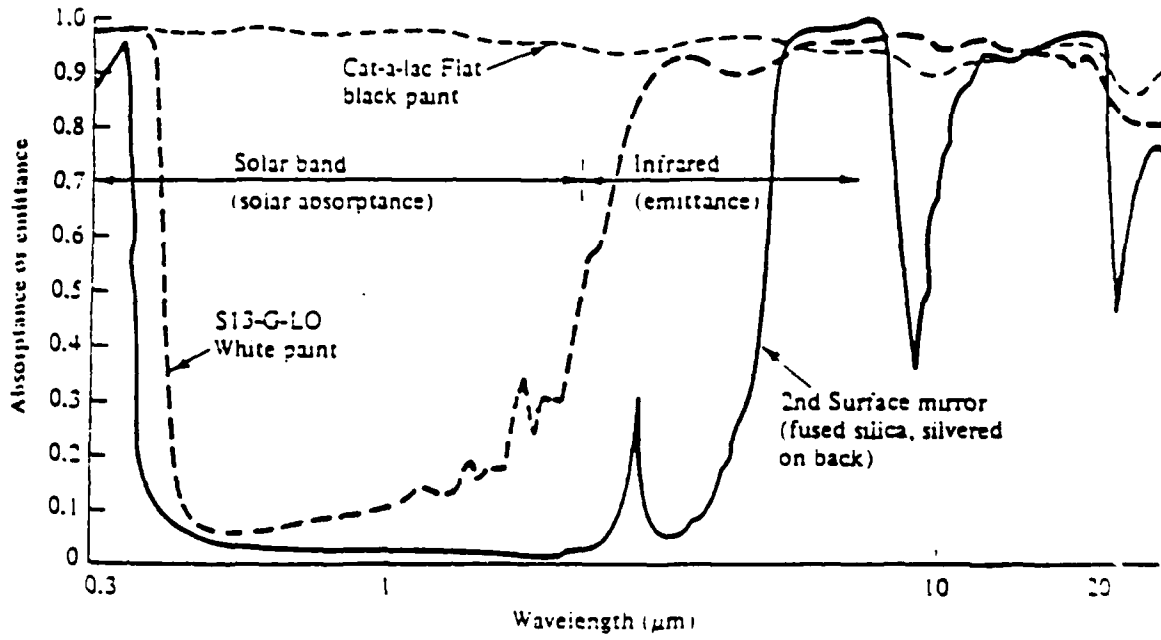


Figure 4.6-19 Emittance of selected surface coatings as a function of wavelength

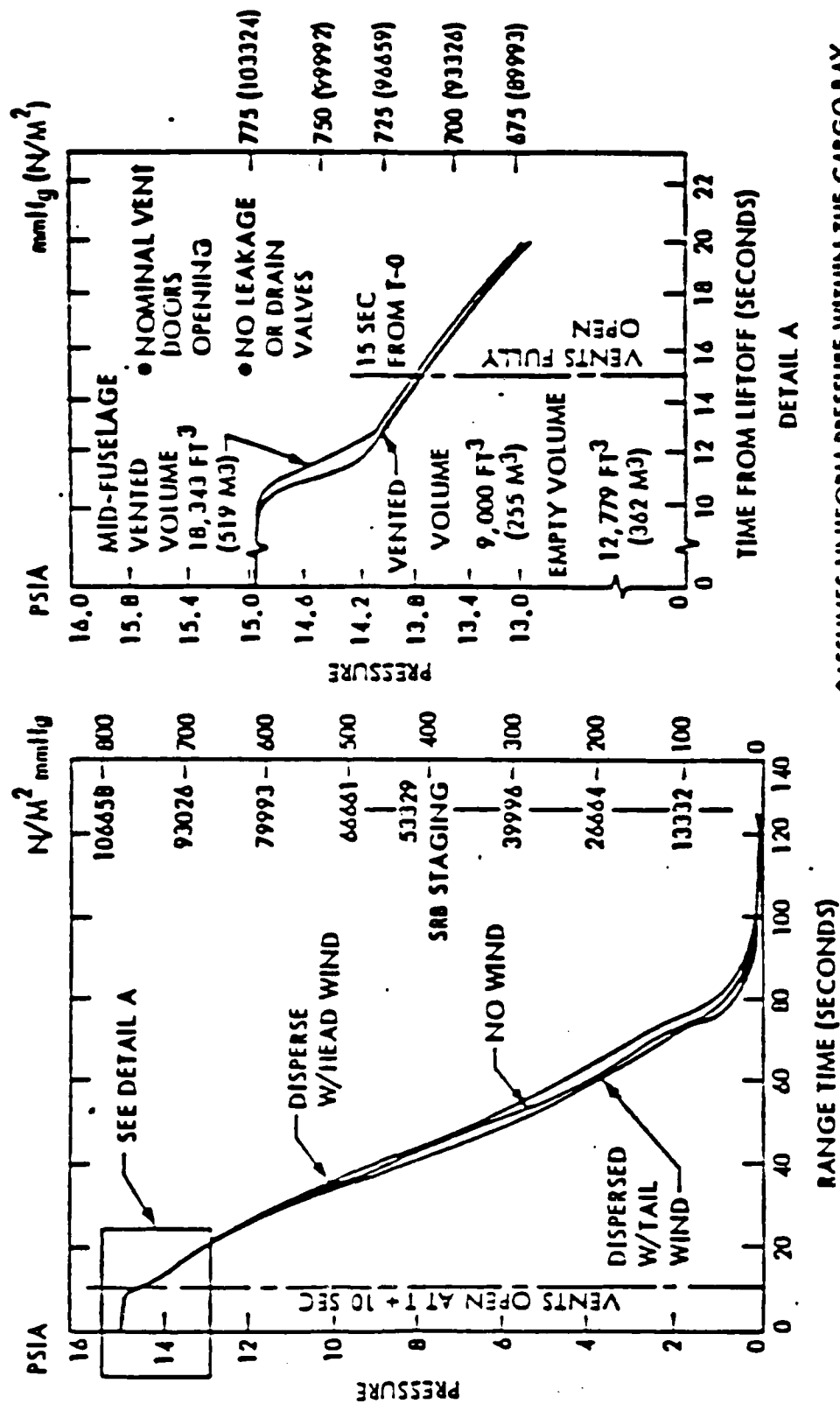


Figure 4.6-20 Cargo bay pressure change vs time after shuttle lift-off

• ASSUMES UNIFORM PRESSURE WITHIN THE CARGO BAY

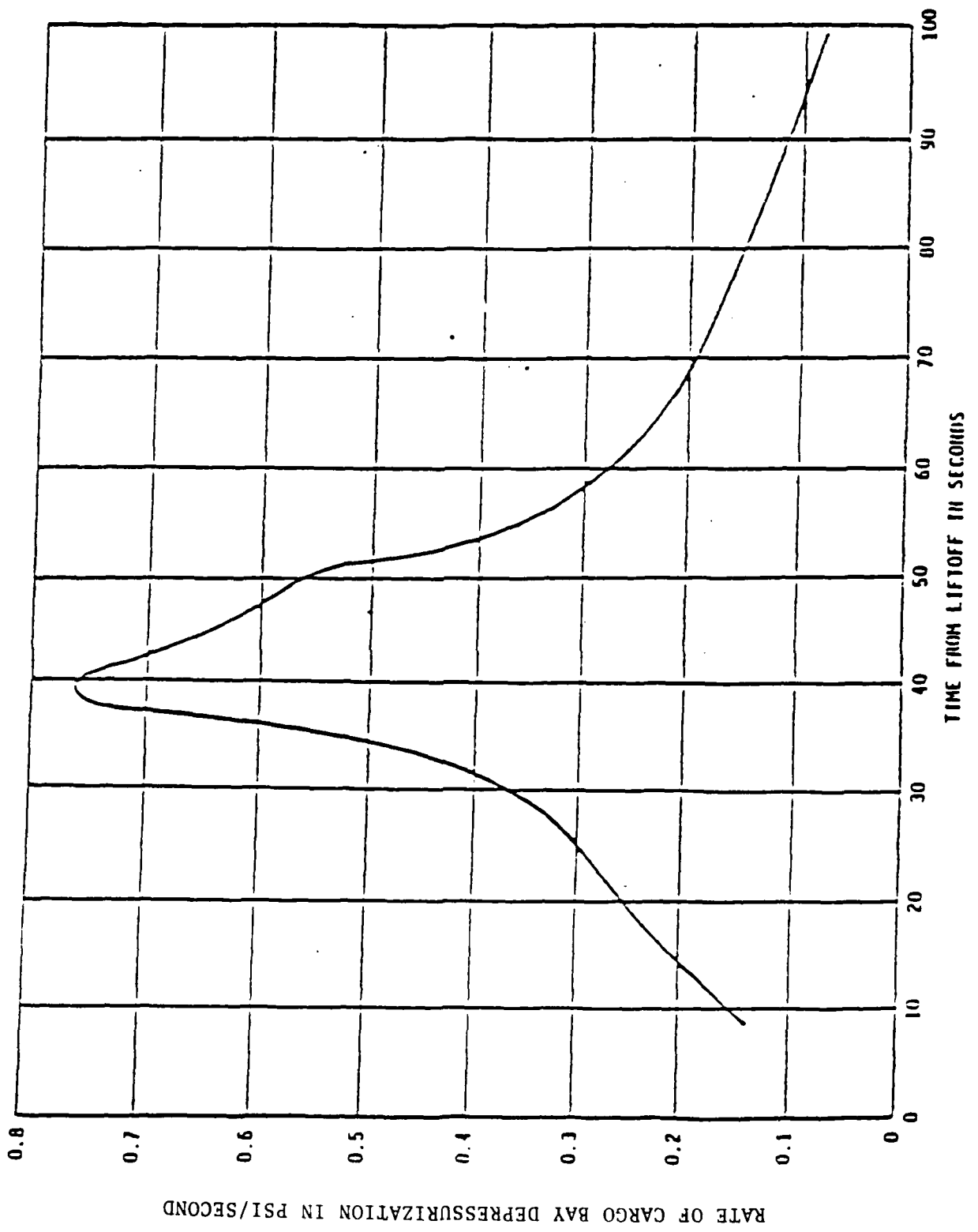


Figure 4.6-21 Maximum cargo bay pressure decay rate during ascent

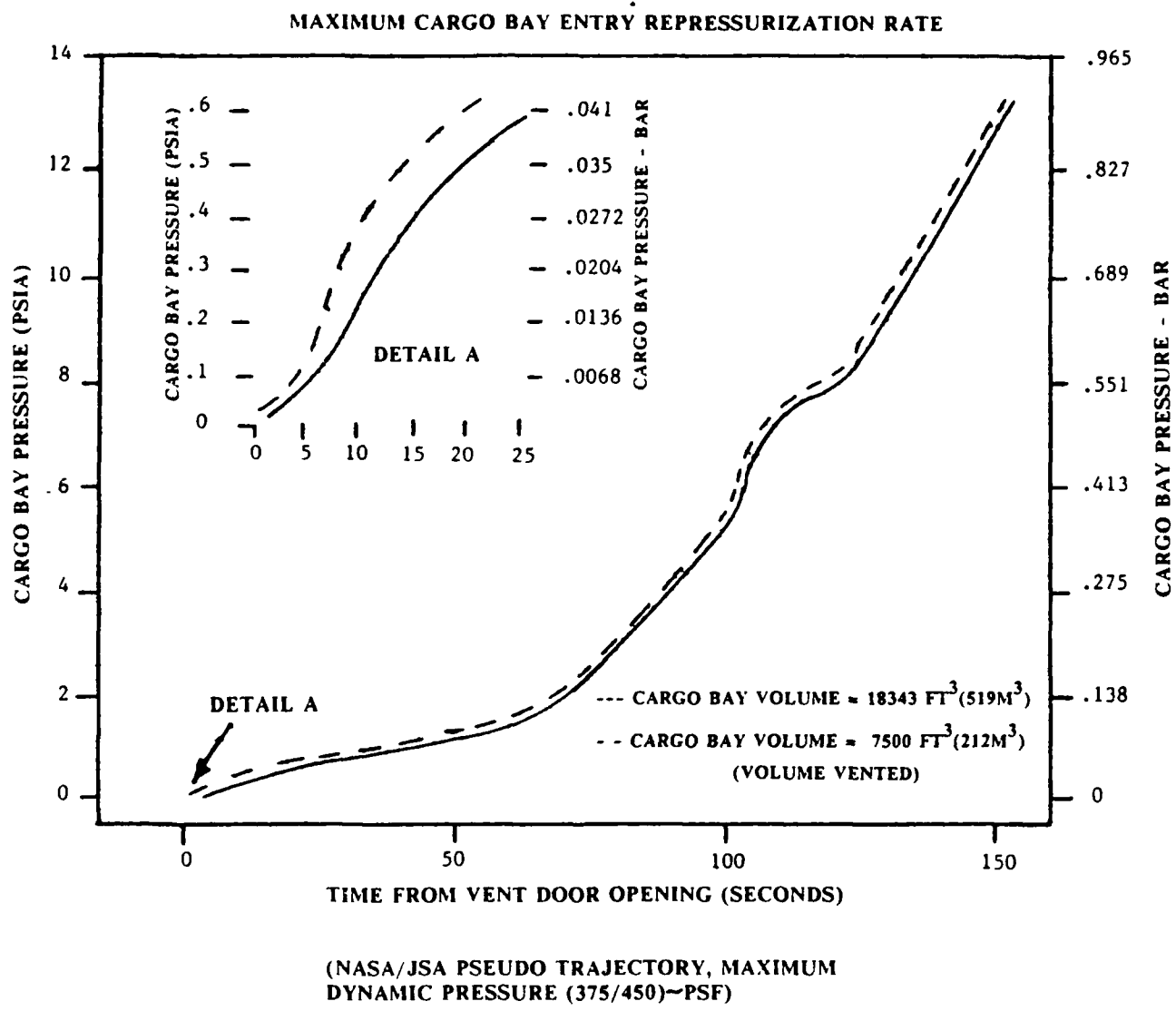


Figure 4.6-22 Cargo bay repressurization during reentry after vent door opens

All Axes

Frequency (Hz)	Design/Qual/Protoflight Level	Flight Acceptance Level
5-13.6	20 mm DA	13.3 mm DA
13.6-35	7.5 g ₀ -pk	5.0 g ₀ -pk
35-80	1.5 g ₀ -pk	1.0 g ₀ -pk

Duration: Design/Qual - Sweep up and down at 2 octaves/minute
Protoflight/FA - Sweep up and down at 6 octaves/minute

Figure 4.6-23 Sinusoidal vibration design and test requirements (SPAS)

20 Hz @ 0.00142 g²/Hz
20-150 Hz @ +6 dB/oct
150-400 Hz @ 0.08 g²/Hz
400-2000 Hz @ -3 dB/oct
2000 Hz @ 0.0011 g²/Hz

Composite = 6.5 g(rms)

Test Duration = 60 seconds each axis

**Figure 4.6-24 Random vibration certification levels
(a) HH-G payloads**

Subsystems/Assemblies Mounted on the Carrier

A. Perpendicular to Plane of Equipment Support Panel

Equipment on support panel loaded by up to 20 kg

Frequency (Hz)	Design/Qual/Protoflight Level	Flight Acceptance Level
20-50	0.025 G ² /Hz	0.010 G ₂ /Hz
50-120	+12 dB/oct	-12 dB/oct
120-360	2.0 G ² /Hz	0.80 G ² /Hz
360-2000	-9 dB/oct	-9 dB/oct
	grms = 29.6	grms = 18.7

Equipment on support panel loaded by between 20 kg and 40 kg

Frequency (Hz)	Design/Qual/Protoflight Level	Flight Acceptance Level
20-45	0.025 G ² /Hz	0.010 G ² /Hz
45-120	+12 dB/oct	+12 dB/oct
120-360	1.3 G ² /Hz	0.52 G ² /Hz
360-2000	-9 dB/oct	-9 dB/oct
	grms = 23.9	grms = 15.1

Equipment on support panel loaded by more than 40 kg

Frequency (Hz)	Design/Qual/Protoflight Level	Flight Acceptance Level
20-40	0.025 G ² /Hz	0.010 G ² /Hz
40-120	+12 dB/oct	-12 dB/oct
120-360	0.74 G ² /Hz	0.30 G ² /Hz
360-2000	-9 dB/oct	-9 dB/oct
	grms = 18.0	grms = 11.4

Duration: Design/Qual: 3 minutes/axis
FA/Protoflight: 1 minute/axis

B. Parallel to Plane of Equipment Support Panel

Frequency (Hz)	Design/Qual/Protoflight Level	Flight Acceptance Level
20-95	0.025 G ² /Hz	0.01 G ² /Hz
95-150	+9 dB/oct	-9 dB/oct
150-600	0.10 G ² /Hz	0.04 G ² /Hz
600-2000	-9 dB/oct	-9 dB/oct
	grms = 8.8	grms = 5.6

Duration: Design/Qual: 3 minutes/axis
FA/Protoflight: 1 minute/axis

Figure 4.6-24 Random vibration certification levels
(b) SPAS payloads

Recommended Payload Acoustic Flight Levels
 (based on empty STS Cargo Bay)
 December 1982

Sound Pressure Level
 (dB re. 20 μ N/m²)

Center Frequency (Hz) 1/3 Octave	Flight 1/3 Octave	Test 1/3 Octave
25	119	122
32	122	125
40	125	128
50	127.5	130.5
63	129.5	131.5
80	129	132
100	129	132
125	129	132
160	129	132
200	129	132
250	129	132
315	129	132
400	127.5	130.5
500	125.5	128.5
630	124	127
800	122	125
1000	120	123
1250	118.5	121.5
1600	116.5	119.5
2000	115	118
2500	113	116
3150	111.5	114.5
4000	109.5	112.5
5000	108	111
6300	106	109
8000	104.5	107.5
10000	103	106
Overall	139.5	142.5
Min. Duration		30 seconds

Figure 4.6-25 Payload acoustic level testing (cargo bay during liftoff)
(a) HH-G payloads

System, Subsystem, Assembly Acoustic Requirement

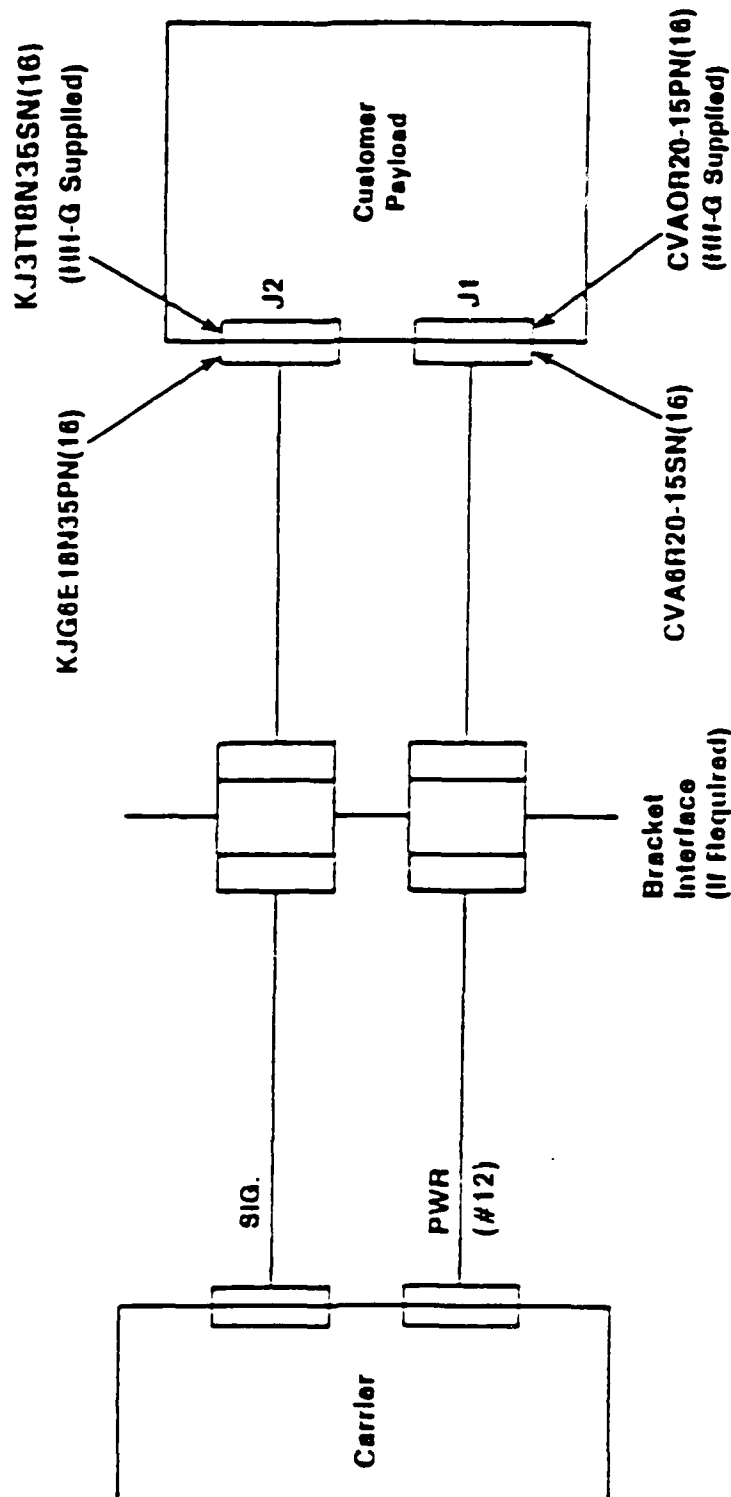
Center Frequency Hz	Design/Qual/ Protoflight Level 1/3 octave band SPL dB	Flight Acceptance Level 1/3 octave band SPL dB
31.5	126.0	122.0
40	128.0	124.0
50	129.5	125.5
63	131.0	127.0
80	132.0	128.0
100	132.5	128.5
125	133.0	129.0
160	133.0	129.0
200	132.5	128.5
250	131.0	127.0
315	130.0	126.0
400	129.0	125.0
500	127.0	123.0
630	125.5	121.5
800	124.0	120.0
1K	121.5	117.5
1.25K	120.0	116.0
1.6K	118.0	114.0
2K	116.0	112.0
2.5K	114.0	110.0
3.15K	112.5	108.5
4K	111.0	107.0
Overall	142.3	138.3

Duration: Qual/Design: 3 minutes;
Protoflight/FA: 1 minute

SBL dB Ref: 20 microNewtons per M²

**Figure 4.6-25 Payload acoustic level testing (cargo bay during liftoff)
(b) SPAS payloads**

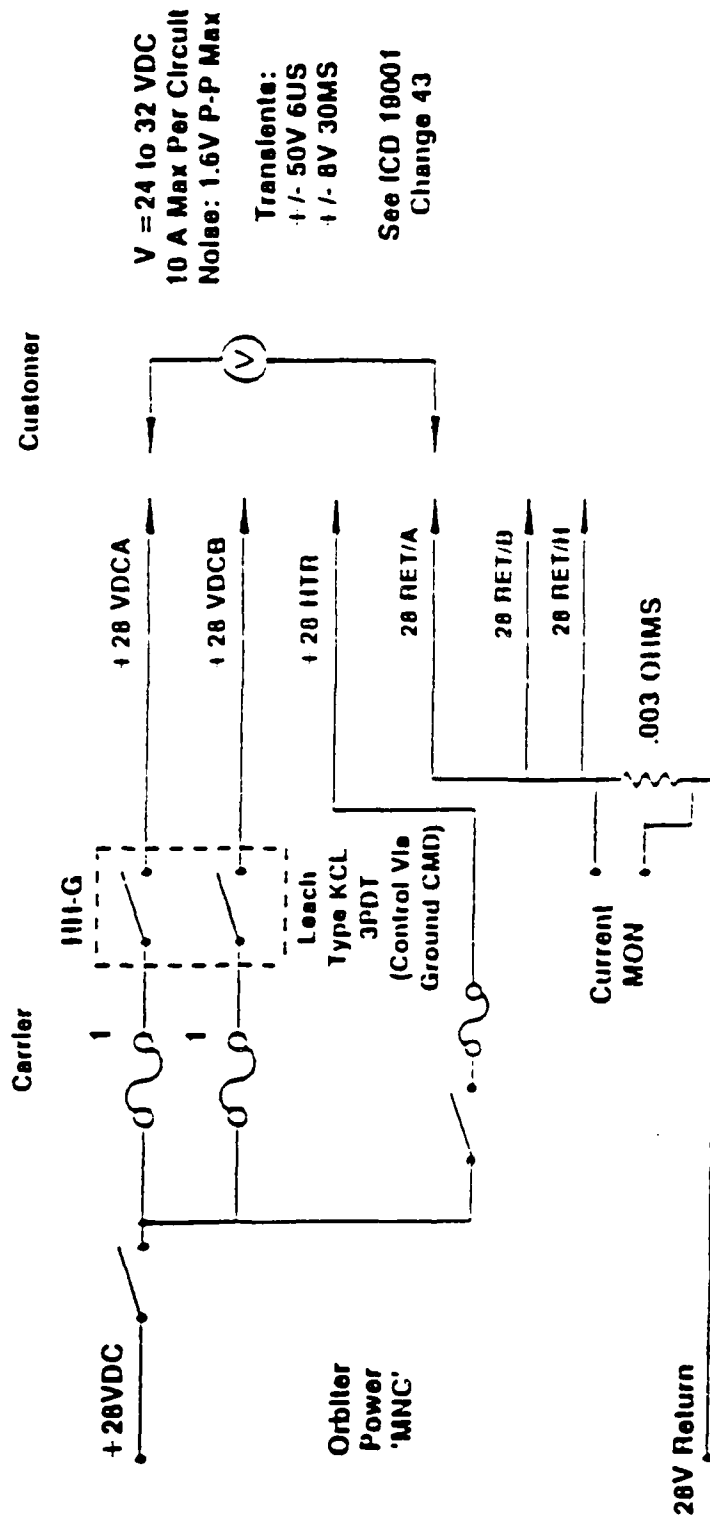
HH-G Standard Interface Cables (Plate Mounted Customer)



**Semi-Rigid Convolute Tube Shielding
Provides External RF Shield and
Mechanical Protection on Power and
Signal Cables**

Figure 4.6-26 Standard interface cabling on HH-G plate mount

Customer Power Interface



- 1 Fuse, 20A, Rated 10A Max for #12 Service Only (Plate)
- Fuse, 15A, Rated 10A Max for #16 Service Only (Gas Can)
- 2 Fuse, 4A Rated 2A Max

Figure 4.6-27 Interface between shuttle power and HH-G payload

HH-G Main Switches

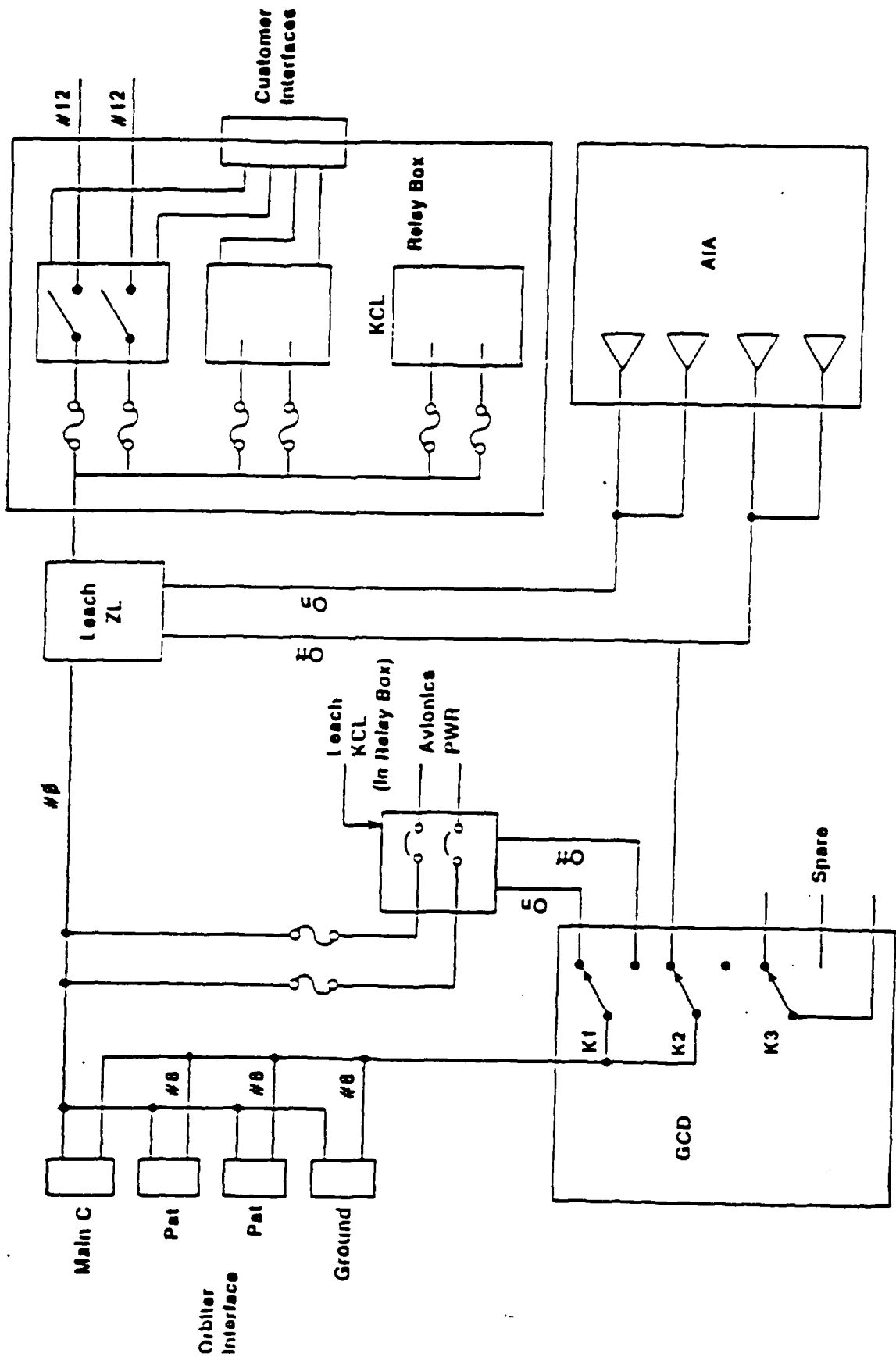


Figure 4.6-28 Schematic of actual payload power interface to HH-G payload

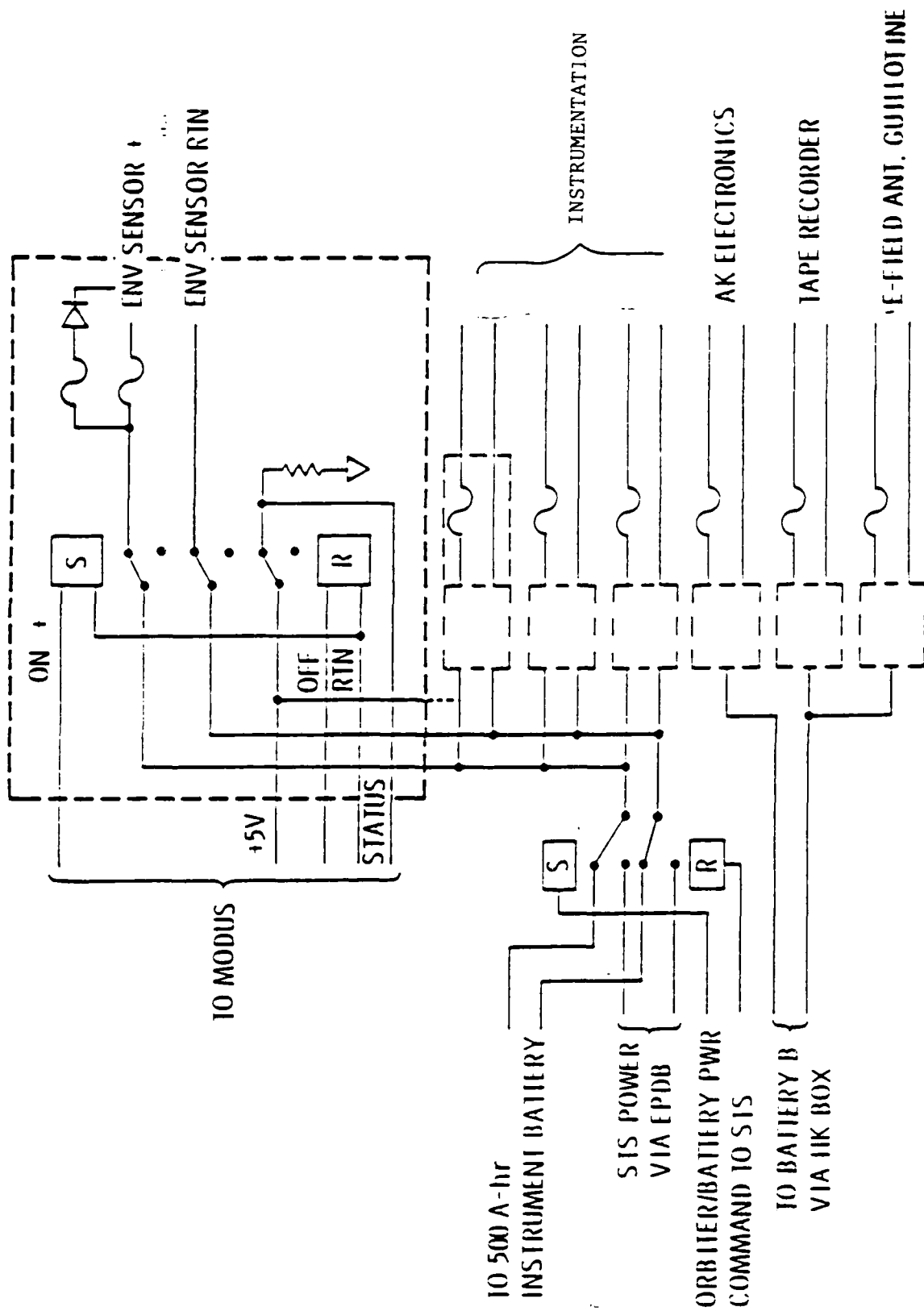


Figure 4.6-29 SPAS power distribution system for experiments

ID	PIN	TYPE	FUNCTION
POMAO	1	A	POM ANALOG DATA
POMINDX	21	A	POM INDEX PULSE
SIGGND	2	A	SIGNAL GROUND
POMCLK	42	A	POM BIT RATE CLOCK
POMENA	32	A	SERIAL DIGITAL ENABLE A
POMENB	33	A	SERIAL DIGITAL ENABLE B
POMDATA	3	A	SERIAL DIGITAL DATA A
POMDATB	4	A	SERIAL DIGITAL DATA B
THER1	14	A	THERMISTOR 1
THER2	15	A	THERMISTOR 2
THER3	16	A	THERMISTOR 3
SHIELD	6	A	SHIELD FOR COMMAND AND DATA SIGNALS
RD-	21	A	RECEIVE DATA ASYNC - FROM SPOC
RD-	22	A	RECEIVE DATA ASYNC - FROM SPOC
SD+	23	A	SEND DATA ASYNC - TO SPOC
SD-	24	A	SEND DATA ASYNC - TO SPOC
BLCMD1	17	A	BILEVEL/PULSE COMMAND 1
BLCMD2	18	A	BILEVEL/PULSE COMMAND 2
BLCMD3	19	A	BILEVEL/PULSE COMMAND 3
BLCMD4	20	A	BILEVEL/PULSE COMMAND 4
SCHCLK	10	A	SERIAL COMMAND CLOCK
SCHENV	11	A	SERIAL COMMAND ENVELOPE
SCHDAT	12	A	SERIAL COMMAND DATA
METMIN	40	A	MET/MET ONE MINUTE PULSE
IRIGMET+	30	A	IRIG-B MET (MET) -
IRIGMET-	31	A	IRIG-B MET (MET) -
FRMGND	49	A	FRAME GROUND
KUMRCLK-	34	A	CUSTOMER GENERATED MR CLOCK -
KUMRCLK-	35	A	MR CLOCK -
KUMRDAT-	43	A	CUSTOMER GENERATED MR DATA -
KUMRDAT-	44	A	MR DATA -
KUMRSHLD	25	A	SHILD FOR KU SIGNALS
UNOTSP1-	61	A	UNDED TSP 1 -
UNOTSP1-	66	A	UNDED TSP 1 -
UNOTSP1	54	A	SHIELD FOR UNOTSP1
UNOTSP2-	62	A	UNDED TSP 2 -
UNOTSP2-	63	A	UNDED TSP 2 -
UNOTSP2	55	A	SHIELD FOR UNOTSP2
UNOTSP3-	56	A	UNDED TSP 3 -
UNOTSP3-	57	A	UNDED TSP 3 -
UNOTSP3	46	A	SHIELD FOR UNOTSP3
UN04	58	A	UNDED 4
UN05	59	A	UNDED 5
UN06	50	A	UNDED 6
UN07	54	A	UNDED 7
UN08	55	A	UNDED 8
UN09	53	A	SHIELD FOR UNDED 4-8
MOAOC	52	A	RESERVED
MOASTP	51	A	RESERVED

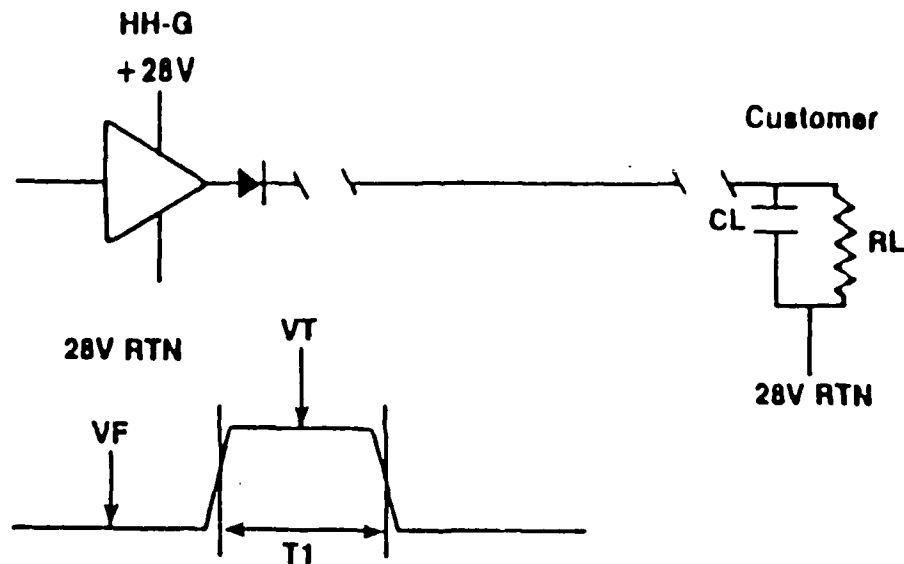
NOTE 1: POWER RETURN PINS B, D AND F MAY BE CONNECTED TOGETHER WITHIN PAYLOAD WIRE TYPE DESIGNATIONS:

A 22 GA
 B 16 GA
 C 12 GA

NOTE 2: CUSTOMER WILL MAKE NO CONNECTIONS TO UNUSED PINS

Figure 4.6-30 Pinout of J2 signal cable connecting HH-G payload to shuttle

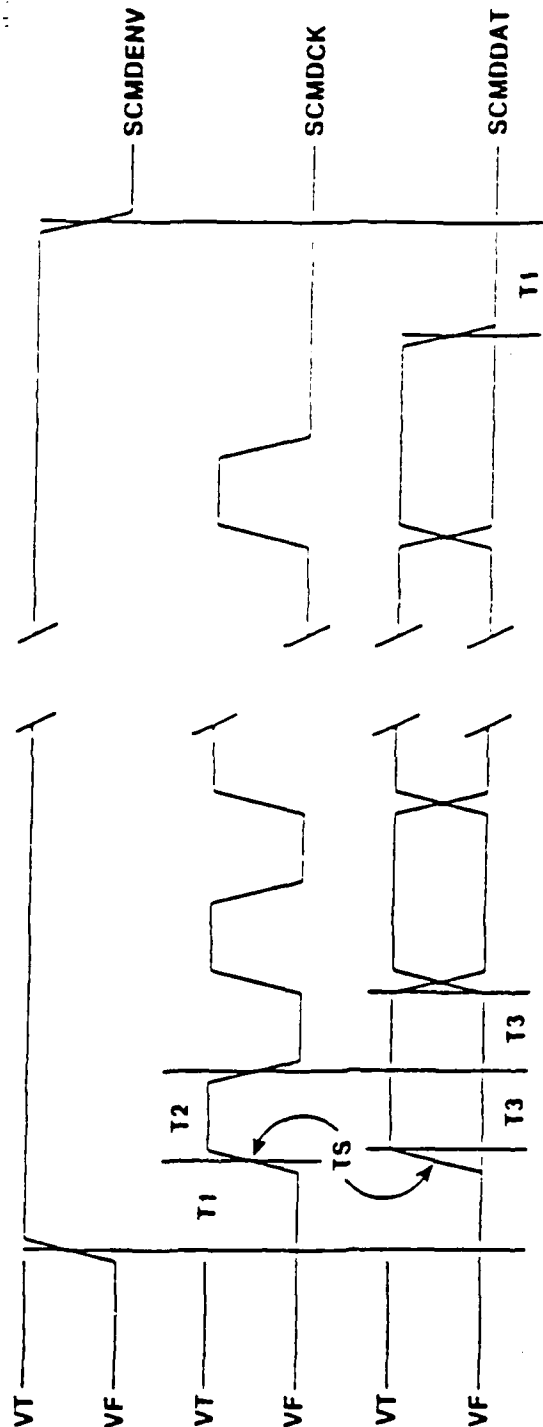
Customer Bi-Level Command Interface



- RL = 3.2K OHMS Min. (Customer Power On or Off)
- RL = 10K Ohms Max, (Source 10 MA Max; Sink 0)
- CL = 1500 PF Max,
- VT = 28 +/- 7V
- VF = 1.5 +/- 1.5V
- VNOISE = 1.6 V P-P (Max)
- TR = TF = 10 Microsec (Min)
- TR = TF = 100 Microsec (Max)
- T1 = 50 +/- 30MS (Pulse Mode)

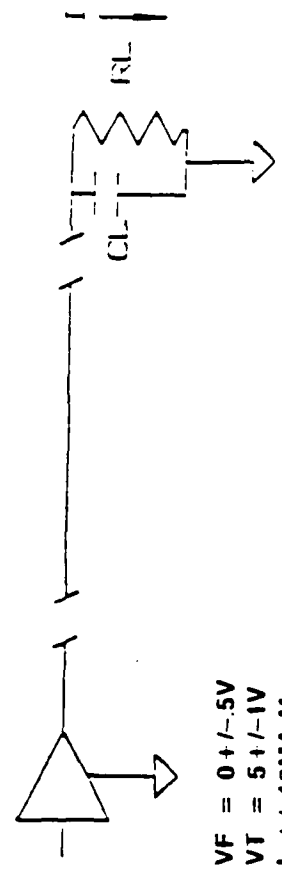
Figure 4.6-31 Bi-level command interface specifications

Customer Serial Command Interface



- TS = Setup Time From Data to Clock = 33 +/- 5 Microsec
- T1 = 8MS Min
- T2 = .5MS Min
- T2 = 15MS Max
- T3 = .5MS Min
- TH = 1 Microsec Min
- TH = 50 Microsec Max
- TF = Same as TH
- CL = 1500 PF Max
- RL = 600 OHMS Min (Payload Power On or Off)
- RL = 4K OHMS Max (Open Input Shall Read As False)

Customer



SPOC

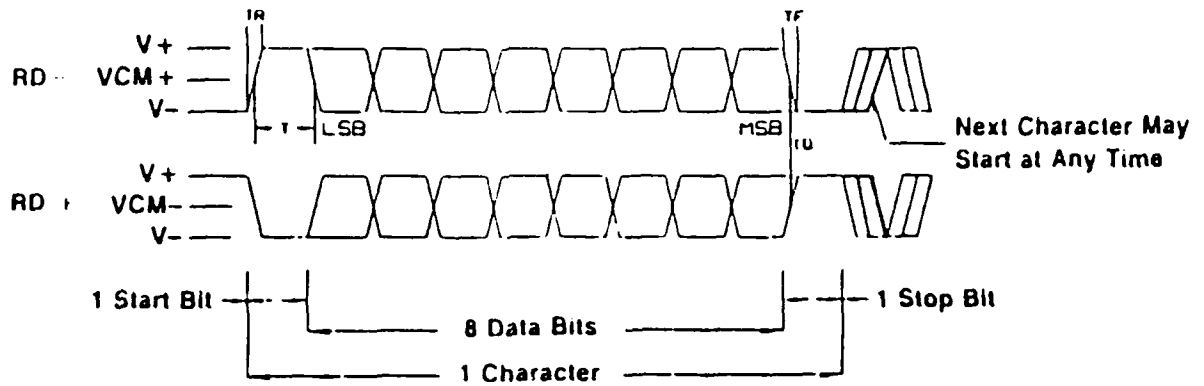
- VF = 0 +/- .5V
- VT = 5 +/- .1V
- I +/- 10MA Max

Figure 4.6-32 Serial command interface electrical characteristics and timing

PARAMETER	DIMENSION		CHARACTERISTICS CARRIER/PAYLOAD INTERFACE	NOTES
Type			Single-Ended	
False ("0")	min	volt	-0.5 (1)	
	max	volt	-0.5 (1)	
True ("1")	min	volt	+4.0 (1)	(1)
	max	volt	+6.0	
Ripple & Noise	max	Milli- volt	400	
Rise/Fall Time (10 to 90%)	min	Microsec	1 (2)	
	max	Microsec	30 (1)	
Bit Rate			bps 100 - 1050	
Transfer			Direct Coupled	Grounded at Carrier
Source Impedance (Carrier)	min	ohm	30	
	max	ohm	100	
Load Imped- ance (Payload)	min	ohm	600	
	max	ohm	4K	(3)
Capaci- tance	max	Pico- Farad	3500	Payload not to Exceed 1500
Pwr Off Impedance	min	ohm	10K (+6 VDC)	Payload shall exceed 600 w/pwr off
Current Drive			Milliamp 10 (Logic "1")	
Current Sink			Milliamp -10 (Logic "0")	= 0.5 volts
Overvoltage Protection	Max	volt	+32	
Fault Voltage Emission	Max	volt	+15	
Fault Current Limitation	Max	Milliamp	+20	
Power-Ground Isolation			Megohms 10	
(1) Reference Signal Ground				
(2) 400 ohm $\pm 5\%$ in parallel with 5 nanofarad $\pm 0\%$ load				
(3) An open input shall not result in an ambiguous logic state				
(4) 0.2 millisecond state uncertainty maximum following power up				

Figure 4.6-33 Additional electrical detail on serial interface characteristics

Customer Asynchronous RD Interface



$T = 1/1200 \text{ sec.}$

$VCM + 1V <= V+ <= VCM + 2.5V$

$VCM - 1V <= V- >= VCM - 2.5V$

$-3V <= VCM +/- <= +3V \text{ WRT SIG. GND.}$

For Both Lines

$TR = TF = .5\mu S$

Slew Rate = 40V/ μS Max

Character Rate = 120 C/S Max, 100 C/S Nom

TD = Differential Time Delay = 10NS Max

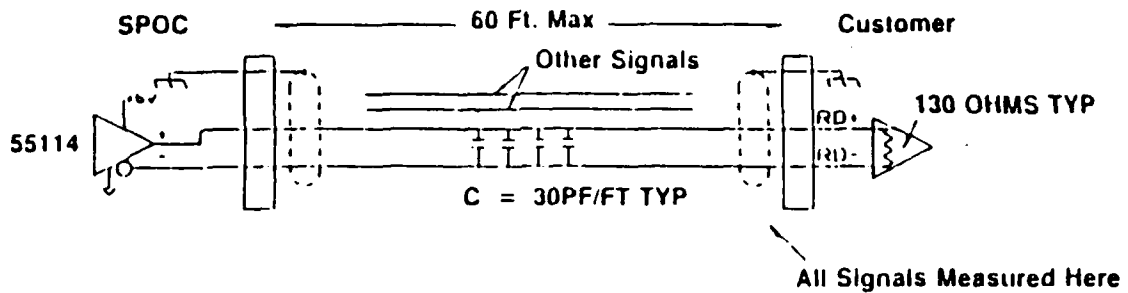
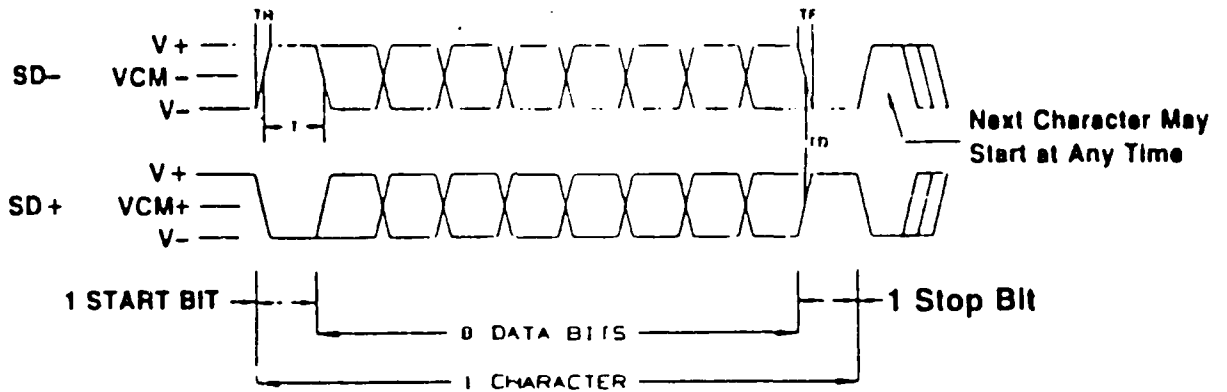


Figure 4.6-34 RD serial link electrical and timing specifications

Customer Asynchronous SD Interface



$VCM + 1V <= V+ <= VCM + 2.5V$
 $VCM - 1V <= V- >= VCM - 2.5V$
 $-3V <= VCM +/- <= +3V$ WRT SIG. GND. } For Both Lines
 $T = .8333$ MS (1200 Baud)
 $VCM+ = VCM- (+/-50MV)$
 $TR = TF = 1\mu S$ Max Input Z = 130 OHMS +/-10%
 $TD =$ Differential Time Delay = 5NS Max

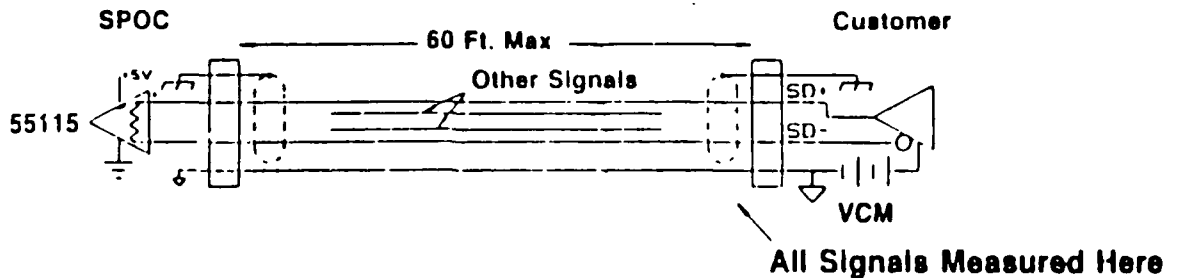
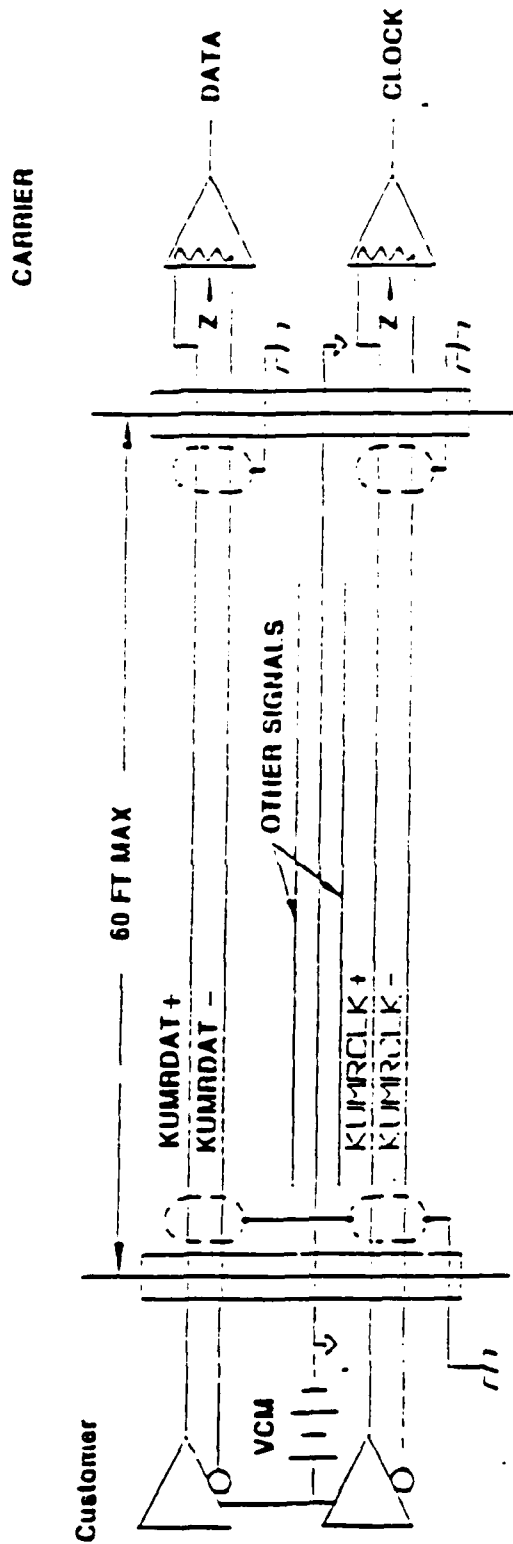


Figure 4.6-35 SD serial link electrical and timing specifications

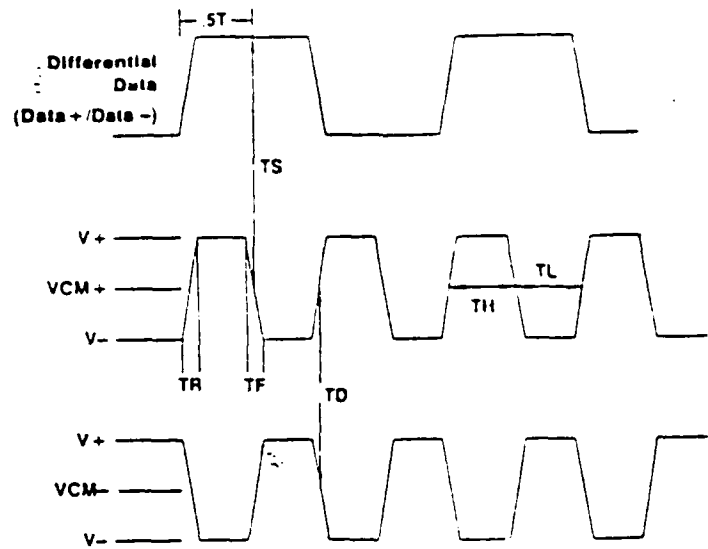
Medium Rate Customer Interface



Z = 70 OHMS MIN. 150 OHMS MAX.

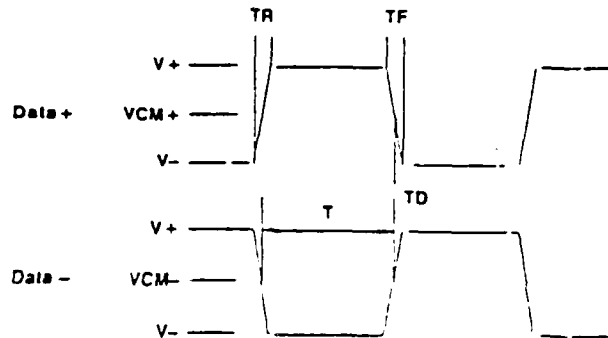
Figure 4.6-36 Electrical interface for KU-band medium data rate link

Medium Rate Customer Clock



Required: $V_{CM+} = V_{CM-} \pm 50\text{mV}$, Then $V_{CM+} = V_{CM-} = V_{CM}$
 Required: $3\text{V} < V_{CM+} < 3\text{V}$ For Clock + and Clock - Lines
 $V_{CM+} + .8\text{ Volts} < V < V_{CM+} + 1.25\text{ Volts}$
 $V_{CM-} - .8\text{ Volts} > V > V_{CM-} - 1.25\text{ Volts}$
 Baud Rate = $1/T$
 $T = T_H + T_L = \text{Baud Period}$ $T_H/T_L = 1 \pm .15$
 $T_D = \text{Differential Delay} = .05T < 20\text{ NS}$
 $T_S = \text{Clock Skew} = \pm .15T$ Max from Middle of Data Bit
 $T_R = T_F < .1T < 1\mu\text{S}$ Measured Between 10% and 90% Amplitude
 Baud Rate Stability $\pm .1\%$ or Better

Medium Rate Customer Data

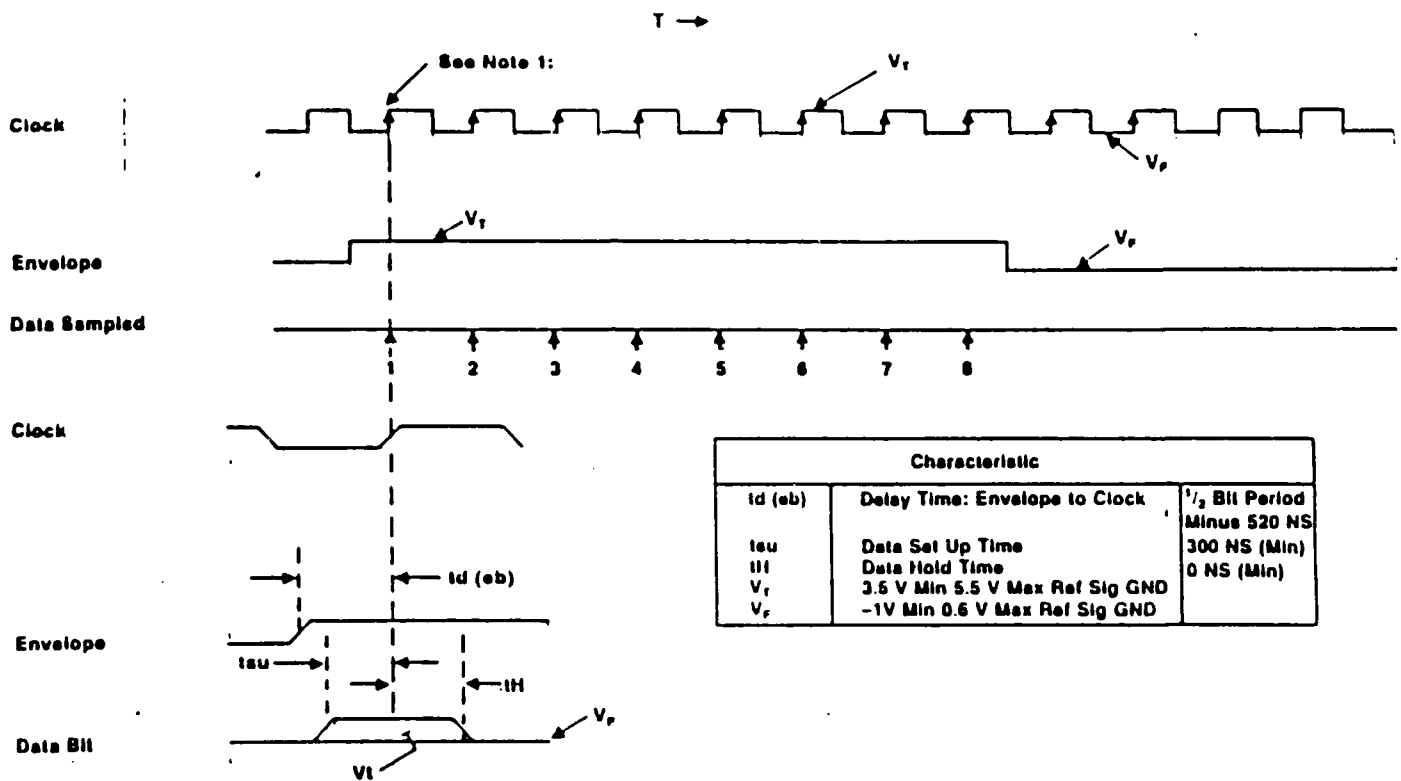


Required: $V_{CM+} = V_{CM-} \pm 50\text{mV}$, Then $V_{CM+} = V_{CM-} = V_{CM}$
 Required: $V_{CM+} + .8\text{ Volts} < V < V_{CM+} + 1.25\text{ Volts}$ For Data +
 Required: $V_{CM-} - .8\text{ Volts} < V < V_{CM-} - 1.25\text{ Volts}$ and Data - Lines
 Required: $-3\text{V} < V = V_{CM} \pm < +3\text{V}$ With Respect To Sig. GND
 $T_R \leq T_F \leq 1\mu\text{S}$

$T = \text{Baud Period} = 1/\text{Baud Rate}$ Baud Rate = $1/T$
 $T = \text{Differential Time Delay} = 10\text{ MS Max}$
 Baud Rate Stability $\pm 0.1\%$

Figure 4.6-37 Data and clock signal timing for medium data rate link

PCM Digital Interface Waveforms



Notes:

- 1) Data Bits
On the Leading Edge of Clock as Shown. Bit 1 (First Bit Out) Should Be Most Significant Bit.

Figure 4.6-38 Digital timing of high speed PCM interface

Customer PCM Data Interfaces

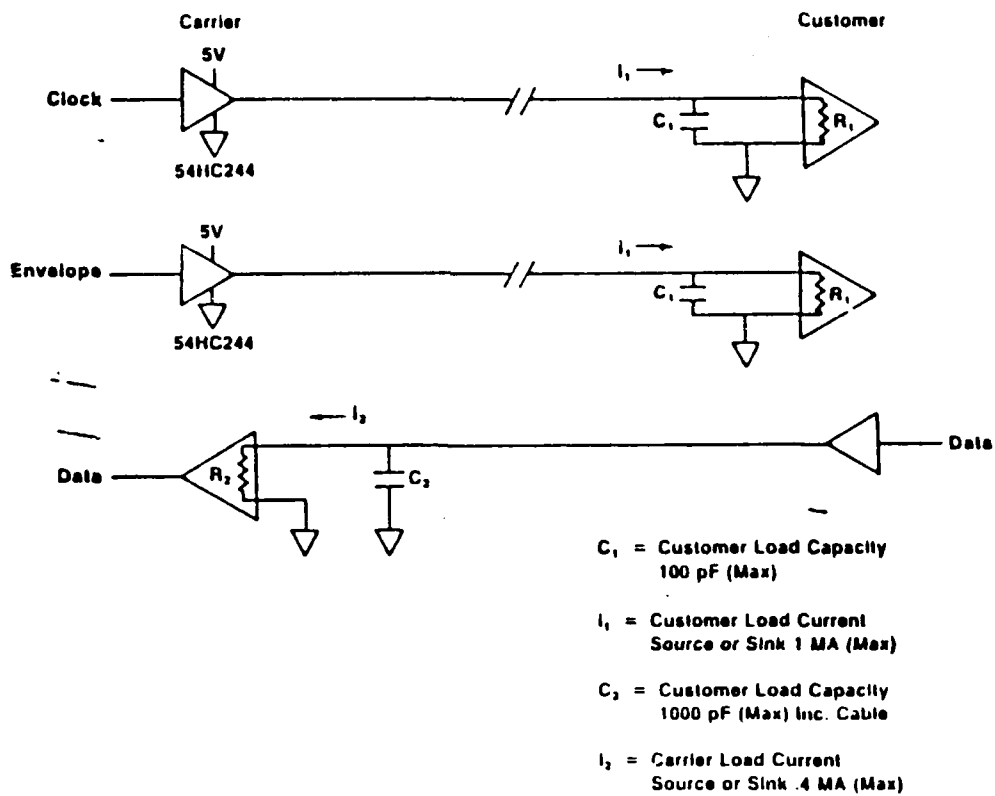


Figure 4.6-39 Electrical details of PCM high speed interface

Customer Interfaces for Time

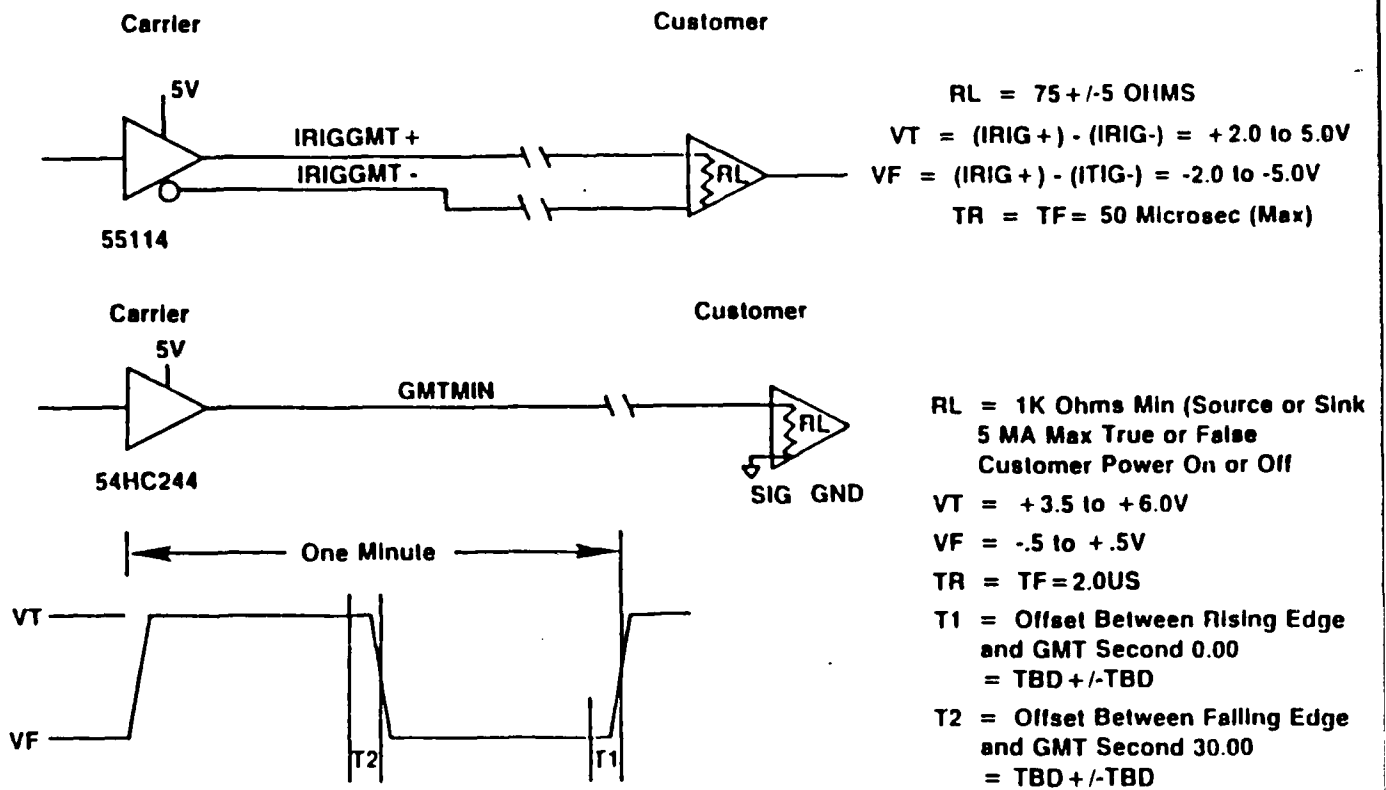


Figure 4.6-40 Electrical characteristics of IRIG-B MET signal provided to payload

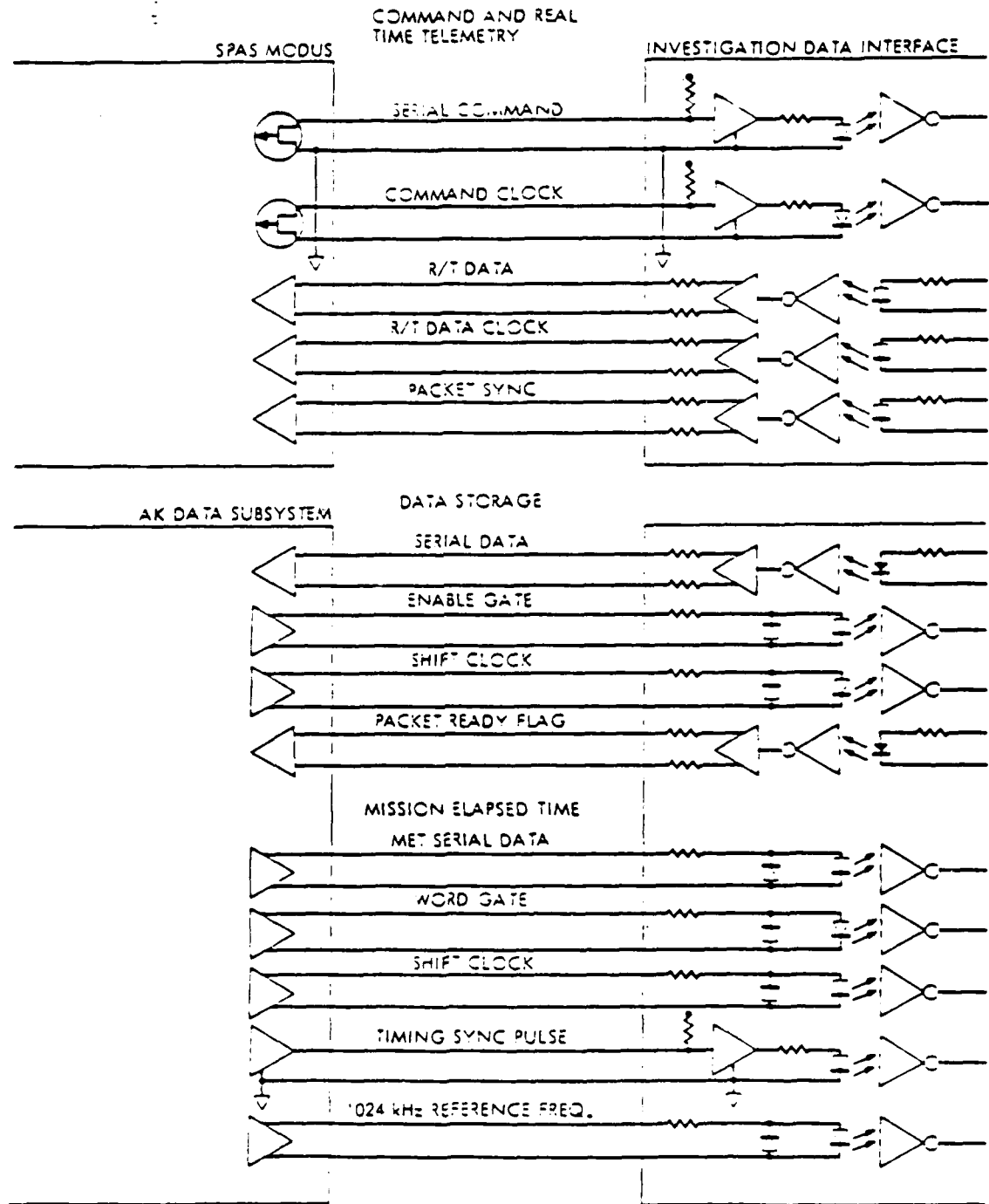
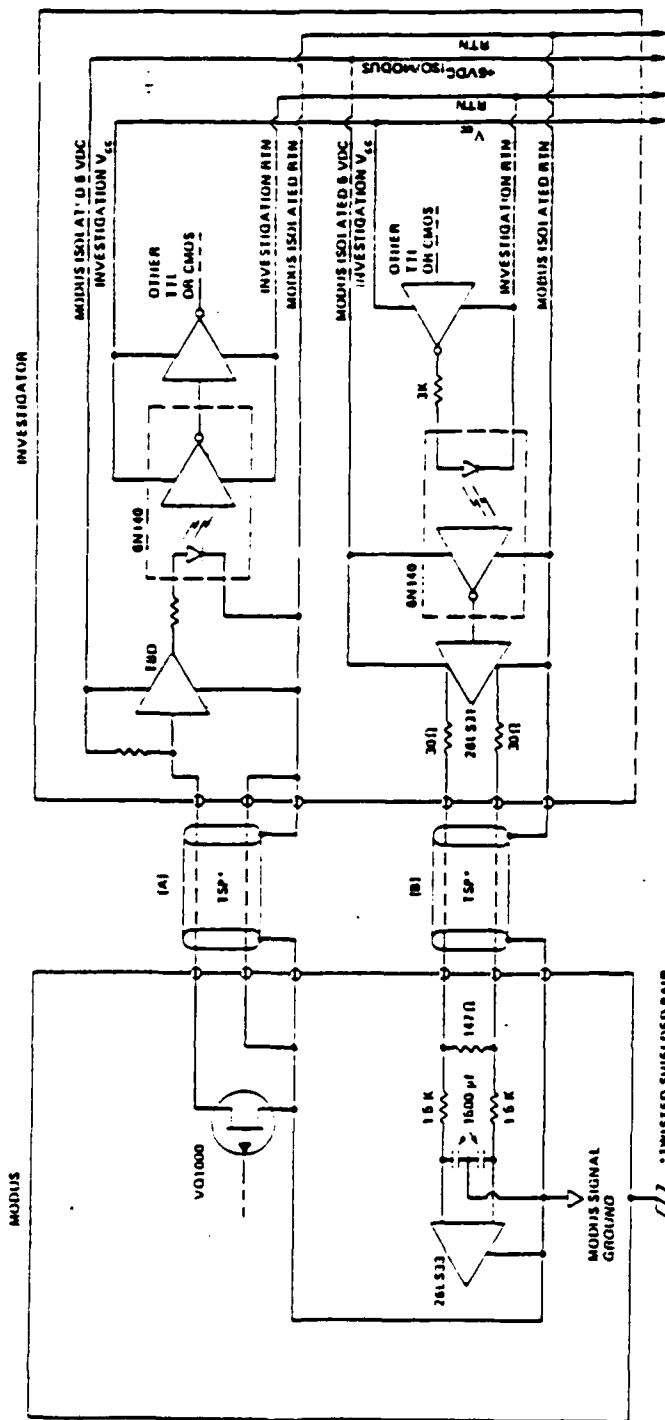


Figure 4.6-41 Command, timing, and interface lines provided in SPAS Data Handling Subsystem (DHS)



Electrical Interface Circuit Diagrams (1 of 4)

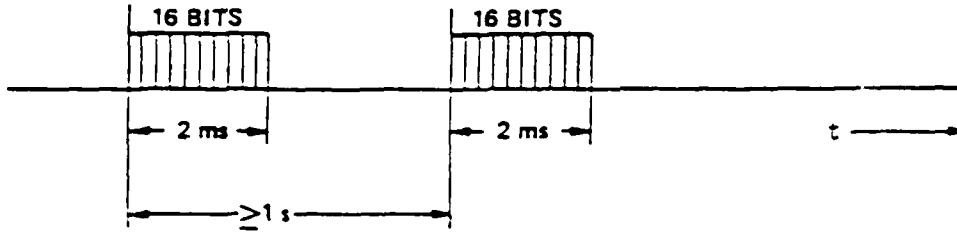
- (A) Modbus → Investigation Single-Ended
- (B) Modbus ← Investigation Differential

Figure 4.6-42 Electrical interface on SPAS payload for each experiment

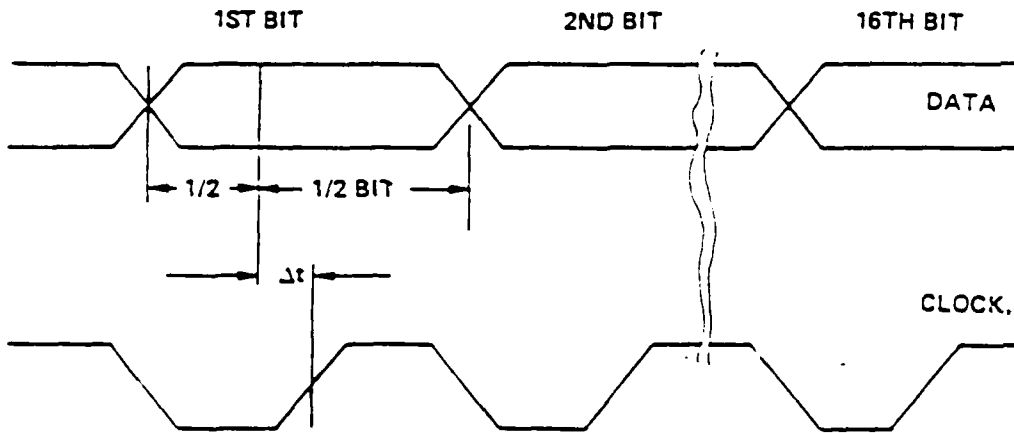
	<u>Interface</u>	<u>Characteristics</u>
A.	Serial Digital Command	Single-ended
	1. code	NRZ-L
	logic 1 level	high
	logic 0 level	low
	data	MSB first, 16 bit word
	2. bit rate	8 Kbps
B.	Command Clock	Single-ended
	1. waveform	(word gate · square wave)
	2. frequency	8 KHz ± TBD
	3. word rate	max. 1 Hz

Figure 4.6-43 Signal characteristics of serial interface on SPAS payload

A. WORD SEQUENCE



B. TIMING: IMPS DHS CHANGES DATA ON NEGATIVE GOING EDGE OF CLOCK, DATA ARE VALID ON THE USER'S SIDE ON POSITIVE EDGE OF CLOCK.



TIME SKEW $|\Delta t| \leq 10 \text{ us}$

t_p, t_f DEPENDENT ON USER LOAD

Figure 4.6-44 Timing of serial interface signals on SPAS serial interface

Characteristics	CLASS A Program	CLASS B Program	CLASS C Program	CLASS D Program
Mission priority or national prestige	Highest	High	Medium to high	Medium to low
Allowed program risk	Lowest feasible	Low	Medium	Medium to high
Management systems imposed in the SOM	Military standards imposed in the SOM	Military standards imposed in the SOM	Reduced compliance to military standards	Only contractor internal management systems
Reviews of contractor	Monthly (formal)	Every two months (formal)	Every three months	Very limited
Program schedule	May take four or more years to launch	May take three or more years to launch	May take two or more years to launch	May take one or more years to launch
Hardware complexity	High, usually involving two or more different experiments	High, often involving two or more different experiments	Low to medium complexity; usually only a single experiment	Low complexity; usually only a single experiment
flight-type vehicles needed for single flight	Two; one for flight, one for qualification tests	Single unit for flight	Single unit for flight	Single unit for flight
flight-type components to support first vehicle	Usually six of each type; (includes two spares and redundancy)	Usually three of each type; (includes one spare and redundancy)	Usually two of each type; (includes one spare)	Usually two of each type; May only be one of each
Contingency plan if there is a hard flight failure	Fly qual. unit with flight spares, or rely on a parallel effort	Repeat program using flight spare, or rely on a parallel effort	Retrieve, repair, then refly; or rely on a parallel effort	Retrieve then refly; or rely on a parallel effort, or repeat program
Acquisition cost	Highest	High	Medium	Lowest

Figure 5.1-1 Comparison of program characteristics of space programs of each payload class

Statement of work items	CLASS A Program	CLASS B Program	CLASS C Program	CLASS D Program
Safety program	MIL-STD-1574 (formal)	MIL-STD-1574 (formal)	MIL-STD-1574 (formal)	MIL-STD-1574
Orbiter safety	NHB 1700.7 (NASA)	NHB 1700.7 (NASA)	NHB 1700.7 (NASA)	NHB 1700.7 (NASA)
Reliability program	MIL-STD-1543 (formal)	MIL-STD-1543	MIL-STD-1543	MIL-STD-1543 (guide)
Reliability analyses	To place part level	To single point failure	To component level	To subsystem level
Failure mode effects and criticality analyses	To place part level MIL-STD-1543	To place part level MIL-STD-1543	To component level MIL-STD-1543 (guide)	To subsystem level MIL-STD-1543 (guide)
Justify single point fail	Required (MIL-STD-1543)	Required (MIL-STD-1543)	For critical items	Not required
Electromagnetic compatibility	MIL-STD-1541 and for STS JSC 07700 Vol. XIV			
Human engineering	MIL-STD-1472 (guide)	MIL-STD-1472 (guide)	MIL-STD-1472 (guide)	MIL-STD-1472 (guide)
Configuration control	DOD-STD-480; MIL-STD-483	DOD-STD-480; MIL-STD-483	DOD-STD-480; MIL-STD-483	Not required
Model survey	Required	Required	Required	Not required
Loads analyses	Iterative analysis (three cycles)	Iterative analysis (three cycles)	Iterative analysis (two cycles)	For safety only
Dynamic loads analyses	Transient events	Transient events	Transient events	As required
Structural test model	Required or use qual.	Use flight item	Use flight item	Use flight item
Computer structural model	Required (software)	Required (software)	Required (software)	For safety only
Computer thermal model	Required (software)	Required (software)	Required (software)	Not required
Thermal verification of computer model	Thermal vacuum test	Thermal vacuum test	Thermal test or thermal vacuum test	Not required
Manufacturing plan	Formal	Informal	Informal	Not required
Program schedule	Formal	Formal	Informal	Informal
Work breakdown structure	MIL-STD-883	MIL-STD-883	MIL-STD-883	Not required

Figure 5.1-2 Items that must be included in statement of work for design and building of payloads of each class

Review Items	CLASS A Program	CLASS B Program	CLASS C Program	CLASS D Program
Program reviews	MIL-STD-1521	MIL-STD-1521	MIL-STD-1521	Limited
Technical reviews	Monthly (formal)	Every two months (formal)	Every three months	Limited
Component level reviews	MIL-STD-1521	MIL-STD-1521	MIL-STD-1521	Limited
Prelim. design review	Required (formal)	Required for new designs	Informal for new designs	Not required
Critical design review	Required (formal)	Required for new designs	Informal for new designs	Not required
Qualification review	Required (formal)	Required for new designs	Informal for new designs	Not required
Component acceptance	Required (formal)	Included in qual. review	Included in qual. review	May be required
Vehicle level reviews	MIL-STD-1521	MIL-STD-1521	MIL-STD-1521	Limited
System design review	Required (formal)	Required (formal)	Not required	Required
Prelim. design review	Required (formal)	Required for new designs	Informal for new designs	Not required
Critical design review	Required (formal)	Required (formal)	Required (informal)	Not required
Phased software reviews	Required (formal)	Required (formal)	Required (informal)	Not required
Qualification reviews	Required (formal)	Required (protoflight)	Required for software	Required for software
Vehicle acceptance	Required (formal)	No. included in protofit	Required (formal)	Required (formal)
Phased safety reviews	Required	Required	Required	Required
Flight accreditation	Required (formal)	Required (formal)	Required (informal)	Not required
Independent readiness review	Required (formal); before acceptance test	Required (formal); before protoflight test	Required (informal); before acceptance test	Safety related
Mission readiness review	Required (formal)	Required (formal)	Required (formal)	Safety related
Flight readiness review	Required (formal)	Required (formal)	Required (formal)	Safety related

Figure 5.1-3 Comparison of review items included in the statement of work for payloads of each class

Characteristics	CLASS A	CLASS B	CLASS C	CLASS D
Mission priority or national prestige	Highest	High	Medium to high	Medium to low
Allowed risk	Lowest feasible	Low	Medium	Medium to high
Specification compliance	Through all tiers	Through all tiers	Through all tiers	Top level only
Flight-type vehicle or experiment	Two; one for flight, one for qualification tests	Single unit for flight	Single unit for flight	Single unit for flight
Acquisition cost	Highest	High	Medium	Lowest
Vehicle complexity	High, usually with two or more different experiments	High, often with two or more different experiments	Low to medium complexity; usually only a single experiment	Low complexity; usually only a single experiment
Typical launch time	Narrow launch windows	Narrow launch windows	Not critical	Not critical
Typical orbit	Free-flyer	Free-flyer	Attached to host vehicle	Attached to host vehicle
Typical on-orbit time	Years	Years	Months	Days
Experiments carried on vehicle	Usually several Class A, but may include Class B, Class C, and/or Class D	Usually several Class A or Class B, but may include Class C or D	Usually one or more Class C, but could include other classes	Usually one or more Class D, but could include other classes
Use of redundancy in vehicle	Used to assure critical functions, & independent failure of experiments	Used to assure critical functions, & independent failure of experiments	Usually a single string; redundancy used if safety critical	Usually a single string; redundancy used if safety critical
Probable failure mode of vehicle	Soft or only partial loss of data	Soft or only partial loss of data	Partial or total loss of data	Partial or total loss of data
Retrievability or in-orbit maintenance	Not usually possible	Not usually possible	Usually retrievable or maintainable in orbit	May or may not be retrievable
Experiment complexity	Usually complex, or with complex interfaces, or both	Usually complex, or with complex interfaces, or both	Usually low or medium complexity	Usually very simple, but can be of low or medium complexity
Use of redundancy in experiment	Redundancy used in all critical functions, where practical	Redundancy used in some critical functions, and where cost effective	Usually a single string; redundancy used if safety critical	Usually a single string; redundancy used if safety critical
Probable failure mode of experiment	Soft or only partial loss of data	Soft or only partial loss of data	Partial or total loss of data	Partial or total loss of data

Figure 5.1-4 Additional comparisons between space payload programs of each class

	CLASS A	CLASS B	CLASS C	CLASS D
Design Factors	Highest feasible	To meet mission life	To meet mission life	May be low
Mean time to fail (See 5.2)	Redundancy used in all critical functions, where practical	Redundancy used in some critical functions and where cost effective	Usually a single string; redundancy used if safety critical	Usually a single string; redundancy used if safety critical
Use of redundancy (See 5.2)	To be avoided if feasible	Avoided if critical or where cost effective	Avoided only if clearly cost effective	Acceptable
Single failure points (See 5.2)	At the piece part and higher levels of assembly	At the piece part and higher levels of assembly	At the component and higher levels of assembly	At the system level
Analyses of failures of flight items (See 5.2)	MIL-STD-1540 definition	MIL-STD 1540 definition	MIL-STD 1540 definition	MIL-STD-1540 definition
Operating environments (See 5.4)	10 deg C; 6 dB	5 deg C; 3 dB	0 deg C; 0 dB	0 deg C; 0 dB
Environ. design margins (See 5.4.4)	MIL-STD-1547	MIL-STD 1547	MIL-STD 1547 (guidance)	Contractor option
Part specifications (See 6.1)	Space quality	Space quality	Space quality	Contractor option
Materials (See 6.1)	MIL 1700.7 (NASA)	MIL 1700.7 (NASA)	MIL 1700.7 (NASA)	MIL 1700.7 (NASA)
Structures (See 6.2 and 6.12)	MIL 1700.7 (NASA)	MIL 1700.7 (NASA)	MIL 1700.7 (NASA)	MIL 1700.7 (NASA)
Pressure vessels (See 6.3 and 6.12)	DOD-A-83577	DOD A 83577	DOD A 83577 (guide)	DOD-A-83577 (guide)
Mechanical assemblies (See 6.4)	DOD E-83578	DOD E-83578	DOD E-83578 (guide)	DOD E-83578 (guide)
Explosive ordnance (See 6.5)	LOD-W-83575	DOD W 83575	DOD W 83575	DOD-W 83575 (guide)
Wiring (harnesses) (See 6.6)	DOD E-898	DOD E-898	DOD E-898 (guide)	DOD E-898 (guide)
Electronic components (See 6.7)	MIL S 83576	MIL S 83576	MIL S 83576 (guide)	MIL-S 83576 (guide)
Bolus arrays (See 6.8)	For lot traceability	For lot traceability	For lot traceability	If required for safety
Product marking (See 6.9)	MIL-STD 1541	MIL-STD 1541	MIL-STD-1541 (emissions)	MIL-STD 1541 (emissions)
Electromagnetic compat. (See 6.10)	MIL-STD-1574	MIL-STD 1574	MIL-STD 1574	MIL-STD 1574
Safety program (See 6.12)	MIL 1700.7 (NASA)	MIL 1700.7 (NASA)	MIL 1700.7 (NASA)	MIL 1700.7 (NASA)
Safety (See 6.12)	SAMTO HB S-100	SAMTO HB S-100	SAMTO HB S-100	SAMTO HB S-100
Ground safety (See 6.12)	MIL-STD-1472 (guide)	MIL-STD 1472 (guide)	MIL-STD 1472 (guide)	MIL-STD 1472 (guide)
Human engineering (See 6.13)				

Figure 5.1-5 Typical design factors used in each of the payload class categories

Computer Resources	CLASS A	CLASS B	CLASS C	CLASS D
Operational computers (See 7.1.1)	2 times the rate and 1.5 times the memory	2 times the rate and 1.5 times the memory	2 times the rate and 1.5 times the memory	As required
Operating system (See 7.1.2)	Existing	Existing	Existing	As required
Application software (See 7.1.3)	Develop to standards	Develop to standards	Develop to standards	As required
Software maintenance (See 7.2)	Delivered facility	Development guide	Development guide	Development guide
Verification/validation (See 10.4.3 - SOW Item)	Independent V & V	Walkthrough and test cases	Walkthrough and test cases	Guidance

Figure 5.1-6 Typical computer resource requirements for space experiments of each class

Construction Factors	CLASS A	CLASS B	CLASS C	CLASS D
Supplier selection	Has controlled process for space quality	Has controlled process for space quality	Has controlled process for space quality	Contractor option
Parts traceability (See 8.1)	Required	Required	Required	Contractor option
Materials traceability (See 8.1)	Required	Required	Required	Contractor option
In-process screening (See 8.1)	To assure performance and quality	To assure performance and quality	To assure performance and quality	Contractor option
Manufacturing processes (See 8.1)	Documented in detail	Documented	Limited documentation	Contractor option
Assembly lots (See 8.2)	For all parts and materials	for all parts and materials	for critical parts and materials	Contractor option
Cleanliness (See 8.3)	For everything	for everything	for everything	Contractor option
Electrostatic discharge (See 8.4)	DOD-HDBK-263	DOD-HDBK-263	DOD-HDBK-263	Contractor option
Outgassing (See 6.1.1 and 8.3.3)	SP-R-0022 (NASA)	SP-R-0022 (NASA)	SP-R-0022 (NASA)	SP-R-0022 (NASA)

Figure 5.1-7 Typical construction requirements for each of the payload classes

Test Requirements	CLASS A	CLASS B	CLASS C	CLASS D
Maximum operating environments	MIL-STD-1540 definitions (component acceptance) for each assembly level	MIL-STD-1540 definitions (component acceptance) for each assembly level	MIL-STD-1540 definitions (component acceptance) for each assembly level	MIL-STD-1540 definitions (component acceptance) for each assembly level
Testing tolerances	MIL-STD-1540	MIL-STD-1540	MIL-STD-1540	MIL-STD-1540
Development tests	As required	As required	As required	Not required
Component acceptance (See 10.4.1)	MIL-STD-1540 (component acceptance)	Not required on test item; protoflight test only	MIL-STD-1540 (component acceptance)	Not required
Component qualification (See 10.4.1)	MIL-STD-1540 (qual.) to design levels	MIL-STD-1540(protoflight) to design levels	Not required (acceptance test only)	Not required
Qual. thermal margin	10 deg C	5 deg C	0 deg C	0 deg C
Qual. vibration margin	6 dB	3 dB	0 dB	0 dB
Qual. acoustic margin	6 dB	3 dB	0 dB	0 dB
Qual. shock margin	6 dB	3 dB	0 dB	0 dB
Experiment acceptance (See 10.4.2)	MIL-STD-1540 (vehicle acceptance)	Not required on test item; protoflight test only	MIL-STD-1540 (vehicle acceptance)	MIL-STD-1540 (vehicle acceptance)
Experiment qualification (See 10.4.3)	MIL-STD-1540 (vehicle qualification)	MIL-STD-1540(protoflight) to design levels	Not required (acceptance test only)	Not required (acceptance test only)
Qual. margins (environ.)	10 deg C; 6 dB	10 deg C; 6 dB	0	0
Vehicle acceptance (See 10.4.3)	MIL-STD-1540 (vehicle acceptance)	Not required on test item; protoflight test only	MIL-STD-1540 (vehicle acceptance)	MIL-STD-1540 (vehicle acceptance)
Vehicle qualification (See 10.4.3)	MIL-STD-1540 (vehicle qualification)	MIL-STD-1540(protoflight) test item to design levels	Not required (acceptance test only)	Not required (acceptance test only)
Qual. margins (environ.)	10 deg C; 6 dB	10 deg C; 6 dB	0	0

Figure 5.1-8 Comparison of test requirements for payloads of each class

Item	CLASS A Equipment	CLASS B Equipment	CLASS C Equipment	CLASS D Equipment
Component development test items	For all newly developed items. Development tests as required.	For newly developed mission-critical items (tests as required)	For newly developed safety-critical items (tests as required)	None required
Number of flight-type components required to support first flight	Usually six of each type	Usually three of each type	Usually two of each type	May only be one of each type
Component serial 1 (first fabricated)	Component qualification tests, then use for reliability margin tests	For flight vehicle (first string) (protoflight tested)	For flight vehicle (single string) (acceptance tested)	For flight vehicle (component tests optional)
Component serial 2 (second fabricated)	For qualification vehicle (first string); then spare; (acceptance tested)	For flight vehicle (second string); (acceptance tested)	A "true" flight spare (acceptance tested)	Flight spare if planned (component tests optional)
Component serial 3 (third fabricated)	For qualification vehicle A (second string); then spare; (acceptance tested)	A "true" flight spare (acceptance tested)	Usually none planned	Usually none planned
Component serial 4 (fourth fabricated)	For flight vehicle (first string) (acceptance tested)	Usually none planned	Usually none planned	Usually none planned
Component serial 5 (fifth fabricated)	For flight vehicle (second string) (acceptance tested)	Usually none planned	Usually none planned	Usually none planned
Component serial 6 (sixth fabricated)	A "true" flight spare (acceptance tested)	Usually none planned	Usually none planned	Usually none planned

Figure 5.1-9 Typical fabrication and test requirements for components to support the first flight item of each class

Commander's Policies (technical)	CLASS A	CLASS B	CLASS C	CLASS D
SDR 540-4 INDEPENDENT MASS PROPERTIES, STABILITY & CONTROL	yes	yes	yes	yes
SDR 540-5 INDEPENDENT STRUCTURAL LOADS ANALYSIS	yes	yes	yes	yes
SDR 540-6 SPACE VEHICLE TESTING	yes	yes	yes	no
SDR 540-8 SPACE SERVICING	yes	yes	yes	yes
SDR 540-9 "B" NUTS	yes	yes	yes	yes
SDR 540-10 FMECA'S	yes	yes	yes	yes
SDR 540-12 PIECE PARTS PROCUREMENT	yes	yes	no	no
SDR 540-17 INDEPENDENT MISHAP RISK ASSESSMENT	yes	yes	yes	yes
SDR 540-18 TIAC SUPPORT PLANNING	yes	yes	yes	yes
SDR 540-23 USE OF MULTILAYER PRINTED-WIRING BOARDS	yes	yes	no	no
SDR 540-25 PRESSURIZED STRUCTURES	yes	yes	yes	yes
SDR 540-39 SPACEFLIGHT ENGINEERS	yes	yes	yes	yes

* NOTE: USAF Space Division Regulations (SDRs), including the Commander's policies in SDR 540, are applicable to all USAF Space Division programs unless the requirement is waived by the Commander. Many policies allow compliance tailored to the actual program needs; however, this matrix is intended to provide guidance to new programs that may consider making a request for a waiver.

Figure 5.1-10 Applicability of Space Division directives for each payload class

Commander's Policies (program management)	CLASS A	CLASS B	CLASS C	CLASS D
SDR 540-3 SYSTEMS ACQ. REVIEWS AND AUDITS	yes	yes	no	no
SDR 540-14 SD/MASA JOHNSON COORDINATION	yes	yes	yes	yes
SDR 540-15 MISSION READINESS	yes	yes	yes	yes
SDR 540-16 SECURITY	yes	yes	yes	yes
SDR 540-21 CONTRACTOR PERFORMANCE	yes	yes	yes	yes
SDR 540-31 ENGINEERING DESIGN REVIEWS	yes	yes	no	no
SDR 540-33 PROGRAM DIRECTOR'S FINAL REPORT	yes	yes	yes	yes
SDR 540-41 OPTIMIZING COMPETITION	yes	yes	yes	yes

* NOTE: USAF Space Division Regulations (SDRs), including the Commander's policies in SDR 540, are applicable to all USAF Space Division programs unless the requirement is waived by the Commander. Many policies allow compliance tailored to the actual program needs; however, this matrix is intended to provide guidance to new programs that may consider making a request for a waiver.

Figure 5.1-11 Applicability of Space Division's commander policies in management requirements for payloads of each class

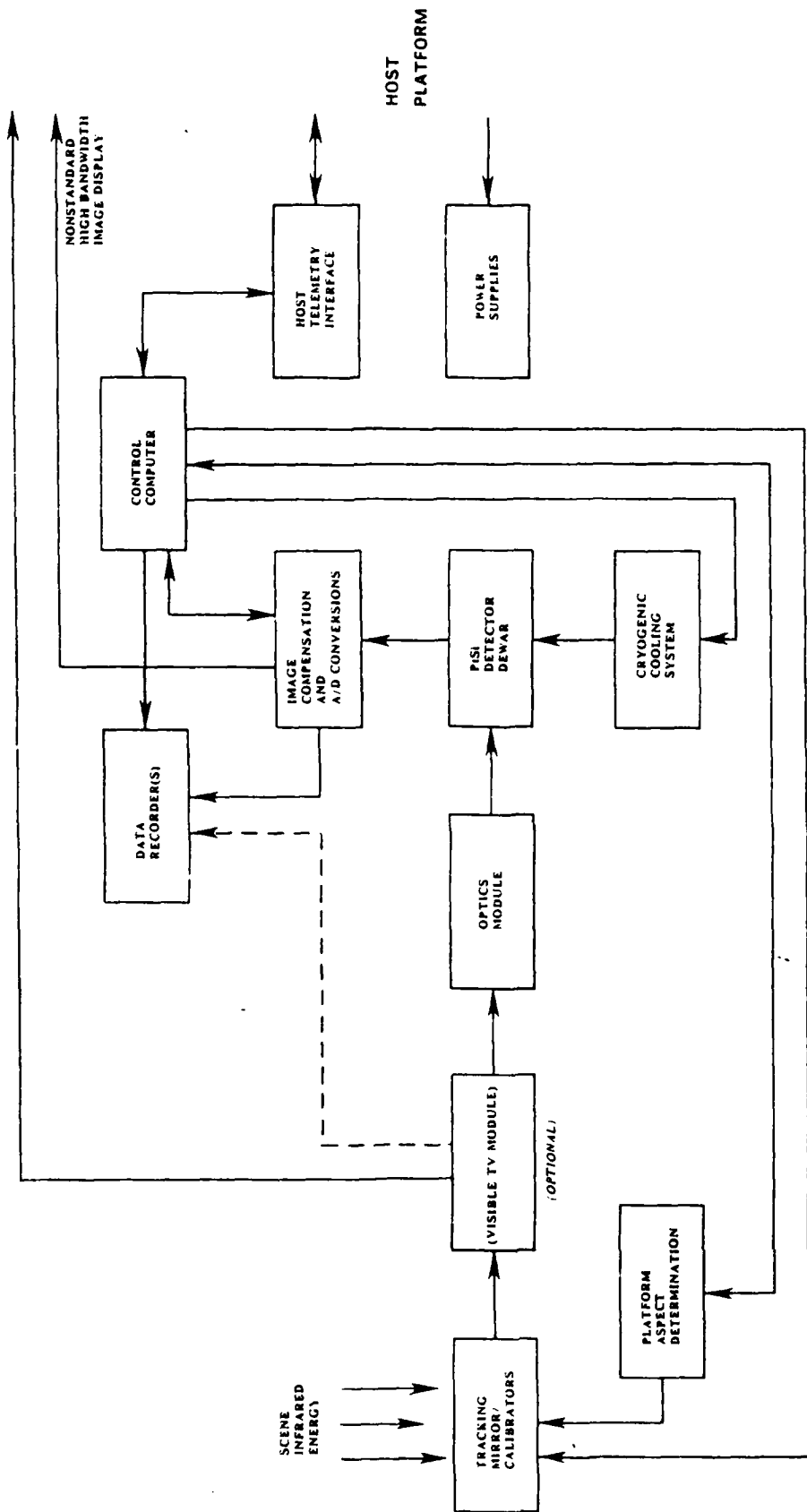


Figure 6.1-1 Component level block diagram of the SBS Camera payload

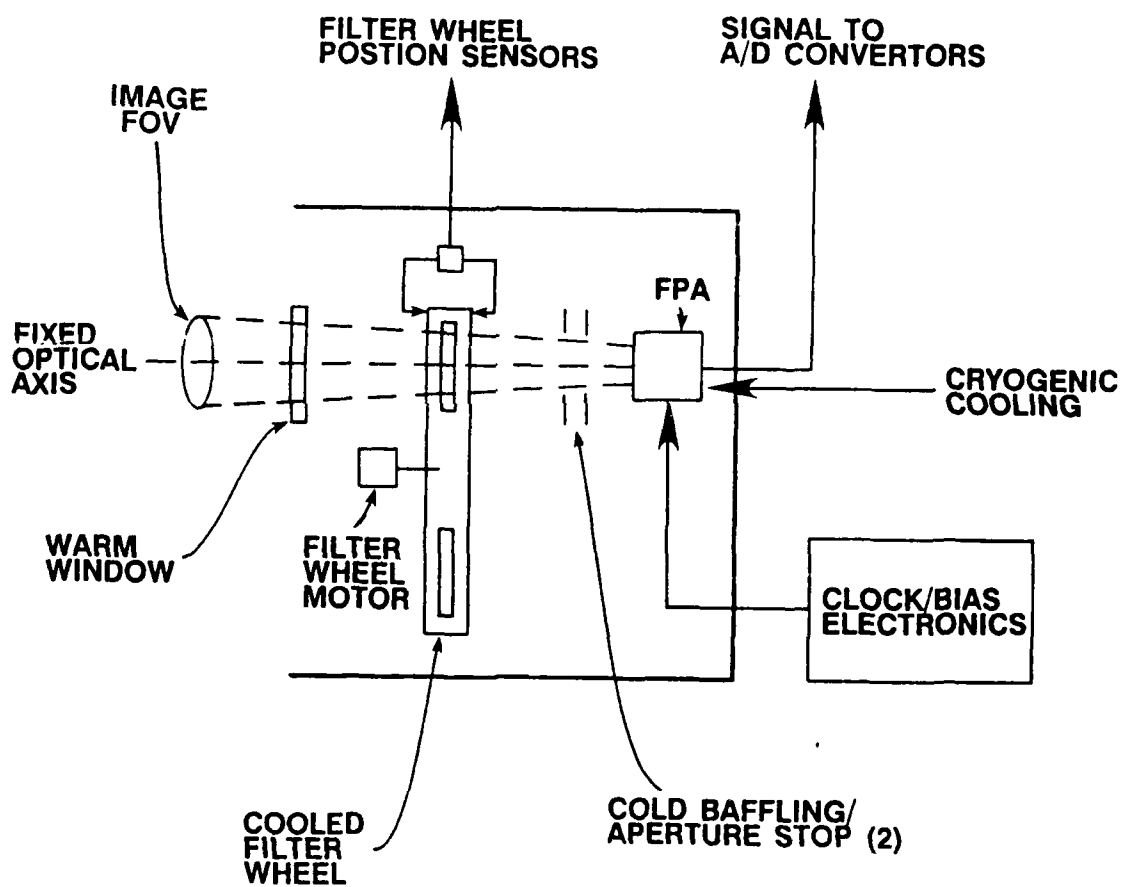


Figure 6.1-2 SBS Camera dewar block diagram

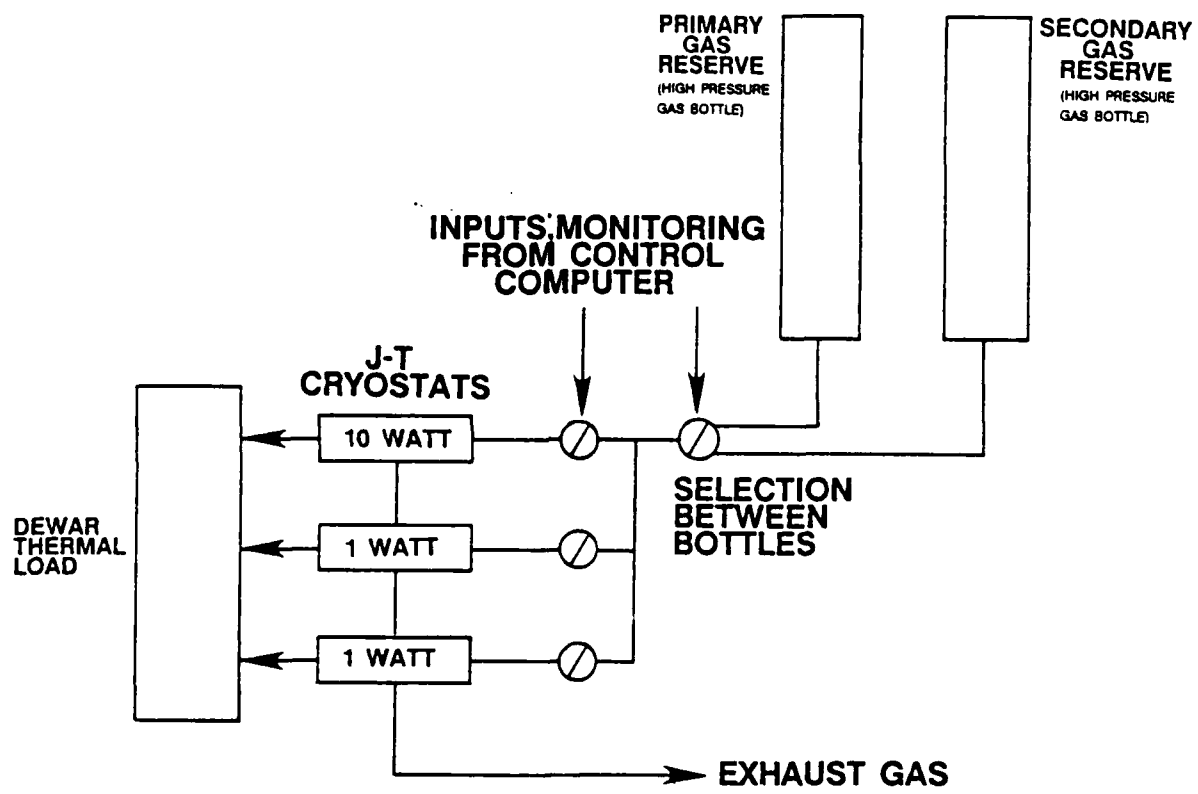


Figure 6.1-3 Cryogenic cooling system block diagram

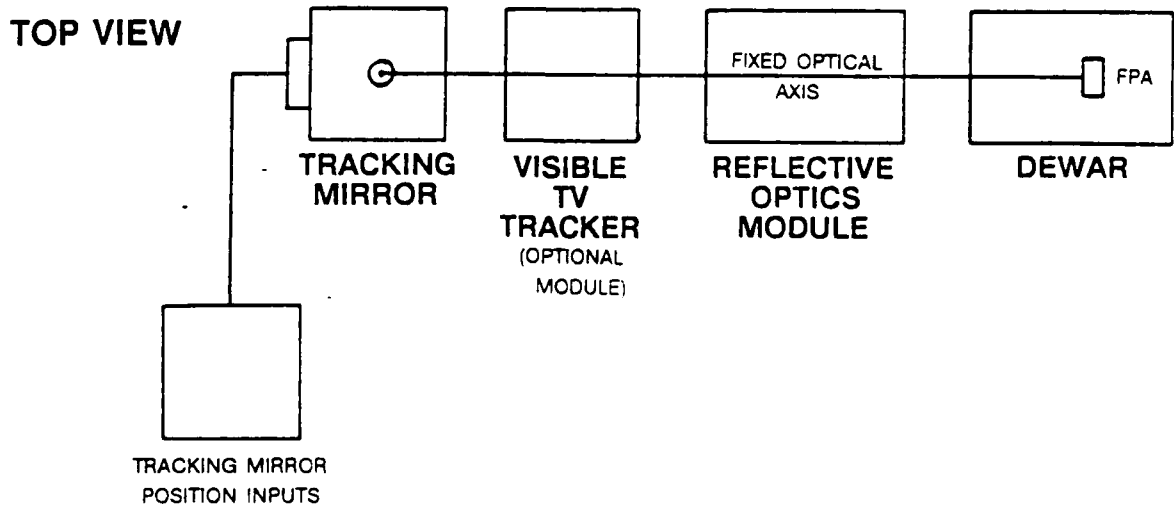
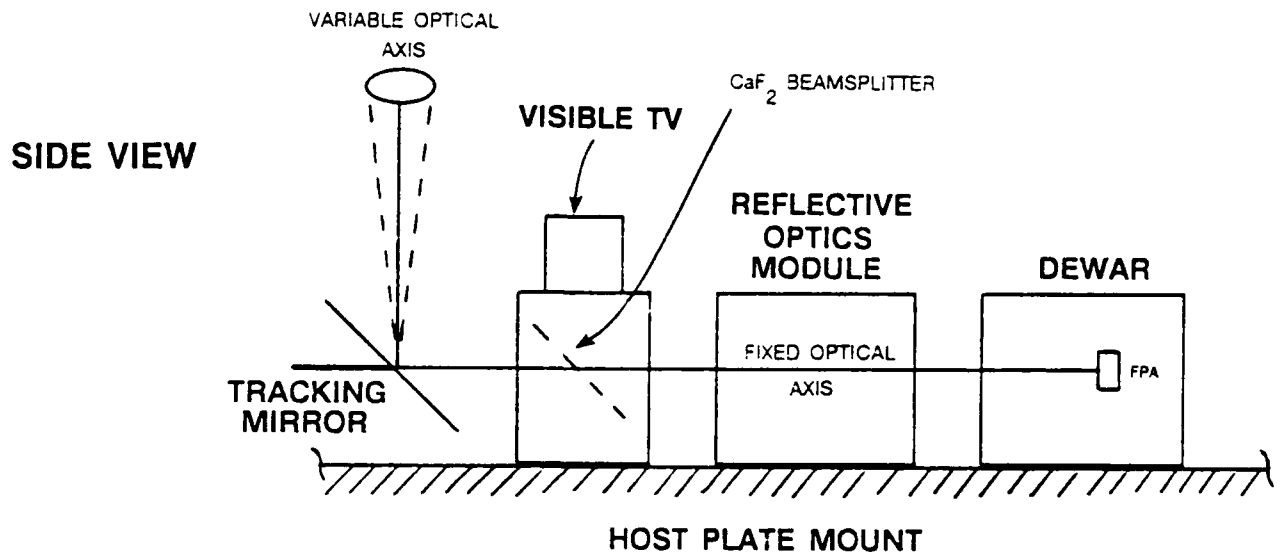


Figure 6.1-4 Major optical components and axes of SBS Camera

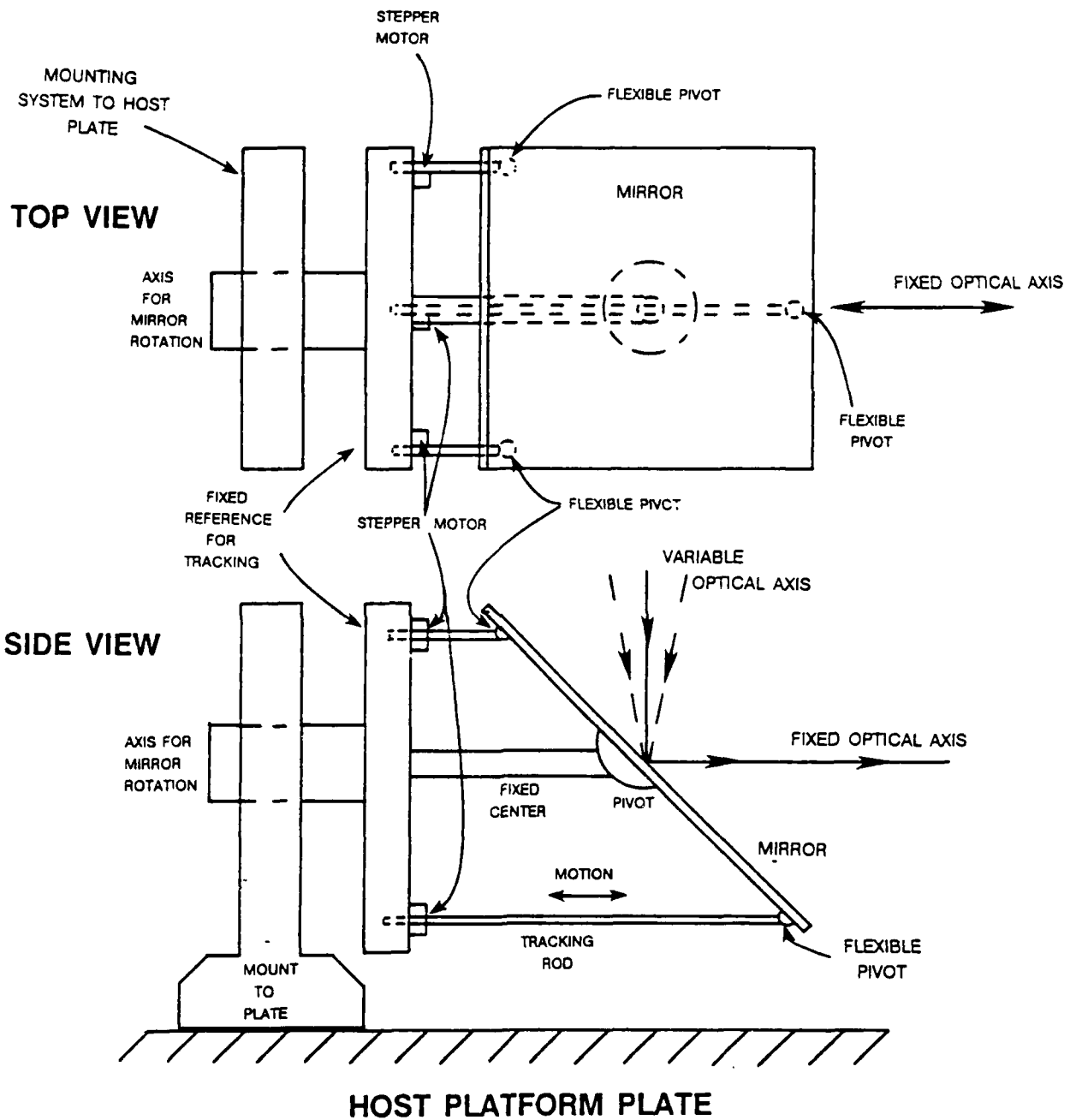


Figure 6.1-5 Diagram of tracking system

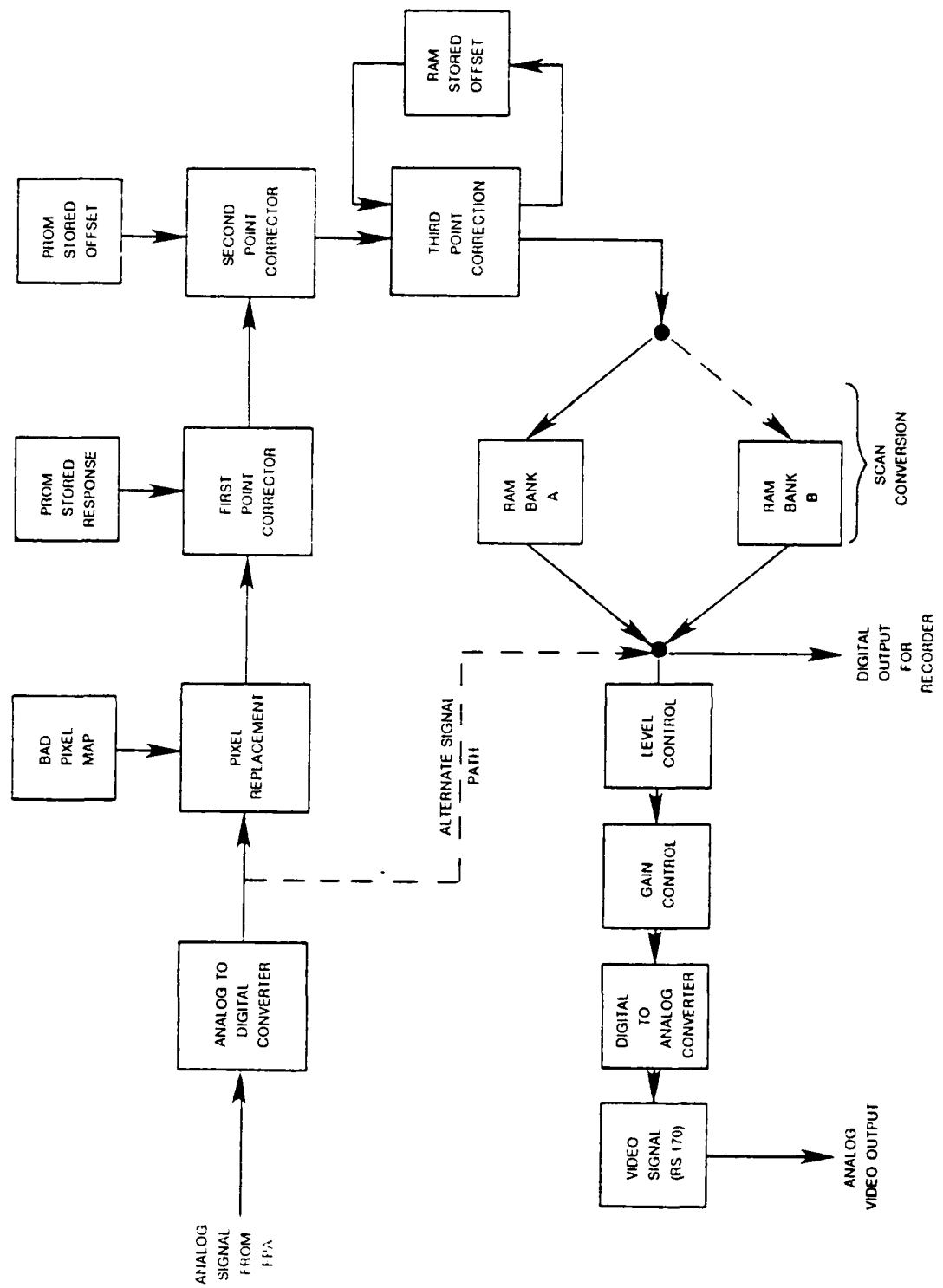


Figure 6.1-6 Image compensator block diagram

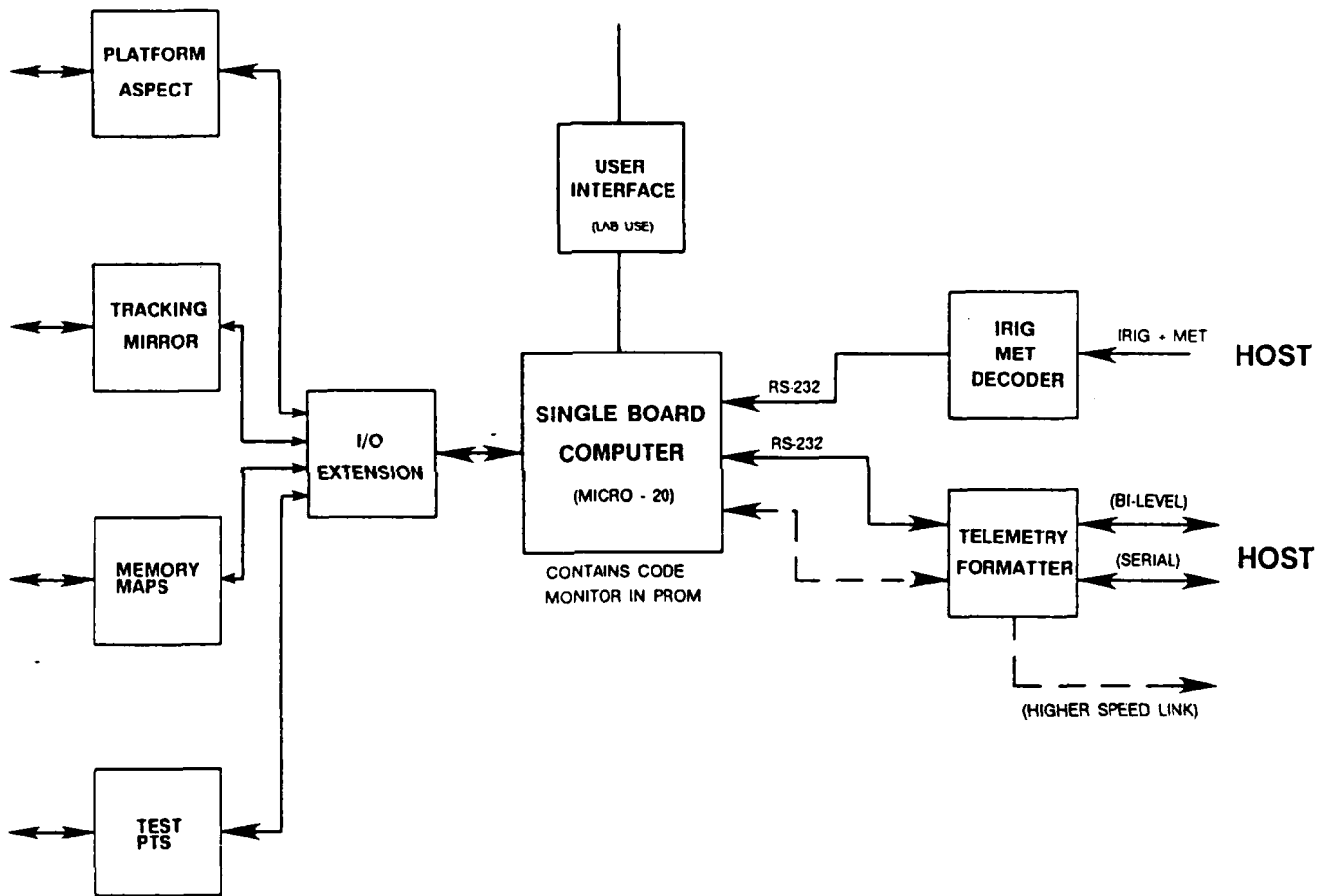


Figure 6.1-7 Block diagram of SBS payload control computer components

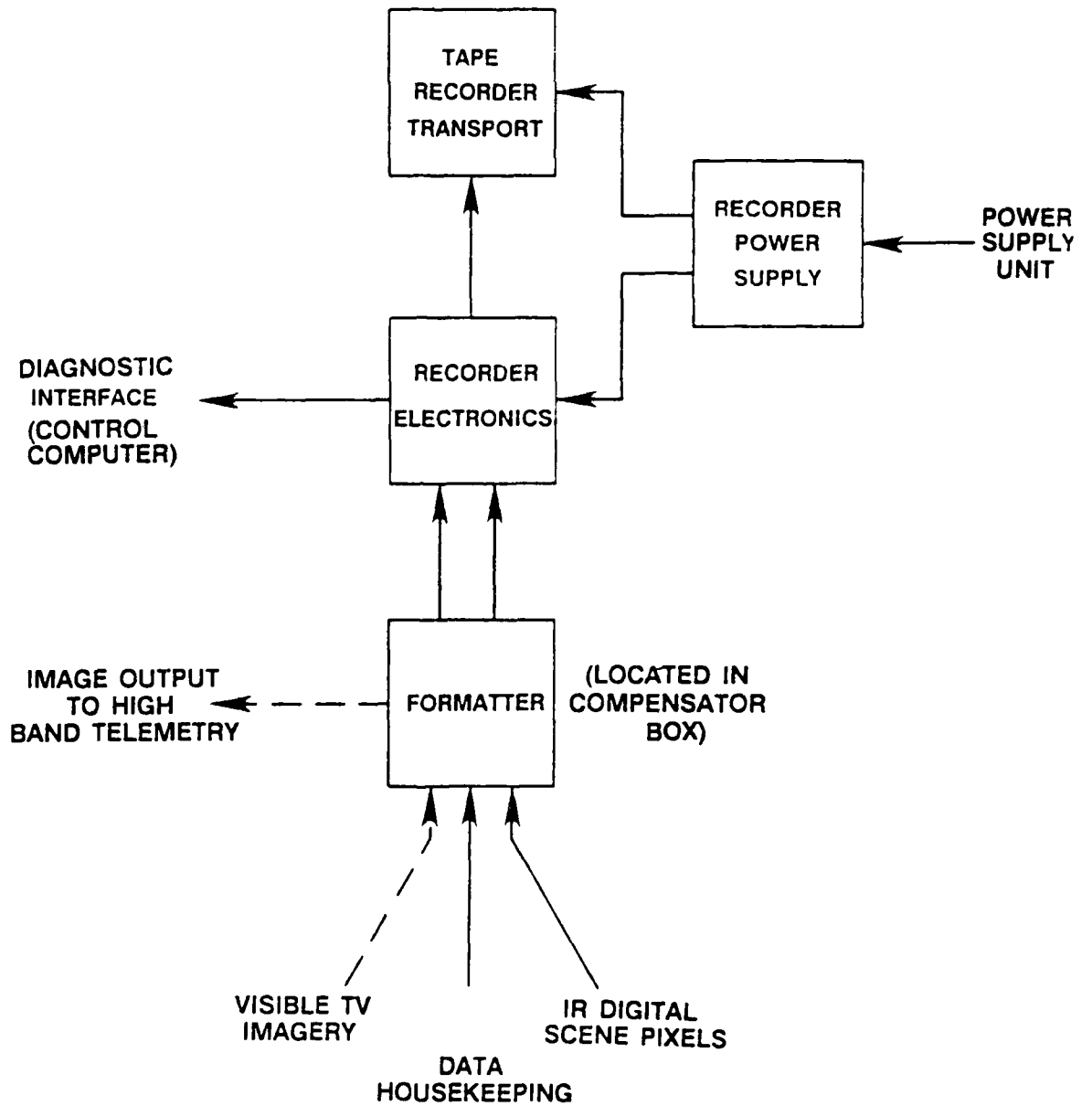


Figure 6.1-8 Data recording system

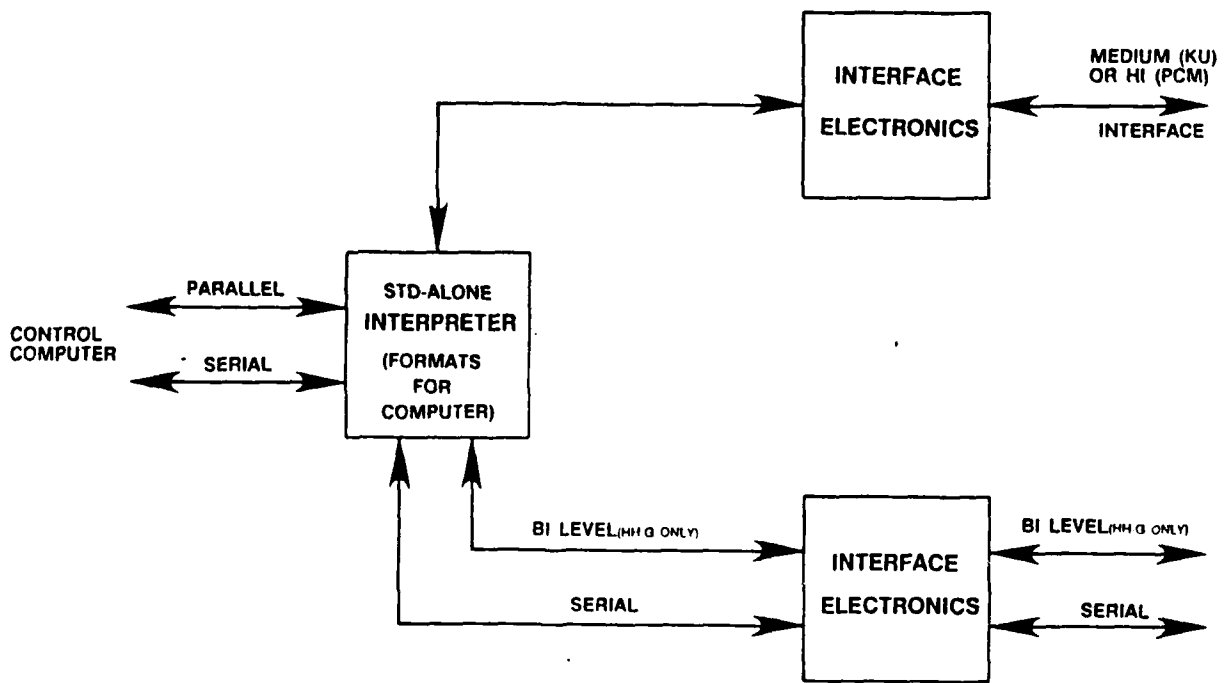


Figure 6.1-9 Payload to host platform telemetry interface

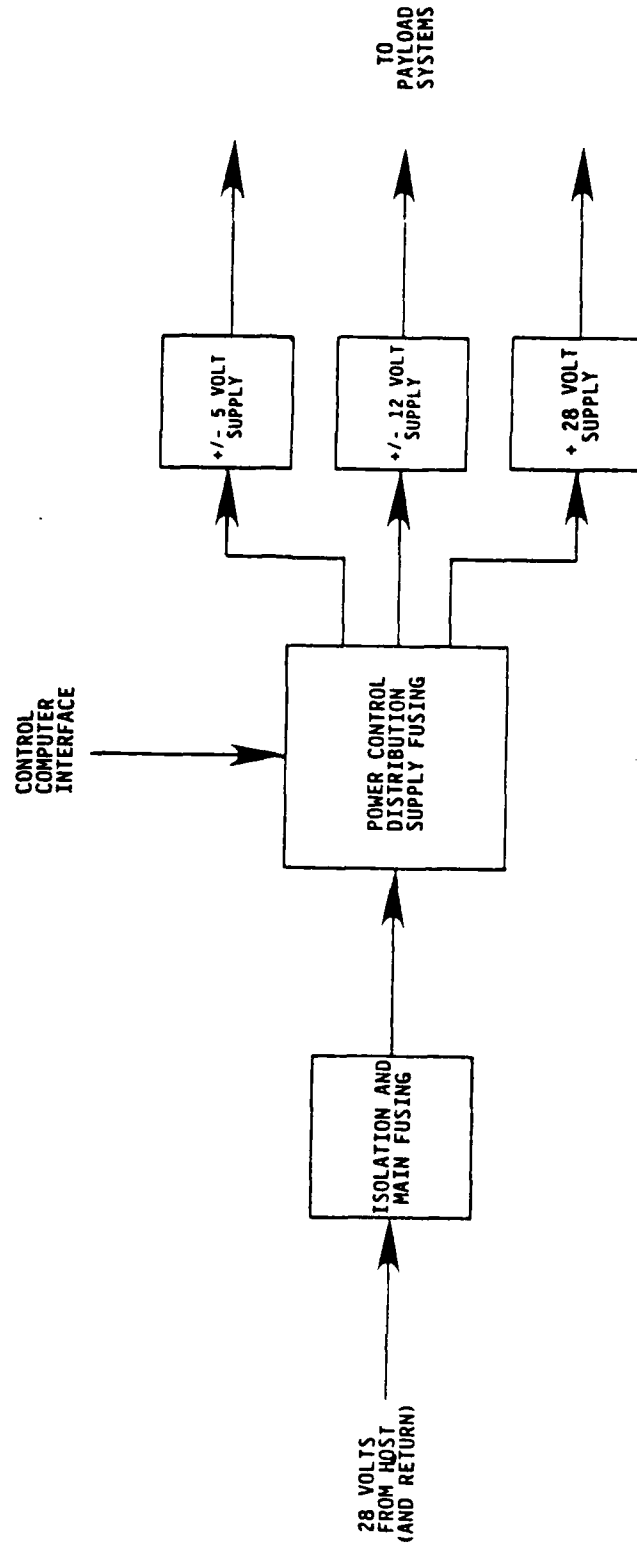


Figure 6.1-10 Block diagram of payload power interface

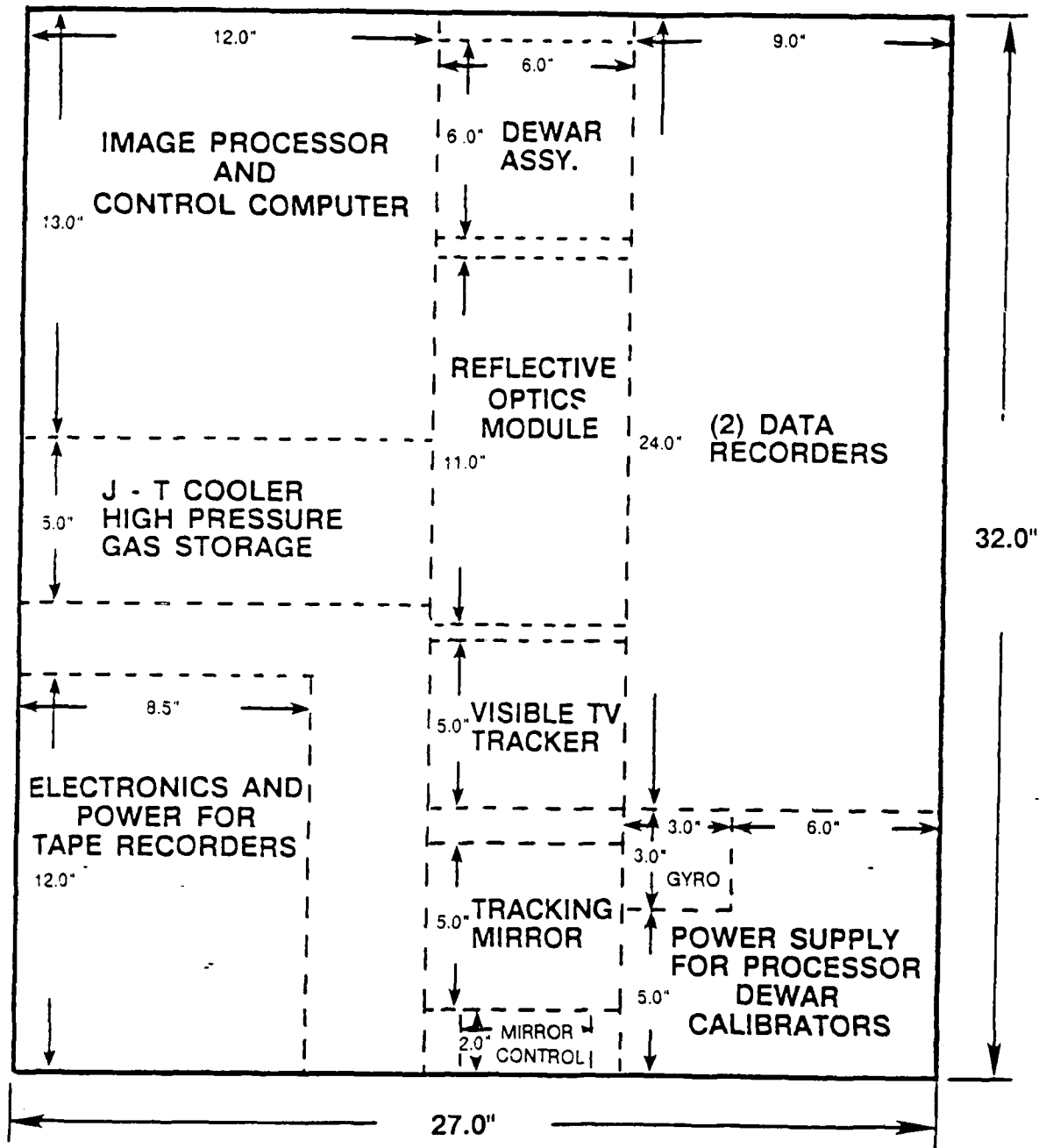


Figure 6.2-1 SPAS Equipment Support Plate mounting payload layout

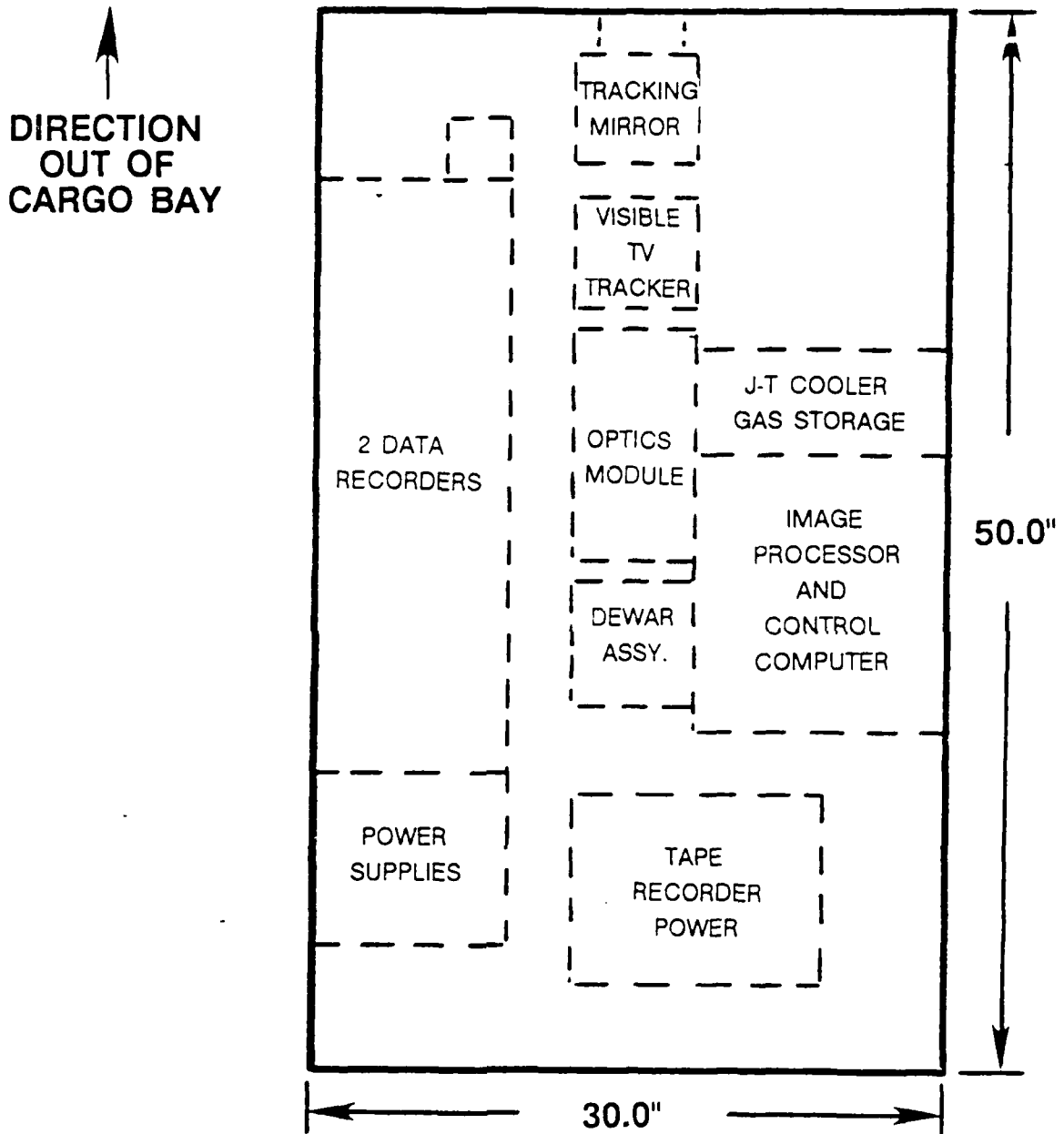


Figure 6.2-2 HH-G plate mount payload layout

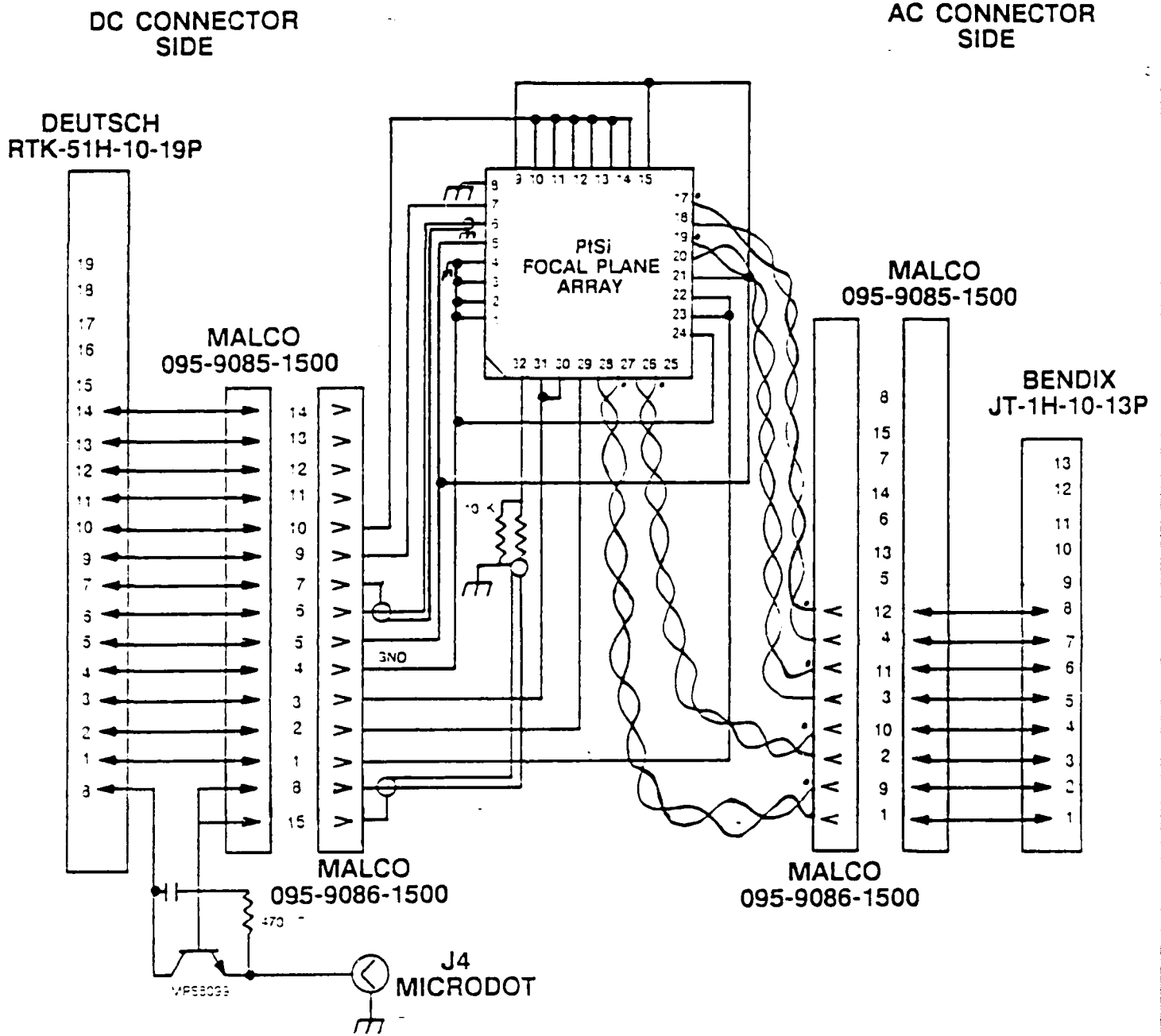
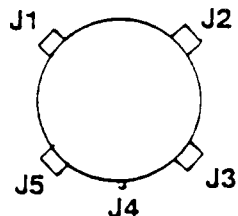


Figure 6.3-1 SAIRS dewar wiring diagram



J1 AND J2 DUPLICATES
OF J3 AND J5 (SECOND FPA)

J3 (A/C CONNECTOR)

- 1 ... ϕ _{2C}
- 2 ... ϕ _{3C}
- 3 ... ϕ _{1B}
- 4 ... ϕ _{2B}
- 5-8 .. N/C
- 9 ... ϕ _{4C}
- 10 ... ϕ _{1C}
- 11 ... ϕ _{3B}
- 12 ... ϕ _{4B}
- 13-15 .. N/C

J5 (D/C CONNECTOR)

- 1 ... G_{1C}, G_{2C}
- 2 ... G_{3C}
- 3 ... V_{DD1}, V_{DD2} (+20 V NOMINAL)
- 4 ... GND
- 5 ... V_{CD}, V_{SA}, V_{DA}, V_{SC} (+20 V NOMINAL)
- 6 ... G_{5C}
- 7 ... G_{5C} RETURN
- 8 ... TEMP SENSOR
- 9 ... G
- 10 ... -20 V (UNUSED CLOCKS)
- 11-19 .. N/C

J4 (MICRODOT)

- 1 ... TEMP READOUT
- 2 ... SHIELD GND

Figure 6.3-2 Connector pinouts used in SAIRS dewar

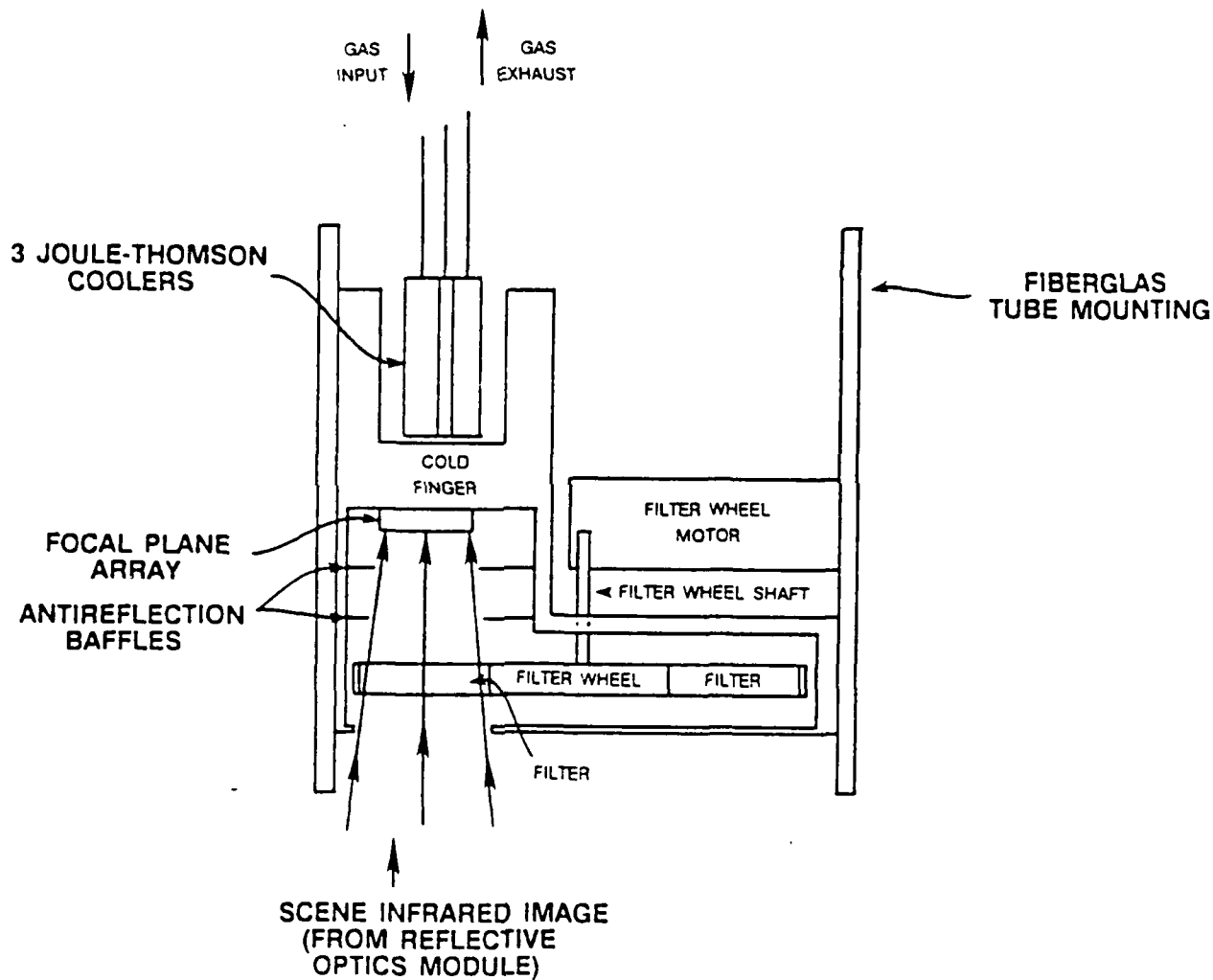


Figure 6.3-3 Internal cooled assembly of detector dewar

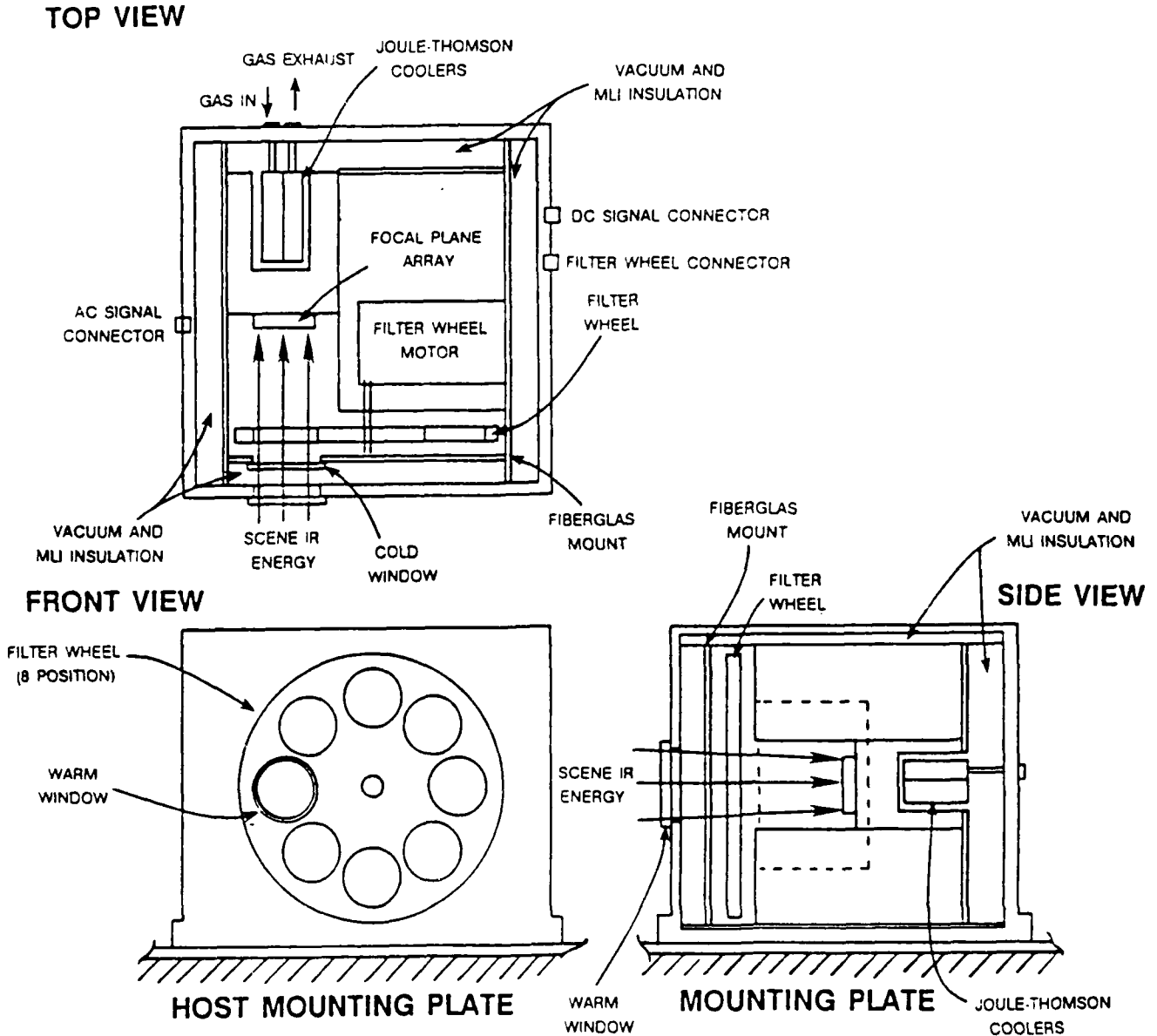


Figure 6.3-4 Mounting of cooled assembly to outer dewar unit

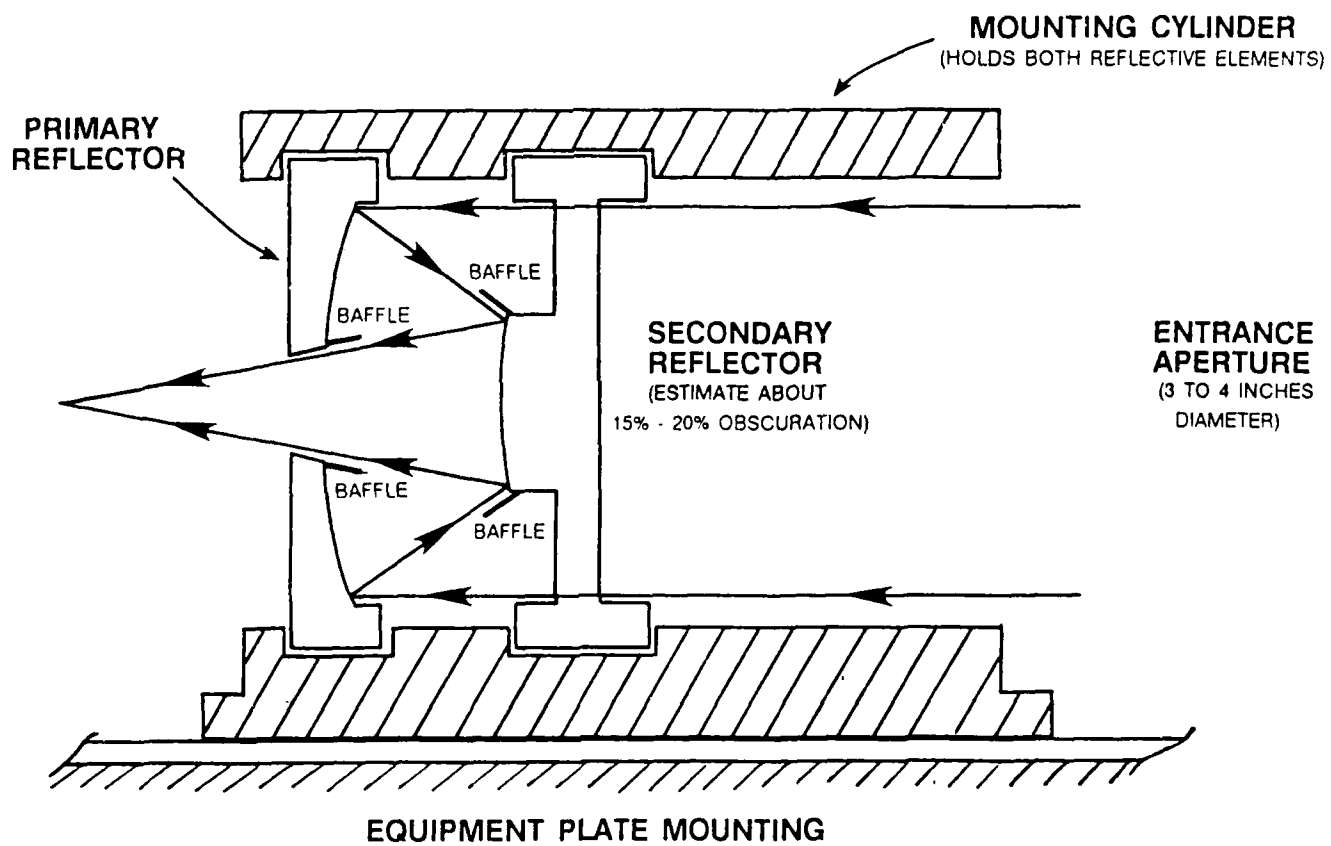


Figure 6.4-1 Physical configuration of camera reflective optics module

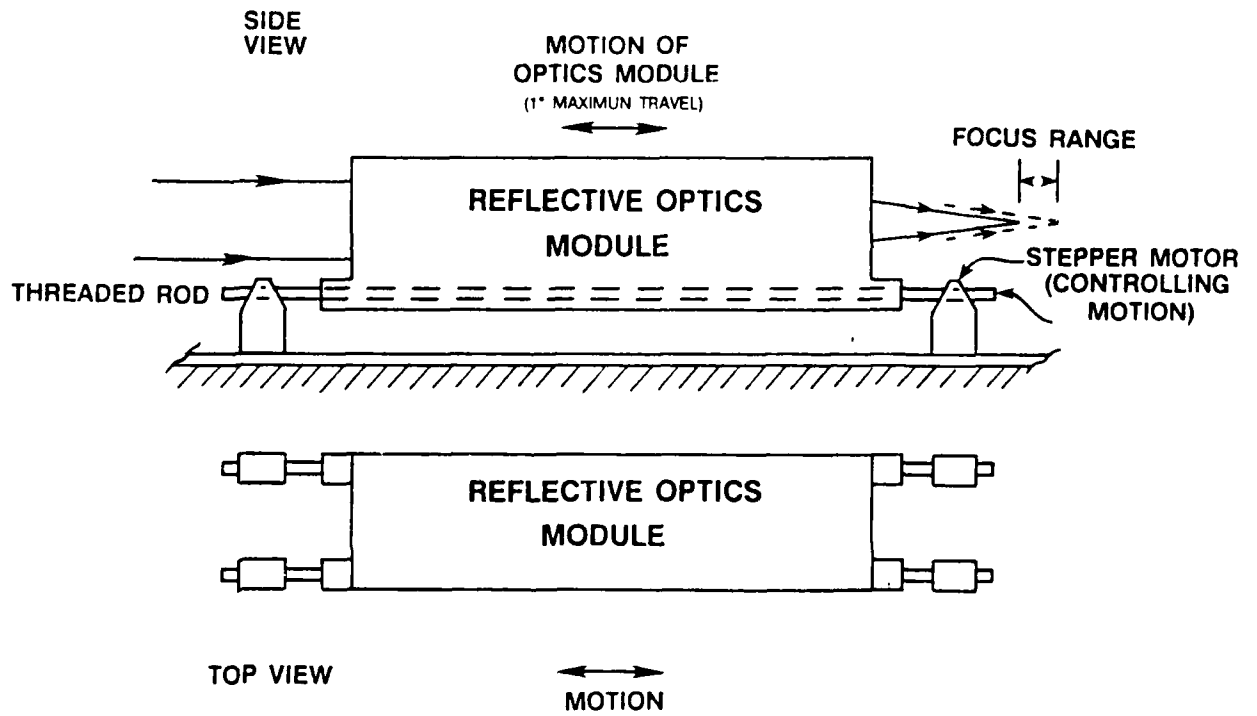


Figure 6.4-2 Implementation of focus control

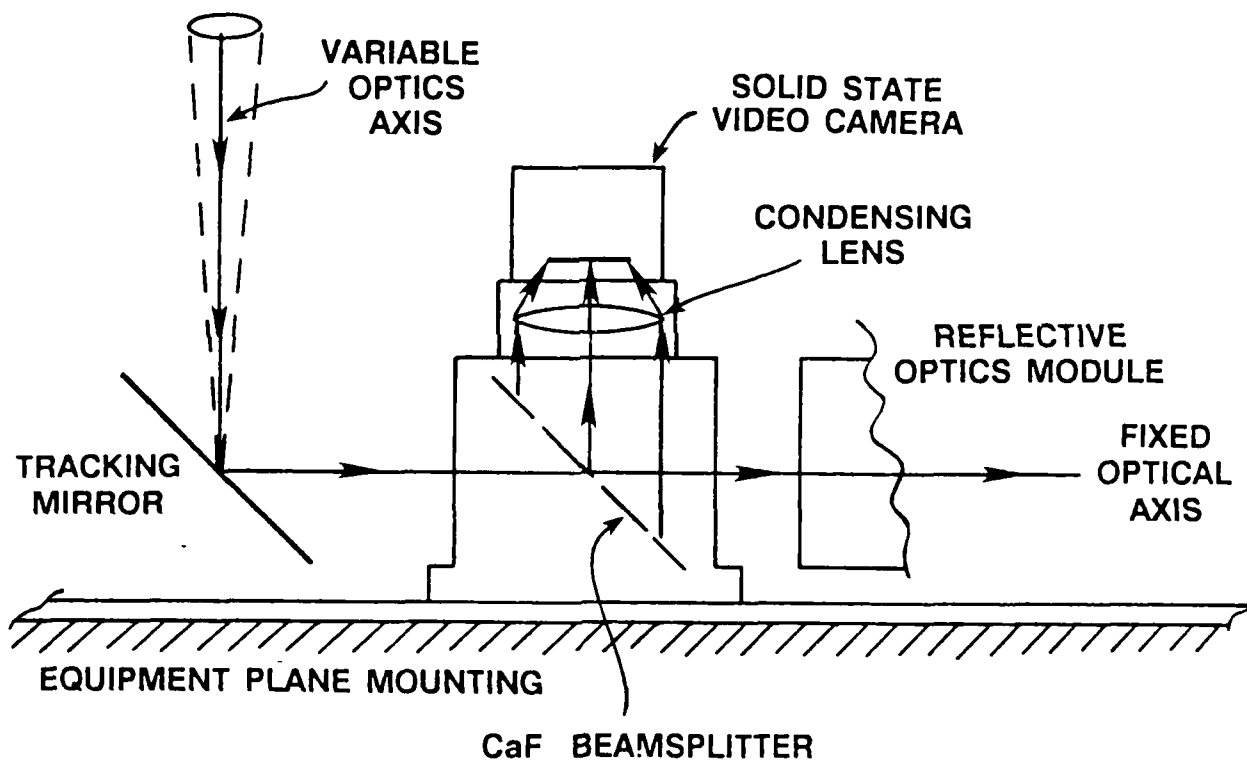


Figure 6.4-3 Visible video camera implementation

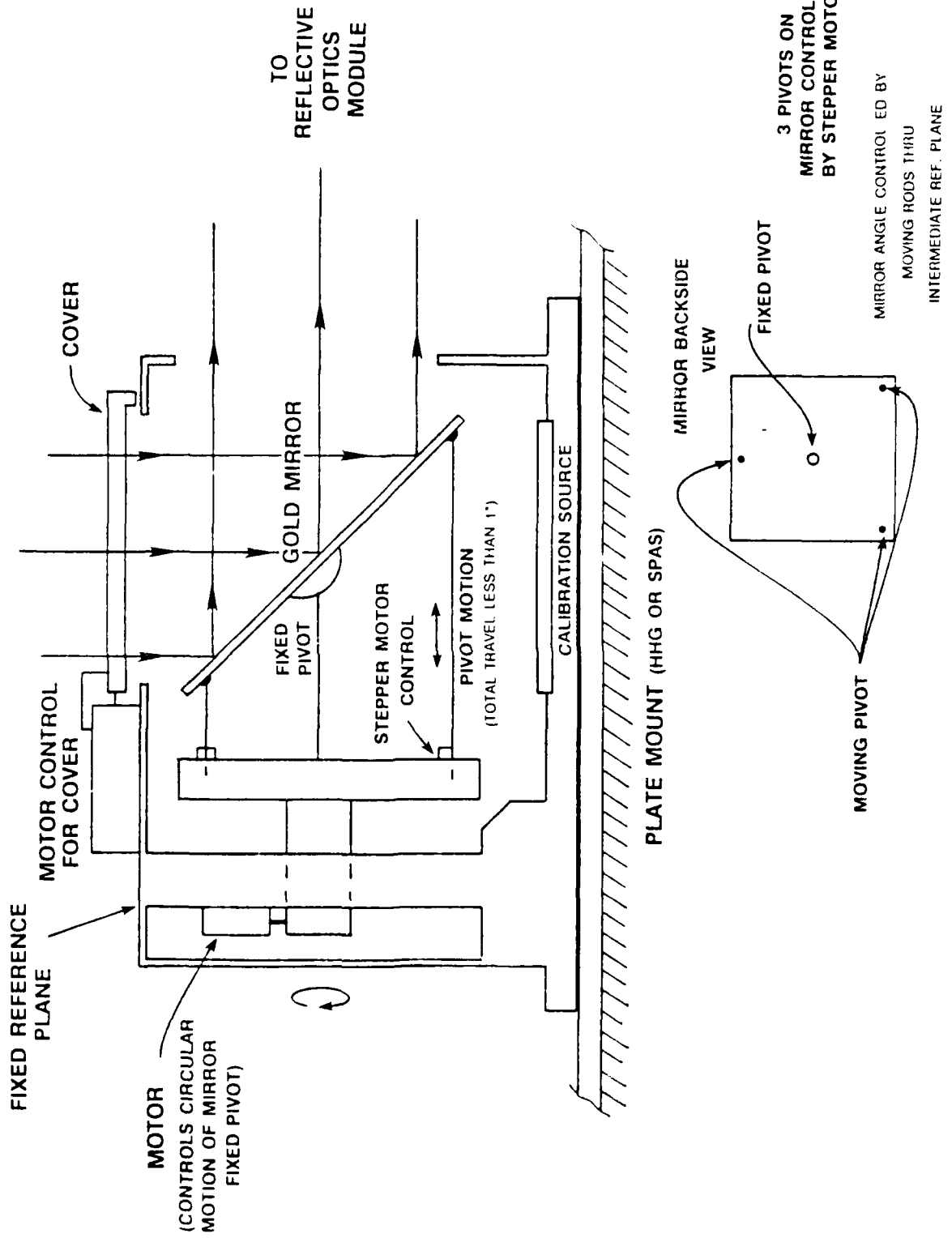


Figure 6.5-1 Drawing of tracking mirror assembly

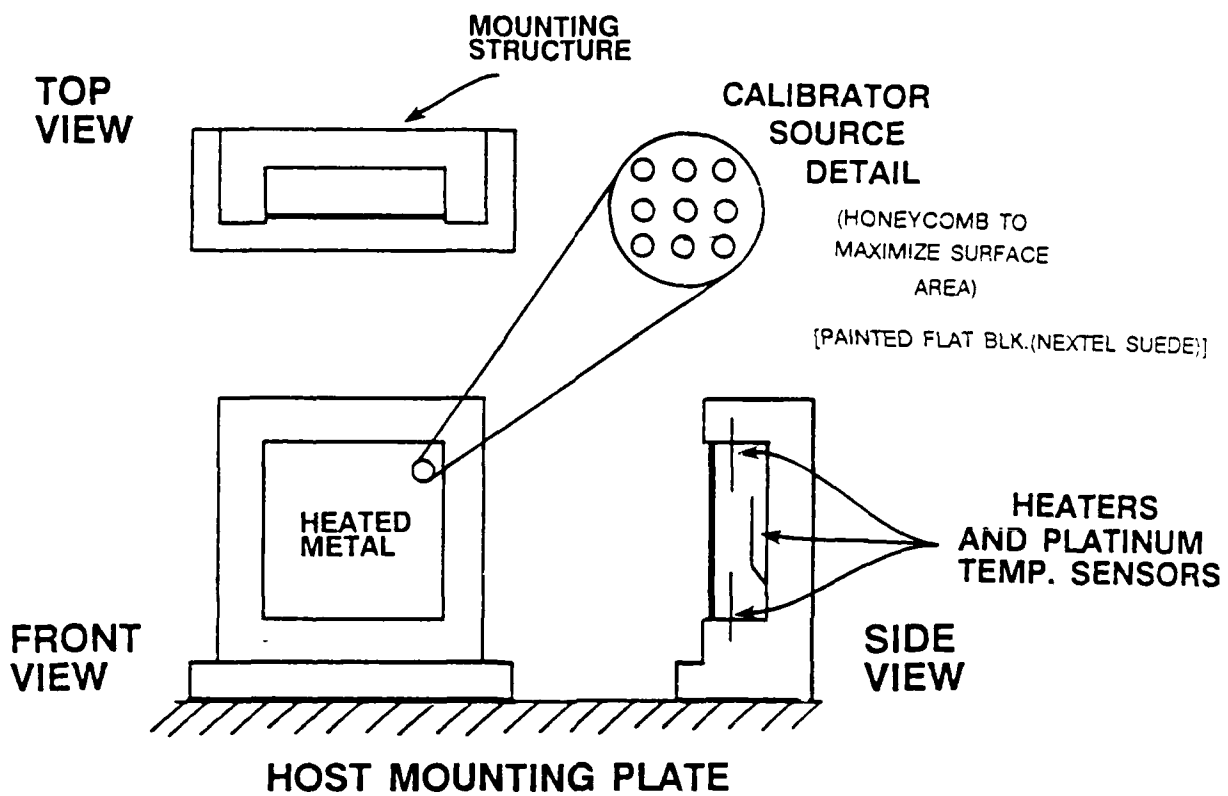


Figure 6.5-2 Extended source calibrators around tracking mirror assembly

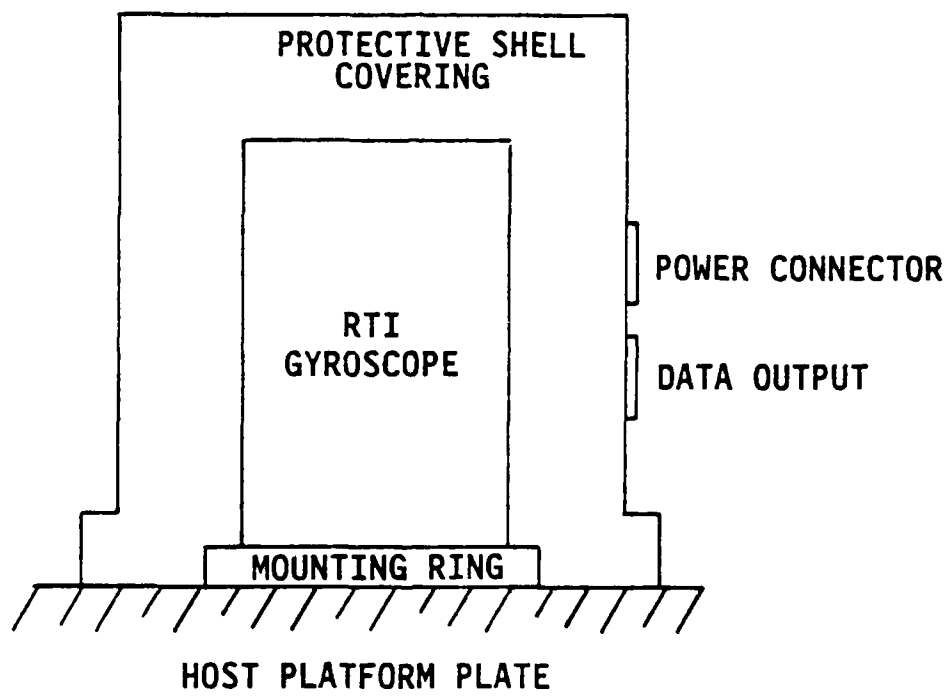


Figure 6.6-1 Sketch showing gyroscope and mounting to plate

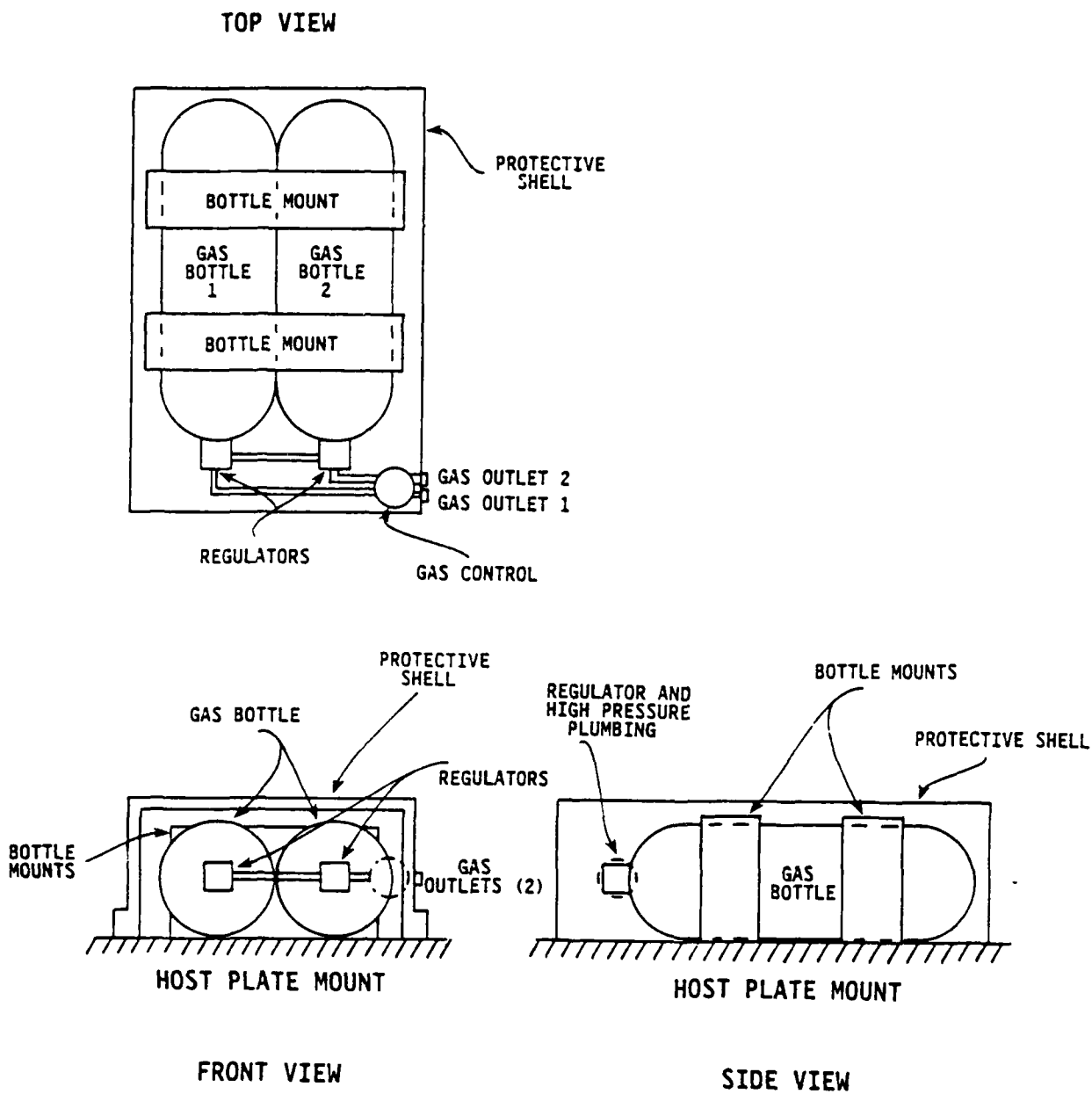
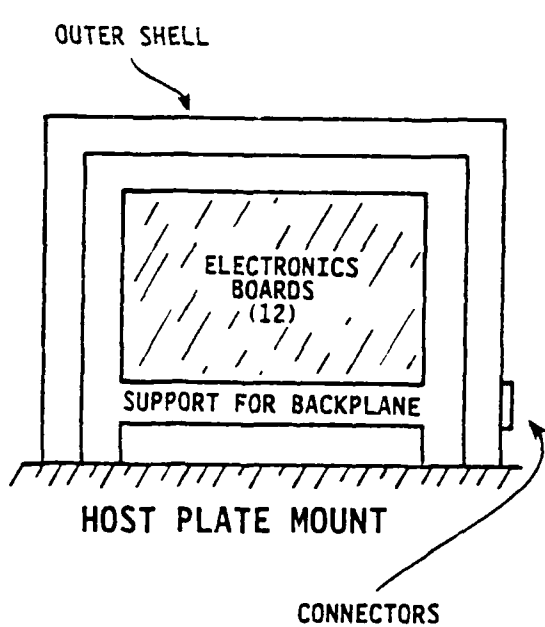
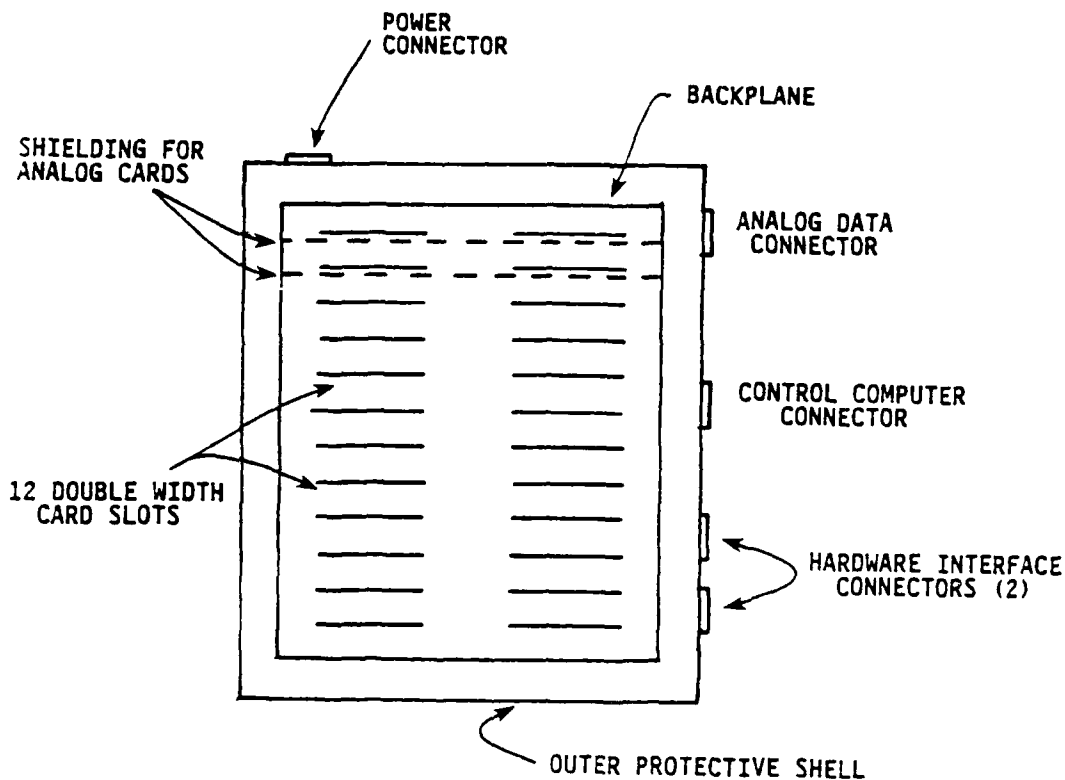
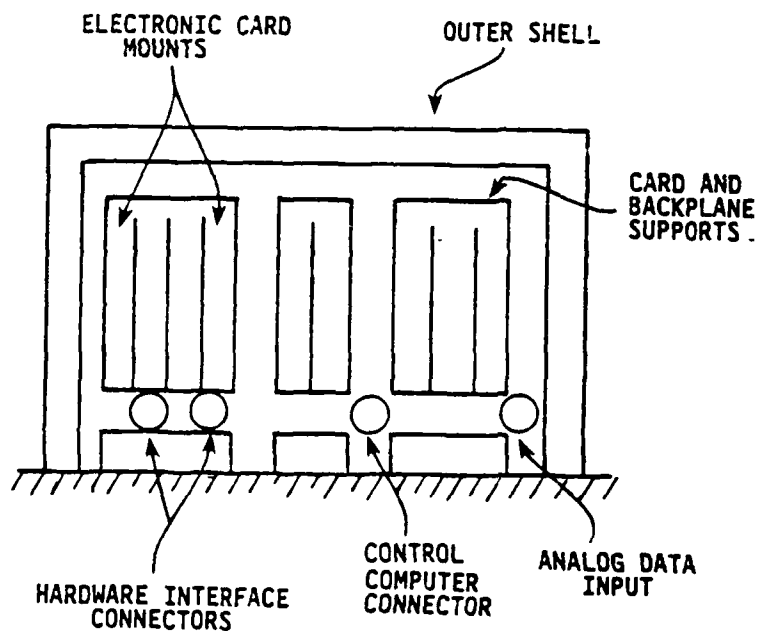


Figure 6.7-1 Gas storage mounting for cryogenic cooling system

TOP VIEW



FRONT VIEW



SIDE VIEW

Figure 6.8-1 Sketch illustrating electronics mounting assembly

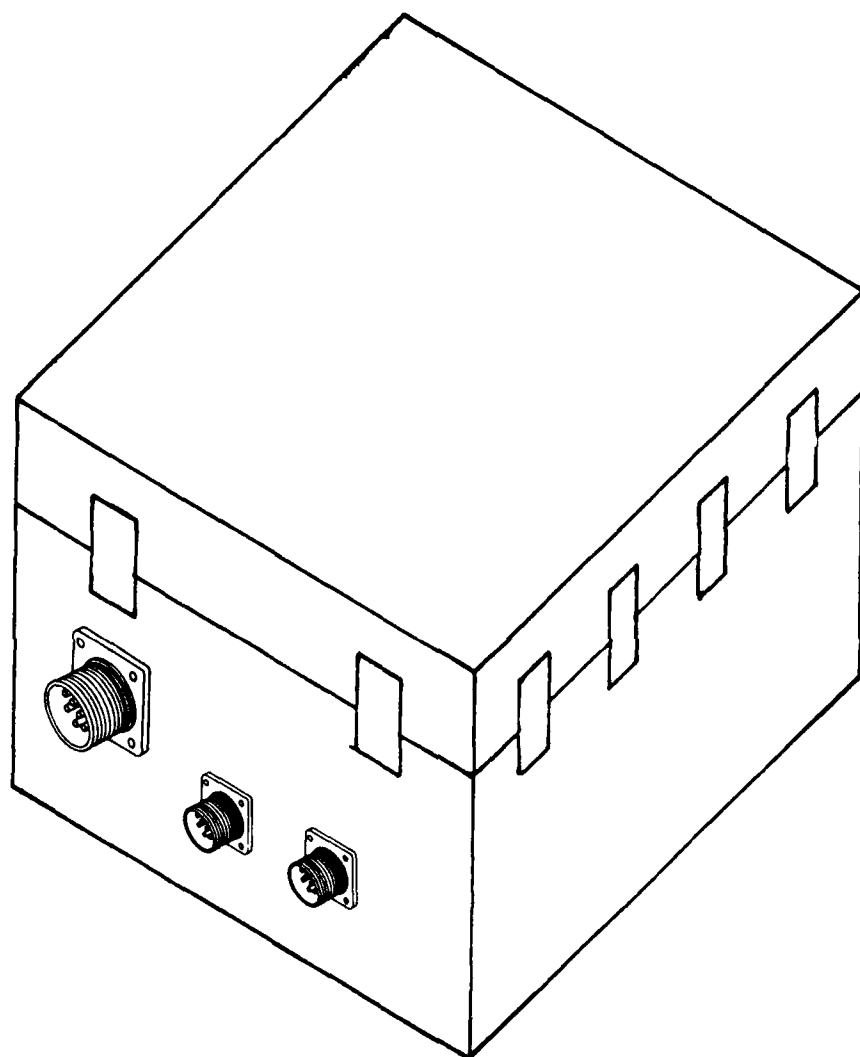


Figure 6.9-1 Outline of Ampex DCRSi recording unit

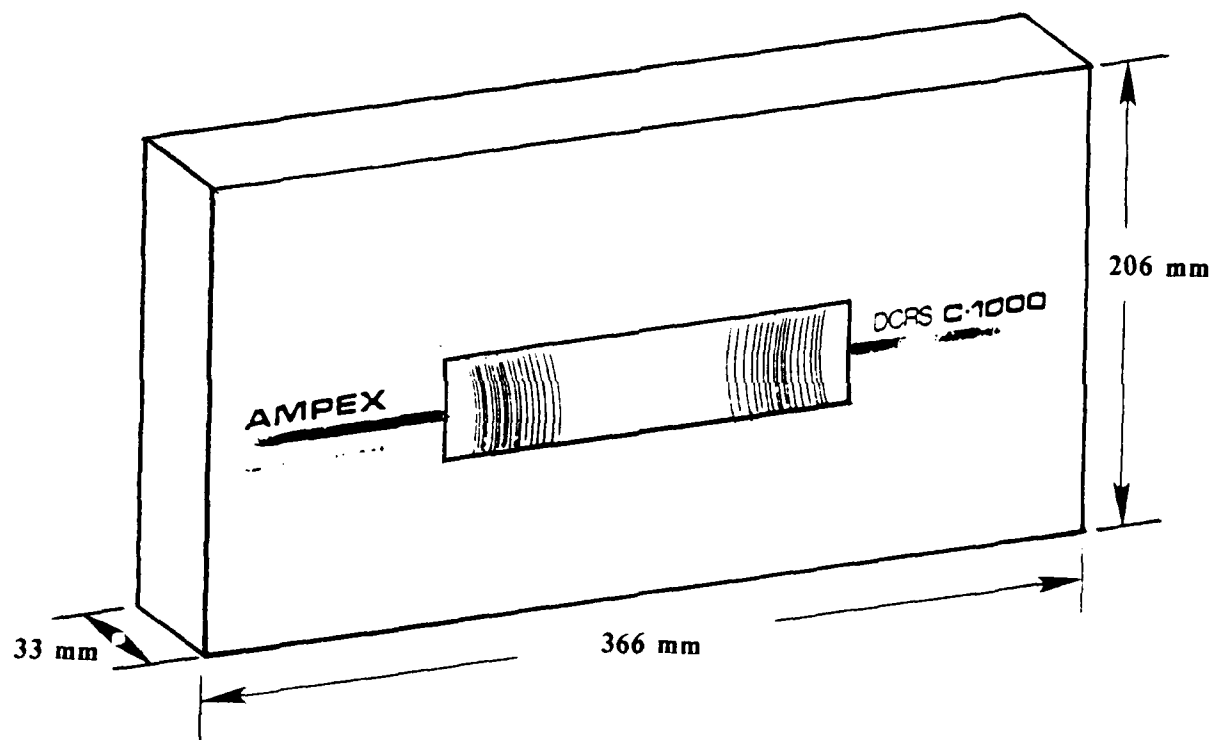
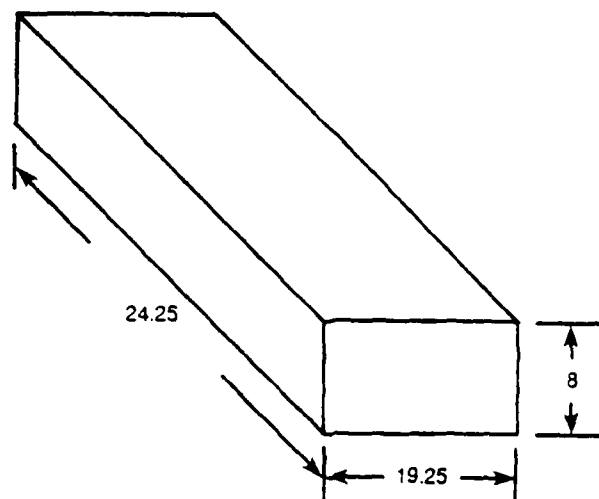
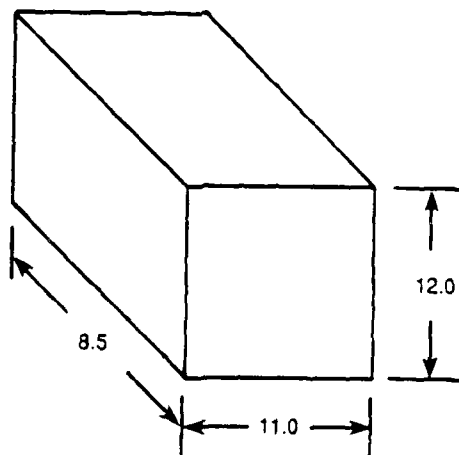


Figure 6.9-2 Tape cassette used in DCRSi recorder



**TAPE UNIT
(T.U.)**



**ELECTRONICS
UNIT
(E.U.)**

Figure 6.9-3 Physical envelopes of each recorder component

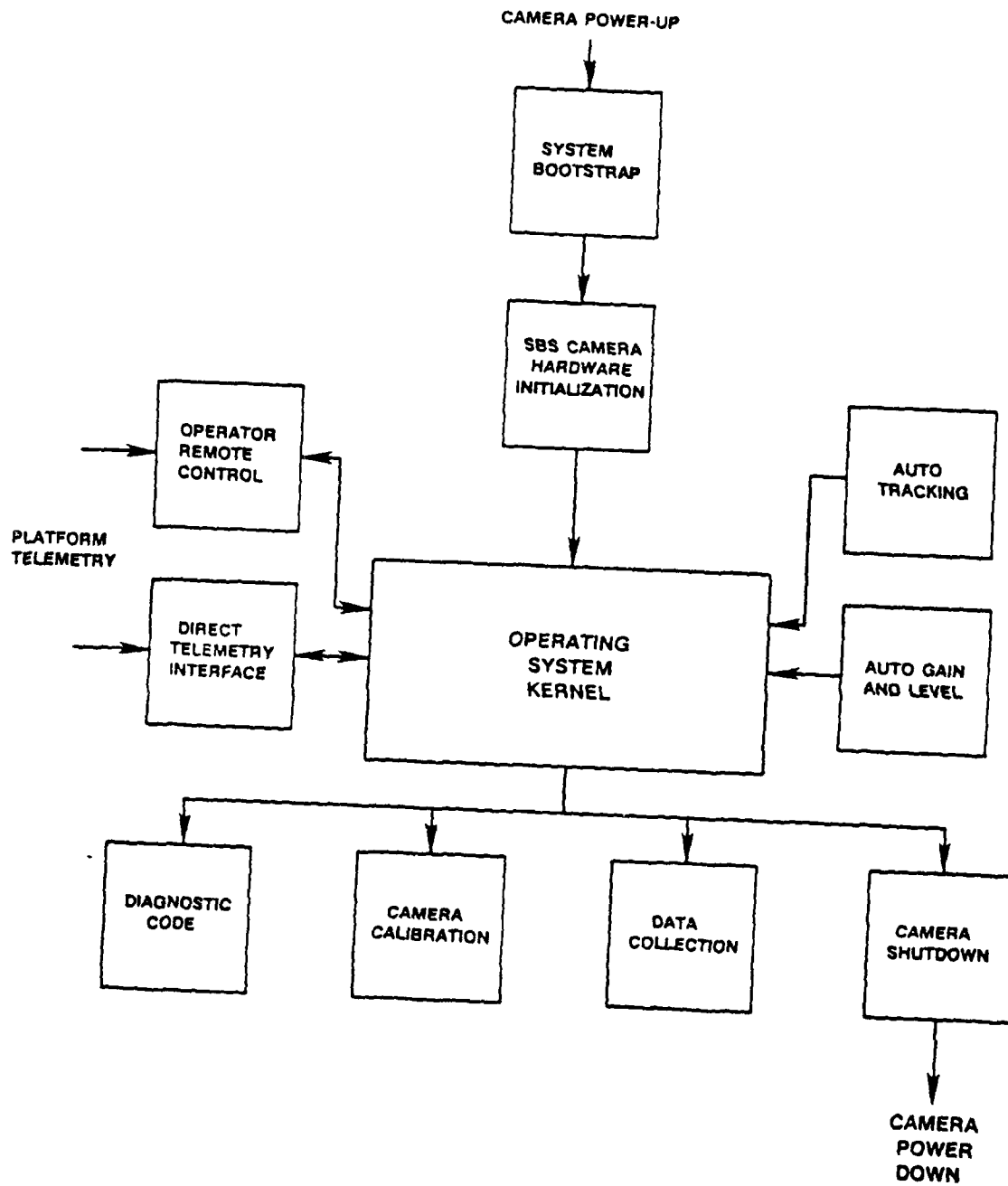


Figure 6.10-1 Functional block diagram of SBS control computer software code